The Development of Novel Cool Asphalt Pavement Structures to Alleviate the Urban Heat Island Effects

by

Mohsen SHAMSAEI

MANUSCRIPT-BASED THESIS PRESENTED TO ÉCOLE DE TECHNOLOGIE SUPÉRIEURE IN PARTIAL FULFILLMENT FOR THE DEGREE OF DOCTOR OF PHILOSOPHY
Ph.D.

MONTREAL, FEBRUARY 6, 2026

ÉCOLE DE TECHNOLOGIE SUPÉRIEURE
UNIVERSITÉ DU QUÉBEC

BOARD OF EXAMINERS

THIS THESIS HAS BEEN EVALUATED

BY THE FOLLOWING BOARD OF EXAMINERS

Mr. Michel Vaillancourt, Thesis Supervisor
Department of Construction Engineering at École de Technologie Supérieure

Mr. Alan Carter, Thesis Co-supervisor
Department of Construction Engineering at École de Technologie Supérieure

Mr. Stéphane Hallé, President of the Board of Examiners
Department of Mechanical Engineering at École de Technologie Supérieure

Mrs. Katherine D'Avignon, Member of the jury
Department of Construction Engineering at École de Technologie Supérieure

Mr. Éric Lachance-Tremblay, Member of the jury
Department of Construction Engineering at École de Technologie Supérieure

Mr. Nam Tran, External Evaluator
National Center for Asphalt Technology, Auburn University

THIS THESIS WAS PRESENTED AND DEFENDED

IN THE PRESENCE OF A BOARD OF EXAMINERS AND THE PUBLIC

ON JANUARY 21, 2026

AT ÉCOLE DE TECHNOLOGIE SUPÉRIEURE

ACKNOWLEDGMENTS

First and foremost, I extend my heartfelt gratitude to my Ph.D. thesis supervisor, Dr. Michel Vaillancourt, whose expertise, knowledge, encouragement, and unwavering support have been invaluable throughout my Ph.D. journey. His mentorship not only shaped the direction of my research but also inspired me to push the boundaries of my capabilities. I am equally indebted to my co-supervisor, Dr. Alan Carter, for his constructive criticism, insightful feedback, and continuous encouragement. His collaborative spirit and dedication to excellence have significantly enriched the quality of my research.

Besides, I extend my sincere appreciation to the ETS technicians, Sylvain Bibeau, Francis Bilodeau, Richard Prowt, Alexis Vadeboncoeur, and Sébastien Ménard, whose technical expertise and assistance have been indispensable in conducting experiments and analyzing data. Their willingness to help and professionalism have made the research process more efficient. I would like to express my sincere appreciation to Dr. Stéphane Hallé, Dr. Katherine D'Avignon, Dr. Éric Lachance-Tremblay, and Dr. Nam Tran for serving on my jury and for their time, expertise, and valuable contributions to the evaluation of this work.

I also acknowledge the Natural Sciences and Engineering Research Council of Canada (NSERC) for providing financial support (funding reference number: RGPIN-2020-04861). Their investment in this project has been crucial, and the completion of this research would not have been possible without their support.

Last but not least, I would like to extend my deepest appreciation to my family for their unwavering love, guidance, encouragement, and belief in my abilities. I am endlessly grateful for their sacrifices and understanding throughout my academic journey.

Développement des nouvelles structures de chaussée en enrobés à froid pour atténuer les effets de l'îlot de chaleur urbain

Mohsen SHAMSAEI

RÉSUMÉ

La température en milieu urbain est généralement plus élevée que celle des banlieues en raison des activités et des travaux humains, tel que la fabrication des revêtements bitumineux. Le revêtement en enrobé bitumineux absorbe et stocke l'énergie solaire pendant la journée et la libère la nuit, engendrant ainsi un phénomène appelé îlot de chaleur urbain (ICU). Deux solutions différentes ont été proposées dans le cadre de cette recherche pour atténuer les effets de l'ICU. Tout d'abord, la chaussée bitumineuse a été recouverte d'enduits superficiels fabriqués à partir de matériaux recyclés afin d'augmenter la réflectivité de la surface et de réduire l'absorption de chaleur pendant la journée, refroidissant ainsi le revêtement de la chaussée. Les propriétés mécaniques, la sécurité et la durabilité de ces nouveaux revêtements ont également été évaluées par temps froid et chaud. Bien que l'absorption de chaleur par le revêtement bitumineux puisse être minimisée par un revêtement réfléchissant, elle ne peut pas être nulle. Par conséquent, la chaleur absorbée dans les couches bitumineuses doit être transférée dans les couches inférieures afin de réduire le gradient thermique entre le revêtement et l'air ambiant. Par ailleurs, moins de chaleur est transférée à l'air ambiant, ce qui atténue l'ICU. À cette fin, la deuxième solution proposée consistait à améliorer le transfert de chaleur à l'interface des couches bitumineuses et des couches granulaires sous-jacentes et à développer une couche de fondation conductrice. Un sous-produit industriel a donc été utilisé pour préparer une couche de fondation et de sous fondation conductrice. Globalement, les expériences en laboratoire et sur le terrain ont montré que la réduction de l'absorption de chaleur par la chaussée et le transfert de la chaleur absorbée vers la couche de base peuvent abaisser la température du revêtement en asphalte, entraînant une moindre libération de chaleur dans l'air ambiant et atténuant ainsi l'ICU associé aux chaussées en asphalte.

Mots-clés: îlot de chaleur urbain, réflectivité, traitement de surface, couche de fondation conductrice, couche de sous fondation conductrice

The Development of Novel Cool Asphalt Pavement Structures to Alleviate the Urban Heat Island Effects

Mohsen SHAMSAEI

ABSTRACT

The urban temperature is usually higher than the suburban temperature due to some human activities and inventions, one of which is asphalt pavement. Asphalt pavement absorbs and stores solar energy during the day and releases it at night, exacerbating a phenomenon named urban heat island (UHI). Two different solutions were proposed in this research to mitigate the effects of UHI. Firstly, the asphalt pavement was coated with chip seals made of some recycled materials to increase the surface reflectivity and reduce heat absorption during the day, cooling the asphalt pavement. The mechanical properties, safety, and durability of these new chip seals were also evaluated for cold and hot weather conditions. Although the heat entering the asphalt pavement can be minimized by reflective pavements, it cannot be zero. Hence, the absorbed heat in the asphalt mixture should be transferred into the layers below to observe a smaller thermal gradient between the asphalt mixture and its surrounding air. As a result, less heat is transferred to the ambient air, mitigating the UHI. For this purpose, the second proposed solution was enhancing the heat transfer at the interface of the asphalt mixture and base course and developing a conductive base course. Therefore, an industrial by-product, steel slag, was utilized to prepare a conductive prime coat and a conductive base course. Overall, the laboratory and field experiments indicated that reducing pavement heat absorption and transferring the absorbed heat into the base course can decrease the asphalt pavement temperature, resulting in less heat release into the ambient air and mitigating the UHI associated with asphalt pavements.

Keywords: urban heat island, reflectivity, chip seal, conductive base course, conductive prime coat

TABLE OF CONTENTS

Page

LIST OF TABLES

Page

LIST OF FIGURES

Page

LIST OF ABBREVIATIONS AND ACRONYMS

3RMCDQ	Association of Building and Demolition Materials Collectors and Recyclers of Quebec
ALD	Average Least Dimension
BPN	British Pendulum Number
BPT	British Pendulum Tester
BNQ	Bureau De Normalisation Du Québec
CBR	California Bearing Ratio
CO_2	Carbon Dioxide
CDW	Construction and Demolition Waste
CMA	Cold Mix Asphalt
CRS-2	Cationic Rapid Setting Type 2
CT	Computed Tomography
CV	Coefficient of Variation
DNI	Direct Normal Irradiance
DSC	Differential Scanning Calorimetry
EAF	Electric Arc Furnace
EOL	End-of-Life
EPP	Expanded Polypropylene
EU	European Union
FWD	Falling Weight Deflectometer
FAC	Fly Ash Cenosphere
FI	Flakiness Index
GHG	Greenhouse Gas
IO	Input-Output
HMA	Hot Mix Asphalt
IBT	Interface Bond Test
LCA	Life Cycle Assessment

LCIA	Life Cycle Impact Assessment
LCI	Life Cycle Inventory
LWT	Load Wheel Test
MTS	Material Testing System
MDD	Maximum Dry Density
MTD	Mean Texture Depth
MTPS	Modified Transient Plane Source
NCHRP	National Cooperative Highway Research Program
NSERC	Natural Sciences and Engineering Research Council of Canada
NIR	Near-Infrared
N_2O	Nitrous Oxide
OMC	Optimum Moisture Content
PCM	Phase Change Materials
RAP	Reclaimed Asphalt Pavement
SD	Standard Deviation
TLS	Transient Line Source
TAC	Transportation Association of Canada
UHI	Urban Heat Island
US	United States
UV	Ultra-Violet
VIS	Visible
XRF	X-Ray Fluorescence

LIST OF SYMBOLS

R_s	Solar reflectance (%)
T_S	Surface temperature (K)
T_1	Top surface temperature (K)
T_2	Bottom surface temperature (K)
T_{air}	Air temperature (K)
V_t	Volume of asphalt mixture (m^3)
α_{abs}	Surface absorptivity
ΔT	Temperature difference (K)
A_g	Initial weight of the specimen (g)
B_g	Final weight after testing (g)
C_g	Asphalt disk weight (g)
V	Volume of sand (mm^3)
C_s	Specific heat capacity at constant pressure ($J.kg^{-1}.K^{-1}$)
ρC_p	Volumetric heat capacity ($J.m^{-3}.K^{-1}$)
C_{vol}	Volumetric heat capacity ($J.m^{-3}.K^{-1}$)
h_c	Convective heat transfer coefficient ($W.m^{-2}.K^{-1}$)
D	Spread sand diameter (mm)
E	Wastage factor for traffic whip-off
G	Bulk specific gravity
H	Average least dimension (mm)
L	Depth of the specimen (m)
m	Mass (kg)

q_{con}	Convective heat flux (W)
q_x	Conduction heat flux (W)
Q	Total transferred energy (J)
A	surface area (m^2)
R	Residual asphalt content of binder (%)
S	Surface condition factor (L/m^2)
A_b	Aggregate absorption factor (L/m^2)
T	Traffic factor
B	Binder application rate (L/m^2)
C	Aggregate application rate (kg/m^2)
V_d	Voids in loose aggregate (%)
W	Loose weight of aggregates (kg/m^3)
M	Median particle size (mm)
V	Volume of the component (m^3)
α_A	Albedo
α	Thermal diffusivity ($m^2.s^{-1}$)
ε	Thermal emissivity ($W.m^{-2}$)
e	Thermal effusivity ($W.\ s^{1/2}.\ m^{-2}.\ K^{-1}$)
k	Thermal conductivity ($W.m^{-1}.K^{-1}$)
ρ	Density ($kg.m^{-3}$)
$R(\lambda)$	Measured spectral data
$E(\lambda)$	Spectral irradiance
ε	Absorption (fraction, dimensionless)
ρ	Reflectance (fraction, dimensionless)

τ	Transmittance (fraction, dimensionless)

INTRODUCTION

Asphalt pavement is the most common type of pavement all over the world. There are many reasons for this worldwide application, including fast implementation, easy maintenance, rehabilitation, comfort, and smoothness for vehicles. However, asphalt pavement can absorb and store thermal energy. This energy is released into the ambient air, especially at night, due to the high thermal gradient between the asphalt mixtures and the air temperature. The outgoing heat of asphalt pavement can exacerbate a phenomenon called urban heat island (UHI) (Mohajerani et al., 2017a). This phenomenon is believed to be one of the causes of climate change (Founda, 2011; Nakayama and Fujita, 2010). This is attributed to the reduction of green places, trees, vegetation, and the transformation of these natural areas into buildings and structures (Stone Brian et al., 2010).

The UHI is an urban area with higher temperatures than its suburbs. This higher urban temperature stems from some human activities and inventions in cities, one of which is asphalt pavement. The temperature difference can be from 5 to 15 ℃ (Santamouris, 2013a). In general, asphalt pavement accounts for a considerable part of the city (Akbari & Rose, 2008), indicating the impact of pavements on the UHI. Although many studies have been conducted to enhance the surface reflectivity and alter the thermal conductivity of asphalt pavement to alleviate the UHI effects, an efficient and practical asphalt pavement structure, that can mitigate the UHI effects, has not been proposed.

Although the mix design of asphalt mixtures affects the heat transfer rate, surface reflectivity is claimed to be one of the most important factors in heat absorption and storage of asphalt pavements, influencing the UHI (Sha et al., 2017). Lower surface reflectivity results in higher heat absorption and higher surface temperature (Silva et al., 2010). One of the common approaches for declining surface temperature and heat absorption is to enhance the albedo of asphalt pavements. Albedo is defined as the ratio of reflected solar radiation to the total incoming solar radiation on the surface. It is a dimensionless parameter that indicates surface reflectivity, ranging from 0 (perfect absorber) to 1 (perfect reflector). Conventional asphalt

pavements typically exhibit low albedo values (0.05–0.15), resulting in significant heat absorption and contributing to elevated surface temperatures and the urban heat island (UHI) effect. Raising the albedo by 0.1 unit can reduce the surface temperature by 2.1 ℃ (Chen et al., 2017). Therefore, increasing pavement albedo through surface treatments or alternative materials is a recognized strategy for mitigating these thermal impacts.

Although the asphalt mixture layer plays the most significant role in heat exchange between the asphalt pavement and the surrounding air, the heat transfer rate between the asphalt mixture and the base course can be important for UHI mitigation. The reason is obvious since the heat absorption of the asphalt mixture can be minimized, but not to zero (Chen et al., 2017). If the absorbed solar energy accumulates in the asphalt mixture and at the top of the pavement, more heat is released into the ambient air because of a higher thermal gradient between the pavement and its surrounding air at night. Therefore, transferring the absorbed heat into the base course and subgrade can reduce the surface temperature, alleviating the UHI (Shamsaei et al., 2022). According to previous studies, the effect of the asphalt mixture and base course interface on heat transfer has been neglected. As air is trapped at the interface, the heat transfer rate is decreased, accumulating heat in the asphalt mixture layer. A prime coat is a thin asphalt binder layer applied at the interface, enhancing the adhesion between the base course and asphalt mixture as well as sealing the surface pores of the base course, reducing the moisture migration (Freeman et al., 2010). Hence, applying a prime coat modified with conductive materials can enhance the heat transfer rate from the asphalt mixture to the base course.

This thesis comprises four chapters that evaluate novel methods and pavement structures for UHI mitigation. Chapter 1 is a literature review, providing a comprehensive overview of the UHI phenomenon, outlining its underlying causes, health and infrastructure impacts, and the key mechanisms of heat transfer involved, namely surface radiation, thermal conductivity, and convection. It further examines the influence of pavement materials and structural characteristics, including color, density, and thermal properties, with a focus on both conventional and recycled materials such as construction and demolition waste (CDW) and steel slag. This chapter also highlights the role of interlayer heat transfer and the presence of voids in influencing pavement thermal behavior. Finally, it surveys existing UHI mitigation strategies, such as increasing surface albedo and the use of cool pavements, and summarizes

key experimental approaches used in the literature to measure thermal properties and evaluate pavement performance.

Chapter 2 outlines the research objectives and presents the comprehensive methodology adopted in this study. This chapter begins by clearly stating the main goals of the thesis, which focus on mitigating UHI effects through the development of asphalt pavement structures that enhance surface reflectivity and promote efficient heat dissipation into underlying layers. The methodology section details experimental design, including both laboratory and field investigations, and provides a rationale for the selection of specific tests based on the thermal and mechanical performance criteria relevant to pavement applications. Tests such as surface and in-depth temperature measurements, mechanical and thermal properties measurements of reflective chip seals, prime coat, and conductive base courses are described, alongside the modified procedures employed to simulate realistic environmental conditions in the laboratory. Each test method is supported by references to appropriate international standards, and the selection of materials, including conventional aggregates and recycled alternatives such as construction and demolition waste (CDW) and steel slag, is justified in terms of both technical and environmental considerations. Special emphasis is placed on understanding the thermal behavior of pavement structures, including the role of surface roughness and void content at the interface in influencing heat transfer between the layers. This chapter also explains the preparation of specimens, the configuration of testing setups, and the protocols for data collection and analysis. Overall, Chapter 2 establishes the experimental foundation upon which the subsequent analysis and findings of this thesis are built.

Chapter 3 presents the details of the first research objective, which is developing novel chip seals, enhancing the albedo and surface reflectivity of asphalt pavements. This includes experimental methodology, results, and analysis related to the use of CDW materials as chip seal treatments for asphalt pavements. The chapter begins by focusing on evaluating the mechanical performance, durability, safety, and thermal behavior of innovative CDW-based chip seals. The methodology section describes the laboratory and field tests conducted to assess surface texture (sand patch method), skid resistance (British Pendulum Tester), binder adhesion and durability (sweep test), cohesion (Vialit test and interface bond test), and surface

degradation. Additionally, more tests were conducted to measure surface reflectivity, albedo, and the impact of material composition on surface and in-depth pavement temperature. All tests were designed following recognized standards to ensure reproducibility and practical relevance. Emphasis is placed on evaluating the potential of these recycled materials not only to meet performance and safety requirements but also to contribute to UHI mitigation through increased surface reflectivity and reduced heat absorption. This chapter provides a comprehensive framework for assessing the technical feasibility and environmental benefits of incorporating recycled concrete, brick, and glass in chip seal applications.

After reducing heat absorption by reflective chip seals, Chapter 4 focuses on the second objective of this research, which is the dissipation of heat into the underlying pavement layers. This chapter investigates the role of prime coats and base course materials in enhancing heat dissipation within pavement structures to mitigate UHI effects. It evaluates and compares the performance of a conventional bituminous prime coat with a specially formulated conductive prime coat, as well as a conductive base course composed of recycled materials with higher thermal conductivity. The aim is to understand how these components influence downward heat transfer, surface cooling, and the reduction of heat re-emission into the ambient air. Laboratory experiments were designed to simulate actual pavement conditions, with temperature sensors installed at multiple depths to capture the thermal behavior of different layer configurations. The experimental program assesses the capacity of conductive treatments to transfer absorbed heat from the surface into the underlying layers more effectively than traditional materials. Through this investigation, Chapter 4 establishes the potential of using thermally conductive interfaces and base layers as a complementary strategy to reflective surface treatments in reducing surface temperature, decreasing the nighttime outgoing heat, and contributing to UHI mitigation.

Finally, the critical discussion of the overall approach taken in this research highlights the combined effects of reflective chip seals and conductive pavement layers on mitigating UHI impacts. It synthesizes the key findings from the experimental investigations and assesses the practical implications, limitations, and potential for large-scale application. The chapter concludes by summarizing the main contributions of the study and offering recommendations for future research and implementation in sustainable pavement design.

Regarding the scientific contributions of this thesis, it introduces several innovative approaches to mitigate the UHI effect, particularly focusing on asphalt pavements. First, novel chip seals using recycled materials are developed. The mechanical properties, safety, and durability of these chips are evaluated to propose a practical solution. Their surface reflectivity and effects on the pavement temperature reduction are then assessed. This approach not only addresses environmental sustainability by reusing waste materials but also enhances the thermal performance of pavements on the UHI by reducing heat absorption. Another novel scientific aspect of this study is to show the role of the interface of the asphalt mixture and base course on temperature reduction and the effect of the conductive base course on UHI mitigation. The thesis explores the often-overlooked aspect of heat transfer at the interface between the asphalt mixture and the base course. By developing a conductive prime coat and a conductive base course using an industrial by-product, the study aims to increase the heat dissipation rate from the pavement to its lower layers. Finally, by combining the analysis of surface albedo enhancement with subsurface heat transfer improvements, this research provides a comprehensive understanding of UHI mitigation strategies for asphalt pavements. This integrated approach goes beyond existing studies that often focus on one aspect in isolation. Overall, these contributions not only advance the field of asphalt pavement engineering but also offer practical solutions to urban planners and policymakers aiming to reduce the adverse effects of UHI. The findings have the potential to influence future pavement design standards and promote the adoption of sustainable materials in urban infrastructure.

CHAPTER 1

LITERATURE REVIEW

1.1 Introduction to Urban Heat Islands

Urban Heat Islands (UHI) refer to the phenomenon in which urban areas experience significantly higher temperatures than their surrounding rural environments. This temperature differential arises due to human activities, high building density, and manmade surfaces such as roads, rooftops, and parking lots. These surfaces absorb and retain solar radiation during the day and release it gradually at night, disrupting the natural thermal balance of the environment (Mohajerani et al., 2017a). The UHI effect is particularly pronounced in densely populated metropolitan regions, where vegetation is sparse, and human-related heat emissions from vehicles, buildings, and industrial processes further contribute to elevated temperatures. Among the various components of the urban landscape, asphalt pavements are one of the major contributors to UHIs due to their low albedo, high thermal mass, and widespread application in urban areas. These pavements not only absorb a significant portion of solar radiation but also release stored heat slowly, especially during nighttime, increasing the thermal stress in urban environments (Chen et al., 2017). Understanding the dynamics of UHIs and their relation to pavement materials and structure is critical for developing effective mitigation strategies. This chapter focuses specifically on the contribution of pavements to the UHI phenomenon and explores both the thermal mechanisms involved and the potential interventions, such as reflective surface treatments and enhanced subsurface heat dissipation, that can reduce their thermal impact.

The UHI phenomenon has been increasingly recognized as a byproduct of rapid urbanization and industrialization. Historically, the roots of UHI can be traced back to the early stages of urban development, where the transformation of natural landscapes into dense city environments began to change local climate conditions. The first formal identification of UHIs occurred in the early 19th century, when Luke Howard, a British meteorologist, documented

elevated temperatures in London compared to surrounding rural areas (Mills, 2008). Since then, expanding urban footprints across the globe have consistently exhibited similar patterns.

Urbanization contributes to UHI formation primarily through the replacement of vegetation with built infrastructure, including buildings, roads, and pavements. These changes disrupt the natural energy balance by reducing evapotranspiration, increasing surface roughness, and introducing materials with higher thermal mass and lower albedo. As cities grow, the concentration of manmade heat sources, such as vehicles, industrial processes, and air conditioning systems, further intensifies local warming (Irfeey et al., 2023). In addition to physical changes in land use, the spatial configuration of urban structures plays a role in trapping heat. Narrow streets surrounded by tall buildings, commonly known as urban canyons, limit longwave radiation loss at night, exacerbating nocturnal temperature differences between urban and rural zones (Rossi et al., 2016). The cumulative impact of these factors over time has led to the persistent development of UHIs, particularly in metropolitan areas with high population densities and limited green infrastructure. Understanding this historical and urban context is essential to identifying the key mechanisms of UHI formation and evaluating strategies for its mitigation, especially in relation to pavement materials and design, which are of particular interest in this thesis.

Among the various contributors to UHI effects, pavements represent one of the most significant sources of excess urban warmth. In many urban environments, pavements, including roads, parking lots, and sidewalks, can account for over 30-40% of the land surface (Akbari and Rose, 2008). These surfaces are typically composed of dark, impervious materials such as asphalt, which are characterized by low solar reflectivity, high thermal conductivity, and substantial heat storage capacity (Akbari and Rose, 2008). Due to their physical and thermal properties, pavements absorb a large proportion of incoming solar radiation during the day and retain heat well into the night, releasing it gradually into the surrounding air. This delayed release of thermal energy contributes to elevated nighttime temperatures, a defining characteristic of UHI effects (Shamsaei et al., 2022). Previous case studies showed that maximum UHI intensities in cities like Nanjing, Shanghai, Beijing, and Hong Kong range between 6 and 10.5 °C due to built infrastructures (Memon et al., 2009; Zeng et al., 2009). The UHI can raise local temperatures

by 5 to 15 °C, and pavements are one of the most significant contributors to UHIs, making the deployment of cooling pavement solutions increasingly vital (Santamouris, 2013a). The surface characteristics and structure of pavements also influence heat transfer dynamics both at the surface level and within underlying layers. Parameters such as albedo, thermal emissivity, material composition, surface texture, and even air void content between layers can impact how heat is absorbed, conducted, and re-radiated. These mechanisms make pavements a crucial target for UHI mitigation strategies (Shamsaei et al., 2024a).

1.2 Primary Causes of the UHI Effects

The UHI effects arise from the combination of environmental modifications and human-induced activities that change the thermal characteristics of urban environments. Population growth is one of the main factors of this transformation, which intensifies urbanization and leads to widespread land development (Rossi et al., 2014). As cities expand to accommodate growing populations, natural landscapes are increasingly replaced by impervious materials such as asphalt and concrete. These low albedo surfaces can contribute to UHI effects, raising the urban temperature (Yamamoto, 2006; Grimmond, 2007; Shamsaei et al., 2022).

The expansion of urban areas also results in the significant loss of vegetation and water bodies. With fewer green spaces and open water surfaces, the capacity for evaporative cooling diminishes, reducing latent heat exchange and further intensifying urban warming. Dense urban layout, shaped by high-rise buildings and narrow streets, restricts airflow and creates heat-retaining microclimates, particularly during nighttime hours when built structures continue to emit stored heat (Stone Brian et al., 2010; Rossi et al., 2016). Besides, population growth contributes to increased heat emissions through greater demand for energy, transportation, and cooling systems. Industrial activity, vehicular traffic, and air conditioning systems release considerable amounts of heat into the ambient air. While air conditioners cool indoor spaces, they discharge warm air outdoors, exacerbating the external heat burden in already dense urban zones (Rossi et al., 2014; Hatvani-Kovacs et al., 2016). Therefore, the low albedo of urban surfaces, coupled with limited air circulation due to obstructive urban geometry, prevents natural heat dispersion. As a result, the UHI phenomenon is intensified,

presenting critical challenges for environmental sustainability, public health, and urban infrastructure resilience. These main causes are illustrated in Figure 1.1.

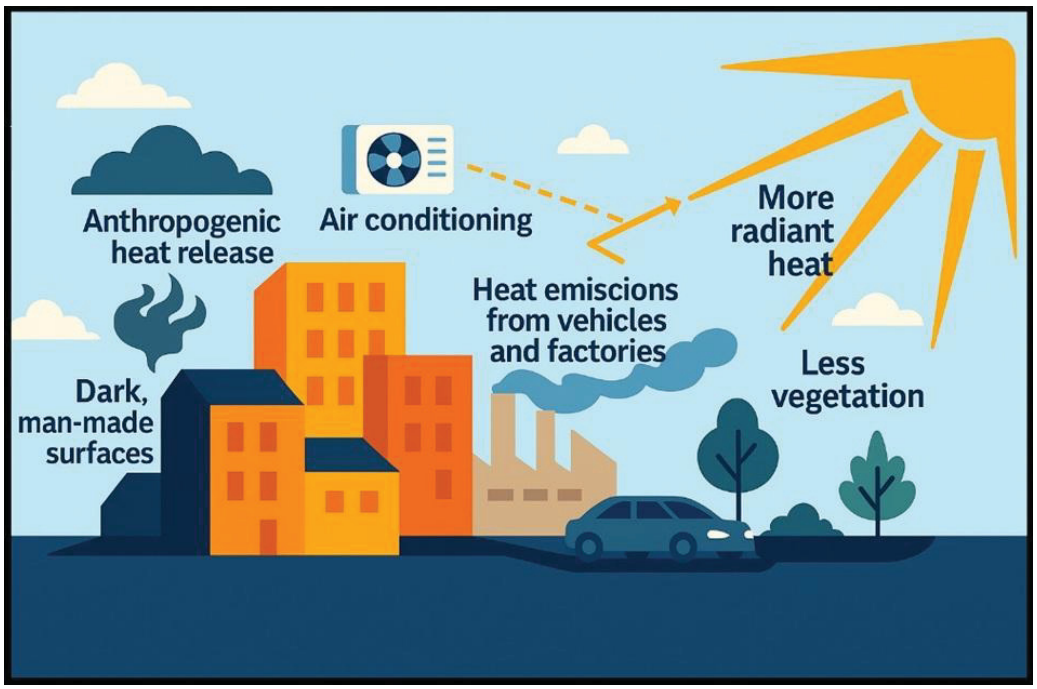

Figure 1.1 The primary causes of UHI

1.3 Problems of the UHI Effects

Urban heat islands represent a significant environmental and engineering challenge in densely built environments, where asphalt pavements are a major contributor due to their extensive coverage and unfavorable thermal properties (Rossi et al., 2014). The disproportionate absorption and retention of solar radiation by these surfaces contribute to elevated urban temperatures, with adverse effects on public health, energy systems, and infrastructure longevity. Conventional pavement designs often neglect their contribution to localized heating. This thesis addresses the urgent need to evaluate and improve pavement systems with respect to their thermal behavior, exploring innovative solutions that can reduce surface temperatures and mitigate UHI effects while maintaining performance and sustainability.

1.3.1 The UHI Effects on Urban Health, Energy Use, and Infrastructure Performance

From a public health perspective, UHIs exacerbate heat-related illnesses, especially among vulnerable populations such as the elderly, children, and individuals with pre-existing health conditions. Higher ambient and nighttime temperatures can intensify the effects of heat waves, increasing risks of heat exhaustion, heatstroke, and cardiovascular complications (Hatvani-Kovacs et al., 2016). Studies have shown a correlation between UHI intensity and elevated mortality rates during extreme heat events. In addition, elevated temperatures contribute to poor air quality by accelerating the formation of ground-level ozone and particulate matter, which can aggravate respiratory diseases such as asthma and bronchitis (Anderson and Bell, 2011; Yang et al., 2019).

In terms of energy consumption, the UHI significantly increases the cooling demand for buildings during warmer months. Urban areas experiencing higher temperatures due to UHI effects rely more heavily on air conditioning, leading to elevated electricity usage. This surge in energy demand strains electrical grids, raises operational costs, and increases greenhouse gas emissions, creating a feedback loop that contributes to further urban warming and climate change (Grimmond, 2007; Ichinose et al., 2008; Rossi et al., 2014).

Regarding infrastructure performance, prolonged exposure to elevated surface and subsurface temperatures can accelerate material degradation, particularly in asphalt pavements. High temperatures soften asphalt binders, reducing their structural integrity and making pavements more susceptible to distress such as rutting, cracking, and fatigue (Chen et al., 2019). Temperature fluctuations significantly influence asphalt mixtures due to the viscoelastic nature of asphalt binders, prompting extensive research into the thermal conductivity of asphalt concrete. At low temperatures, binder stiffening leads to the formation of thermal cracks (D. Zhang et al., 2019). In contrast, elevated temperatures exacerbate rutting, as the binder's rheological behavior and reduced viscosity under heavy traffic loads make the pavement more susceptible to deformation (Morea et al., 2011; Tong et al., 2020). Rutting is largely attributed to high surface temperatures and repetitive loading, and while it can affect both surface and underlying layers, studies show that 85% to 95% of rutting typically occurs in the asphalt

concrete layer (Coleri et al., 2008). Rutting can cause many problems, including penetration of the accumulated water in ruts, safety issues, and increasing maintenance and rehabilitation costs (Tian and Yu, 2017). The thermal expansion and contraction caused by daily and seasonal temperature fluctuations can also compromise the performance of roadways, bridges, and utility lines. These thermal-induced stresses reduce the lifespan of infrastructure, increase maintenance costs, and disrupt urban mobility and economic activity (Gilbert et al., 2017; Yinfei et al., 2018; Li et al., 2021). Considering the thermal susceptibility of asphalt binder, heat transfer in the asphalt pavement is of great importance. This property affects both the performance of asphalt pavement and the ambient air (Kataoka et al., 2009; Ma et al., 2016). Therefore, the UHI phenomenon represents not only an environmental and sustainability challenge but also a multidimensional urban management concern. Mitigating UHI effects is therefore essential for enhancing public health resilience, reducing energy consumption, and extending the service life of infrastructure, all of which are vital for building sustainable cities.

1.3.2 Pavement's Contribution to Urban Temperature Increase

Asphalt pavements are one of the major contributors to the UHI, resulting in higher urban temperatures. Unlike vegetated or lighter-colored surfaces, pavements typically exhibit low albedo values, meaning a greater proportion of incoming solar energy is retained rather than reflected. The surface temperature and thermal conductivity of asphalt concrete are measured in many studies. This retained energy elevates surface and subsurface temperatures, especially during hot seasons (Golden and Kaloush, 2006). Hence, the dark surface and dense composition of conventional pavement materials allow them to reach much higher temperatures than vegetated or natural surfaces under similar solar exposure. Studies have shown that pavement surfaces can be 20–30°C hotter than surrounding shaded or grassy areas, directly increasing the near-surface air temperature. This effect is most pronounced during summer months and in regions with intense solar radiation (Bobes-Jesus et al., 2013). It was concluded that this temperature could reach up to 60 ℃ in summer (Higashiyama et al., 2016). In detail, asphalt pavements absorb a substantial amount of incoming solar radiation during the day and release the stored heat gradually during the night, leading to sustained high surface and ambient temperatures well after sunset. This prolonged heat retention exacerbates the

temperature differential between urban and surrounding rural areas (Silva et al., 2010; Synnefa et al., 2011).

Moreover, the lack of moisture retention and evaporative cooling in pavement surfaces eliminates one of the key natural mechanisms for dissipating heat. Unlike vegetated areas that cool through evapotranspiration, asphalt and concrete pavements trap and re-radiate heat, intensifying the urban heat island effect (Liu et al., 2018). Due to the extensive coverage of pavements in cities, often accounting for more than one-third of urban land, pavements have a broad and cumulative impact on urban thermal environments (Akbari and Rose, 2008). Therefore, as more surface area is paved in expanding urban centers, the potential for heat accumulation increases, intensifying the temperature increase trend during heat waves and contributing to long-term urban warming trends.

1.3.3 High-Temperature Environment and Low-Albedo Surfaces Challenges

High-temperature urban environments present some challenges that go beyond the general impacts of urban heat. Regarding the heat absorption of low-albedo surfaces of asphalt pavements and the subsequent heat release, the lack of nighttime cooling becomes a critical issue (Aletba et al., 2021). Without sufficient temperature drops at night, the urban surface hardly fully resets thermally, resulting in a cumulative heating effect known as thermal lag. This phenomenon is particularly severe in cities with compact layouts, limited vegetation, and widespread pavement surfaces, where airflow is restricted and natural cooling is minimal (Parker, 2010; Rossi et al., 2016). Furthermore, these environments with higher temperatures often experience a feedback loop. This means that higher surface temperatures increase energy demand for indoor cooling, which in turn generates more heat through air conditioning systems. This extra heat is released into the urban atmosphere, further amplifying the UHI effect (Grimmond, 2007). Additionally, rising temperatures can accelerate chemical degradation in pavement binders and increase the rate of oxidative aging, leading to reduced pavement durability even before visible distress occurs (Yang et al., 2023). Another challenge is the mismatch between traditional pavement design standards and the actual thermal conditions experienced in hot climates. Pavement materials and structural configurations

optimized for temperate climates may fail to perform adequately when subjected to sustained high heat, highlighting the need for localized thermal performance testing and specific design guidelines (Gudipudi et al., 2017). Lastly, the radiative properties of low-albedo surfaces contribute to human thermal discomfort. Dark pavements absorb more solar radiation and reach higher surface temperatures, leading to increased emission of longwave infrared radiation. This elevates the mean radiant temperature experienced by pedestrians and increases the risk of heat-related illnesses in vulnerable populations (Anand and Sailor, 2022). Consequently, addressing low-albedo pavements in hot urban climates is not only an engineering priority but also a public health and urban livability concern.

1.4 Mechanisms of Heat Transfer in Pavements

Understanding the mechanisms of heat transfer in pavement structures is vital to mitigating the UHI effect and improving thermal performance. Pavements are thermally dynamic systems where energy is absorbed, stored, conducted, and released through various physical processes (Xue et al., 2013). These include radiation from the sun, conduction within and between pavement layers, convection with the surrounding air, and energy storage related to material-specific heat capacity and diffusivity. Each of these mechanisms is influenced by the material composition, structural design, and environmental conditions (Chen et al., 2017; Shamsaei et al., 2022).

1.4.1 Surface Radiation

Surface radiation is a fundamental mechanism by which pavements interact thermally with their ambient air, primarily through the absorption and emission of solar energy. Radiation involves the emission or transmission of thermal energy in the form of electromagnetic waves or particles through space or materials. Pavement surfaces absorb a significant portion of solar radiation due to their low albedo (Gui et al., 2007). Albedo is generally shown with α, but in this thesis, it is presented as α_A to be differentiated from other parameters shown with the same symbol (α). Albedo depends on how much a material's surface can absorb solar radiation and is determined using Equation 1.1 (Pomerantz et al., 2003).

$$\alpha_A = 1 - \alpha_{abs} \tag{1.1}$$

In this equation, α_{abs} denotes the surface's absorptivity, while α_A refers to the albedo of the material. This equation shows that higher absorptivity leads to lower albedo. Moreover, albedo is not a fixed property for asphalt pavements; it can vary with time of day based on incident angle and surface temperature. Studies have shown that albedo tends to drop as surface temperature increases. The correlation between albedo and surface temperature is demonstrated in Figure 1.2 (Li et al., 2013).

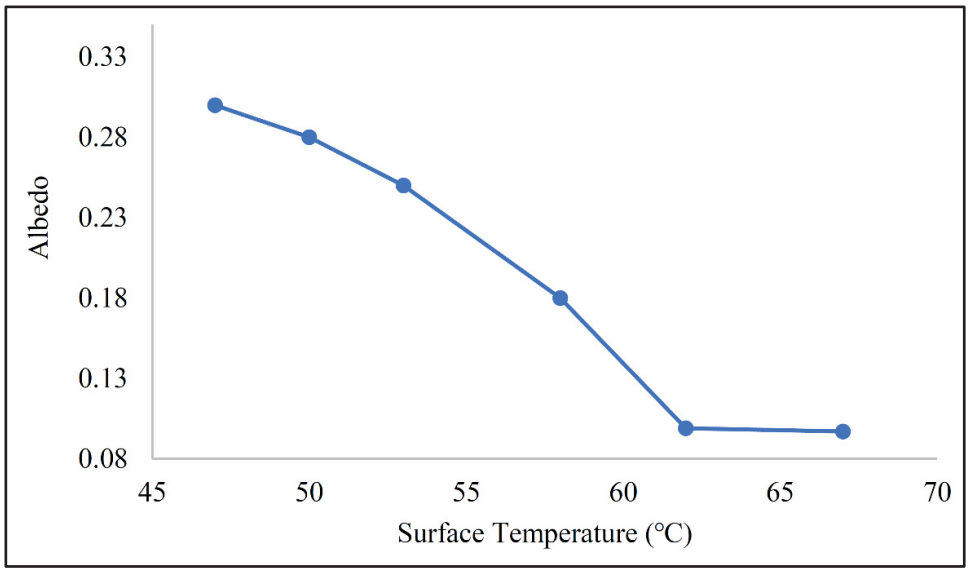

Figure 1.2 The relationship between albedo and the surface temperature
Adapted from Li et al (2013)

Albedo and solar reflectance are closely related radiative properties, but they are not identical. Solar reflectance represents the fraction of incident shortwave solar radiation that is reflected by a surface, including both diffuse and specular reflection components, and is defined over the full solar spectrum unless otherwise specified. Albedo, by contrast, refers specifically to the diffuse hemispherical reflectance of a surface with respect to solar radiation, also generally integrated over the entire shortwave spectrum. Both properties may be reported as broadband values or expressed as spectral reflectance curves as a function of wavelength, depending on the measurement method and application. While solar reflectance characterizes the total

reflective behavior of a material, albedo is particularly relevant for evaluating surface–atmosphere energy exchanges under outdoor conditions. In other words, both albedo and solar reflectance are defined over the shortwave solar spectrum, but they differ in how reflected radiation is treated. Albedo represents the diffuse hemispherical reflectance of a surface under solar illumination and is therefore particularly relevant for evaluating surface–atmosphere energy exchanges in outdoor conditions. Solar reflectance represents the total reflected fraction of incident solar radiation, including both diffuse and specular components, and may be measured as a broadband value or as a spectral function of wavelength using standardized methods such as ASTM E903 or ASTM C1549.

Solar absorptivity is another property that quantifies the ability of a material to absorb solar radiation, and it represents the retained portion. Together, these properties dictate the energy balance at the pavement surface (Brennan et al., 2014). New asphalt pavements typically have a very low albedo, around 0.05, reflecting only 5% of incoming solar radiation while absorbing the remaining 95%. Consequently, the surface temperature of such asphalt can rise up to 30 °C above the surrounding air temperature due to intense heat absorption (Richard et al., 2015).

In addition to albedo and absorptivity, emissivity is a critical factor governing surface radiation and is denoted by ε. Emissivity is a dimensionless property, with values ranging between 0 and 1, that represents the fraction of thermal radiation emitted by a real surface relative to that emitted by an ideal blackbody at the same temperature. It therefore characterizes how efficiently a material emits thermal radiation, rather than the absolute amount of electromagnetic energy emitted (Maria et al., 2013). Pavement surfaces typically have high emissivity (around 0.90–0.95), which enables them to emit heat effectively during nighttime. However, during the day, the rate of incoming solar radiation often exceeds the rate of thermal emission, leading to net heat gain and elevated surface temperatures (Pasetto et al., 2019). As emissivity represents the fraction of thermal radiation emitted by a real surface relative to that emitted by an ideal blackbody at the same temperature, this energy is always equal to or less than the energy emitted by a blackbody. To determine this parameter, the energy radiated per unit area is measured in watts per square meter, based on the Stefan-Boltzmann law (Bergman et al., 2017). Factors such as surface finishing and texture influence emissivity, and heating

can increase the amount of emitted infrared radiation. As a result, infrared energy can be used to estimate a material's surface temperature. Higher emissivity typically corresponds to a lower surface temperature, as illustrated in Figure 1.3 (Marceau and VanGeem, 2007).

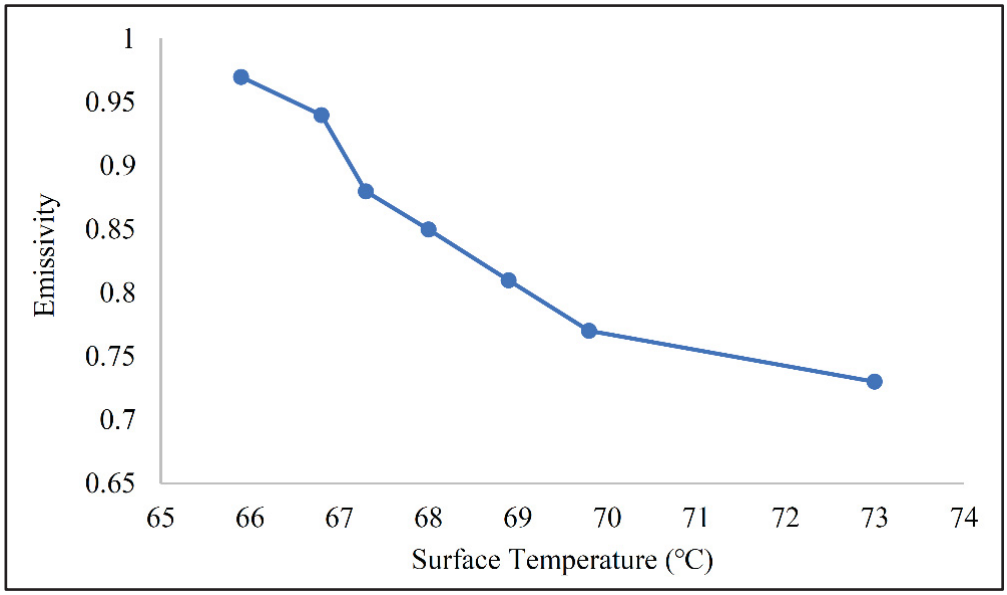

Figure 1.3 The relationship between emissivity and the surface temperature
Adapted from Marceau and VanGeem (2007)

Emissivity can be determined using ASTM C1371 and ASTM E408 standards (ASTM, 2013; ASTM, 2015). To measure emissivity, both thermocouples and infrared cameras are commonly employed. In this process, the specimen is heated to a predefined temperature, and thermocouples record its temperature while accounting for environmental factors such as humidity and ambient air temperature. Simultaneously, an infrared camera captures the surface temperature of the specimen. When the readings from both instruments align, the corresponding emissivity value is determined (Adesanya, 2015; Rakrueangdet et al., 2016).

Another key aspect influencing surface radiation is the spectral response of pavement materials. This refers to how different materials interact with various wavelengths of solar radiation. Dark-colored pavements absorb broadly across the solar spectrum, including visible and near-infrared wavelengths, further intensifying heat accumulation. Lighter-colored or

specially coated pavements, in contrast, are designed to reflect more of the solar spectrum, particularly in the near-infrared range, which is responsible for a large portion of solar heat (Singh and Garg, 2013).

Some environmental conditions, such as solar angles, cloud cover, and urban geometry (e.g., shading from buildings), also affect surface radiation. Urban canyons can trap reflected radiation between surfaces, creating feedback loops that amplify heat retention (Rossi et al., 2016). Thus, mitigating the radiative heat gain through material selection and surface modification is a primary strategy in designing thermally responsive pavement systems.

1.4.2 Thermal Conductivity and Conduction

Thermal conductivity (k) is a fundamental material property that determines how effectively heat is transferred through a substance via conduction. Conduction refers to the internal transfer of thermal energy through the interaction of particles and electron movement; in this process, energetic molecules in the warmer region collide with adjacent molecules, passing on their kinetic and potential energy (Shi et al., 2019). In detail, it governs how efficiently heat moves from warmer regions to cooler ones through microscopic interactions within materials. Essentially, thermal conductivity defines a material's capacity to conduct heat. One of the most widely used methods for calculating this property is Fourier's law in steady-state conditions and one dimension, which can be expressed in Equation 1.2 (Chen et al., 2015).

$$q_x = kA\frac{T_1 - T_2}{L} \tag{1.2}$$

In this equation, q_x (W) is conduction heat transfer rate which represents the amount of heat conducted per unit time in the x-direction, k ($W.m^{-1}.K^{-1}$) represents the thermal conductivity measured in $W.m^{-1}.K^{-1}$, A (m^2) denotes the surface areas, L (m) is the thickness of the material in meters, while T_1 (K) and T_2 (K) refer to the temperatures at the top and bottom surfaces of the specimen, respectively, measured in Kelvin. A material with low thermal conductivity results in a slower rate of heat transfer, which is why this property is crucial for designing pavements with high thermal resistance. Several factors influence a material's thermal conductivity, including its mineral composition, inherent physical properties, aggregate gradation, moisture levels, and specific gravity (Chen et al., 2017). Standard methods for

determining thermal conductivity include ASTM C177, along with other protocols outlined in prior research (ASTM, 2019; Kuvandykova & Bateman, 2013).

In the context of pavement engineering, thermal conductivity plays a pivotal role in governing the temperature distribution within asphalt and concrete layers. This parameter directly affects the rate at which heat from solar radiation or ambient air is dissipated into the underlying pavement structure, thus influencing both surface temperatures and subsurface thermal behavior (Shamsaei et al., 2022). In pavements, the ability to dissipate heat downward into cooler layers can significantly mitigate surface heating, particularly in urban environments where the accumulation of heat contributes to the UHI effect (Chen et al., 2020). Materials with higher thermal conductivity can reduce the intensity and duration of surface temperature peaks by allowing heat to flow more efficiently from the top layer into deeper, cooler layers. Conversely, pavements with low thermal conductivity trap heat at the surface, intensifying heat accumulation and elevating surface temperatures during the day (Deng et al., 2019; Jiao et al., 2020a; Chen et al., 2020).

The thermal conductivity of asphalt concrete is not uniform and is influenced by various factors, including the type of binder used, the characteristics of aggregates, and the presence of specific additives (Ahmad Nazki et al., 2020). Asphalt binders themselves typically have lower thermal conductivity compared to mineral aggregates. Therefore, the volume ratio between binder and aggregate significantly affects the overall thermal behavior of the composite material. Denser mixes with higher aggregate content tend to exhibit higher thermal conductivity, facilitating better heat transfer (Abdushafi Hassn et al., 2016). Aggregate type and gradation also play a crucial role. For instance, granite and basalt aggregates generally have higher thermal conductivity than limestone or recycled materials. In addition, aggregate shape and surface texture can impact the thermal pathways within the pavement matrix. Well-compacted, angular aggregates promote better contact and reduce voids, enhancing thermal transfer between particles (Ahmad Nazki et al., 2020).

Additives and modifiers are increasingly being introduced into asphalt mixes to alter their thermal properties. For example, the inclusion of metallic fibers, conductive fillers (e.g.,

graphite, carbon black), or phase-change materials (PCMs) can significantly improve heat conduction or thermal regulation properties (Vo et al., 2017; Vo and Park, 2017; Shamberger and Bruno, 2020). These innovations aim to create pavement materials that are not only structurally suitable but also capable of managing thermal loads more efficiently, which is particularly relevant in the design of cool or thermally responsive pavements (Si et al., 2020). Therefore, optimizing thermal conductivity in pavement design requires a careful balance between material selection, environmental context, and functional requirements. By selecting materials with appropriate thermal behavior, engineers can contribute to reduced surface temperatures, prolonged pavement life, and mitigate the UHI effects.

1.4.3 Convection

Convection refers to the transfer of thermal energy between a surface and a moving fluid, in the case of pavements, between the pavement surface and the surrounding air. Convection occurs due to the movement of fluids, transferring heat from one area to another. This mechanism is typical in gases and liquids and can also occur in porous solids containing air (Petkova-Slipets and Zlateva, 2018). While this mode of heat transfer is inherently dynamic and influenced by environmental conditions, its contribution to the total heat exchange in pavement structures is generally less significant than conduction or radiation. Nonetheless, convection becomes important when assessing the cooling capacity of surface-air interactions, especially under varying wind conditions (Aletba et al., 2021). According to Newton's law of cooling, the convective heat transfer coefficient is influenced by several factors, including the characteristics of the fluid, surface roughness, geometry, and airflow conditions (Nellis and Klein, 2009). When wind speed and air movement are minimal, the convective heat transfer coefficient (h) is reduced, limiting convective heat removal from the pavement; as a result, the pavement surface temperature can rise under solar loading, potentially increasing the pavement–air temperature difference (Ting, 2012). A practical illustration of this is found in permeable pavements, which feature greater surface roughness and higher air void content than traditional pavements. These properties promote airflow within the pavement structure, leading to a reduction in surface temperature (Li, 2012). The convective heat transfer rate can be calculated based on Newton's Law of Cooling, in one-directional and steady state conditions, as shown in Equation 1.3 (Bergman et al., 2017).

$$q_{con} = h_c A(T_S - T_\infty) \tag{1.3}$$

Where q_{con} (W) is convective heat transfer rate, which the amount of heat transferred per unit time from the surface to the fluid (or vice versa), T_S denotes the surface temperature (K), T_∞ indicates the fluid temperature (K), A is the surface area, and h_c refers to as the convective heat transfer coefficient ($W.m^{-2}.K^{-1}$). Regarding asphalt pavements, typical values for h_c are 5 $W.m^{-2}.K^{-1}$ for low wind, 12 $W.m^{-2}.K^{-1}$ for moderate wind, and 30 $W.m^{-2}.K^{-1}$ for high wind conditions (Aletba et al., 2021). These values demonstrate that under compact urban zones and poorly ventilated street canyons, the convective cooling effect is minimal, which contributes to greater retention of heat at the pavement surface. Thus, in field scenarios, forced convection can play a more notable role. Vehicle-induced airflow over the pavement, particularly on highways and arterial roads, can increase convective heat loss. Similarly, natural convection may be enhanced in open suburban areas where vegetation and building density allow better airflow (Rossi et al., 2016).

Laboratory simulations often aim to isolate thermal properties by controlling or eliminating convective effects. In lamp tests (which simulate solar radiation) or infrared thermography setups, specimens are often placed in enclosures or controlled environments to minimize heat loss through convection. For instance, some studies use wind tunnels or enclosed test chambers to standardize the effect of air movement during thermal testing, which was also used in this thesis (Rakrueangdet et al., 2016; Pirouzfam and Sendur, 2021). The heat transfer modes in asphalt pavements are shown in Figure 1.4.

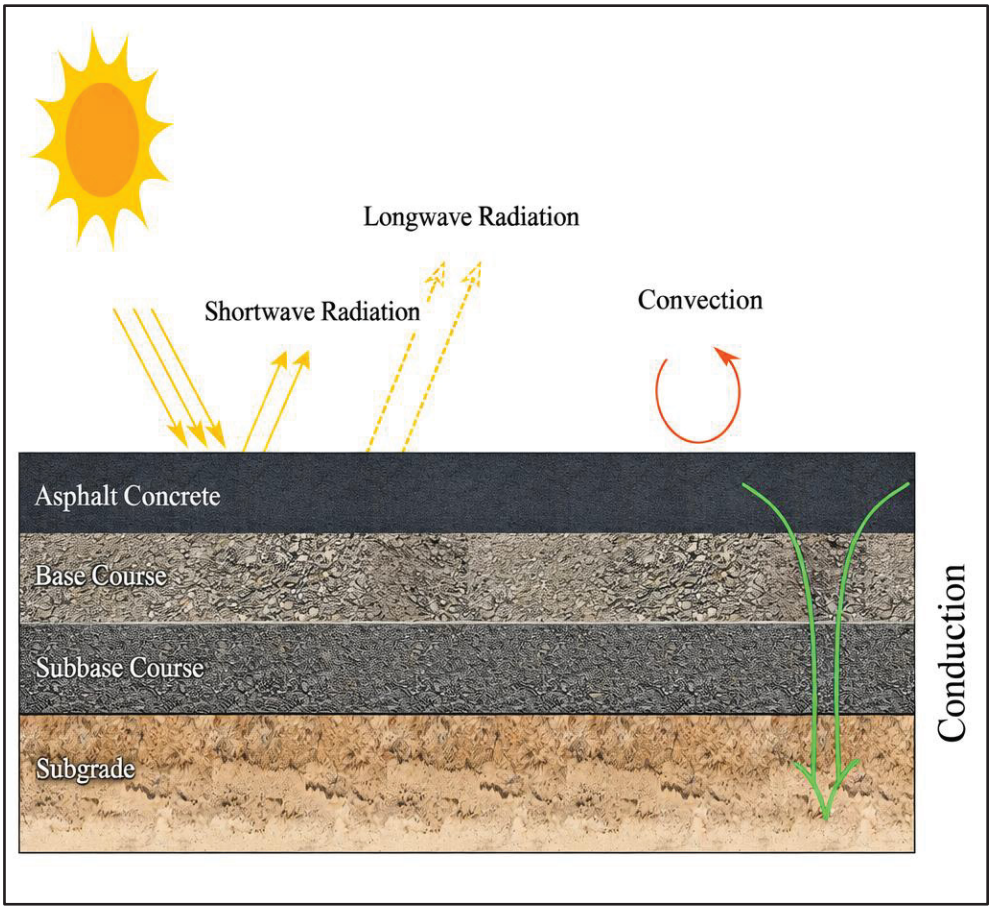

Figure 1.4 Different heat transfer modes in asphalt pavements
Taken from Shamsaei et al. (2022)

In summary, although convection typically contributes less to heat transfer in pavements than radiation or conduction, it must be considered in comprehensive energy balance models and experimental protocols. Neglecting convective effects can lead to overestimation of a surface's thermal retention in both laboratory and simulation-based analyses.

1.4.4 Volumetric Heat Capacity and Thermal Diffusivity

In the thermal analysis of pavement materials, volumetric heat capacity and thermal diffusivity are fundamental parameters for understanding how heat is stored and transmitted through pavement structures. These properties significantly influence the pavement's thermal response to daily and seasonal temperature fluctuations and therefore affect surface temperature regulation and potential distresses such as rutting and thermal cracking (Yinfei et al., 2018).

Volumetric heat capacity, C_{vol} (J.m^{-3}.K^{-1}) quantifies the ability of a material to store thermal energy per unit volume per degree of temperature change, which refers to the quantity of energy required to increase the temperature of one unit of a material by one degree. It is calculated based on density, ρ, (kg.m^{-3}), and specific heat capacity at constant pressure, C_s, (J.kg^{-1}.K^{-1}), depicted in Equation 1.4 (Mirzanamadi et al., 2018).

$$C_{vol} = \rho . C_s \tag{1.4}$$

C_s is the specific heat capacity at constant pressure, defined as the amount of heat needed to increase the temperature of a unit mass of a material by 1 degree. This rise in C_S means that more heat energy is required to raise the material's temperature (Gui et al., 2007). Therefore, using materials with a higher specific heat capacity in pavement structures requires more thermal energy to raise their surface temperature. Regarding asphalt pavements, volumetric heat capacity can be calculated using Equation 1.5 (Mirzanamadi et al., 2018).

$$C_{vol} = \frac{(C_S.\rho.V)_{aggregate}+(C_S.\rho.V)_{bitumen}+(C_S.\rho.V)_{moisture}+(C_S.\rho.V)_{air}}{V_t} \tag{1.5}$$

In this equation, V is the volume of the individual component (m³), while V_t refers to the total volume of the asphalt concrete (m³). The moisture content may exist in both liquid and frozen states. Specific heat capacity is typically measured using the differential scanning calorimetry (DSC) method, following the guidelines set by ASTM C351. The parameters involved in calculating C_p are outlined in Equation 1.6 (Roesler and Sen, 2016; Geng and Heitzman, 2019).

$$Q = C_s m\, \Delta T \tag{1.6}$$

In this equation, Q denotes the total energy transferred in joules (J), C_s stands for the specific heat capacity of the object (J.kg^{-1}.K^{-1}), m represents the object's mass in kilograms (kg), and ΔT refers to the change in temperature in Kelvin (K).

Thermal diffusivity reflects the rate at which heat moves through a material. Materials with high thermal diffusivity tend to experience a rapid increase in internal temperature. Conversely, selecting a material with low thermal diffusivity leads to reduced thermal

conductivity while increasing its heat storage capacity. This is a derived property that combines thermal conductivity, density, and specific heat, and can be determined by Equation 1.7.

$$\alpha = \frac{k}{C_s.\rho} \tag{1.7}$$

In this equation, α represents thermal diffusivity ($m^2.s^{-1}$), k stands for thermal conductivity ($W.m^{-1}.K^{-1}$), ρ is the material's density ($kg.m^{-3}$), and C_s denotes the specific heat capacity ($J.kg^{-1}.K^{-1}$). Thermal diffusivity measures how quickly a material can respond to temperature changes by conducting heat relative to its ability to store it. Materials with low thermal diffusivity heat up and cool down slowly, providing thermal stability, which is desirable in pavements subjected to cyclic thermal loads (Mirzanamadi et al., 2018).

Pavement materials vary widely in these properties. For instance, asphalt concrete generally has a higher volumetric heat capacity than Portland cement concrete due to its denser composition and lower thermal conductivity. Aggregates, air void content, and moisture levels also affect both properties. Fine-grained materials with high moisture retention typically exhibit higher heat capacity and lower diffusivity, without causing sharp changes in surface temperature variations (Shamsaei et al., 2022).

Various test methods are employed to measure these properties in previous studies. For example, Transient Line Source (TLS) and Modified Transient Plane Source (MTPS) methods are commonly used in laboratory settings. TLS measures the temperature response to a linear heat source embedded in the material, whereas MTPS uses a flat sensor to evaluate the response over a defined surface. Both methods provide accurate, repeatable measurements, although they differ in sensitivity to surface condition and contact resistance (Shamsaei et al., 2024a, 2025). Understanding the interplay between volumetric heat capacity and thermal diffusivity is vital for developing and selecting pavement materials that are suitable for mitigating urban heat islands. By choosing materials with optimized thermal response characteristics, engineers can design pavement structures that not only perform well under mechanical loads but also contribute to urban thermal comfort.

All the aforementioned parameters significantly influence heat transfer in asphalt pavements. However, previous studies have shown that two factors, in particular, have a more pronounced

impact on the absorption and transfer of solar energy. The first is the albedo of the pavement surface, which determines the proportion of solar radiation reflected versus absorbed (Li et al., 2013). A higher albedo leads to less heat absorption, making it a crucial element in reducing surface temperatures. The second is thermal conductivity, which dictates how efficiently the absorbed heat is transmitted through the asphalt layers (Vo et al., 2017). Due to their strong influence on pavement thermal performance, these two parameters have been the primary focus of many studies in the field.

1.5 Influence of Pavement Materials on Pavement Thermal Behavior

The thermal behavior of asphalt pavements is not only formed by external conditions such as solar radiation or ambient temperature. In fact, their thermal behavior is deeply influenced by the materials' properties used and the structural design of pavement systems (J. Zhang et al., 2019). Different pavement components, including surface coatings, asphalt binders, aggregates, and even base layers, play an important role in determining how heat is absorbed, stored, and dissipated. These factors collectively affect surface temperature dynamics, energy efficiency, and the magnitude of the UHI effects (ShengYue et al., 2014; Tong et al., 2020). The selection of materials, including their physical characteristics such as color, texture, density, and thermal capacity, alongside structural features like layer thickness, compaction, and air void content, can substantially change the pavement’s thermal behavior (Stempihar et al., 2012; Chu et al., 2020). This section affects how these variables influence heat transfer and thermal performance in both conventional and sustainable pavement systems.

1.5.1 Physical Properties of Materials

The physical properties of pavement materials critically influence how they interact with solar radiation and manage the absorbed thermal energy. Among these properties, surface color and texture, thermal properties, and density are particularly important in controlling surface temperature and heat flow within the pavement structure (Mohajerani et al., 2017a; Yinfei et al., 2014).

Surface color significantly affects a material's albedo. Dark-colored materials, such as traditional asphalt, tend to absorb more solar radiation due to their low albedo values (around 0.05–0.15), leading to higher surface temperatures (Pomerantz et al., 2003; Shi, 2014). In contrast, light-colored materials reflect more sunlight and remain cooler under the same conditions, thus offering a practical mitigation strategy against the UHI effect (Shamsaei et al., 2024a). In addition to surface color, surface texture can also impact the interaction of pavements with both radiation and convective air currents. Rougher surfaces tend to disrupt laminar airflow, which may improve convective cooling to some extent (Nellis and Klein, 2009; Ting, 2012). This airflow decreases the pavement's temperature (Li, 2012). Moreover, surface roughness can affect the reflectivity of the material by changing the angle of incoming solar radiation, resulting in the effective albedo (Li et al., 2013).

All in all, these physical characteristics not only affect the immediate thermal response of pavements but also contribute to their long-term performance, durability, and contribution to urban microclimates. Understanding and optimizing these properties are essential for designing pavement systems that minimize heat storage and mitigate the UHI impacts.

1.5.2 Standard Flexible Pavement Materials and Structures

Conventional flexible pavements are composed of several layers, each of which plays an important part in mechanical performance and structural integrity. These include the seal coat, asphalt concrete surface layer, tack coat, binder course, prime coat, granular base and sub-base layers, and the subgrade (Huang, 2004). Different layers of flexible pavement with their thicknesses are shown in Figure 1.5. Some of these layers might be omitted due to the project's economy and necessity.

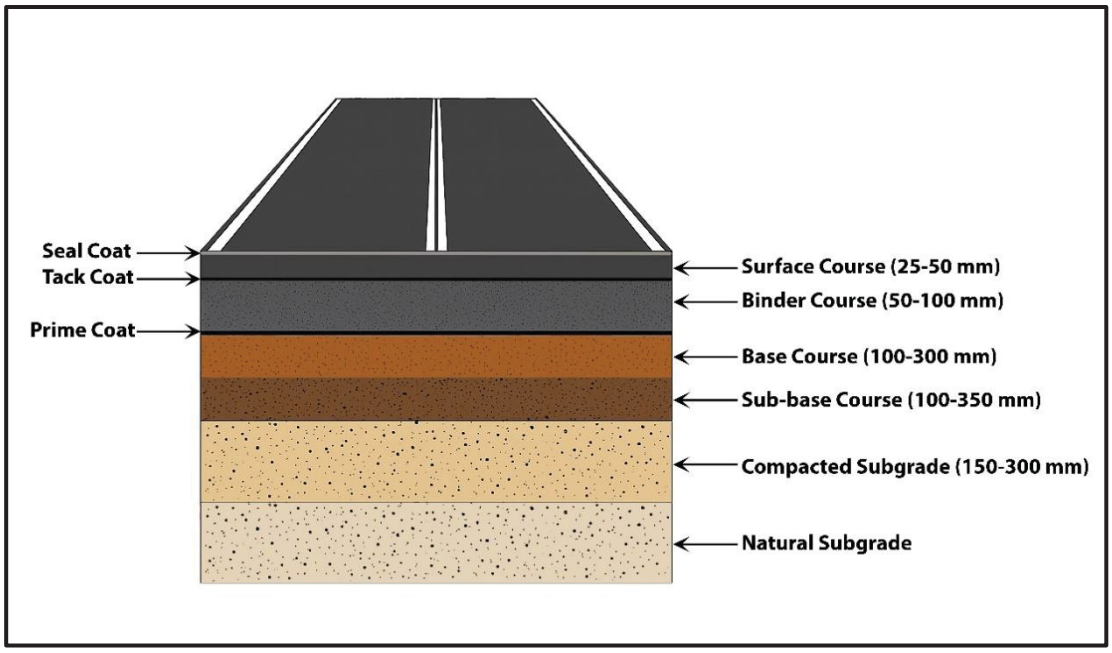

Figure 1.5 The cross-section of flexible pavements

The seal coat, which is a thin asphalt layer, is the uppermost protective layer applied over the asphalt concrete, extending pavement life by preventing water infiltration, sealing minor cracks, and improving surface friction of polished aggregates. This layer may or may not be covered with aggregate (Huang, 2004). However, its dark color and low albedo contribute to additional solar heat absorption, making it a critical factor in surface temperature increase. The implementation of this layer is not common, though.

The surface course is placed at the top of the asphalt pavement. It is usually made of hot mix asphalt (HMA). This layer should be tough enough to resist traffic loads, and it should have a skid-resistant and smooth surface to provide a suitable riding quality (Asphalt Institute, 2007). Moreover, it should be waterproof to avoid the weakening of the pavement system due to water penetration (Huang, 2004). Although this layer is designed for load distribution and surface durability, its low albedo and high thermal conductivity make it a major contributor to surface heat retention and the UHI effects.

The binder course is situated under the surface layer. The first reason for using this layer is that the asphalt concrete has a considerable thickness and may not be compacted well when it is

one layer (Asphalt Institute, 2007). The second reason is that this course can have larger aggregates and less asphalt binder. Besides, the quality of aggregates can be lower than the surface course. Therefore, using this layer can be economical (Huang, 2004). The tack coat is an asphalt binder to increase the adhesion between the surface and binder layers. This layer should be thin and cover the whole surface. The prime coat is an asphalt binder with lower viscosity that binds the asphalt layer to the base course. The difference between this layer and the tack coat is that this layer should penetrate the base layer to reduce the air void and increase its resistance to water penetration. However, the tack coat does not penetrate its underlying course (Huang, 2004). Prime coat may be omitted to reduce the construction costs. However, it can play an important role in surface temperature reduction and alleviating the UHI effects by transferring the accumulated heat in the surface layer to the base and subbase courses.

The base layer is placed under the surface or binder layers, and it consists of crushed slag, crushed stone, gravel, and other stabilized or untreated materials (Asphalt Institute, 2007). The layer beneath the base layer is named the subbase layer. The reason why two different layers are used is their economic benefits. Instead of performing a base course with higher-quality aggregates, cheaper and local materials can be used for the subbase layer (Huang, 2004).

Finally, the subgrade is the natural soil beneath all pavement layers. The top of this layer, usually 152 mm in depth, is scarified, and it is then compacted to reach a suitable density. Regarding its materials, selected materials and or local soil can be utilized for this course (Holtz et al., 2011). This layer plays a critical role in overall thermal storage and dissipation. The moisture content, compaction level, and mineral composition of the subgrade can significantly impact the upward or downward flow of heat within the pavement system (Mammeri et al., 2023b). Although pavement subgrades in Québec are typically deep, the present study focuses on thermal processes occurring within the surface and base layers, which primarily govern short-term (diurnal) heat storage and release relevant to urban heat island effects. Heat penetration to the subgrade is limited over daily cycles; therefore, deeper subgrade layers were not explicitly modeled in this study.

The thermal limitations of conventional pavement materials, particularly their low albedo and insufficient dissipation capabilities, present significant challenges in designing thermally

efficient roadways in urban areas. While most of these layers are essential for the mechanical strength of flexible pavements, their collective thermal behavior causes challenges for mitigating surface temperature rise in urban environments. Traditional materials in these layers are not optimized for thermal performance, as conventional pavement design prioritizes structural capacity over thermal behavior, emphasizing the need for new material strategies to reduce heat storage and enhance urban thermal comfort.

1.5.3 Recycled and Sustainable Pavement Materials

Regarding growing environmental concerns and the need for sustainable infrastructure, the use of recycled and alternative materials in pavement engineering has gained significant attention in recent years. These materials can reduce the demand for virgin resources and provide opportunities to enhance the thermal performance of pavement systems, potentially mitigating urban heat island effects (Aghayan et al., 2021; Mammeri et al., 2023a, 2023b).

1.5.3.1 Construction and Demolition Waste (CDW)

Due to ongoing global urbanization, the volume of construction and demolition waste (CDW) has been increasing (Duan et al., 2019). This type of waste includes metals, glass, plastic, wood, asphalt shingles, and mineral-based debris like concrete, bricks, and tiles, resulting from construction and demolition activities (Menegaki and Damigos, 2018). The United States, the European Union, and China have been ranked among the major contributors to CDW generation (Kabirifar et al., 2020). In detail, the United States, European Union, and China produced approximately 600, 372, and 1,704 million tonnes (Mt) of CDW in 2018, respectively (Zhang et al., 2022). In Canada, CDW is also a significant issue, accounting for almost 27% of the municipal solid waste, kept in landfills (Yeheyis et al., 2013). Globally, it is estimated that around 10 billion tonnes of CDW are generated each year, highlighting the urgent need for effective management solutions (Molla et al., 2021). While the United States, European Union, and Canada report relatively high overall recovery rates for construction and demolition waste (CDW), China's recovery rate remains below 10% (Huang et al., 2018). Nevertheless, the recycling rates specifically for mineral-based construction waste, such as concrete and bricks, are still very low in the US, EU, and Canada, due to challenges related to material

contamination, separation complexity, variable quality, and limited end-use applications. These materials make up the largest portion of CDW from building construction, accounting for approximately 59%, which are discharged in landfills (Ulubeyli et al., 2017; Umar et al., 2017; Menegaki and Damigos, 2018).

Waste glass also has a high generation rate from the construction and food industries. According to environmental assessments in 2013, the United States produced approximately 10.37 million tons of waste glass from food and beverage containers, and only 27% was recycled, while around 7.59 million tons ended up in landfills (Epa, 2015). In the same year, in the European Union countries, roughly 15.9 million tons of waste glass from packaging and 1.5 million tons from construction and demolition activities were generated (Hestin et al., 2016; Mohajerani et al., 2017b). Additionally, global glass waste production in 2007 was estimated at 130 million tons per year (IEA, 2007). Although glass has a high potential for recovery, strict remanufacturing requirements limit the portion that can be reused. Initially, the collected waste glass must be sorted by color. However, sorting becomes difficult if the glass is broken, mixed during collection, or contains impurities or composite materials (Kadirgamar, 2014). Furthermore, different chemical compositions among different types of glass can result in incompatible melting points, making mixed glass unsuitable for reuse. In fact, just 5 grams of non-recyclable glass can contaminate an entire ton of recyclable glass (Afshinnia and Rangaraju, 2015).

In addition to contributing to environmental pollution, the rising accumulation of CDW has caused serious global safety concerns. For example, in Shenzhen, China, approximately 10 million tons of CDW had piled up in a landfill that collapsed in 2015, triggering a landslide that destroyed several buildings and resulted in 73 fatalities (Yang et al., 2016). A similar incident occurred in Chennai, India, in the same year, where excessive CDW buildup contributed to severe flooding, damaging infrastructure, and financially impacting over 400 families (Narasimhan et al., 2016). Furthermore, landfill collapses in Sri Lanka and Ethiopia in 2017 led to 30 and 115 deaths, respectively (Duan et al., 2017). These tragedies highlight that inadequate CDW recycling rates not only harm the environment but also pose significant threats to human life.

According to previous studies, approximately 50% of CDW has the potential to be recycled using different methods, depending on the type of CDW materials (Ulubeyli et al., 2017). For example, recycling most building materials using common current methods can lead to significant emissions of greenhouse gases such as methane, nitrous oxide (N_2O), carbon dioxide (CO_2), and fluorinated gases, contributing to air pollution (Teh et al., 2017). Hence, using alternative methods, such as reusing some CDW, such as concrete, clay bricks, and tiles, in the construction sector for different purposes, such as noise buffer walls, the base of sports grounds, landscape construction, and pavements, can be a more sustainable solution. This approach not only supports the efficient recycling of CDW but also decreases the reliance on nonrenewable raw materials in construction projects (Fatemi and Imaninasab, 2016). For example, Contreras Llanes et al. (2022) used waste materials such as clay, ceramic, and mortar as aggregates in concrete paving. Test results showed that these additions increased water absorption and higher apparent porosity in the concrete, reducing both its splitting tensile and compressive strengths. However, replacing aggregates with these materials at rates up to 50% still met the minimum strength requirements for concrete paving applications.

Considering the environmental benefits of using CDW materials as construction materials, these materials have also been used to develop new asphalt mixes. For instance, Pasandín and Pérez (2013) investigated the effects of substituting up to 30% recycled concrete as aggregates in HMA mixtures. The mechanical properties were examined, including stiffness, moisture sensitivity, fatigue life, and permanent deformation. Results indicated that increasing CDW content improved stiffness, resistance to rutting, and moisture susceptibility. However, it also negatively reduced the fatigue life of HMA. Besides, recycled concrete powder has also been utilized as a filler in cold mix asphalt (CMA). Findings indicated that incorporating 1–3% of concrete powder by the total weight of the mixture enhanced the CMA's performance by increasing fatigue life, tensile strength, rutting resistance, stability, and resistance to moisture and abrasion (Deb and Singh, 2022). Furthermore, Mammeri et al. (2023) replaced 100% of the virgin aggregates in HMA with recycled glass to explore its potential in reducing the UHI effects. Thermal tests revealed that this substitution raised surface temperatures during the day, potentially increasing the risk of rutting, but helped reduce surface temperatures at night.

Compared to the control mix, the glass-based HMA absorbed and released 34% and 47% less heat, respectively (Mammeri et al., 2023b). Javani et al. (2019) added waste glass and polypropylene fibers to asphalt pavement. Their mechanical testing showed that adding glass up to 5% by weight enhanced the Marshall stability of the asphalt by approximately 12%. In addition to HMA, Lu et al. (2019) replaced fine aggregates with waste glass up to 50% in pervious concrete. While this substitution decreased the compressive strength, it significantly improved water permeability, attributed to the smooth texture and low water absorption of the glass aggregates.

The application of CDW materials extends beyond the surface layer of pavements, and it is also used in unbound layers such as the base and subbase. Arisha et al. (2018) utilized up to 100% CDW, comprising recycled clay masonry and concrete aggregates, as base and subbase materials. Repeated load triaxial and static triaxial shear tests showed that increasing the proportion of clay masonry reduced both the initial matric suction and resilient modulus compared to mixtures with higher concrete content. Besides, the predictive model indicated that pavements constructed with these CDW materials demonstrated improved resistance to fatigue cracking and rutting. Additionally, Zhang et al. (2021) used CDW aggregates (100% by weight) in the subgrade layer of pavement systems. Their performance under freeze-thaw cycles was evaluated, revealing that increasing matric suction results in higher dynamic resilient modulus and compaction levels. Conversely, freeze-thaw cycles reduced both the matric suction and dynamic resilient modulus. In another research, Xiao et al. (2020) employed natural aggregates in the base course that were replaced with waste glass, and the mixture was stabilized using a waste glass powder-based geopolymer cement. Findings indicated that incorporating more than 10% waste glass aggregates significantly reduced the California Bearing Ratio (CBR). However, the addition of the stabilizing agent improved the mechanical strength of the base course, allowing for a higher percentage of glass content by weight. In another research, Yaghoubi et al. (2021) used fine-sized waste glass in subgrade soil at proportions of 10%, 20%, and 30% by weight. Both experimental tests and numerical simulations showed that incorporating 30% waste glass increased the resilient modulus by 113%. Despite this improvement, the addition of glass reduced both tensile and compressive

strains. Consequently, this strain reduction could enhance the pavement's resistance to rutting and extend its fatigue life.

In conclusion, CDW materials account for a large amount of solid waste globally. Reusing CDW in pavement structures can support circular economy principles, reduce landfill loads, and conserve natural aggregates. CDW typically includes concrete, bricks, tiles, glass, and asphalt debris, which can be crushed for use in the surface layer or beneath layers of pavements. Regarding the thermal properties of CDW materials, they are different depending on their source and composition. Despite the potential benefits of incorporating CDW in pavement materials, several challenges remain. These include variability in material composition, contamination with deleterious substances, inconsistent mechanical properties, and reduced fatigue performance at higher replacement levels. In addition, processing requirements, quality control, and limited standardization can restrict large-scale implementation. As a result, the use of CDW in pavement applications requires careful material selection, performance evaluation, and adherence to agency specifications to ensure long-term durability and reliability. However, due to the lighter colors of some of these materials, they can be used for surface treatments of pavement to increase the reflectivity and mitigate the UHI effects.

1.5.3.2 Steel Slag

Various strategies have been explored by researchers to propose new ways for recycling some conductive by-products and mitigating the UHI effects associated with asphalt pavements. This can be either due to the environmental benefits of recycling industrial waste materials or mitigating the UHI effects. As some of these materials can transfer the absorbed heat into the base course and subgrade, which can reduce the surface temperature of pavements. Steel slag is one of these conductive materials that has been used as a pavement material for different purposes. For example, Jiao et al. (2020b) employed steel slag aggregates as a substitute for up to 60% of the asphalt mixture volume, which resulted in an 8.23% rise in thermal conductivity. However, exceeding this amount caused a decline in conductivity, attributed to the increased porosity of the steel slag. Additionally, another study, Cao et al. (2022) reported that while steel slag used as aggregate in asphalt mixtures contains active minerals like iron

oxides, which can enhance thermal conductivity, the presence of micropores on the aggregate surfaces tends to reduce it, depending on the steel slag aggregate size. The highest growth in thermal conductivity, recorded at 4.78%, was observed for mixtures containing 60% of steel slag aggregates (3-5mm).

Apart from the thermal benefit of steel slag aggregates in HMA, this industrial by-product has also been utilized as aggregate in base courses and subgrade layers in several studies. Yildirim and Prezzi (2017) have shown that using steel slag in subgrade mixtures can improve bearing capacity, resulting in reduced uneven settlement. It also helps prevent soil swelling and grouting. Moreover, utilizing steel slag also increased the resilient modulus, water permeability, and drainage capabilities of subgrade soils (Zaika and Djakfar, 2016). In another study, Behiry (2013) utilized up to 90% steel slag aggregates in subbase and base courses. The experiments on resilient modulus and CBR indicated that 70% steel slag had the highest strength, while increasing it to 90% further improved resistance to vertical deformation. Furthermore, this material was used up to 75% of conventional aggregates in the base course, and the mixture was stabilized using 19% fly ash and 6% lime to form layers with 150 mm and 250 mm thicknesses. The results revealed that the stiffness of the base course was improved. Additionally, data from falling weight deflectometer (FWD) tests showed reduced peak deflections and an extended service life (Pai et al., 2021).

Therefore, the global application of steel slag as an aggregate in pavement surface, base, and subbase layers is growing. In particular, the United States, Japan, and Europe utilized around 41%, 32%, and 70% of this industrial by-product, respectively, in road construction (Nippon Slag Association, 2016; Liu et al., 2022) However, the impact of steel slag on the thermal conductivity of base layers, the interface of layers, and its role in alleviating UHI effects has been neglected.

1.5.3.3 Environmental Considerations and Life Cycle Assessment

There has been a global emphasis on sustainable infrastructures, indicating the importance of evaluating environmental impacts associated with recycled pavement materials, which can be done through life cycle assessment (LCA). LCA provides a comprehensive framework for assessing the energy consumption, greenhouse gas (GHG) emissions, and ecological footprint

of materials from extraction to disposal or reuse (Aghayan et al., 2021). Regarding the recycled materials used in this thesis, the application of CDW and steel slag into pavement structures represents a more environmentally friendly approach for recycling these materials as well as reducing the demand for raw materials. As the LCA is not part of the scope of this study, the general environmental benefits are presented briefly in this section.

Regarding recycled materials used in this research, including recycled concrete, clay bricks, glass, and steel slag materials, are generated in large quantities due to ongoing urbanization and infrastructure renewal. The improper disposal of them not only contributes to environmental degradation and landfill overuse but also creates potential hazards, such as slope instability and flooding (Narasimhan et al., 2016; Yang et al., 2016). Therefore, reusing these materials as pavement materials offers significant environmental benefits. The first benefit is a reduction in natural resource depletion. Utilizing these materials as aggregates in pavement layers decreases the demand for virgin aggregates, reducing quarrying activities and preserving natural resources (Chiu et al., 2008). Another merit is the reduction of accumulated waste in landfills. In fact, by using these materials in pavement surface and base layers, the volume of waste stored in landfills is significantly reduced. This alleviates pressure on municipal waste management systems (Medina et al., 2023). Moreover, studies have shown that the application of CDW in pavement construction can lead to considerable reductions in carbon emissions, especially when local recycled materials are used, minimizing transportation emissions (Zhao et al., 2021). Decreasing energy consumption is also attributed to reusing these materials in pavements. Recycling processes, especially mechanical crushing and sorting, typically consume less energy than the extraction and processing of raw materials, contributing to overall energy savings (Zhang et al., 2020).

In addition to recycling CDW materials in pavements, reusing steel slag decreases the burden on industrial waste disposal and mitigates the negative environmental impacts of slag landfilling, such as the leaching of heavy metals (Georgiou and Loizos, 2021). This material has high reusing potential. For example, in countries like the United States, Japan, and across Europe, significant proportions of steel slag are already used in road construction, revealing its feasibility as a sustainable pavement material (Nippon Slag Association, 2016; Liu et al.,

2022). While the production of steel consumes high energy, using steel slag as aggregates avoids the environmental cost of producing virgin aggregates. This can compensate for part of the generated carbon footprint associated with steel production (Hassan et al., 2024). More importantly, due to its high stiffness and load-bearing capacity, steel slag can improve pavement service life, decreasing the required pavement repairs and the consumed energy associated with maintenance cycles (Díaz-Piloneta et al., 2021).

Despite the advantages of reusing CDW and steel slag materials in pavements, some significant points need to be taken into consideration. The environmental performance of CDW materials depends on their type and treatment process. For example, some recycling methods may release pollutants or GHGs, especially when processes demand high temperatures or intensive mechanical treatments (Abedin Khan et al., 2024). Therefore, the selection of low-emission recycling techniques and proper quality control is essential to ensure sustainable outcomes. Similar points must be considered for steel slag aggregates. The environmental acceptability of steel slag depends on its chemical composition, particularly the presence of free lime and magnesia, which may cause volumetric instability or leaching issues if not properly stabilized (Pasetto et al., 2023). Therefore, environmental monitoring and pretreatment are vital when employing steel slag at a large scale in pavements.

To support environmental evaluation, several LCA methodologies and software tools can be utilized to assess the environmental impacts of recycled materials such as CDW and steel slag in pavement applications. First of all, the ISO 14044 standard provides the general principles, techniques, and guidelines for conducting LCA studies (ISO 14044 Standard, 2006). Based on this standard, LCA is a scientific method used to quantitatively evaluate the environmental impacts of a system across all stages of its life, from the extraction of raw materials to its final disposal. The pavement LCA includes some stages, including material production, construction, usage, maintenance, rehabilitation, and the end-of-life phase, depicted in Figure 1.6 (Medina et al., 2023). Although LCA provides a comprehensive framework for assessing impacts across the pavement life cycle, it was not within the scope of this thesis. Accordingly, environmental performance was discussed qualitatively based on findings reported in the literature rather than through a full LCA.

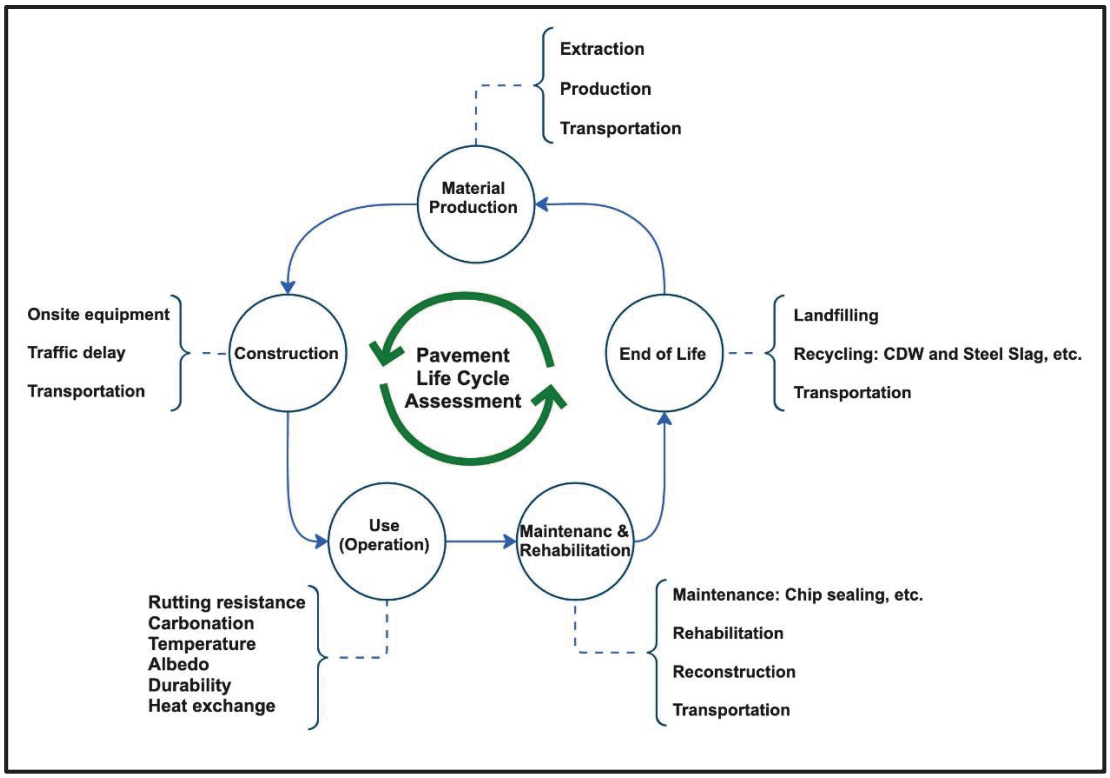

Figure 1.6 Pavement life cycle stages

Three main life cycle assessment (LCA) approaches are used to evaluate recycled solid waste materials, such as construction and demolition waste and steel slag, in pavement construction: cradle-to-gate, which considers processes from raw material extraction to construction; cradle-to-grave, which assesses the full life cycle from extraction through use to end-of-life; and cradle-to-cradle, a closed-loop approach in which materials are recycled back into the production cycle rather than being disposed (Stripple, 2001; Weil et al., 2006; Ding et al., 2016). These LCA types are demonstrated in Figure 1.7. Considering the importance of LCA for the use of recycled materials in this thesis, this assessment is recommended to be done in future relevant studies.

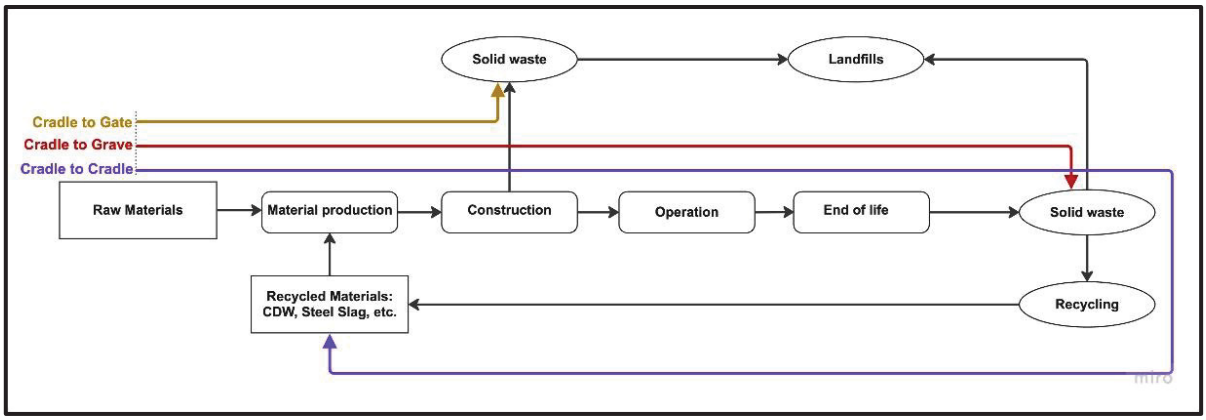

Figure 1.7 Different Pavement LCA methods

1.5.3.4 Chip Seal Development Using CDW Materials

Replacing deteriorated pavements is expensive, and using corrective or preventive maintenance strategies, such as chip sealing, which can be rapidly implemented on existing pavement surfaces, is of great importance (Serigos et al., 2017). Chip sealing involves applying a thin layer of bitumen emulsion, comprising 60–70% asphalt cement, deionized water, and an emulsifying agent, followed by one or more layers of aggregates, which are then compacted using rollers before the setting of the emulsion (You et al., 2019). This method is recognized as one of the most economical bituminous surface treatments, which is suitable for both asphalt and concrete pavements (Montoya et al., 2017).

In recent years, chip seals have attracted researchers' attention, and several studies have been conducted on the use of various aggregate types for chip sealing. For instance, You et al. (2019) examined the performance of chip seals made with trap-rock and granite, using the Vialit test at low temperatures and Michigan Tech's Interface Bond Test (IBT) under both cold and normal conditions. The findings revealed that chip seal durability is negatively affected by freeze–thaw cycles, primarily due to moisture infiltration into the aggregate–binder interface. During freezing, water expansion induces microcracking and weakens adhesion, while repeated freeze–thaw cycles accelerate aggregate loss and surface degradation. This highlights the importance of selecting aggregates with low water absorption and adequate frost resistance for cold climates. In another study, Gheni et al. (2017) used recycled crumb rubber as an aggregate replacement in chip seals. Evaluations using the sand patch method, skid resistance

testing, and image analysis demonstrated that crumb rubber achieved adequate embedment depth and skid resistance, indicating its potential to partially or fully replace natural aggregates in chip seals. Moreover, reclaimed asphalt pavement (RAP) has also been investigated as an alternative chip-sealing aggregate, and the test results showed that RAP aggregates could meet chip-seal mix design standards (Durrani, 2021).

Despite the promising environmental and engineering advantages of using CDW materials in pavement applications, these materials have not been used for chip seal development. More importantly, since chip seals are applied as the top layer of pavements with exposed aggregates, they can enhance pavement reflectivity using light-colored recycled aggregates. Hence, CDW materials can be used as chip seal aggregates to enhance the surface reflectivity and mitigate the UHI effects. Thus, firstly, the mechanical properties, safety, and durability of chip seals developed with CDW materials should be assessed due to the novelty of using these materials as chip seal aggregates. Their impact on albedo and temperature reduction must then be evaluated with experimental methods.

1.5.4 Effect of Air Voids and Interfaces

The thermal behavior of pavement systems is significantly influenced by the void content within each layer and the layers' interfaces. The air void affects the pavement's ability to transfer and dissipate heat, which is critical for UHI mitigation strategies (Abdushafi Hassn et al., 2016).

1.5.4.1 Air Void Content and Thermal Performance

Air voids significantly influence the thermal capacity and conductivity of asphalt pavements. Their content ranges from 4% to 30%, and this variation can impact both the mechanical and thermal behavior of asphalt concrete (Garcia et al., 2015). Therefore, air void content plays a significant part in the pavement's heat transfer. In fact, asphalt concrete surface with high temperatures can release greater amounts of heat into the ambient air through infrared radiation (Wong and Chen, 2008). Air voids of pavement structures, particularly in asphalt and base layers, can disrupt the continuity of thermal conduction. Since air has a much lower thermal conductivity than aggregates and binder, higher air void content generally reduces the overall

thermal conductivity of the pavement. This thermal resistance slows down the transfer of heat from the surface to deeper layers, increasing surface temperature and exacerbating UHI effects (Abdushaffi Hassn et al., 2016).

Asphalt pavements absorb a significant amount of solar energy, and air voids are important in terms of temperature control. If the air voids are filled with water, this energy is used to evaporate the water, reducing the surface temperature (Hendel et al., 2015). Firstly, capillary action moves the water toward the surface for evaporation (Vorhauer et al., 2010). This evaporation process cools the surface rapidly (Garcia et al., 2015). However, once the surface dries out, the evaporation rate declines as water vapor diffusion from the internal voids becomes the limiting factor, allowing solar radiation to raise the surface temperature. Although a few studies have explored the connection between thermal conductivity and water evaporation (Dawson et al., 2012; Zhou et al., 2013), most research has been limited to field observations or basic simulation models (Yavuzturk et al., 2005; Gui et al., 2007; Novo et al., 2013).

Some studies have investigated how air voids influence the thermal properties of asphalt pavement. Stempihar et al. (2012) revealed that asphalt concrete's thermal behavior is affected by multiple factors, among which air void content and its interaction with other variables play a significant role. However, most studies were based on field data without climate control rather than laboratory experiments under controlled conditions. Besides, regarding the controlled laboratory tests, Abdushafi Hassn et al. (2016) examined how air void levels impact asphalt's thermal conductivity in a study. Results showed that as air voids increased, both thermal conductivity and specific heat capacity decreased. More importantly, asphalt concrete samples with higher air void content had higher surface temperatures. This was attributed to the trapped heat accumulating in the asphalt mixture, since it could not dissipate effectively. Besides, the heat flux decreased with greater air voids. Thus, in dry conditions, the high surface temperature can be related to reduced thermal conductivity. Moreover, the emissivity of asphalt concrete also declined with increased air voids (Abdushaffi Hassn et al., 2016).

To observe and compare air void content in asphalt specimens, X-ray computed tomography (CT) can be used. As shown in Figure 1.8, black areas represent air voids. Image (a) has the

lowest void content, while image (e) has the highest. The difference between 5% and 25% air void is visible between these two samples. Increasing the air void content from 5% to 25% caused approximately a 2% reduction in specific heat capacity and a 30% drop in thermal conductivity (Abdushaffi Hassn et al., 2016). Hence, air voids have a much greater effect on thermal conductivity in comparison to specific heat. The air void ratio also affects volumetric heat capacity and thermal diffusivity. Materials with higher air voids tend to have lower volumetric heat capacity, having higher surface temperature fluctuations due to reduced thermal inertia. Consequently, samples with high air void ratios tend to store heat rather than dissipate it, resulting in asphalt concrete with higher surface temperatures. In contrast, dense and well-compacted pavements offer better thermal conduction and slower heat accumulation, providing lower temperatures during peak solar exposure.

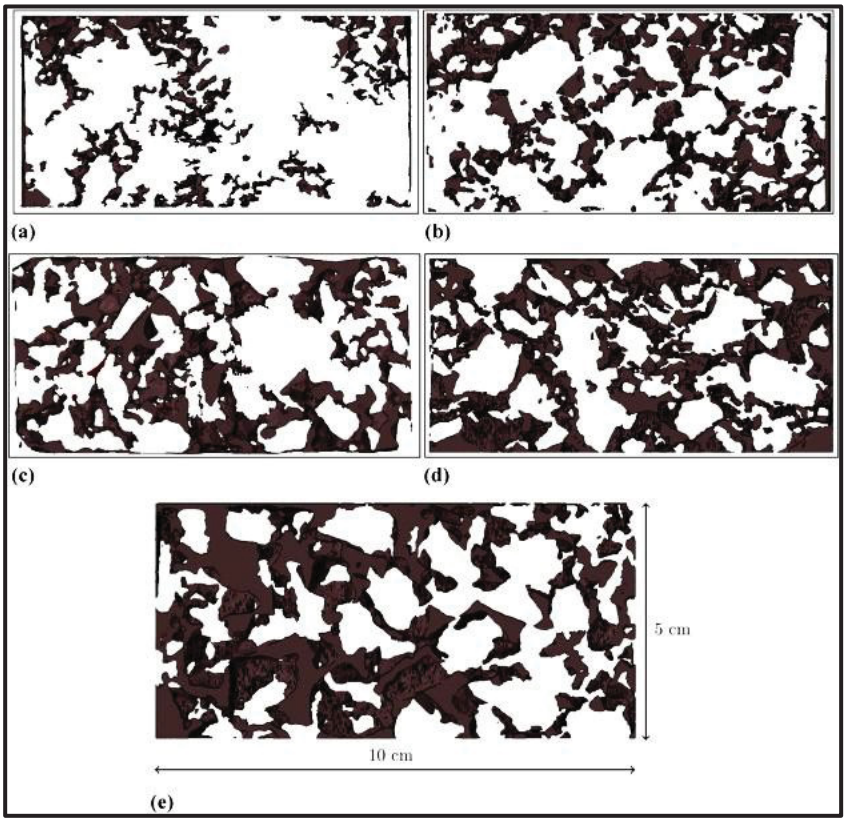

Figure 1.8 X-ray CT scan of specimens containing 5% (a), 13.2% (b), 17.4% (c), 21.5% (d), and 25.3% (d) air voids
Taken from (Abdushaffi Hassn et al., 2016)

Several factors influence the air void content in asphalt mixtures, including aggregate gradation, compaction techniques and intensity, and binder content (Xu et al., 2019). Using dense-graded aggregates reduces air voids because fine particles can fill the gaps more effectively. In contrast, open-graded aggregates typically cause higher air void content, as they lack sufficient fine material to fill the spaces (Fang et al., 2019). However, this type of gradation may require more binder, decreasing the air voids (Zaniewski and Yan, 2014). Both the aggregate gradation and binder amount significantly influence the compaction process. Open-graded mixes are also more susceptible to aggregate breakdown during compaction. Furthermore, the compaction level correlates with the target air void percentage; higher air voids generally mean lower compaction and density (Pouranian and Haddock, 2020). As a result, adjusting the thermal conductivity of asphalt mixtures through air void modification can be achieved by changing the gradation, binder content, and compaction level.

1.5.4.2 Interfaces Between Pavement Layers and Heat Dissipation

Proper bonding between the asphalt mixture layer and base course is of major significance, and low adhesion can cause early pavement failures such as stripping, rutting, or cracking. Most previous studies focused on the mechanical properties of the pavement associated with the interface, such as mechanical interlock and shear resistance, which can lead to pavement deterioration under repeated traffic loads (Le et al., 2020). Based on previous research, a rough surface on the base course is essential to facilitate mechanical interlock and enhance bonding. If the surface is too smooth, it reduces interfacial friction and bond strength. Therefore, a rough surface is recommended before applying the asphalt mixture layer, ensuring proper adhesion between these layers (Freeman et al., 2010). This rough surface can increase the trapped air at the interface, reducing the heat transfer rate from asphalt concrete to the base course. This thermal barrier can trap heat in the asphalt mixture layer, increasing the pavement's contribution to UHI effects. Applying the prime coat at the interface can fill the voids and facilitate the heat transfer between layers. In Figure 1.9, the prime coat impact at the interface is demonstrated.

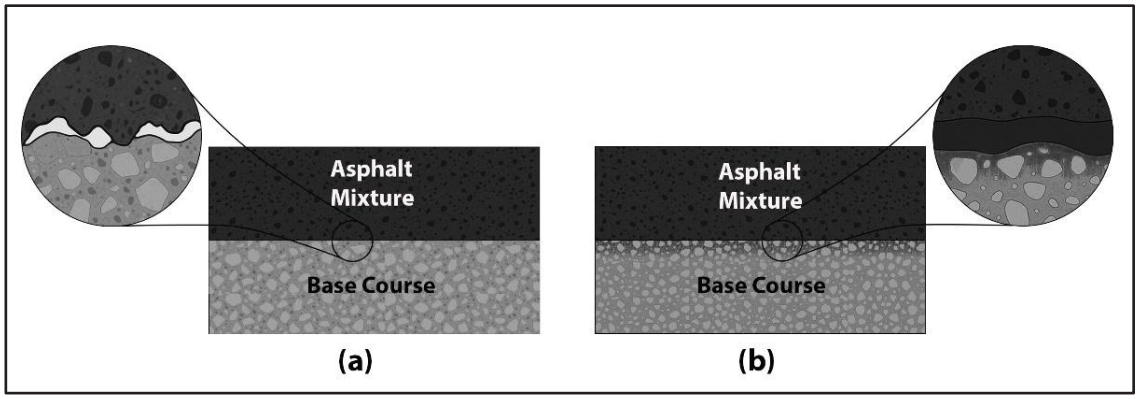

Figure 1.9 The interface of pavement layers before (a) and after (b) applying a prime coat

Regarding the impacts of the prime coat in enhancing the heat transfer rate between pavement layers, investigation on this topic has been neglected. In fact, using conductive materials, such as steel slag, can alter interface properties and improve heat dissipation at the interface. Therefore, understanding the interface behavior is critical for designing thermally optimized pavements. This is especially relevant in urban environments, where controlling surface temperature can have significant impacts on the UHI effects. Hence, this subject will be examined thoroughly in this thesis.

1.6 Existing Common UHI Mitigation Approaches

After recognizing the significant contribution of pavements to the UHI effects, various strategies have been developed to create cooler pavement structures. These developed cool pavements are constructed using special materials and design techniques to decrease pavement surface temperatures compared to conventional pavements. Although many studies focused on UHI mitigation, most approaches fall into three primary categories, including enhancing pavement reflectivity, modifying thermal conductivity using either conductive or insulating materials, and using water potential to drop pavement temperatures (Mohajerani et al., 2017a; Anting et al., 2018; Du et al., 2020). The maximum surface temperature of pavement plays an important role in heat exchange with the surrounding air, and reducing the maximum pavement surface temperature can be achieved by either increasing the albedo or thermal inertia (Qin,

2015). Hence, reflective pavements, evaporative pavements, and thermally modified pavements are the three primary types of pavements designed to mitigate UHI effects.

1.6.1 High-Albedo Pavements

One of the most widely used strategies to enhance the albedo of asphalt pavements is the application of pigments and heat-reflective coatings. High-albedo pavements reflect a larger portion of incoming solar radiation, reducing the amount of absorbed heat. For instance, a commonly used approach to enhance the reflectivity of asphalt pavements is to apply light-colored sealing materials on the surface of pavements (Tran et al., 2009; Akbari and Matthews, 2012). This type of sealed surface is comprised of spreading a thin layer of asphalt binder over existing aged pavement, and fine aggregates are then placed. The resulting reflectivity largely depends on the color of the aggregates used and pavement aging (Pomerantz et al., 2003). Light-colored slurry seals have also been shown to improve pavement albedo (Tran et al., 2009). However, their practicality is limited due to the need for modifying emulsion formulations, bringing about higher construction costs. Alternative methods, such as incorporating light-colored materials in micro-surfacing treatments or applying surface coatings like reflective paints, can similarly enhance pavement surface reflectivity (Tran et al., 2009).

In addition to slurry seals, researchers also applied ten different types of coatings to improve pavement reflectivity. Results indicated that surfaces achieved visible light reflectance levels of up to 60% and near-infrared reflectance as high as 95% (Xie et al., 2019). Similarly, nanocomposite reflective coatings were tested, showing that they could reduce pavement heat radiation and convection by 66% and 50%, respectively, decreasing surface temperatures and improving thermal comfort for pedestrians (Zheng et al., 2019). Moreover, Chen et al. (2022) developed a specialized heat-reflective coating based on epoxy resin emulsion using functional fillers such as titanium oxide, diatomite, silicon dioxide, and fumed silica. It was found that filler content should remain below 30% of the coating's weight, and using 2% iron oxide to produce a light gray coating had optimal cooling performance and visual comfort. When this coating was applied at a rate of 0.8 kg/m², pavement surface temperatures dropped by approximately 10 °C.

While applying such pigments and coatings can effectively drop pavement temperatures and alleviate the urban heat island effect, they may also compromise drivers' visibility and decrease the skid resistance of the pavement surface. These pavements with high reflectivity can sometimes cause some issues for drivers, such as glare due to the reflection of visible light. To mitigate this issue, non-white or light colored pigments were designed that were capable of reflecting near-infrared rather than visible light, improving pavement reflectivity without negative effects on its comfort for drivers (Maria et al., 2013). Although surfaces treated with these pigments appear dark, their albedo values can still range between 0.4 and 0.7 (Nishioka et al., 2006). Additionally, the texture of the pavement surface influences its reflectivity, and smoother surfaces tend to reflect more radiation (Santamouris, 2013b). However, smooth surfaces can compromise skid resistance. To combat this, special sand or ceramic particles were incorporated to enhance surface friction, with tests showing a 50% improvement in skid resistance (Zheng et al., 2015). However, the durability of fillers and particles for increasing the skid resistance of pavements containing these coatings has been questionable

Furthermore, these coatings degrade over time when exposed to natural weathering. To address this issue, anti-aging additives were incorporated into the pigments. Test results indicated that the reflectance variation remained below 10% for white coatings and under 5% for colored coatings (Xie et al., 2020). Various coatings made from materials like inorganic red, organic green, and combinations of organic and inorganic black pigments, all of which offer enhanced reflectivity, are illustrated in Figure 1.10. Some of these pigments have harmful chemical compositions that are not environmentally friendly. More importantly, considering all requirements for pavements coated with these pigments with sufficient skid resistance and durability can increase pavement construction and maintenance costs.

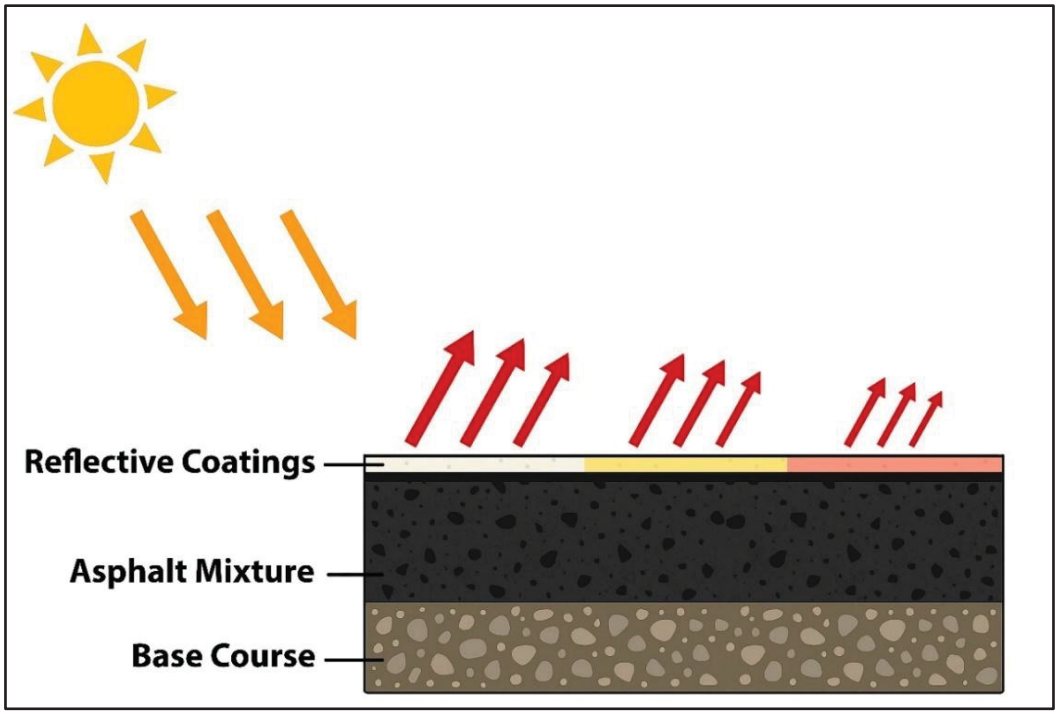

Figure 1.10 Using reflective coating to increase pavement albedo

While reflective pavements have lower surface temperatures during summer, they also reduce surface temperatures in winter, which is not desirable. Ideally, pavements should reflect more sunlight in summer and less in winter. Thermochromic materials offer a solution, as their albedo changes with temperature, with transition ranges between 17°C and 38°C or higher (Ma and Zhu, 2009). In another study, thermochromic materials were added to the asphalt binder, resulting in pavement surfaces that were 6°C cooler in summer and 3°C warmer in winter compared to traditional binders (Hu and Yu, 2013). Although some advances have been made to increase the pavement albedo and reduce the pavement temperature, the durability, cost effectiveness, environmental friendliness, and practicality of these advances are questionable. Hence, novel reflective pavements using recycled materials such as chip seals made of CDW materials can be a practical solution to mitigate the UHI effects.

1.6.2 Water-Based Cooling Pavements

The pavement temperature can be reduced by utilizing water cooling potential, mitigating the UHI effects. Researchers have investigated various types of pavements with this potential,

including evaporative and heat-harvesting pavements. Evaporative pavements are designed to retain water within their structure, enabling temperature reduction through the process of water evaporation. This cooling mechanism can significantly drop surface temperatures in urban environments. These pavements have high air voids, allowing water to infiltrate and be stored within the material. As water evaporates, a substantial portion of the absorbed heat is dissipated, reducing the pavement temperature. However, these pavement systems are most effective in regions where runoff water is readily available. In contrast, applying evaporative pavements in hot, arid areas can have the opposite effect, potentially leading to even higher temperatures compared to traditional pavements due to lower thermal conductivity (Santamouris, 2013b).

Permeable, porous, and pervious pavements are the three main types of evaporative pavements, which have different mechanisms. Permeable pavements have a specially designed top layer that allows water to spread across the pavement structure without penetrating the lower base layer. Due to their rougher surface texture, these pavements tend to reflect less sunlight compared to smoother surfaces, but their design can reduce UHI effects owing to the water cooling mechanism (Li, 2015; Qin, 2015). Typically, permeable pavements have a layer of fired-clay bricks or concrete, and in arid climates, they can retain more heat than dense asphalt concrete (Mullaney and Lucke, 2014). In contrast, pervious pavements function differently, as they allow water to pass directly through the surface layer into the base course, making them less suitable for high-traffic roads. These pavements are constructed using concrete or asphalt binders mixed with large and single-sized aggregates to create void spaces for water infiltration. Additionally, porous pavements are characterized by numerous open spaces or voids, which are often filled over time with gravel, dirt, or vegetation. Once these voids are filled, the cooling benefits are negatively affected, and the pavement functions similarly to conventional mixtures, showing minimal impact on temperature reduction (K. W. Lee et al., 2012).

Heat-harnessing pavements have been introduced as an innovative method to indirectly utilize water's cooling potential inside pavement structures. These pavements are designed to capture solar energy and transform it into another form of energy, reducing the pavement temperature

(Pascual-Muñoz et al., 2013). This is typically achieved by using pipes filled with water beneath the pavement surface, where absorbed solar heat warms the water, which is then transported to a storage reservoir (Gao et al., 2010). However, this technique has practical limitations. It is generally unsuitable for areas with heavy traffic, as conventional pavements may not withstand the modifications without specialized reinforcement. Additionally, the installation and maintenance of such systems significantly increase construction costs, making them less economically feasible for widespread application (Bobes-Jesus et al., 2013). The overall mechanism of this system is illustrated in Figure 1.11.

While evaporative and heat-harnessing pavements offer promising potential for reducing surface temperatures and UHI effects, their practical application across urban environments remains highly limited. These specialized pavement types often involve complex designs, such as high air void content or integrated water storage and piping systems, which are not compatible with the structural demands of existing high-traffic urban roads. Their effectiveness is also dependent on the climate, while beneficial in regions with high rainfall, evaporative pavements can worsen thermal conditions in arid, dry environments. Moreover, the implementation of these systems requires the replacement of current pavement structures, which is economically unfeasible for most cities due to the high material, installation, and maintenance costs. The ongoing maintenance challenges, such as preventing void clogging in porous pavements or managing the mechanical wear of heat-harnessing systems, further limit their practicality. Replacing existing infrastructure with these technologies across most cities is neither cost-effective nor realistic, making them unsuitable as widespread solutions for UHI mitigation in most urban areas. Therefore, finding a practical solution that can be used for most existing pavements with the minimum cost is of major significance, and the importance of a reflective top layer is undeniable.

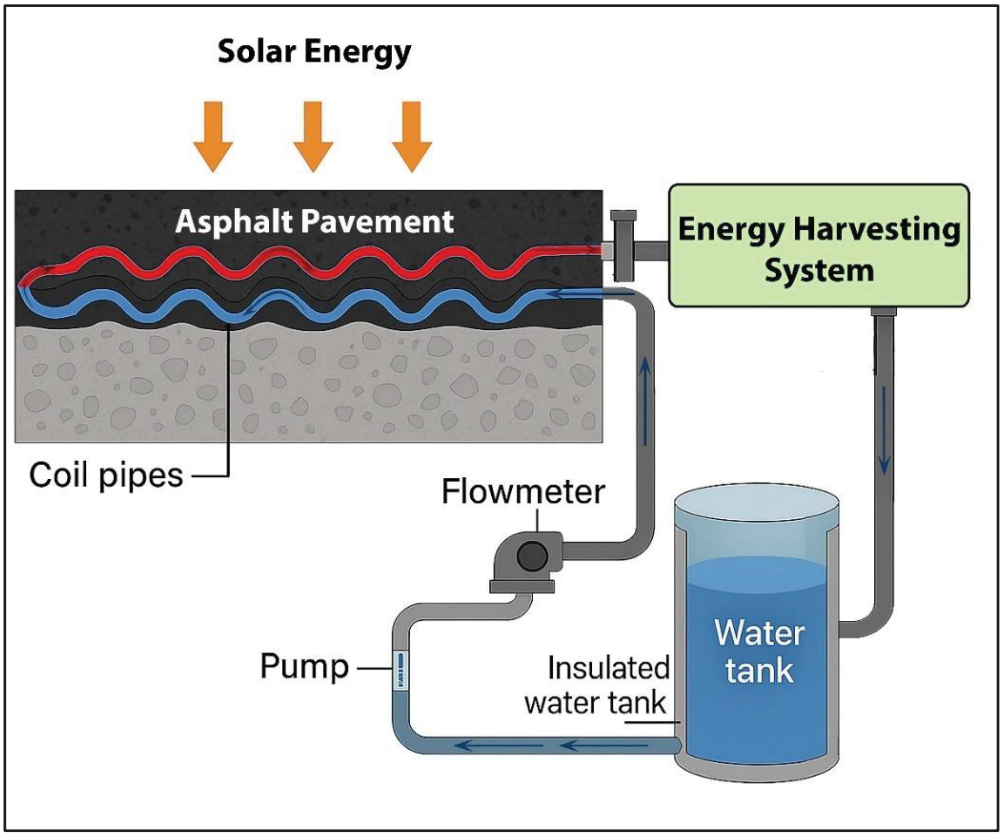

Figure 1.11 The heat-harvesting pavement system

1.6.3 Thermally Modified Asphalt Mixtures

As the top layer of pavement, the asphalt mixture, plays the most important part in heat absorption and transfer, changing the asphalt mix design has been one of the most common ways to mitigate the UHI effects. The materials used in asphalt mixtures significantly influence their thermal behavior. Various insulation and conductive aggregates, fillers, and binder additives have been utilized to modify the thermal properties of the asphalt mixture. Since aggregates typically account for the largest portion of asphalt mixtures, approximately 90–95% by weight or 75–85% by volume, their role in determining thermal performance is of major significance (Asphalt Institute, 2007). Therefore, the selection and composition of these materials are critical to alter the thermal behavior of asphalt mixtures. Most previous research has focused on altering asphalt mixture materials for two main objectives, including either enhancing or reducing the thermal conductivity and heat transfer rates of asphalt mixtures. The

outcomes of these material modifications and their impact on pavement heat transfer are explained in this section.

Many researchers have emphasized raising the thermal conductance and enhancing the thermal conductivity and heat transfer rate of asphalt mixtures to avoid heat accumulation in the asphalt mixture layer and transfer the absorbed heat to the layers below. A variety of materials have been added to asphalt mixtures to enhance their thermal conductivity and heat transfer rate. In general, the specific heat capacity and thermal conductivity of hot mix asphalt (HMA) laboratory specimens range from 1120 to 1368 ($J.kg^{-1}.K^{-1}$) and from 1.4 to 1.8 ($W.m^{-1}.K^{-1}$), respectively (Luca and Mrawira, 2005). Researchers have experimented with several additives, including carbon black powder, thermochromic powders, graphite powder, synthetic acrylic polymers, and waste engine oil residues, to improve the thermal conductivity of asphalt pavements (Cong et al., 2014; Yinfei et al., 2014; Hu and Yu, 2016; Vo et al., 2017; Petkova-Slipets and Zlateva, 2018; Shi et al., 2019; Wang et al., 2020). A summary of the results from the relevant studies in which thermal conductivity and heat transfer have been improved is presented in Table 1.1.

Enhancing the heat transfer rate and thermal conductivity can decrease pavement surface temperatures during summer. Pavements with higher conductivity transfer absorbed heat faster to the lower pavement layers, allowing the surface to cool more efficiently. This surface cooling results in reduced heat emissions due to lower thermal gradient with the ambient air, better air quality, decreased energy use, and mitigates UHI effects (Shi, 2014; Vo et al., 2017). However, previous research has not investigated the impact on night-time temperatures. While conductive asphalt mixtures may remain cooler during the day, they may potentially release more heat at night, leading to higher nighttime surface temperatures (Asaeda et al., 1996; Mohajerani et al., 2017a). This approach may not be suitable in cities where cooler night-time conditions are essential. London, for example, experiences more intense UHI effects at night, with temperatures rising 5 to 8°C higher than during the day, indicating significant nighttime heat release and exacerbation of the UHI (Asaeda et al., 1996; Givoni, 1998; Watkins et al., 2002; Kolokotroni et al., 2012).

Table 1.1 Materials used to enhance the thermal conductivity of the asphalt pavements

Literature	Type of materials added to the asphalt mixture	Thermal conductivity ($W.m^{-1}.K^{-1}$)	Specific heat capacity ($J.\ kg^{-1}.\ K^{-1}$)	Conclusion
(Park et al., 2014)	20 % Graphite powder	2.09 (control: 0.7-1.2)	810	Raising the thermal conductivity, as a result, reduces snow-melting time.
(Vo et al., 2017)	1% chopped carbon fiber, 20 % milled carbon fiber, and 20 % graphite powder	2.2	818-841	Increasing the thermal conductivity, which cooled down the surface and melted the snow faster, and enhanced the tensile strength
(Vo and Park, 2017)	Up to 4% carbon fiber and 20 % graphite powder (by volume of asphalt binder)	2.8	-	Enhancing the thermal conductivity by up to 58 % and accelerating the snow-melting process
(Jiao et al., 2020b)	Up to almost 5% steel slag in asphalt concrete by volume	1.7-2.1	-	Increasing the thermal conductivity by 8.23% and enhancing the snow-melting efficiency by 14.7%.
(Chen et al., 2020)	Up to 100% quartzite coarse aggregates	3.65	-	Growing the thermal conductivity by 30% and reducing the skid resistance
(Cong et al., 2014)	Up to 26% carbon black by volume of the asphalt binder	0.77	-	Raising thermal conductivity (up to 48 %) and enhancing anti-aging and high-temperature performance
(Ahmad Nazki et al., 2020)	Up to 2% graphene by weight of the asphalt binder	0.188-0.247	-	50-80 % increase in thermal conductivity of binder, and increasing the shear modulus

The thermal conductivity of asphalt pavements was enhanced to transfer the heat rapidly from the heated surface to the underlying layers in summer or from the underlying layers to the surface in winter (Wang et al., 2010; Liu and Wu, 2011; ShengYue et al., 2014). This strategy offers advantages in both summer and winter conditions. In winter, pavements with higher thermal conductivity can accelerate snow-melting processes, which is especially critical for safety on infrastructure such as tunnel exits, bridge decks, slopes, and airport runways (Park et al., 2014; Vo et al., 2017). Moreover, using conductive materials as asphalt mixture aggregates can raise surface temperatures in colder regions, reducing the risk of cracking caused by low temperatures (Hu and Yu, 2016). In fact, when temperature differences between the top and bottom surfaces of asphalt concrete are minimized, the material exhibits greater resistance to thermal cracking (Shi et al., 2019).

In contrast to approaches aimed at increasing thermal conductivity, some researchers have focused on reducing thermal conductivity to create thermally resistant asphalt pavements. This technique is considered effective for decreasing the temperature at the bottom of asphalt concrete while raising the surface temperature (Doulos et al., 2004). Various materials have been utilized to decrease heat transfer rates, such as ceramics, expanded polypropylene (EPP) beads, fly ash cenospheres (FAC), and lightweight aggregates coated with resin, such as volcanic rock, shale ceramsite, pottery sand, diatomite, and bauxite. These materials have reduced thermal conductivity and heat transfer rate in asphalt mixtures (Mallick et al., 2004; Huang et al., 2009; González-Corrochano et al., 2011; Feng et al., 2013; Ren et al., 2014; Pancar, 2016; Wang et al., 2018; Shi et al., 2019; Wang et al., 2019; Yinfei et al., 2020; Deng et al., 2019).

There are several reasons for the development of thermal-resistant asphalt pavements, the first one of which is the reduction of overall pavement structure temperatures (Yinfei et al., 2014, 2016). These pavements serve as insulating layers that prevent the thawing of permafrost (D. Zhang et al., 2019; Du et al., 2020). Research has shown that up to 30% of the total absorbed heat from solar radiation in the asphalt pavement can be absorbed in the center of the subgrade, which may lead to permafrost thawing and increase the subgrade's moisture content. This added moisture can cause structural issues such as subgrade collapse, pavement cracking, and roadbed deformation (Epps, 2000; Wu and Niu, 2013; Yu et al., 2015). Another objective for

enhancing the thermal resistance of asphalt mixtures is to minimize oxygen aging of bitumen (Hou et al., 2018). However, the use of insulating materials may result in greater heat accumulation at the pavement surface, potentially intensifying heat exchange with the surrounding ambient air. Further research is needed to fully assess the effectiveness of thermally resistant pavements in mitigating UHI effects. Some studies in which materials were used to lower the thermal conductivity of asphalt concrete, with their brief results, are provided in Table 1.2.

Since both high and low thermal conductivity asphalt pavements offer advantages and disadvantages, some studies have explored the combination of these materials to develop optimum pavement structures. These investigations involved dividing the asphalt concrete into two or three layers, each with different thermal properties. For example, Yinfei et al. (2015) investigated the use of a heat-reflective thin surface layer and an insulating material, such as floating beads, in the top layer to reduce thermal conductivity. The middle layer contained both insulating and conductive materials separately, and in the bottom layer, graphite powder was used to enhance the heat transfer rate. Results showed that this multilayer pavement emitted the least amount of heat to the surroundings at night, with the bottom layer exhibiting a lower surface temperature and less solar heat absorption. This layered structure also improved resistance to permanent deformation, with rutting depth reduced by up to 65%. The details of this pavement structure, including thermal conductivities and thicknesses of each layer, are illustrated in Figure 1.12.

However, the negative aspect of these kinds of structures is related to the thermal-resistant top layer, which may trap heat, increasing surface temperatures. More importantly, these innovative pavement systems require high costs, advanced levels of implementation, and higher maintenance costs, which make them impractical for real situations. To address UHI effects more effectively, increasing reflectivity and transferring heat to the lower layers can be a more efficient strategy.

Table 1.2 Materials used to decrease the thermal conductivity of the asphalt pavement

Literature	Type of materials added to the asphalt mixture/biner	Thermal conductivity ($W.m^{-1}.K^{-1}$)	Specific heat capacity ($J.\ kg^{-1}.\ K^{-1}$)	Conclusion
(Khan and Mrawira, 2008)	Lightweight ceramic coarse aggregates	0.77–0.87	-	Decreasing the thermal conductivity and frost penetration
(Yinfei et al., 2014)	Up to 15% floating beads as fine aggregates	0.6529	1541	Diminishing the thermal conductivity by up to 35 % and the rutting depth by up to 44 %
(Shi et al., 2019; Wang et al., 2019)	Expanded polypropylene (EPP) beads	1.3	-	Reducing the thermal conductivity (up to 32%), heat capacity (up to 27 %), and the tensile strength
(D. Zhang et al., 2019)	Up to 75% floating beads as mineral filler in asphalt concrete	0.895	-	dropping the thermal conductivity (by 36.5 %) and the rut depth (by 27%)
(Deng et al., 2019)	Up to 33% shale ceramsite (by weight) of fine aggregates	0.84-1.045	1039-1237	Decreasing the thermal conductivity by up to 35.3% and the temperature by 4.39 °C, and increasing the rutting resistance.
(Du et al., 2020)	Up to 100% fly ash cenosphere as filler of asphalt mastic	0.23	-	diminishing the thermal conductivity (by 37.8 %) and the fatigue life

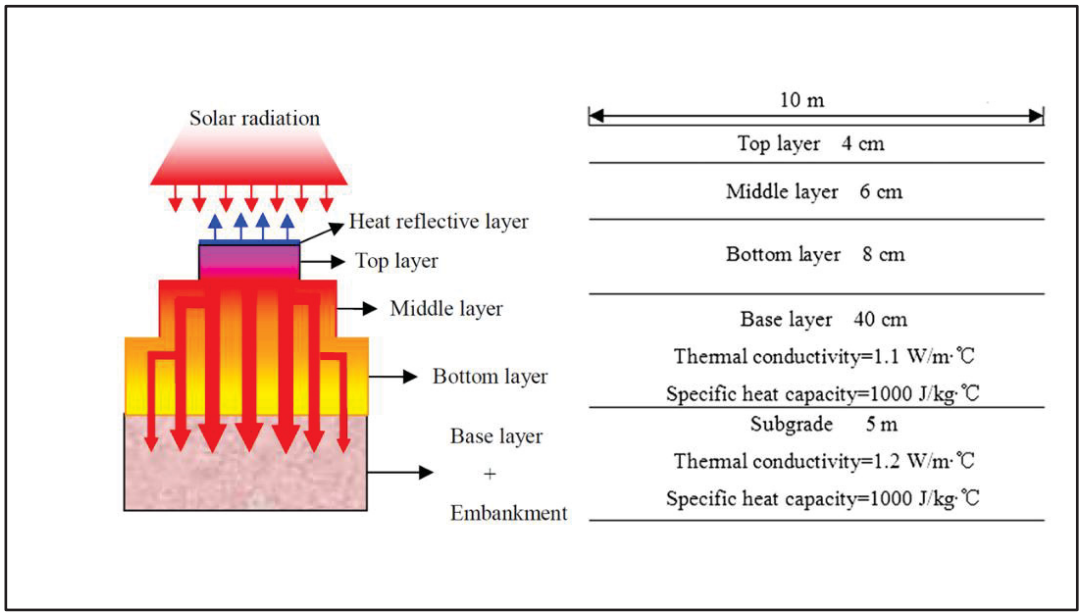

Figure 1.12 The heat conduction mechanism of pavement consists of 3 layers of asphalt mixtures for UHI mitigation
Taken from Yinfei, Qin, et al (2015)

1.7 Experimental Techniques and Performance Tests in Literature

To effectively assess the thermal and mechanical behavior of pavement systems and their capacity to alleviate UHI effects, a range of experimental techniques has been employed in previous studies. For evaluating thermal properties of pavements, different devices and sensors, including the C-Therm device, DRE-2C and DRM-II devices, the Thermal Constants Analyzer, the Hilton Heat Transfer Unit, and the QuickLine device, were employed. Most of these devices have similar mechanisms to measure the thermal properties. However, these methods differ in sensitivity, sample size requirements, and response time, providing flexibility for laboratory and field-based evaluations, which is explained in this section. In addition to thermal properties measurement devices, other experimental and field tests, including indoor infrared lamp setups for cooling effect measurements, pyranometers for albedo assessment, and spectrometers for evaluating reflectance across different wavelengths, are mentioned in this section.

Apart from the thermal properties, different tests have been done to evaluate the mechanical properties and durability of chip seals, including the sand patch test, sweep test, the British Pendulum tester (BPT), the interface bond test, and the Vialit test. Although there are not many standards to assess the chip seals' properties, these tests have been developed in previous studies. These tests and the most common methods for creating chip seal mix designs in North America are explained in this section.

1.7.1 Measurement of Thermal Properties

Evaluating pavement thermal properties is critical for assessing climatic performance and UHI mitigation potential, with key parameters including thermal conductivity, specific heat capacity, and thermal diffusivity. Several experimental techniques have been developed to measure these properties accurately under both laboratory and field conditions. Several studies have employed specialized fillers to modify the thermal conductivity of asphalt binders. In a study, Petkova-Slipets and Zlateva (2018) used the C-Therm device for measuring thermal conductivity, which was formerly known as the TCi thermal conductivity analyzer. This device does not have a specific model number, and the MTPS conforms to the ASTM D7984 standard (ASTM D7984, 2021). Based on this standard, MTPS is equipped with a flat, one-sided heat source, and a surrounding guard ring positioned perpendicular to the heat source is placed in contact with one side of the test sample. This setup allows a brief heat pulse to be transmitted into the material for testing purposes. Regarding pavement testing, a solid asphalt binder layer is placed directly onto the MTPS sensor, with a weight applied on top to ensure contact. The analyzer then directly measures parameters such as thermal conductivity and thermal effusivity. With these values, other thermal properties can be calculated using corresponding equations (Petkova-Slipets and Zlateva, 2018). Although the TCi analyzer can also be used for asphalt concrete specimens, certain limitations exist. The high surface roughness of asphalt mixtures can damage the sensor, and not all sensor types ensure adequate contact with the irregular surface of the samples. Additionally, asphalt mixtures are not thermally uniform at the surface due to the differing conductivities of the binder and aggregate materials. As a result, multiple measurements are required to obtain a reliable average value. As a result of these limitations, the TCI analyzer was found to be more suitable for measurements on asphalt

binders than on rough asphalt mixture surfaces within the context of the study, unless specimens were cut and prepared to provide a flat and smooth contact surface.

Additionally, two other apparatuses that follow a similar measurement principle are the DRE-2C and DRM-II models (Jiao et al., 2020a; Yinfei et al., 2020). Both these models conform to ISO 22007-2 (ISO 22007-2, 2022). Based on this standard, this technique provides instructions for evaluating materials that are homogeneous and isotropic, as well as those with a uniaxial anisotropic structure. It assumes that the material's uniform properties extend across the entire specimen and that no thermal discontinuities exist within the probing depth, other than those adjacent to the probe. These devices generate heat in a specially designed rutting plate to vary the internal temperature of the sample and evaluate its thermal conductivity using transient heat transfer equations (Jiao et al., 2020a; Yinfei et al., 2020). The use of this method for assessing asphalt mastic is demonstrated in Figure 1.13. Compared to other techniques, these instruments offer certain advantages. First, they allow for direct measurement of heat transfer, which significantly reduces testing time. Second, because they rely on transient rather than steady-state heat transfer, their results are less influenced by thermal contact resistance (Jiao et al., 2020a; Yinfei et al., 2020). However, these devices require the sample surface to be flat, or the sample must be in powdered form to ensure accurate readings. Furthermore, due to the small size of their sensors, they are particularly well-suited for testing asphalt binders and mastics, rather than Asphalt mixtures and inhomogeneous solids.

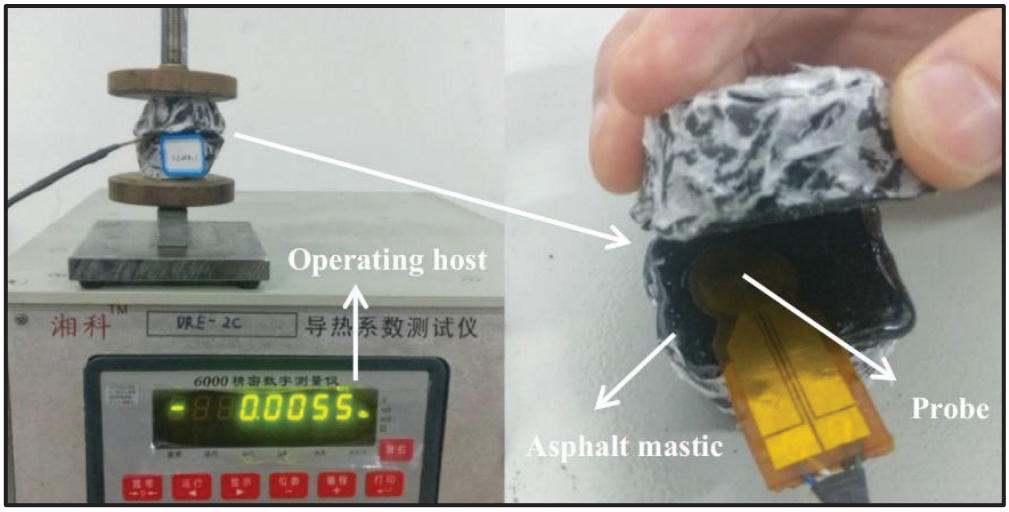

Figure 1.13 Thermal conductivity measurement process
Taken from Yinfei et al (2020)

In addition to instruments designed for measuring the thermal conductivity of asphalt binders and mastics, other devices are specifically developed to assess the thermal conductivity of asphalt concrete. One such device is the QuickLine (Model TM-30), which operates in accordance with the ASTM D5334 standard (ASTM D5334, 2022). Based on this standard, this testing procedure outlines a method for measuring the thermal conductivity of soil and rock through a transient heat technique. It can be applied to both undisturbed and reconstituted soil samples and is effective in both laboratory and field settings. While it is ideally suited for homogeneous materials, it can also provide a reliable average thermal conductivity value for heterogeneous materials. This testing method is suitable for dry, unsaturated, or saturated materials capable of maintaining a cavity for sensor insertion. This method utilizes a 5-cm surface probe and employs a dynamic measurement technique that significantly shortens testing time. During operation, a constant electrical current is applied while the probe is in contact with the asphalt sample. As heat is generated, the change in temperature from the initial to the final state is recorded and used to determine thermal conductivity (Vo et al., 2015, 2017). While this device is well-suited for testing solid materials such as asphalt mixture samples.

Another widely used technique involves the Hot Disk Instrument (Model TPS 2500S), which utilizes a hot disk thermal sensor that works as both a heat source and a temperature detector. This thermal analyzer meets the ISO 22007-2 standard (ISO 22007-2, 2022), which was

explained for DRE-2C and DRM-II models. The device supports a range of testing capabilities, including standard assessments of isotropic materials, evaluations of rod-like specimens, analyses of thin films, coatings, or adhesive layers, measurements of highly conductive sheets or panels, testing of ultra-light and low-conductivity materials, and investigations of anisotropic materials or layered configurations. One benefit of this device is that it can be used for solids, liquids, and powders. This sensor is made of an ultra-thin nickel foil (10 μm thick) arranged in an electrical pattern similar to a hot disk and is coated with a 70 μm Kapton insulation layer. To conduct the test, asphalt concrete samples are typically cut into two or three sections, and the hot disk is placed between them. Once the nickel foil is heated, thermal energy transfers into the surrounding material (Chen et al., 2015; Liu et al., 2017; Mirzanamadi et al., 2018; Shi et al., 2019; Chen et al., 2020). This method is recognized as one of the most precise for determining thermal properties (Liu et al., 2017). One of its main advantages is its effectiveness in testing heterogeneous materials like asphalt mixtures. It is also capable of evaluating large specimens with multiple layers, which many other devices cannot accommodate. Furthermore, the broader surface area of the TPS sensor enables enhanced contact with both the asphalt binder and the aggregates, improving the reliability of thermal conductivity measurements, as shown in Figure 1.14.

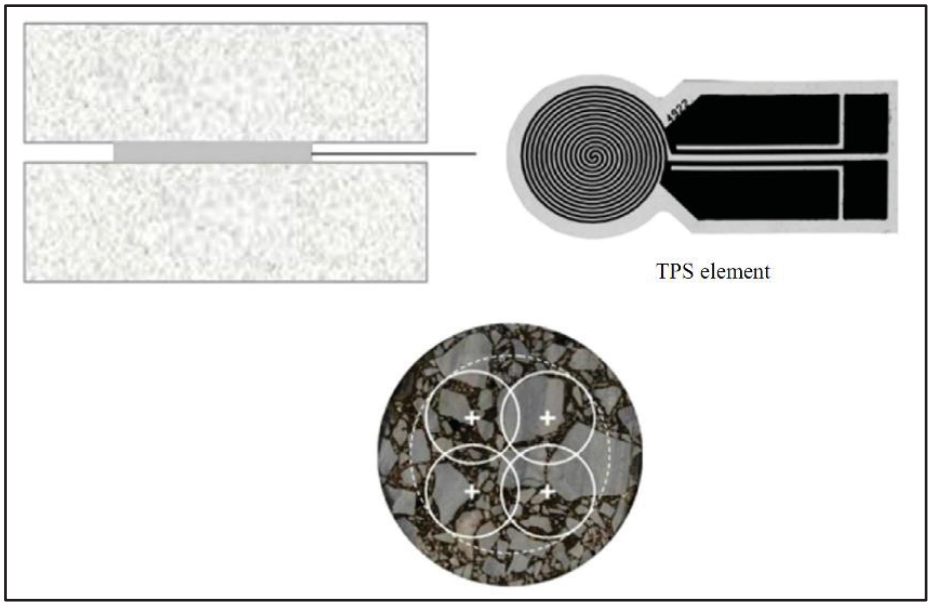

Figure 1.14 Thermal conductivity measurement with the hot disk thermal analyzer
Taken from Liu et al (2017)

Choosing the most suitable device to measure the thermal properties of asphalt binder, asphalt mixture, aggregates, and base course blend depends on many factors, such as the availability of different sensors based on the surface of materials. Among all the above-mentioned apparatuses, the C-Therm device (no model), a trident thermal conductivity instrument, has a wide range of sensors, all of which work based on the transient heat transfer method that can be used for pavement structures. The modified transient plane source (MTPS) and Transient Line Source (TLS) needle sensors of this device are recommended for measuring the thermal properties of aggregates, binder, and granular materials.

Regarding the MTPS sensor, it works based on the transient heat transfer and the ASTM D7984 standard (ASTM D7984, 2021). Thermal effusivity is calculated based on how the surface temperature changes over time. The extent of the temperature increase is inversely related to the material's thermal effusivity. This device can be used for measuring thermal conductivity and thermal effusivity parameters of solid materials. The minimum diameter of the solid sample for this sensor is 18 mm, and the sample should have a flat surface. Based on the recommendation of the manufacturer, a special paste provided can be applied on the surface of the sample to minimize the voids and maximize the contact. The C-Therm device has some

reference samples on which this thermal paste can be used, and checks the measured thermal properties before and after using this agent, which will remain unchanged. Therefore, this is a suitable sensor for measuring the thermal properties of asphalt mixture, asphalt binder, and construction aggregates.

TLS Needle sensor works based on the transient heat transfer and complies with several international standards and guides, including IEEE 442, ASTM D5930, and ASTM D5334 Standards (ASTM D5930, 2017; IEEE 442, 2017; ASTM D5334, 2022). The IEEE 422 provides procedures for measuring the thermal resistivity of various materials used in underground cable installations, including soil, concrete, engineered backfills, grout, rock, sand, and other encasing materials. Understanding the thermal characteristics of these materials is essential for accurately designing, rating, and loading buried cable systems. The measurement technique relies on the principle that the rate at which temperature increases from a linear heat source is influenced by the thermal properties of the surrounding material. Additionally, the guide includes designs for thermal probes suitable for both laboratory and field applications. The TLS Needle sensor is specifically designed for measuring the thermal conductivity of materials like polymer melts, semi-solids, and soil. However, it is not ideal for low-viscosity fluids, as convection may interfere with accurate readings. The sensor is 150 mm in length and requires a relatively large sample volume, with a minimum of 80 mL. Hence, this is a suitable sensor for measuring the thermal properties of the base course granular materials.

To accurately assess the thermal properties of various pavement materials used in this study, including asphalt binder and mastic, construction aggregates, and base course blends, the C-Therm device equipped with MTPS and TLS sensors was selected. This decision was based on the need for precise and versatile testing methods capable of handling a wide range of materials with different thermal behaviors and physical forms, as well as the availability of the device and its previous successful usage in other studies. The MTPS sensor is well-suited for homogeneous solid materials like asphalt binder, mastics, and cut, smooth-surfaced aggregates due to its high precision, rapid measurement time, and ability to operate over a broad temperature range for solids. Its flat, guarded heat source allows for reliable surface contact and direct measurement of thermal properties. For granular materials, such as base course

aggregates, the TLS needle sensor provides effective thermal properties measurements based on transient heat conduction along a line source. Its design enables testing materials with more variable structures, making it ideal for engineered soils and aggregates. The combined use of MTPS and TLS within a single device ensures that a comprehensive range of pavement material types can be tested with high accuracy and consistency. Thus, employing the C-Therm system with both sensors offers a flexible and robust approach to characterizing the thermal behavior of key pavement materials in this research, which is essential for both performance prediction and UHI impact assessment. The details of thermal properties measurements of the devices are summarized in Table 1.3.

Table 1.3 Thermal properties measurements device specifications

Device	Thermal conductivity range ($W.m^{-1}.K^{-1}$)	Thermal effusivity range ($W. s^{1/2}. m^{-2}. K^{-1}$)	Temperature range (°C)	Sample limitations
C-Therm device (MTPS)	0.01 - 500	5 to 40,000	Up to 200	Flat solid
C-Therm device (TLS)	0.1 - 6	-	up to 300	Powders & liquids
DRE-2C & DRM-II	0.010 - 500	-	Up to 725	Flat solids & powders
QuickLine (Model TM-30)	0.04 - 1	-	up to 100	Solids larger than 5cm with a maximum thickness of 32mm
Hot Disk Instrument (Model TPS 2500S)	0.005 - 1800	20 - 55,000	Up to 1000	Flat solids

1.7.2 Albedo and Surface Reflectance Tests

The role of pavement reflectivity and albedo in mitigating the UHI effect has been highlighted in previous studies. The albedo of pavements can be determined using the method outlined in ASTM E1918 (ASTM E1918, 2021). This technique involves the use of a pyranometer to

record both the total incoming solar radiation and the amount reflected off the horizontal surface and low-sloped pavement surfaces under natural sunlight conditions. This procedure is particularly suitable for evaluating large surface areas, such as pavements and roofing materials, in outdoor environments. The method involves placing a pyranometer above the test surface to record the incoming solar irradiance and then inverting the sensor to measure the reflected radiation from the same surface. To ensure accuracy, measurements must be taken under clear sky conditions, ideally between solar noon ± 2 hours, when the sun is highest in the sky, to minimize shadowing and variation in solar angle. The test surface must be dry and clean, and the pyranometer should be mounted at a specified height (around 1 meter) directly above the surface to capture a representative hemispherical reflectance. The ratio of reflected to incoming radiation is the albedo value, which provides an important indicator of the surface's ability to reflect solar energy and reduce heat absorption, making this method essential in studies targeting UHI mitigation. This measurement procedure is illustrated in Figure 1.15.

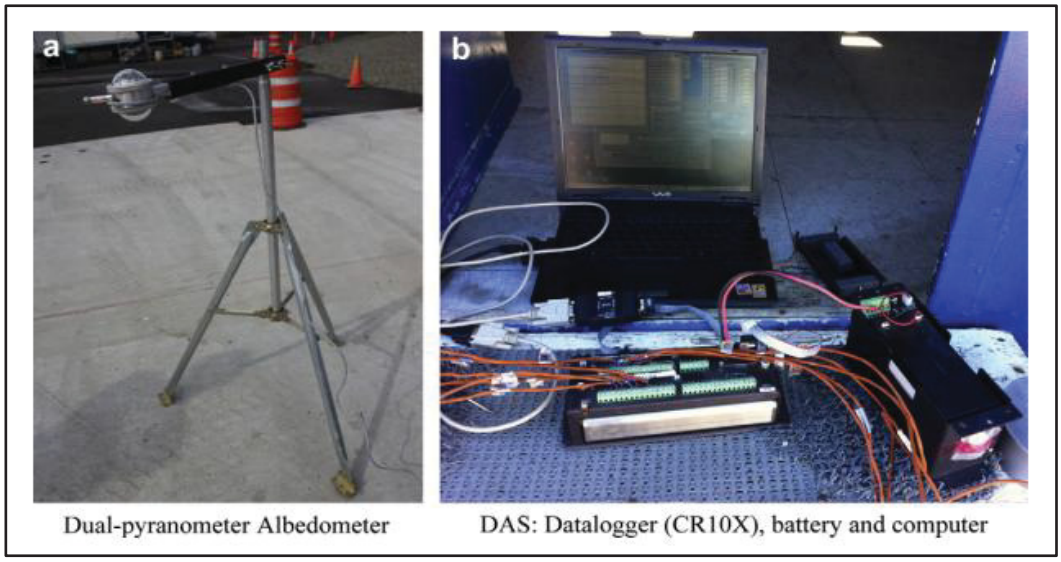

Figure 1.15 A dual pyranometer for albedo measurement; (b) Data logger
Taken from Li et al (2013)

Conducting field experiments to assess pavement reflectivity has challenges due to the influence of changing weather conditions. As an indoor alternative test, the UV/Vis/NIR

spectrometer has proven to be a practical tool for measuring pavement reflectance for different wavelengths. This device captures the reflective spectral data in the ultraviolet, visible, and near-infrared regions, offering a reliable indication of asphalt pavement reflectivity (Cao et al., 2015; Xie et al., 2019). In controlled laboratory conditions, a pyranometer can also be utilized, with solar radiation simulated by an infrared lamp that emits wavelengths similar to natural sunlight. In cases where physical reflectivity tests with pyranometers are unfeasible, such as when the required large pavement area cannot be constructed, laboratory-scale samples can be tested with the UV/Vis/NIR spectrometer at a lower cost, making the spectrometer a reliable and efficient solar simulation method for laboratory-based reflectivity assessments. In addition to its practicality and cost-effectiveness, the UV/Vis/NIR spectrometer offers high-resolution spectral analysis that enables detailed characterization of pavement materials' optical properties across the solar spectrum. This capability is crucial for evaluating surface albedo and understanding how different binder types, aggregate compositions, and surface treatments influence solar reflectance and heat absorption. For instance, studies have shown that pavements with higher reflectance in the NIR range can significantly reduce surface temperatures, mitigating the UHI effect (Cao et al., 2015). The spectrometer allows researchers to identify specific wavelength ranges where material modifications show the greatest thermal benefits.

1.7.3 Indoor Cooling Effect Test Using Solar Energy Simulation

The asphalt pavement cooling effect test is a widely used approach for assessing the rate of heat transfer at various depths within asphalt layers and the cooling effect of newly developed pavement systems. To simulate the effects of solar radiation, an infrared lamp of 275 W in power is utilized. These lamps can be positioned at adjustable heights between 40 cm and 90 cm above the specimen surface (Jiang and Wang, 2020). Both beam-shaped and cylindrical samples are suitable for testing, and insulation materials such as liquid foam are applied around the sides to prevent lateral heat loss. Multiple temperature sensors are embedded at the surface, at various internal depths, and at the base of the specimens to monitor thermal changes. A computer continuously logs temperature increases during the heating phase. After a certain heating period, the lamps are switched off to observe and record the cooling behavior of the

pavement samples (Wang et al., 2018; Deng et al., 2019; Jiao et al., 2020b). This experimental test method is illustrated in Figure 1.16.

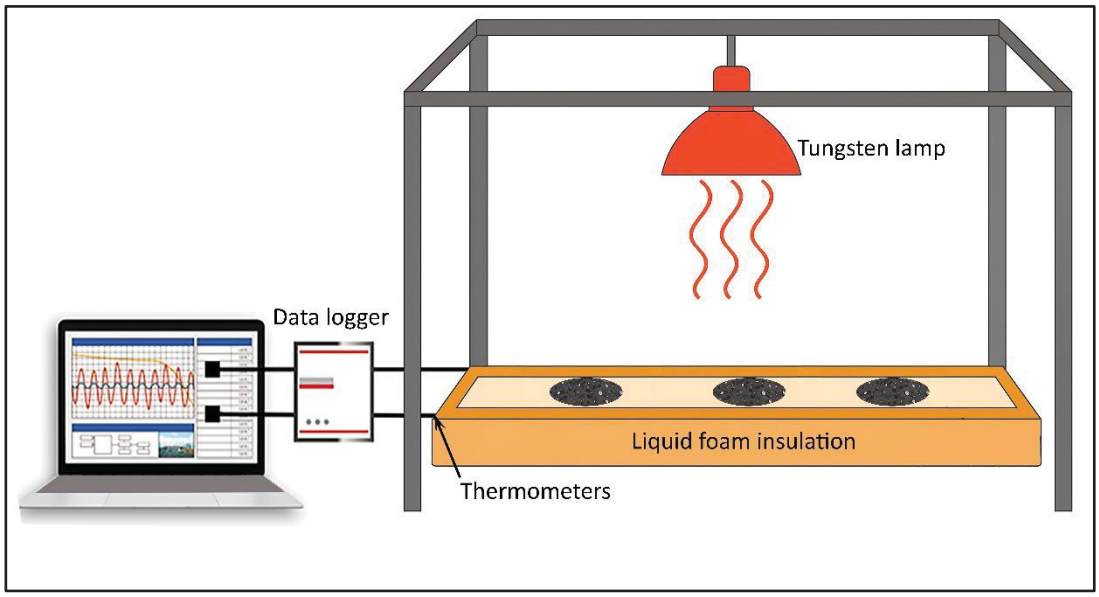

Figure 1.16 Typical indoor solar simulation test

Solar radiation spans a broad range of wavelengths, primarily between 200 and 2500 nanometers, accounting for approximately 96.3% of the total irradiance (Thuillier et al., 2003). Various methods have been developed to simulate solar radiation in laboratory settings, among which infrared lamps are the most frequently used tools for studying heat transfer in asphalt pavements (Jiang and Wang, 2020). While these lamps typically have a color temperature of around 3200 K, the actual brightness temperature of natural sunlight falls between 5600 K and 6000 K. This discrepancy arises due to the limited ultraviolet and shortwave visible light emitted by infrared lamps, making their spectral output different from real sunlight. To improve accuracy, optical filters are often applied to these lamps, which help produce more realistic simulation results. Nonetheless, even with filtering, these lamps do not perfectly replicate the visible light spectrum of natural sunlight, resulting in only a partial match (Pirouzfam and Sendur, 2021).

Overall, the use of infrared tungsten lamps provides a practical method for simulating solar-induced heating in laboratory-based asphalt pavement testing within the scope of this study.

This conclusion is based on their ability to deliver stable, repeatable radiant heat fluxes, enabling controlled observation of heating and cooling behavior across pavement depths. Although these lamps do not fully reproduce the spectral characteristics of natural sunlight, particularly in the ultraviolet and shortwave visible ranges, their consistent heat output allows reliable comparison between pavement configurations under identical laboratory conditions. By adjusting lamp wattage, installation height, and lateral insulation, the experimental setup enabled controlled and repeatable testing. As a result, infrared lamp-based simulation offers a cost-effective and adaptable approach for comparative thermal assessment of pavement materials under laboratory conditions.

1.7.4 Chip Seal Mix Design and Performance Tests

Chip seal is a cost-effective pavement preservation technique that involves the application of an asphalt binder followed by a layer of aggregate chips. The performance and durability of chip seal treatments depend heavily on the appropriate mix design, which ensures adequate aggregate coverage, binder application, and surface friction while minimizing aggregate loss and bleeding (Wood et al., 2006). There is no widely accepted standard for chip seal design across North America. In both research and practical applications in the United States, several design methods are commonly used, including the McLeod, Kearby, modified Kearby, and modified McLeod approaches (Kearby, 1953; McLeod et al., 1969; Stockton and Epps, 1975). These methods aim to determine the appropriate application rates of aggregate and asphalt emulsion to achieve an aggregate embedment between 50% and 80% of the median aggregate size. One of the most widely accepted methods for chip seal mix design in North America is the McLeod Method, which balances binder application rate and aggregate size based on aggregate gradation, traffic volume, surface condition, and climatic factors. In Canada, the modified McLeod method is preferred because it has been specifically calibrated for the climatic and operational conditions typical of northern regions. Unlike earlier U.S. formulations, the modified version incorporates correction factors for cold temperatures, seasonal moisture variation, and the use of emulsified binders that perform better in freeze-thaw cycles, such as adjustments to binder application rates and the use of slow-setting or polymer-modified emulsions that provide improved adhesion and durability under cold climates. Canadian road agencies have adopted this approach as it provides more accurate

estimates of aggregate embedment and binder application rates under local weather and traffic conditions. The McLeod method begins by selecting a single-size aggregate and determining its flakiness index, average least dimension (ALD), and bulk specific gravity. Based on these characteristics and adjustments for traffic and surface absorption, the optimal binder application rate is determined. The target is to achieve one-layer embedment of aggregates into the binder while avoiding excessive binder that can cause bleeding or flushing. In National Cooperative Highway Research Program (NCHRP) Synthesis 342, an overview of successful chip seal practices in the United States and Canada is provided, showing very similar practices for these two countries. The statistics for employing different chip seal mix designs in North America are shown in Table 1.3. As it is shown, the McLeod and Modified McLeod methods are the most popular methods for chip seal design in Canada. The literature review and survey findings indicated that two main chip seal design methods are commonly used across North America. The two principal chip seal mix design approaches are the Kearby/Modified Kearby and McLeod/Modified McLeod methods. Although some agencies have developed independent procedures, most rely on empirical approaches or do not follow a formal design method (Chip Seal Best Practices, 2005). Given the similarity between northern U.S. and Canadian climates, Canadian agencies commonly recommend the Modified McLeod method based on the Minnesota seal coat handbook (Davidson et al., 2005; Wood et al., 2006).

Table 1.4 Chip seal design methods in North America (Chip Seal Best Practices, 2005)

Chip seal design method	United States (%)	Canada (%)
McLeod/Modified McLeod (Asphalt Institute)	11	45
Empirical/Past experience	37	33
No formal method	26	22
Kearby/Modified Kearby	7	0
Own formal method	19	0

There are four main chip seal types that can be used based on different factors. Single chip seal is the most frequently used chip seal type. It involves one layer of binder application followed by the placement of a uniformly graded aggregate layer, as illustrated in Figure 1.17(a). This type of chip seal is typically chosen for standard applications where no unique conditions

require an alternative design (Chip Seal Best Practices, 2005). It is important to note that the figures provided are schematic representations, and different variations of these designs may be implemented in actual practice. Another type is the double chip seal, which involves applying two successive layers of bituminous binder followed by two layers of uniformly graded aggregate, as illustrated in Figure 1.17(b). The aggregate used in the second layer is generally about half the size of that in the first layer. Compared to single chip seals, this method offers better noise reduction, improved waterproofing, and increased durability. As a result, double chip seals are typically employed in high-stress conditions, such as roads with heavy truck traffic or steep inclines (Sprayed Sealing Guide, 2004). Moreover, a racked-in seal is another specialized form of chip seal where a single-layer chip seal is temporarily reinforced by adding choke stone, which fills the voids between the larger aggregate particles, as shown in Figure 1.17(c). This smaller aggregate helps interlock the larger particles, preventing them from becoming loose before the binder has completely set. Racked-in seals are particularly suitable for locations with frequent turning traffic, where the additional locking of aggregates is needed to maintain surface integrity during the curing process (Davidson et al., 2005). Cape seals, originating from the Cape region in South Africa, are another type that consists of a single chip seal layer followed by the application of a slurry seal, as illustrated in Figure 1.17(d). While the original method in South Africa used relatively large base aggregates (up to 19mm), implementations in North America and other regions typically use smaller-sized aggregates. Cape seals are known for their durability and offer shear resistance levels comparable to those of conventional asphalt surfaces. Three other types are the inverted seal, sandwich seal, and geotextile-reinforced seal, which are not commonly used (Sprayed Sealing Guide, 2004).

The choice of aggregate determines the thickness of a chip seal layer, as this surface treatment is designed to be only one stone thick. Typically, agencies select aggregates with a nominal size of 9.5 mm. Larger aggregate sizes create a rougher surface texture, which can lead to increased road noise and a bumpier ride. Moreover, using larger stones raises the risk of windshield damage due to loose aggregate being dislodged and projected by passing vehicles. The final aspect of aggregate selection involves choosing the type of stone to be used in the chip seal. Options include both natural and synthetic aggregates. At this stage, it is important

to note that transportation costs for suitable aggregates often constrain the choices available to the designer. However, since the aggregate serves a critical role in shielding the binder, which acts as a barrier against water penetration, it is recommended that designers perform a life-cycle cost analysis rather than relying solely on upfront price comparisons. This approach helps determine whether investing in a higher-quality aggregate is cost-effective over time. Once the aggregate is chosen, the binder design can then be addressed (Sprayed Sealing Guide, 2004).

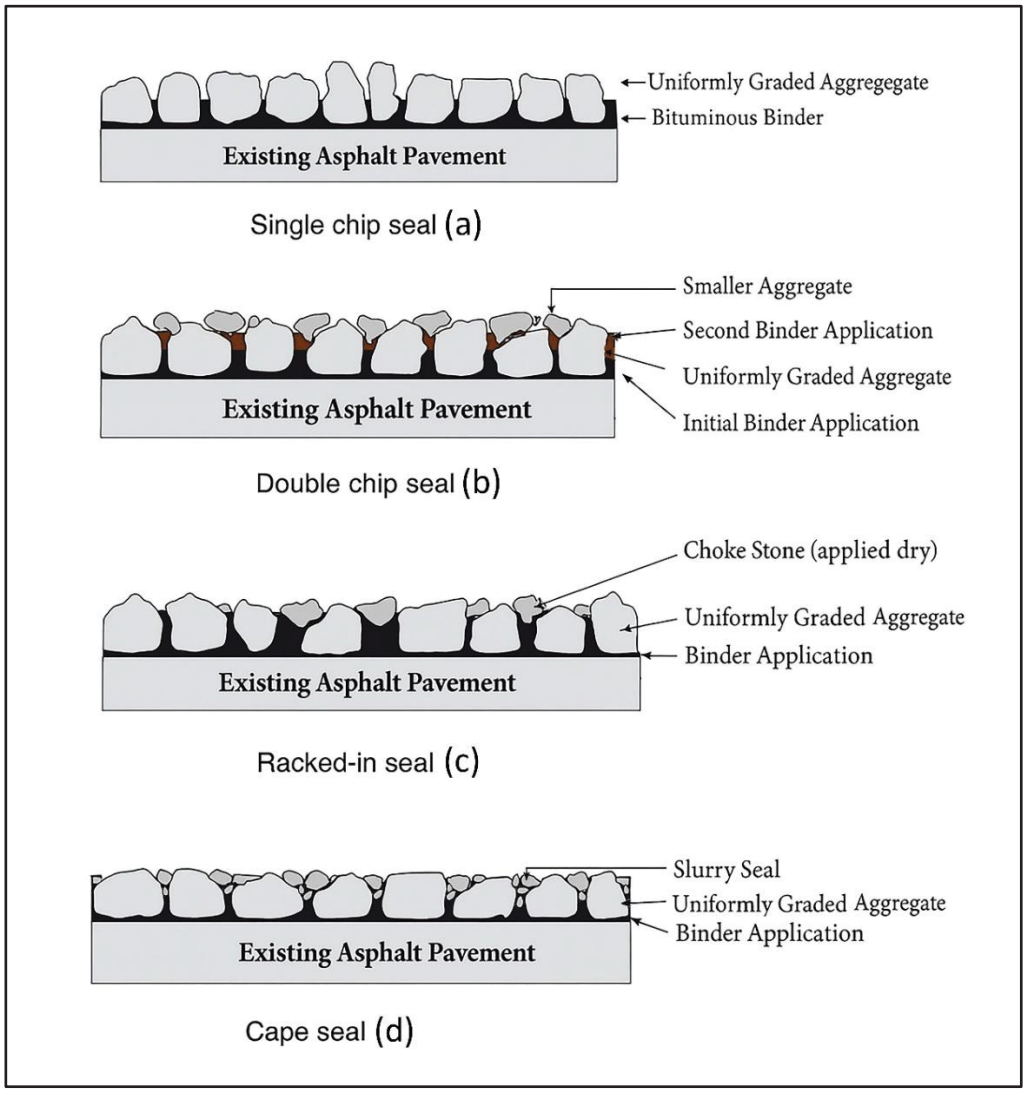

Figure 1.17 Different common chip seal types

Table 1.4 presents the different types of aggregates utilized in chip seal projects both in North America and internationally. Among these, limestone, granite, and natural gravel are the most

commonly used materials across North America. The majority of agencies in the United States and Canada do not apply precoating to chip seal aggregates. In contrast, all surveyed agencies from Australia, New Zealand, and South Africa confirmed the use of precoated aggregates with asphalt binder (Chip Seal Best Practices, 2005).

Table 1.5 Natural aggregates for chip sealing (Chip Seal Best Practices, 2005)

Aggregate type	North America (%)	Australia, New Zealand, United Kingdom, South Africa (%)
Limestone	37	13
Quartzite	13	38
Granite	35	38
Trap Rock	13	25
Sandstone	10	25
Natural Gravels	58	25
Greywacke, Basalt	4	88

Regarding the binder, chip seal projects primarily use two types of binders, asphalt binder and bitumen emulsion. The choice between them is influenced by climate and weather conditions. Key factors to consider in binder selection include surface temperature, aggregate properties, and regional climate at the time of construction (McLeod et al., 1969). Among environmental factors, ambient air temperature is critical, as it directly impacts the quality of the chip seal (Buss et al., 2016). In hot conditions, using a harder binder or emulsions can reduce the risk of bleeding. Conversely, in cooler weather, or when there is high humidity or moisture on aggregates and pavement surfaces, emulsified asphalts tend to perform better than hot-applied binders (Sprayed Sealing Guide, 2004).

Emulsified asphalts or bitumen emulsions consist of three components: asphalt cement, water, and an emulsifying agent (A basic asphalt emulsion manual, 1997). The emulsifier suspends the asphalt cement within the water. When the emulsion is applied, the water begins to evaporate, leaving behind residual asphalt that adheres to the aggregate. A critical challenge in working with emulsions is timing the application of aggregates. As the water evaporates, a process known as breaking, the binder changes color from brown to black. It is essential to

spread and roll the aggregate chips before the emulsion breaks. If the aggregate is applied too late, the effectiveness of compaction is significantly diminished, making it harder for the rollers to embed the chips properly (Gransberg and Zaman, 2005).

Emulsions are classified as either anionic or cationic, depending on the type of emulsifying agent. Cationic emulsions are generally preferred for chip seal applications because they tend to perform better in varying weather conditions, and they are electrostatically compatible with a wider range of aggregates (McHattie, 2001). These emulsions carry a positive charge, which allows them to be attracted to negatively charged aggregate particles, promoting quick and strong adhesion between the emulsion and the aggregate or pavement surface. As water reduces binder viscosity, emulsions can be applied at significantly lower temperatures than asphalt cement. Emulsions are typically classified by their setting time and viscosity. Cationic Rapid Setting (CRS) is one of the most common types of bitumen emulsion, which is used in North America. Specifically, CRS-2 has been used for chip seal preparation in Quebec, Ontario, British Columbia, Manitoba, Nova Scotia, and Saskatchewan (Chip Seal Best Practices, 2005).

The bond between aggregate and binder relies on several factors, the most important of which is aggregate type. This adhesion depends on mechanical, chemical, and electrostatic interactions (Yazgan, 2003). Factors such as aggregate surface dust, moisture levels, and the temperature of the binder during application can impact mechanical and chemical bonding. Electrostatic compatibility is also crucial; effective bonding occurs when the aggregate and binder possess opposite electrical charges (Sprayed Sealing Guide, 2004). Without this polarity difference, a strong bond may not form, leading to aggregate loss or raveling. Consequently, selecting locally available aggregate is essential in choosing the appropriate chip seal type, binder formulation, and construction approach. Additionally, aggregate porosity and surface moisture can affect how well the binder adheres (Gransberg, 2005). Besides, most aggregates, including brick, concrete, and glass, especially those with high silica content, can develop a negative electrostatic charge. This occurs because electrons tend to accumulate on the surface of the aggregate particles, resulting in a negatively charged surface (Behrens and Grier, 2001; Allahdin et al., 2015; Lee and Ahn, 2016). Therefore, using cationic bitumen emulsion is recommended for chip seal development. Moreover, there are more factors that can impact the

adhesion between the chip seal and asphalt pavement, and aggregate-binder adhesion. For instance, the presence of functional groups like carboxyl and hydroxyl in the binder can improve bonding through chemical interactions with the aggregate surface. So, modified binders or emulsions containing polar groups tend to form stronger adhesive bonds. Microscopic surface roughness improves the contact area between the binder and aggregate, reinforcing the chip seal adhesive bond (Yuan et al., 2024). Adequate aggregate embedment ensures sufficient resistance to dislodgement during service. High aggregate surface roughness and angularity increase mechanical interlocking between the binder and aggregates (Zheng et al., 2022). Another influential aggregate factor is porosity and absorptive behavior. Moderately porous aggregates can absorb part of the binder, enhancing the bonding surface area. However, overly porous aggregates may absorb too much binder, weakening the effective binder film. Hence, aggregates with balanced porosity, sufficient to allow limited binder absorption and increased bonding area, but not so high as to excessively absorb binder and weaken the effective binder film, are suitable for chip seal applications (Gransberg, 2005).

According to the main guideline for chip seal design and performance tests, the three main essential tests are texture depth measurements, skid resistance, and sweep tests (Chip Seal Best Practices, 2005; Wood et al., 2006; Buss et al., 2016). Some recent studies developed more tests for assessing the mechanical properties and durability of chip seals, including the interface bond and Vialit tests (You et al., 2019; Baran et al., 2025). Each of these methods plays a crucial role in evaluating chip seals, and they will be described in detail to highlight their specific objectives and procedures.

The sand patch method is a standardized procedure to assess the macrotexture of pavement surfaces by measuring the surface voids, calculated using a certain volume of fine material (Ottawa sand) based on ASTM E965 (ASTM E965, 2019). The test works on the principle that deeper surface textures retain more sand, thus allowing the calculation of mean texture depth (MTD) by spreading a certain amount of sand over the pavement surface and measuring the resulting diameter of the sand circle. The MTD is then calculated by the equation mentioned in ASTM E965. This test was selected in this thesis because it provides essential insight into the surface texture of chip seals constructed with different recycled aggregates such as concrete, brick, and glass. These materials can differ significantly from natural aggregates in

terms of shape, angularity, and texture, all of which directly influence macrotexture and surface performance. In chip seals, texture depth is also closely linked to aggregate embedment, an important indicator of proper aggregate retention and binder application. Achieving the recommended embedment range (typically 50–70%) ensures the chip seal provides adequate durability and skid resistance. Furthermore, surface texture plays a critical role in safety performance, particularly in Canadian climates, where snow and ice require pavements with sufficient macrotexture to maintain tire grip and minimize skidding risk. Thus, the sand patch test was selected not only to assess aggregate suitability, but also to verify adequate aggregate embedment and effective binder–aggregate interaction under conditions representative of regional performance requirements.

The performance of chip seals in terms of aggregate retention is evaluated using the sweep test, conducted in accordance with ASTM D7000 (ASTM D7000, 2019). In this procedure, asphalt felt disks with a 300 mm diameter are first cured at 50 °C for 48 hours, followed by 48 hours of curing at ambient temperature (23 °C ± 2 °C) to ensure flatness. Their weights were recorded prior to specimen preparation. The chip seal specimens are then prepared using the same material quantities and procedures as in the sand patch test. These specimens are cured at 35 °C for 4 hours before loose aggregates are gently removed using a brush, and their weights are recorded as the initial sample weights. The sweep test is then conducted using a modified mixer fitted with a nylon brush rotating at a certain rate for 60 seconds. After brushing off the dislodged aggregates, the final specimen weights are measured. Aggregate losses are calculated using the measured parameters and the equation mentioned in ASTM D7000. This test was selected in this thesis because aggregate retention is a direct indicator of chip seal durability: premature loss of aggregates leads to rapid surface degradation, reduced skid resistance, increased susceptibility to moisture damage, and accelerated need for maintenance or resealing. As a result, sweep test performance provides a practical measure of the long-term functional durability of chip seals used as surface treatments in Canada. Given that recycled aggregates may exhibit different bonding behavior due to variations in surface texture, angularity, size, and porosity, evaluating aggregate retention is particularly important under cold-climate conditions such as those in Quebec, where snowplowing and winter traffic impose

high mechanical stresses on the pavement surface. The sweep test simulates the mechanical action that pavements experience under traffic, evaluating how well each aggregate type remains bonded to the binder. This is critical for ensuring chip seal performance, safety, and maintenance efficiency under harsh Canadian weather and operational conditions.

Another essential test for evaluating the chip seal specification is the skid resistance test, which is assessed using the British Pendulum Tester (BPT) based on the ASTM E303 standard (ASTM E303, 2013). This test evaluates friction value, a key indicator of surface safety. According to the standard, specimens must measure at least 89 mm × 152 mm to ensure adequate contact with the pendulum slider. A 5 kg roller can be used to uniformly compact the aggregates. Curing of chip seal specimens can be performed in two stages: initially at 35 °C for 48 hours and then at ambient temperature (23 °C ± 2 °C) for an additional 48 hours, to ensure adequate water evaporation from the emulsion. As the skid resistance of chip seals is compromised in high temperatures due to softer bitumen, the chip seal specimens can be tested in higher temperatures (Gheni et al., 2017). Regarding one of the highest pavement temperatures in Canada, around 60 °C, this test is recommended to be done once the chip seal specimens are at this temperature (Mills et al., 2009; Gheni et al., 2017). The British Pendulum Test was selected for this thesis due to its ability to provide a quantitative measure of surface friction, which is critical for traffic safety, particularly under wet or high-temperature conditions. In Canada and especially Quebec, where climate extremes range from icy winters to hot summers, maintaining adequate skid resistance is essential to minimize the risk of vehicle skidding. Recycled aggregates of this study have different surface textures and bonding characteristics that directly influence friction. Additionally, traffic loads and elevated pavement temperatures may cause chip seal aggregates to shift, compromising surface grip. By evaluating skid resistance at both 23 °C and 60 °C, it can be ensured that the selected recycled aggregate types can provide safe, durable performance across the full range of seasonal and operational conditions in Canada.

One of the supplementary tests, which can be used to assess the adhesion and bond between the chip seal and asphalt pavement surface, is the interface bond test, which was designed by Michigan Technological University (You et al., 2019). This bond is crucial because inadequate adhesion can lead to premature stripping, making the chip seal ineffective as a pavement

preservation treatment. After preparing the asphalt mixture specimens coated with different chip seals, the interface bond strength can be measured using a Material Testing System (MTS). As bitumen has brittle behavior in the cold temperatures of Canada, this test can be done on specimens that are conditioned at -10 °C and 0 °C, as well as at the ambient temperature (23 °C ± 2 °C). This test was utilized in the thesis because the effectiveness and longevity of developed chip seals depend on the integrity of the bond at the interface with the existing asphalt surface. This is especially critical when using recycled aggregates, such as concrete, brick, and glass, for the first time, whose bonding characteristics differ significantly from natural aggregates due to surface texture, porosity, and chemical composition. Moreover, in Canadian climates, subzero temperatures can weaken the interface, leading to early deterioration. By testing at −10 °C, 0 °C, and 23 °C, realistic conditions were used in this study, determining which aggregate types can maintain strong adhesion under diverse weather conditions. The results will ensure that only aggregates with reliable performance across Canadian environmental conditions are considered suitable for chip seal applications, supporting pavement durability and cost-effectiveness in cold regions.

To evaluate the cold-climate performance of chip seals using recycled aggregates, which is necessary in the Canadian climate, the Vialit test was conducted according to BS EN 12272-3 (BS EN 12272-3, 2003). While this test does not directly measure the physicochemical mechanisms of bitumen–aggregate adhesion, it serves as a practical and standardized impact test to assess the retention of aggregate particles after mechanical shock, offering insight into the effectiveness of the adhesion system under simulated field-like stress conditions. Although the Vialit test is impact-based, it effectively evaluates functional adhesion, showing how well the aggregate remains attached to the binder under mechanical stress (BS EN 12272-3, 2003). Chip seals are exposed to traffic-induced stresses (such as tire impact, vibration). The Vialit test replicates one of the most damaging forces, which is direct impact (Adams et al., 2017). Good adhesion resists not only static forces but also dynamic forces such as shock or sudden dislodgment. Aggregates with poor adhesion are more likely to detach upon impact. Lastly, the number of retained aggregates provides a measurable indicator of the adhesive strength between the aggregate and binder, under conditions that closely simulate field performance

(Baran et al., 2025). In this thesis, this test was selected to assess the durability and practical performance of bitumen–aggregate adhesion in chip seals containing recycled aggregates under cold-climate conditions of Canada. Unlike molecular-scale adhesion tests, the Vialit test provides macro-level evidence of whether the bitumen can retain aggregate under impact, which is critical for evaluating chip seal reliability during harsh winters and snowplowing. The cold-temperature adaptation of this test enhances its relevance to Canadian contexts, where aggregate loss due to debonding can cause early chip seal failure.

1.8 Identified Research Gaps and Motivation for This Thesis

Despite the growing emphasis on urban heat island mitigation policies associated with asphalt pavements, after reviewing the relevant literature, several critical research gaps can be observed, especially in terms of an environmentally friendly and safe surface treatment that can enhance the reflectivity and minimize heat absorption. The other would be a lack of specially designed pavement structures, which can reduce its temperature with minimal emission of heat into the ambient air. Therefore, this study aims to address these gaps by proposing some novel pavement structures made of recycled materials that can both minimize the heat absorption and heat release, alleviating the UHI effects.

1.8.1 Lack of Research on Chip Seals for Enhancing Reflectivity

Current methods for increasing pavement surface reflectivity, particularly in UHI mitigation strategies, rely on reflective surface coatings. While these chemical treatments can initially increase albedo, they suffer from critical limitations, including reduced durability under traffic and weather exposure, high maintenance costs, and most notably, a negative impact on surface friction, which compromises skid resistance and road safety. These drawbacks present a significant challenge in developing sustainable and safe reflective pavements, minimizing the heat absorption of pavements. Although chip seals are known as preventive or corrective pavement maintenance methods in North America, their effectiveness on the UHI mitigation has not been investigated. Unlike the chemical coating, chip seals increase the skid resistance and pavement service life, providing a safe solution to increase the reflectivity of pavements. More importantly, some construction and demolition waste materials cannot be recycled, and

they could be used as chip seal aggregates to increase the surface reflectivity and proposing a new way to reuse these waste materials. Therefore, this study addresses a critical gap by investigating the feasibility of using CDW (concrete, brick, and glass) chip seals to simultaneously improve surface reflectivity, mechanical performance, and environmental sustainability under Canadian climate conditions. It represents a novel approach by integrating reflective design objectives with recycled material applications in chip sealing, an area that has received no attention in previous research.

1.8.2 The Overlooked Role of Asphalt Mixture and Base Course Interface

Another important overlooked subject is the role of the asphalt mixture–base course interface in heat transfer in the pavement and its impacts on UHI effects. As the asphalt pavement can store thermal energy during the day, if the vertical downward heat transfer rate to the base course and subgrade is low due to discontinuity or air voids at the interface, higher thermal gradients between the surface of the pavement and the surrounding air exist, emitting more heat to the ambient air. So, investigating the interface and its effects on the heat dissipation and asphalt mixture temperature reduction is of great importance, which has been neglected in previous studies. Besides, the heat transfer to the layer below can be enhanced using normal or conductive prime coats, which have not been investigated. Therefore, the use of prime coats or thermally conductive asphalt mastic at the interface may play a transformative role in managing subsurface heat storage and facilitating faster thermal dissipation. Conductive prime coats, made of conductive materials such as steel slag powder, might act as thermal bridges, reduce heat entrapment, and accelerate surface cooling, contributing to UHI mitigation. Overall, current pavement research and design guidelines typically overlook such design possibilities.

1.8.3 Neglected Role of Base Course for Heat Dissipation in Pavement

A critical overlooked opportunity for UHI mitigation lies in the thermal management of the pavement's subsurface layers, specifically, the base course. Most UHI reduction efforts concentrate on altering surface reflectivity, and they rarely consider strategies to actively dissipate the absorbed heat from the surface to deeper layers. Although some studies have

focused on developing conductive asphalt mixtures to transfer the absorbed and stored heat to the base course and subgrade (Cong et al., 2014; Vo et al., 2017; Chen et al., 2020; Jiao et al., 2020b), the effect of using a conductive base course to facilitate the heat dissipation in pavement depths has not been evaluated. The asphalt mixture composition has the highest impact on emitting heat into the ambient air due to its direct exposure. However, considering pavement as a system comprised of multiple layers and the role of each layer in dissipation of the absorbed heat may contribute to UHI mitigation effectively. One promising approach can be the integration of thermally conductive materials in the base course, which can facilitate faster heat transfer from the asphalt concrete layer to the subgrade, thereby reducing surface temperatures. Such an approach could minimize the nighttime heat release from pavements due to a lower thermal gradient between the pavement surface and its ambient air. Nevertheless, the concept of using conductive base materials as a thermal channel has not been integrated into current pavement design policies or UHI mitigation strategies. There are some conductive waste materials or industrial by-products, among which, steel slag aggregates may offer both high thermal conductivity and mechanical strength.

1.9 Compliance of Selected Materials with Canadian Road Construction Standards

Some CDW materials, including recycled concrete, clay bricks, and glass, are used as chip seal aggregates in this study. Since these materials have never been used before for chip seal development, there is no recommendation or prohibition of using them in Canadian road construction guidelines. However, in terms of mechanical and environmental aspects, the usage of these materials has been reviewed for road construction. Based on Bureau de normalisation du Québec (BNQ) 2560-600 standard, recycled concrete is allowed and recommended with proper processing and quality control for road construction. Moreover, recycled brick can be used in lower percentages (less than 30% of the total aggregate mix), but it is less favored due to durability issues (BNQ 2560-600, 2024). Although the utilization of glass aggregates has not been mentioned in relevant standards in Quebec, such as Ministère des Transports du Québec (MTQ), the use of recycled glass in asphalt mixture has been investigated in previous research done in the LCMB research group at École de technologie supérieure (ÉTS) in Montreal, Canada (Lachance-Tremblay et al., 2016). The usage of Electric

Arc Furnace (EAF) steel slag for road construction in Quebec is recommended in accordance with the BNQ standards. Regarding Canadian regulations, the Transportation Association of Canada (TAC) specifically provides comprehensive guidelines for using these recycled materials. There is color coding for these materials based on technical and environmental factors. The green highlight signifies that the material is currently both technically and environmentally suitable to replace natural aggregate. The yellow highlight suggests that the material has potential for use; however, certain technical, environmental, or economic concerns need to be addressed. The red highlight means that while the material may have been previously tested or considered viable, major technical, environmental, or economic challenges currently prevent its use. This information is presented in Table 1.5 (Transportation Association of Canada, 2013). Therefore, these recycled materials can be used for road construction as all of them are reported in green and yellow categories. The significant parts of the literature review and research advancements are summarized in Tables 1.6 and 1.7.

Table 1.6 Recycled materials used in Canada as substitutes for natural aggregates (TAC, 2013)

Recycled or By-product Material	Asphalt Concrete	Concrete Pavement	Granular Base and Subbase
Reclaimed Concrete Material	Yellow	Green	Green
Waste Glass	Yellow	Yellow	Green
Steel Slag	Yellow	-	Yellow
Bricks	Yellow	-	Green

Table 1.7 Summary of literature review and research advancement

Sections	Focus of the literature review	Key findings from this literature review	Research advancement
1.1 Introduction to urban heat islands	Defining the UHI phenomenon and identifying asphalt pavements as one of the major contributors to elevated urban temperatures.	Urban areas are typically 5–15 °C warmer than surrounding regions due to some human inventions, such as low-albedo Pavements, accounting for 30–40 % of urban areas.	Establishing the problem scope: Modified pavement systems can reduce UHI intensity.
1.2 Primary causes of UHI	Reviewing urbanization, low-albedo surfaces, anthropogenic heat sources, and loss of vegetation.	Population growth, dense construction, and air-conditioning exhaust amplify surface heat retention and limit natural cooling.	Highlights the need for material-based cooling strategies in highly built environments where vegetation solutions are limited.
1.3 Problems of UHI effects	Evaluating health, energy, and infrastructure consequences of UHIs	UHIs increase mortality during heat waves, raise building-cooling demand, and accelerate pavement rutting, cracking, and binder aging	Supporting the societal and economic importance of thermally resilient pavements
1.4 Mechanisms of heat transfer	Explaining radiation, conduction, convection, and thermal storage processes	Albedo and thermal conductivity are the dominant parameters influencing pavement temperature	Enhancing surface reflectivity and subsurface heat conduction
1.5 Influence of pavement materials	Discussing the effects of aggregate type, density, color, and air-void content	Light-colored, dense, conductive materials, and a lower surface temperature	Supporting the use of CDW for higher reflectivity and steel slag for improved conductivity

Table 1.7 Summary of literature review and research advancement (continued)

Sections	Focus of the literature review	Key findings from this literature review	Research advancement
1.6 Existing UHI mitigation approaches	Summarizing reflective, water-based, and thermally modified pavements	Reflective coatings reduce surface temperature; water-cooling is location-specific; conductive pavements show high potential	Filling the research gap by integrating both reflective (surface) and conductive (subsurface) cooling mechanisms
1.7 Experimental techniques	Compiling testing standards for mechanical and thermal evaluation	Significant tests: reflectance, thermal properties, solar simulation, and skid-resistance measurement	Forming the experimental foundation of this thesis, ensuring consistency with international testing practices
1.8 Research gaps and motivation	Identifying deficiencies in prior studies	(1) Limited research on reflective chip seals, (2) Neglected interface heat transfer, (3) Overlooked conductive base-course role	Defining this research's novelty: dual enhancement of surface and subsurface thermal performance using recycled and conductive materials
1.9 Material standards in Canada	Reviewing the compliance of materials with Canadian pavement specifications	Recycled aggregates (CDW, steel slag) meet Transport Canada and TAC requirements for road construction	Confirming the feasibility of applying the developed materials under Canadian climatic conditions.

In this chapter, the main mechanisms, materials, and experimental approaches related to the thermal behavior of asphalt pavements and their contribution to the urban heat island effect were reviewed. The literature shows that low-albedo asphalt surfaces absorb and retain large amounts of solar radiation, resulting in higher surface temperatures and increased nighttime heat release. Although different mitigation strategies have been proposed, including reflective coatings, high-albedo surfaces, water-retentive pavements, and conductive additives, most of these studies have addressed the UHI, focusing on the surface layer, without integrating both surface and subsurface thermal management. More importantly, limited attention has been given to the role of the interface between asphalt mixtures and base course materials in heat dissipation, or to the use of recycled materials in reflective surfaces like recycled chip seals. These gaps highlight the need for approaches that combine surface reflectivity enhancement with efficient subsurface heat transfer. Accordingly, this research aims to develop novel pavement structures using recycled chip seals to increase surface reflectivity and conductive base and prime coats to promote downward heat flow, mitigating UHI effects while maintaining mechanical and safety performance.

CHAPTER 2

PROBLEM DESCRIPTION AND OBJECTIVES

2.1 Problem Statement

Asphalt pavements exacerbate an environmental issue called urban heat islands (UHI). This means that the dark surface of asphalt pavements absorbs solar energy and releases this heat into the air, increasing the air temperature, especially at night. The higher temperature of cities can bring about some problems, including higher energy consumption due to cooling demands, increasing costs, dropping air quality and life comfort, heat-related illnesses, and more water consumption. UHI effects are also believed to contribute to global warming and heat waves (Ichinose et al., 2008; Hatvani-Kovacs et al., 2016; Shamsaei et al., 2022).

In addition to this significant environmental issue, construction and demolition waste (CDW) has been increasing throughout the world. China generated 1704×10^6 tons of CDW due to urbanization in 2018 (Zhang et al., 2022). Nevertheless, less than 10% of this waste can be recycled in China (Huang et al., 2018). The USA and Europe produced approximately 600×10^6 and 372×10^6 tons of CDW, respectively (Zhang et al., 2022). Regarding Canada, a considerable amount of CDW (27% of municipal solid waste) is generated annually, mostly discharged into landfills (Yeheyis et al., 2013). The total CDW generation is more than 10 billion tons in the world (Molla et al., 2021). The recycling rate of CDW material is less than 10% and most of them are usually discharged to landfills (Menegaki and Damigos, 2018). Some of these materials can be used for surface treatment of asphalt pavements, such as chip seals, to increase their surface reflectivity, mitigating the UHI Effects.

Besides CDW materials, the generation of some industrial by-products, such as steel slag, is high, demanding new approaches for reusing and recycling these materials. Using steel slag aggregates in the surface, base, and subbase layers of pavements has been increasing in recent years. The US, Japan, and Europe use approximately 41%, 32%, and 70% of this industrial by-product material as road construction aggregates (Nippon Slag Association, 2016; Liu et al., 2022). However, the effects of this recycled aggregate as base course aggregates and the UHI have been neglected.

This research aims to address the challenge of UHI mitigation using recycled materials, which is a sustainable waste management policy through an innovative, thermally efficient pavement design utilizing CDW and steel slag aggregates.

2.2 Deficiencies in Current Relevant UHI Mitigation Approaches

The current methods for increasing the surface reflectivity of pavements and in-depth heat dissipation of pavement structures for UHI mitigation have shortcomings. Regarding the enhanced surface albedo methods, most of them use chemical coatings, which have some issues, including lower skid resistance and durability, chemical and high maintenance costs. These safety, environmental, and maintenance problems have made these methods impractical for real-world applications. Chip seals, which can even increase the skid resistance and extend the pavement service life, have not been investigated for alleviating the UHI effects. Despite the proven mechanical applicability of CDW aggregates for chip seal construction, their reflective and thermal properties have not been examined.

The other previous studies mostly focused on the asphalt mixture mix design to mitigate the UHI effects, using insulation or conductive materials. Although increasing the surface reflectivity reduces the heat absorption, asphalt pavements still absorb some heat, which can be released during the night when the air temperature is lower than the pavement temperature. Hence, considering the whole pavement structure is vital to proposing a practical solution for the UHI. Considering the pavement as a system, the important role of the asphalt mixture and the base layers' interface can be captured for UHI mitigation. Besides, the base course materials and their role in transferring the absorbed heat to the subgrade and cooling the asphalt mixture layer, contributing to UHI mitigation, have been neglected in current approaches. Therefore, the potential of some conductive by-products, such as steel slag aggregates, as base course materials has not been evaluated for alleviating the UHI effects.

Considering all the aforementioned issues of the current methods for mitigating the UHI effects associated with asphalt pavements, finding practical solutions that can be applied to all existing pavements in urban areas is of great importance.

2.3 Research Questions and Hypotheses

This thesis is driven by some critical research questions, which will be mentioned in this section. Answering this question can reveal novel pavement structures, which can reduce urban air temperatures.

- Can chip seals increase the surface reflectivity of asphalt pavements and reduce their temperature? Can CDW materials be used as chip seal materials?
- Are there any restrictions on using CDW as chip seal materials? Can all of the employed CDW materials be used for all traffic loads?
- How do CDW materials change the surface reflectivity, albedo, and pavement temperature?
- Can CDW materials mitigate the UHI effects?
- What is the role of the interface between the asphalt mixture layer and base course in terms of temperature reduction of the surface layer?
- How should the interface be modified to transfer the absorbed heat more efficiently to the base course as a UHI mitigation policy? Can this modification contribute to UHI mitigation? What kind of materials can be used for this purpose?
- Do base course materials play an important role in pavement temperature reduction? Can conductive materials, such as steel slag, enhance the heat dissipation in pavement depth to mitigate the UHI? What are the optimum percentages of steel slag for prime coat and base course preparation? What are the effects of these materials on the UHI?
- What is the proper pavement structure that can minimize heat absorption and release the least amount of heat into the ambient air?

This research is guided by two testable hypotheses investigated through comprehensive laboratory testing. The first hypothesis is that the application of chip seals incorporating selected construction and demolition waste (CDW) materials increases pavement surface reflectivity, thereby reducing solar heat absorption and mitigating urban heat island (UHI) effects. The second hypothesis is that enhancing thermal conduction at the pavement interface promotes heat transfer into the base course, where higher volumetric heat capacity enables

greater heat storage, resulting in lower surface temperatures and reduced heat release to the ambient air. The combined effect of these mechanisms is hypothesized to produce pavement structures with reduced surface heating and improved UHI mitigation performance.

2.4 Research Objectives

The objective of this research project is to develop cool asphalt pavement structures to mitigate the impact of pavements on UHI using recycled materials. For this aim, some important parameters, including surface reflectivity, thermal properties, the interface between the asphalt concrete and the base course, and the base course, are modified using recycled materials. The effects of developed pavement structures on the UHI are then evaluated with laboratory and field methods.

Therefore, the first main objective is to assess the effect of increasing pavement surface reflectivity of asphalt pavements to minimize heat absorption and reduce the surface and in-depth temperatures. For this purpose, novel chip seals are developed with recycled materials. The durability, safety, and mechanical properties of the developed chip seals are also investigated to propose a practical solution. In the next step, reflectivity, albedo, surface, and in-depth temperatures of asphalt pavement coated with chip seals are assessed employing laboratory and field methods. These experimental results are then analyzed in terms of UHI mitigation. Therefore, this objective is to minimize heat absorption and reduce the pavement temperature, providing lower thermal gradients with the surrounding air. Although enhancing the surface reflectivity reduces heat absorption, some solar energy is still absorbed and stored in the asphalt mixture layer. This shows the necessity of the second main objective, which will be explained in this section.

The second main objective is to examine the role of subsurface thermal transfer by transferring the absorbed and accumulated heat in the asphalt mixture layer to the layer below, reducing the thermal gradient between the surface of the pavement and its surrounding air and outgoing heat flux. For this aim, the effects of the asphalt mixture and base course interface on the heat transfer to the base course and UHI are evaluated using conventional prime coats. A conductive prime coat containing a recycled by-product is then developed to facilitate heat transfer at the

asphalt mixture and base course interface and reduce the asphalt mixture temperature. Subsequently, the base course heat transfer rate is improved using conductive aggregates to transfer the pavement's absorbed heat into the subgrade and to reduce asphalt mixture temperature. In addition to the UHI mitigations, these solutions can also propose novel methods to recycle construction and demolition waste (CDW) and industrial by-products as road construction materials.

2.5 Research Plan and Methods

Understanding the heat transfer process, thermal parameters, and previous and current methods for mitigating UHI effects, and the research gap in the previous research is of great importance. Therefore, in Chapter 1, a literature review of UHI effects, causes, problems, heat transfer mechanisms in pavements, the role of pavement materials in heat transfer, common UHI mitigation methods, experimental techniques for UHI studies, and research gaps and compliance of recycled materials with the Canadian pavement construction guideline is investigated. After being aware of current methods, challenges, and problems, some hypotheses were made. Firstly, the surface reflectivity and albedo of asphalt pavement can play an important part in temperature reduction and heat absorption. Hence, some novel chip seals were developed using recycled CDW materials to enhance surface reflectivity and minimize heat absorption, presented in Chapter 3.

In Chapter 3, the chip seal mix designs, mechanical properties, safety, and durability of these layers were evaluated to propose a practical solution. In detail, different laboratory tests, including sand patch, sweep, the British Pendulum tester (BPT), interface bond, and Vialit tests, were conducted to evaluate the mechanical properties, durability, and safety of the developed chip seals in different weather conditions. After evaluating the durability and safety of the developed chip seals for real-world projects, the effects of these chip seals on the surface and in-depth temperatures, reflectivity, albedo, and nighttime heat release of asphalt pavements were investigated using different laboratory and field methods. Regarding the laboratory methods, UV-Visible-NIR spectrometer reflectance, a trident thermal properties measurement equipped with an MTPS sensor, and a solar simulation cooling effect laboratory setup were

used. The albedo and cooling effects of the developed chip seals were also assessed with a pyranometer and thermocouples through a field experiment. Once the asphalt heat absorption is reduced, the next phase of the thesis was done in Chapter 4, which is transferring the absorbed heat of the asphalt mixture to the base course and subgrade, causing less thermal gradient between the asphalt mixture layer and its surrounding air to mitigate the UHI.

In Chapter 4, the role of the interface between the asphalt mixture layer and the base course, and the base course thermal conductance modification, is evaluated. In detail, first, the impacts of using a prime coat at the interface to facilitate the heat transfer from the asphalt mixture to the base course and surface temperature reduction were examined. Steel slag, as a conductive material, was then used to prepare a conductive prime coat and a base course to develop pavement structures with conductive in-depth heat channels. Thus, two novel pavement structures were developed to mitigate the UHI effect. The first structure consists of a conventional asphalt mixture with a conductive prime coat and a conventional base course. The second one comprises a conventional asphalt mixture and a conductive base course without a prime coat. The physical and mechanical properties of the developed base course were first evaluated by modified Proctor compaction and California Bearing Ratio (CBR) tests. The two developed pavement structures, including control asphalt mixture specimens, were placed in a solar simulation setup, including an infrared lamp, insulation foams, thermocouples, and a heat flux sensor. Besides, the thermal properties of the developed conductive base course and prime coat were also investigated with the C-Therm device using two MTPS and TLS sensors. The research outline of this thesis is demonstrated in Figure 2.1.

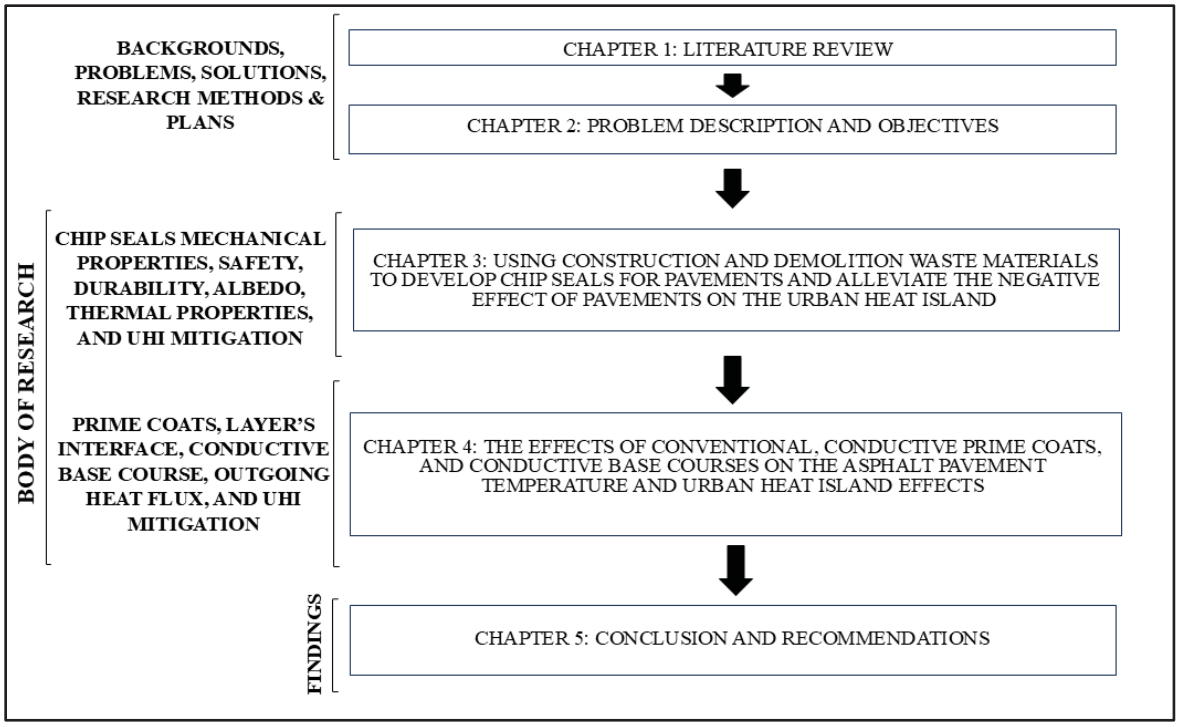

Figure 2.1 The thesis outline

Overall, the two main objectives of this thesis were to minimize the heat absorption and transfer the absorbed heat to the layers below to utilize the higher thermal capacity of the base course and subgrade. Both of these purposes result in cooler pavement surfaces, providing a lower thermal gradient between the pavement surface and its surrounding air, alleviating the UHI effects. The correlations between different chapters and the research plan are shown in Figure 2.2

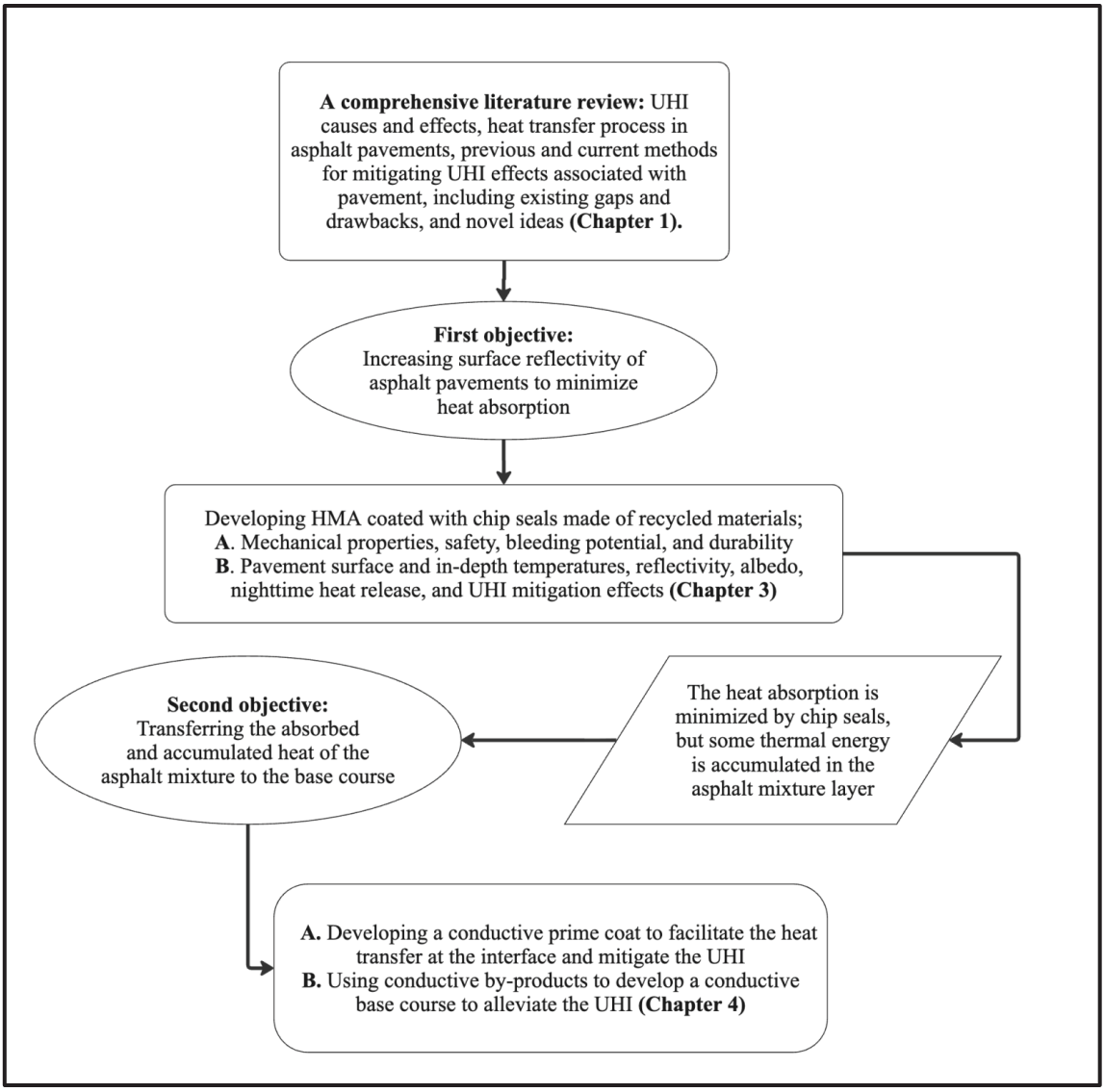

Figure 2.2 The correlation between different chapters and the research plan

CHAPTER 3

USING CONSTRUCTION AND DEMOLITION WASTE MATERIALS TO DEVELOP CHIP SEALS FOR PAVEMENTS AND ALLEVIATE THE NEGATIVE EFFECT OF PAVEMENTS ON THE URBAN HEAT ISLAND

3.1 Introduction

Asphalt pavements can exacerbate the urban heat island (UHI) effects due to their potential for absorbing and storing solar energy during the day and releasing this absorbed heat to the ambient air, since pavement temperature is higher than its surrounding temperature. Based on the discussion in Chapter 1, surface reflectivity and albedo of pavements play an important part in temperature reduction and heat absorption. Chip seals, due to the exposure of aggregates on the pavement surface, can be a practical solution to increase the surface reflectivity if developed with light-color aggregates. Hence, in this chapter, some novel chip seals were developed using construction and demolition waste (CDW) materials, including recycled concrete, two different clay brick, and glass aggregates. Chip seals are known as a cost-effective pavement correction or prevention maintenance method. Chip seals involve spraying a layer of asphalt emulsion or asphalt binder on the existing pavement surface, followed by the application of aggregate compacted by a roller. The result skid-resistant surface that extends pavement life, seals minor cracks, and improves the safety of the roads (Montoya et al., 2017; You et al., 2019). In general, chip seal aggregates are natural stones such as granite, basalt, or limestone, owing to their strength and durability (Serigos et al., 2017). However, the environmental impact of extracting and transporting virgin natural aggregates, as non-renewable resources, has raised concerns about the long-term sustainability of using them.

In response to the growing demand for environmentally friendly road construction materials in recent years, CDW has emerged as a suitable alternative aggregate source. These materials have high rates of generation and low rates of recycling, mostly discharged into landfills (Ulubeyli et al., 2017; Menegaki and Damigos, 2018). In Canada, CDW materials form 27% of municipal solid waste, almost 59% of which is concrete and brick waste materials, mostly

accumulated in landfills (Umar et al., 2017; Yeheyis et al., 2013). Some waste clay bricks, accumulated in a landfill in Montreal (Canada), are shown in Figure 3.1.

Figure 3.1 Waste clay brick (3RMCDQ landfill in Montreal)

Utilizing these materials in chip seals has a dual benefit. Firstly, it reduces waste from landfills and reduces the need for virgin aggregate extraction, promoting the circular economy and sustainable development. More importantly, certain CDW materials, such as crushed concrete and bricks, can increase the surface reflectivity due to a lighter color than asphalt if used as chip seal aggregates, making them a suitable option to combat the UHI effects. Thus, by using high-albedo CDW aggregates for developing chip seals, it may be feasible to decrease pavement surface temperatures and mitigate UHI effects without compromising surface performance and safety of roads.

In this chapter, the feasibility of using CDW aggregates in chip seal applications is evaluated based on a combination of mechanical performance, safety, durability, and thermal effectiveness criteria. Specifically, feasibility is assessed through laboratory and field testing of aggregate retention, skid resistance, surface texture, reflectance, albedo, and pavement temperature response. By examining these performance indicators, the study determines

whether high-albedo CDW aggregates can reduce pavement temperatures and mitigate UHI effects without compromising surface performance or road safety. Unlike common current approaches that rely on surface coatings or pigments, which can reduce skid resistance and lead to higher maintenance costs, this chapter proposes a new strategy that enhances both surface reflectivity and friction while also sealing existing pavement cracks and extending pavement life. This chapter includes two different types of testing. The findings of this research serve as a critical step toward developing sustainable and thermally efficient asphalt pavements for cooling urban environments.

Regarding the first stage, the mechanical performance and feasibility of using certain CDW materials, including recycled concrete, clay bricks, and glass as complete replacements (100%) for conventional chip seal aggregates, were evaluated. A cationic rapid-setting bitumen emulsion (CRS-2) is utilized as the binder. Since these recycled materials have not previously been employed as complete replacements for conventional chip seal aggregates, an expanded set of experimental tests was required to verify their mechanical performance, adhesion, and durability under service conditions. Accordingly, both essential and supplementary experimental tests were conducted to ensure that the developed chip seals meet performance and safety requirements under Canadian climatic conditions (Chip Seal Best Practices, 2005; Wood et al., 2006; Buss et al., 2016; You et al., 2019; Baran et al., 2025). These tests include the sand patch test, sweep test, British Pendulum Tester (BPT), interface bond test, and Vialit tests, which will be explained in this chapter. These tests provide insightful results on how the developed chip seals behave under both hot and cold climatic conditions of Canada.

In the second stage, both laboratory and field experiments were conducted to evaluate the reflectance, albedo, and cooling effects of the developed chip seals. Laboratory testing included utilizing a spectrometer to assess reflectivity across ultraviolet (UV), visible, and near-infrared (NIR) wavelengths, measurements of thermal properties of materials using the C-Therm trident device equipped with an MTPS sensor, and infrared solar simulation tests. Field testing involved albedo measurements using a pyranometer, and surface and internal temperature monitoring using infrared imaging and thermocouples. These experimental

methods can reveal how these chip seals impact the pavement reflectivity, temperature reduction, and UHI mitigation. The outline of this chapter is shown in Figure 3.2.

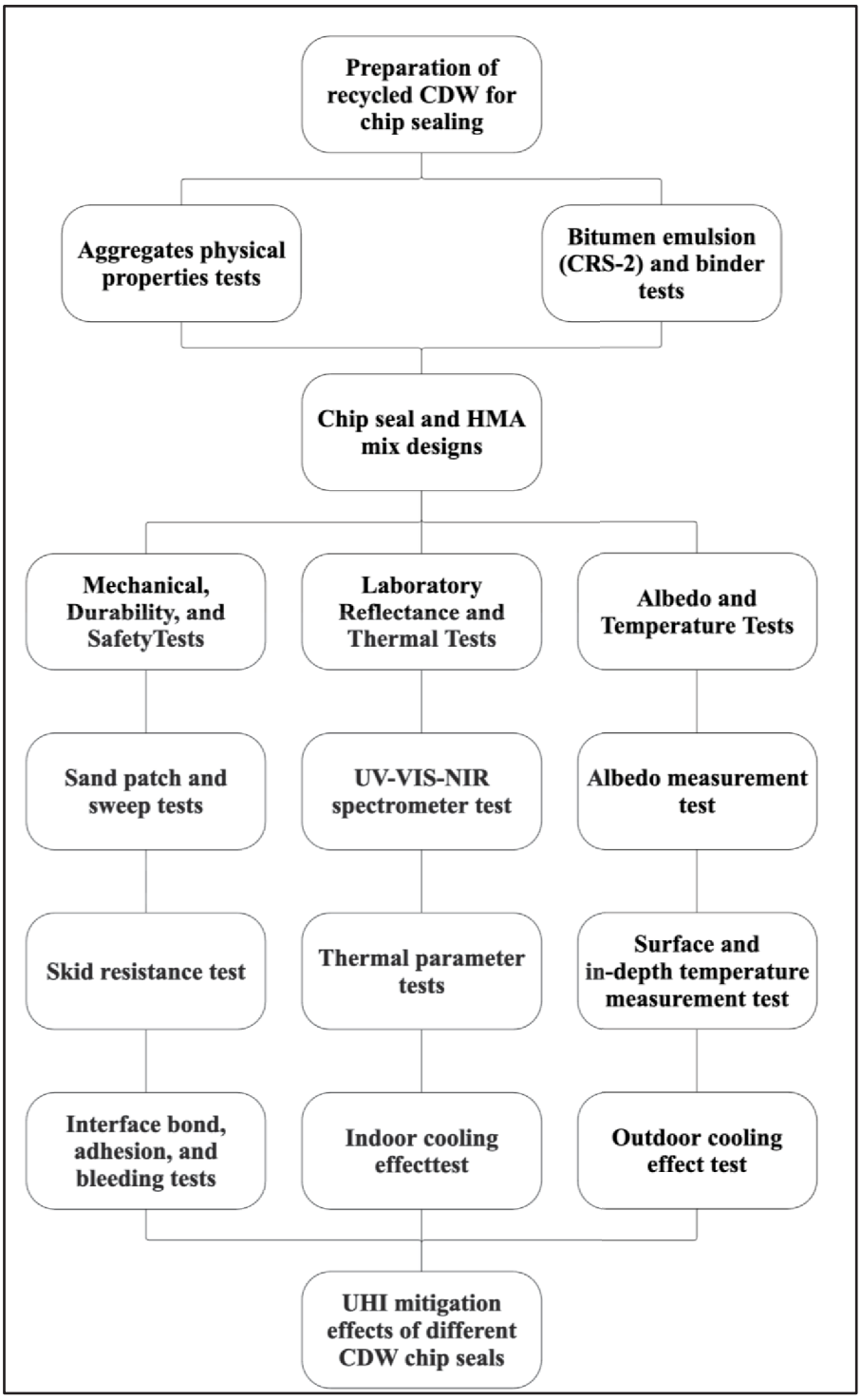

Figure 3.2 The outline of Chapter 3

3.2 Materials and Methods

3.2.1 Materials

Chip seals consist of aggregates applied on a layer of bitumen emulsion. In this research, four types of recycled aggregates, including concrete, yellow brick, red brick, and glass, were utilized. The reason for choosing these materials was their lighter color compared to conventional pavement surfaces. The local waste materials were sourced from the Association of Building and Demolition Materials Collectors and Recyclers of Quebec (3RMCDQ) in Canada. The materials were received in bulk form and subsequently crushed under controlled laboratory conditions. Initial size reduction was performed manually using a hammer, followed by further crushing with a laboratory jaw crusher (Model: Pulverisette 1), shown in Figure 3.3. The crushed aggregates were then sieved to obtain the required size fractions.

Figure 3.3 The Laboratory Jaw Crusher for aggregate preparation

The crushed forms of these materials at their application sizes are demonstrated in Figure 3.4. The clay bricks (both yellow and red) and recycled concrete were used as single-size coarse aggregates with a maximum size of 10 mm. Since all these materials were crushed using the same machine, aggregate gradations were relatively similar. Single-size gradations were selected to comply with common chip seal design practices and to isolate the effect of aggregate type on mechanical and thermal performance, avoiding additional variability associated with blended gradations.

The glass aggregates, however, were smaller, ranging from 2.36 mm to 6.3 mm. This size difference is because larger glass particles were more likely to be flaky and unsuitable for use based on chip seal standards (Chip Seal Best Practices, 2005).

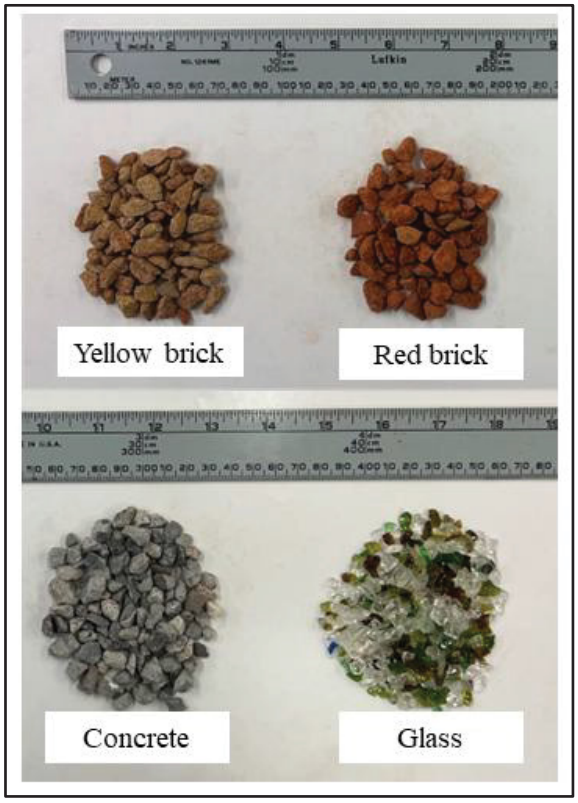

Figure 3.4 Crushed materials used in this study

The physical characteristics of all selected materials were examined based on relevant standards. Additionally, chemical composition was analyzed using the X-ray fluorescence

(XRF) technique, summarized in Tables 3.1 and 3.2, respectively. The chemical compositions were used for understanding the chemical stability and adhesion with bitumen.

Table 3.1 Physical properties of aggregates

Properties	Standard	Concrete	Yellow brick	Red brick	Glass
Density (kg/m^3)	(ASTM C127, 2015)	2369	1932	1906	2490
Loose unit weight (kg/m^3)	(ASTM C29/C29M, 2017)	1513	1116	1121	1485
Water absorption (%)	(ASTM C127, 2015)	4.7	13.55	14.12	0.15
Los Angeles (%)	(ASTM C131/C131M, 2020)	23	39	41	44
Flakiness index (%)	(ASTM D4791, 2019)	15	20	22	31
Median particle size (mm)	(ASTM C136/C136M, 2019)	6.5	6.7	6.8	4.7

Table 3.2 The chemical composition of aggregates

Chemical Composition (%)	Concrete	Yellow brick	Red brick	Glass
SiO_2	34.97	59.03	62.07	73.30
Al_2O_3	7.34	14.53	16.14	1.68
Fe_2O_3	3.31	6.44	5.07	0.38
CaO	47.19	11.90	5.45	11.41
MgO	1.90	2.44	3.38	1.11
SO_3	1.17	0.61	0.68	0.14
K_2O	1.47	2.80	3.69	0.50
Na_2O	1.34	1.10	2.34	10.70
TiO_2	0.40	0.72	0.75	0.04
P_2O_5	0.13	0.12	0.16	0.02
LOI	0.78	0.31	0.27	0.72

The characteristics of the Cationic Rapid Setting Type 2 (CRS-2) bitumen emulsion used in all chip seal specimens, provided by the supplier, are outlined in Table 3.3. This type of emulsion

is widely recognized as a standard material for chip seal applications in Canada (Chip Seal Best Practices, 2005). According to the supplier's specifications, the recommended application temperature ranges between 60°C and 85°C. Therefore, a consistent temperature of 65°C was maintained for the bitumen emulsion during specimen preparation for all specimens. Besides, to evaluate water breakout behavior, the emulsion's weight loss was measured at 35°C, as illustrated in Figure 3.5. As seen, the bitumen emulsion lost almost 25% of its weight after 6 hours of curing and 30% weight after 24 hours of curing due to water breakout. Therefore, the curing time of chip seal specimens should be 24 to 48 hours at 35°C.

Table 3.3 The characteristics of bitumen emulsion

Tests	Unit	Test method	Result For CRS-2	Specifications	
				Min	Max
Residue by distillation (by weight)	%	(ASTM D6997, 2020)	69	65	-
Oil distillate (by volume)	%	(ASTM D6997, 2020)	0.3	-	3
Demulsibility	%	(ASTM D6936, 2017)	85	40	-
Saybolt Furol viscosity at 50 °C	Sec	(ASTM D7496, 2018)	223	100	400
Settlement and storage stability, 1 day	%	(ASTM D6930, 2019)	0.31		1
Penetration, 25°C, 100 g., 5 s.	0/1mm	(ASTM D5, 2013)	153	100	250
Particle Charge	-	(ASTM D7402, 2017)	Positive	-	-
Ductility, 4°C, 5 cm/min	cms	(ASTM D113, 2017)	75	40	-
Solubility in TCE	%	(ASTM D2042, 2015)	99.5	98.5	-

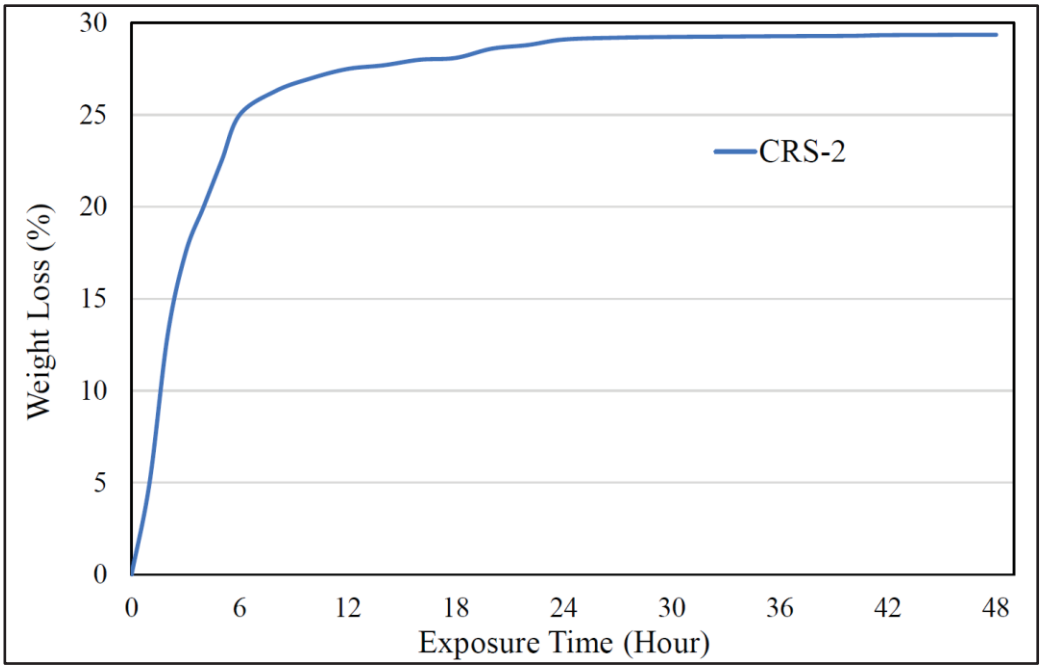

Figure 3.5 The bitumen emulsion's weight loss during curing

3.2.2 Chip Seal Mix Design

Although there is currently no unified standard for chip seal design across North America, in both academic research and practical applications in the United States and Canada, several methods are commonly employed, including the McLeod, Kearby, modified Kearby, and modified McLeod approaches (Kearby, 1953; McLeod et al., 1969; Stockton and Epps, 1975). Among all these methods, the modified McLeod is the most popular method in Canada (Chip Seal Best Practices, 2005). The chip seal design was conducted using the modified McLeod method, a procedure derived from the Minnesota Seal Coat Handbook for the Canadian climate. This method determines aggregate and binder application rates based on aggregate properties, surface condition, and traffic level to achieve 50-80 % aggregate embedment while preventing bleeding. As mentioned in the literature review (Table 1.3), this method was selected because it is the most commonly adopted approach for chip seal design under Canadian climatic conditions (Shuler et al., 2011; Wood et al., 2006). According to this method, the aggregate application rate is influenced by factors such as aggregate shape, gradation, and specific gravity, while the binder application rate is further determined by

aggregate absorption, particle shape, traffic loading, the condition of the existing pavement, and the residual asphalt content in the emulsion. Consequently, employing the modified McLeod method ensures that chip-seal surfaces achieve the desired durability, skid resistance, and resistance to bleeding when exposed to Canada's wide temperature range. The detailed explanation of the chip seal design is provided in Appendix I.

Based on experimental testing of the recycled aggregates and bitumen emulsion, along with calculations using McLeod's method, mentioned in Appendix I, the determined aggregate application rates are reported in Table 3.4. To validate these calculated rates, molds were prepared with heights equal to the average least dimension of each aggregate type. The specified quantities of aggregates and bitumen emulsion, based on the samples' areas, were then applied and compacted. The materials filled the molds, and considering that the bitumen emulsion contained approximately 30% water (as shown in Figure 3.5), the anticipated aggregate embedment after water evaporation would be around 70%. It is worth noting that the McLeod method assumes that the desired level of aggregate embedment will be achieved over a two-year service period under normal traffic and environmental conditions.

Table 3.4 The application rates of aggregates and binder based on McLeod's method

Type of aggregate	Aggregate application rate (kg/m²)	Binder application rate (L/m²)
Concrete	7.88	1.50
Yellow brick	6.11	1.88
Red brick	6.02	1.90
Glass	4.85	1.44

The differences in aggregate and binder application rates presented in Table 3.4 result from variations in aggregate physical properties and the application of the McLeod design method. Aggregates with higher density, angularity, and surface texture, such as recycled concrete and bricks, require higher aggregate application rates to achieve the target embedment level. Similarly, binder application rates are adjusted to account for differences in aggregate absorption, surface area, and particle shape, ensuring adequate coating and adhesion. In contrast, glass aggregates, which are smaller, smoother, and less absorptive, require lower

aggregate and binder application rates. These variations are consistent with chip seal design practice and reflect material-specific adjustments.

3.2.3 Asphalt Mixture Design

The laboratory asphalt mixture specimens were produced based on the Quebec standard (Québec, 2016). A dense-graded hot mix asphalt with a nominal maximum aggregate size of 10 mm (ESG-10) was used, using PG 58-28 asphalt binder modified with an anti-stripping additive to enhance aggregate–binder adhesion and moisture resistance. The properties of the asphalt mixture and binder, along with the aggregate gradation including MTMD limits, are presented in Table 3.5 and Figure 3.6, respectively. According to the standard, the mixing temperature was set at 150°C, and compaction was carried out at 135°C using a gyratory compactor to produce cylindrical specimens.

Table 3.5 The properties of the asphalt mixture and binder

PG 58-28 asphalt binder properties	Values	ESG-10 asphalt mixture Properties	Values
Density at 25 °C (g/cm^3)	1.025	G_{mm} (g/cm^3)	2.538
Viscosity at 135 °C (Pa·s)	0.247	Binder (%)	5.45
Viscosity at 165 °C (Pa·s)	0.075	Absorbed binder (%)	1.02
G*/sin δ at 58 °C for virgin binder (kPa)	1.254	Effective binder (%)	12.2

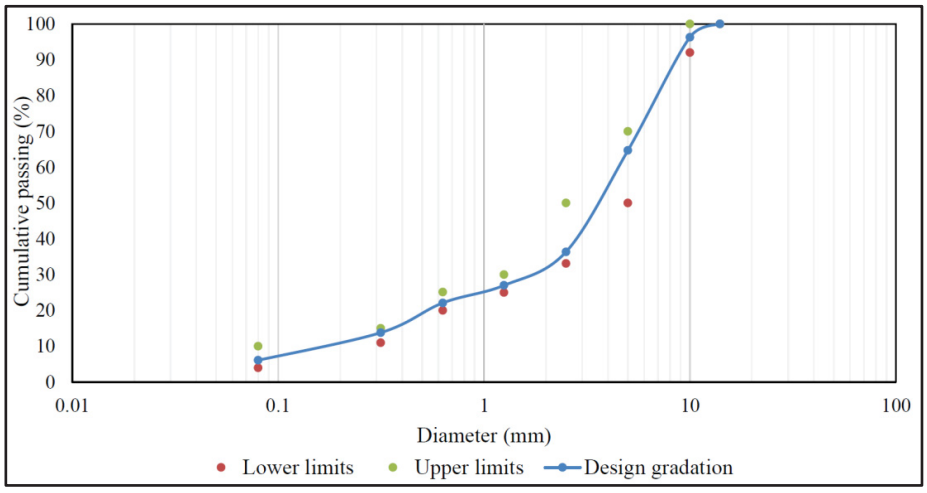

Figure 3.6 Asphalt mixture specimens' aggregate gradation

3.2.4 Description of Mechanical Properties, Durability, and Safety Tests

As mentioned in Chapter 1, the primary guidelines for chip seal design and performance evaluation identify three key tests as essential, including texture depth measurement tested by the sand patch method, skid resistance, and the sweep test (Chip Seal Best Practices, 2005; Wood et al., 2006; Buss et al., 2016). In recent years, additional testing methods have been introduced to better assess the mechanical behavior and durability of chip seals, specifically the interface bond test and the Vialit test (You et al., 2019; Baran et al., 2025). In addition, this thesis introduces a novel experimental approach to evaluate the bleeding potential of chip seals, addressing a performance aspect that is not adequately captured by conventional test methods. Together, these tests provide a comprehensive evaluation of mechanical performance, durability, and safety. Each of these testing procedures serves a specific purpose in evaluating different aspects of chip seal performance, and all are described and applied in this chapter. Based on previous published research, the recycled materials investigated in this study have not been systematically evaluated for chip seal applications under Canadian climatic conditions, particularly with respect to combined mechanical performance, durability, and safety in both hot and cold temperatures.

The selected laboratory tests were chosen to comprehensively evaluate the mechanical integrity, surface texture, and safety performance of the developed chip seals in accordance with the research objectives. Specifically, the sand patch test quantifies the macrotexture depth, which directly affects skid resistance and surface drainage, which are critical factors for pavement safety and albedo measurement. The sweep test evaluates aggregate retention and binder adhesion, ensuring the durability of the chip seal under traffic. The British Pendulum Tester (BPT) measures skid resistance under different temperature conditions, revealing surface safety and frictional performance. The interface bond test evaluates the adhesion strength between the chip seal and underlying asphalt mixture, which is vital for structural integrity and load transfer. Besides, the Vialit test determines the cohesion of the binder–aggregate system, indicating its resistance to raveling in cold temperatures and under mechanical stresses. Finally, the bleeding susceptibility test identifies the tendency of excess binder to migrate to the surface under heat or heavy traffic, ensuring that the chip seals maintain proper texture and do not lose reflectivity or skid resistance over time. Overall, these tests were

chosen to provide a comprehensive assessment of the functional, mechanical, and safety performance of the developed chip seals since these aggregates have not been used for chip sealing. It means that these tests ensure that the developed chip seals not only improve surface reflectivity but also maintain the required mechanical and safety performance standards.

3.2.4.1 The Sand Patch Test

Texture depth is an important parameter to ensure sufficient aggregate embedment of chip seals. As these aggregates have not been used for chip seal preparation before, this test is essential to measure the texture depth, indicating the correct aggregate and binder application rates. Thus, this test was conducted to assess the macrotexture of the chip seal surface. For the 300 mm diameter of the test specimens, the appropriate quantities of aggregates and bitumen emulsion were calculated based on the sample's area, which is about 0.0706 m^2. Based on the application rates provided in the Chip Seal Design section, the amounts of aggregates and bitumen emulsion are calculated by multiplying the surface areas of samples by aggregate and bitumen emulsion application rates, mentioned in section 3.2.2. These quantities are shown in Table 3.6.

Table 3.6 Sample area and materials application rates

Chip seal type	Binder rate (L/m^2)	Aggregate rate (kg/m^2)	Sample surface area (m^2)	Required emulsion (g)	Required aggregates (g)
Concrete	1.50	7.88	0.0706	106	557
Yellow brick	1.88	6.11	0.0706	133	432
Red brick	1.90	6.02	0.0706	134	425
Glass	1.44	4.85	0.0706	102	343

Once the specified amount of bitumen emulsion was applied to the asphalt felt discs, the aggregates were distributed over the surface to form a one-layer aggregate chip seal. The aggregate and bitumen emulsion amounts are mentioned in Table 3.6. The samples were then compacted using a standard compaction device weighing 7500 g, with a curved base radius of 550 mm, in accordance with the ASTM D7000 standard (ASTM D7000, 2019). After preparation, the samples were rotated by 90° to dislodge any loose aggregates. A two-stage

curing process was then applied to facilitate water evaporation from the bitumen emulsion. In the first stage, the specimens were cured at 35 °C for 48 hours, followed by an additional 48 hours at ambient temperature (23 °C ± 2 °C). The sand patch test, in accordance with ASTM E965 (ASTM E965, 2019), was performed on the cured specimens to determine the mean texture depth (MTD). Twelve specimens were tested in total, representing four aggregate types with three repetitions for each chip seal type. As per the standard, a certain amount of Ottawa sand (75 ml in this study) was evenly distributed from the center of the specimen in multiple directions using a stiff rubber applicator. The diameters of the spread sand layer were then measured. The MTD was then calculated using Equation 3.1.

$$MTD = \frac{4V}{\pi D^2} \tag{3.1}$$

In this equation, V represents the volume of sand (mm^3), D denotes the spread diameter (mm), and MTD refers to the mean texture depth (mm). The procedures for specimen preparation and the sand patch testing process are illustrated in Figure 3.7.

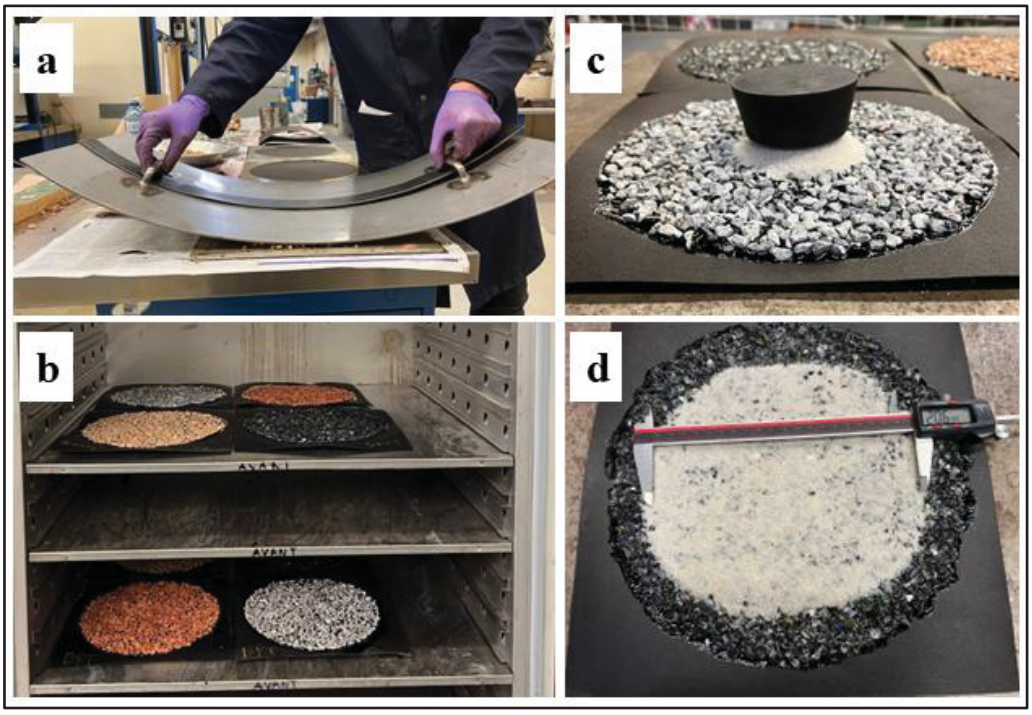

Figure 3.7 Sand patch test procedure: (a) specimen compaction, (b) curing process, (c) uniform distribution of sand, (d) measurement of spread sand diameter

3.2.4.2 The Sweep Test

The sweep test was used to evaluate the aggregate retention performance of chip seals by quantifying the percentage of aggregate loss under simulated mechanical sweeping. This test indicates how well aggregates are bonded to the binder, which is a critical factor in chip seal durability, especially during early service life when loose chips can pose safety and maintenance concerns. The evaluation of chip seal performance in terms of aggregate loss was conducted following ASTM D7000 (ASTM D7000, 2019). Asphalt felt disks with a 300 mm diameter were prepared and cured at 50°C for 48 hours, followed by an additional 48 hours at ambient temperature (23 °C ± 2 °C) to flatten the disks. The disks were weighed before sample preparation.

The chip seal specimens were prepared using the same material quantities and procedures as described in the sand patch test, preparing twelve samples. After preparation, the specimens were cured at 35°C for 4 hours. Loose aggregates were then removed from the surface using a brush, and the samples were weighed to obtain their initial weights. In the next stage, the sweep test apparatus, which is a modified mixer equipped with a nylon brush, was operated at 0.83 gyrations per second for 60 seconds to simulate sweeping, as shown in Figure 3.8. The loosened aggregates were brushed away, and the samples were weighed again to determine their final weights. The aggregate loss percentage was calculated using Equation 3.2.

$$Agreegate\ Loss\ (\%) = \left(\frac{A_g - B_g}{A_g - C_g}\right) \times 100 \times 1.33 \tag{3.2}$$

In this equation, A_g denotes the initial weight of the specimen (g), B_g represents the final weight after testing (g), and C_g is the weight of the asphalt disk (g).

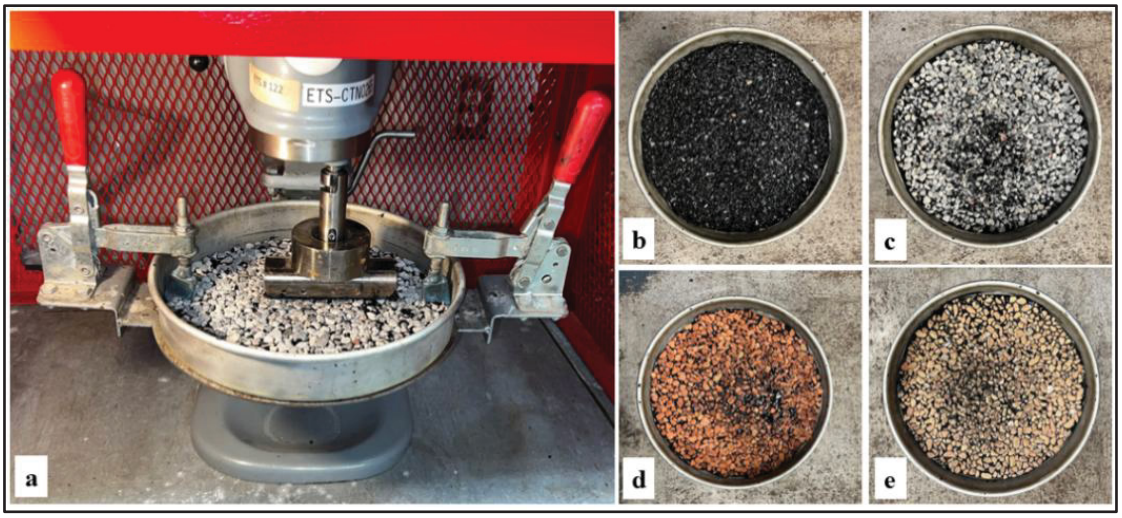

Figure 3.8 (a) The sweep test procedure; (b) glass; (c) concrete; (d) red brick; and (e) yellow brick specimens after the test

3.2.4.3 The British Pendulum Tester (Skid Resistance)

Skid resistance is a critical safety parameter for pavement surfaces, directly influencing vehicle traction, braking efficiency, and accident risk. As mentioned in Chapter 1, one of the most significant issues of reflective coatings is low skid resistance. Hence, measuring this property is essential to propose a way to mitigate the UHI with sufficient safety. For chip seals, which are intended to provide both surface sealing and adequate friction, measuring skid resistance ensures that the selected aggregate type and surface texture deliver sufficient grip throughout the service life. Since environmental factors, especially high temperature, can alter binder viscosity and aggregate embedment, it is important to evaluate the skid resistance of chip seals under both standard and high pavement temperatures.

The skid resistance of the chip seal specimens was assessed using the British Pendulum Tester (BPT), following the procedures provided in ASTM E303 (ASTM E303, 2013). According to this standard, the minimum specimen size should be 89 mm × 152 mm to ensure sufficient contact with the pendulum slider. For this study, custom steel molds with internal dimensions of 100 mm × 170 mm were fabricated to produce flat surfaces with adequate test contact area. Specimens were prepared using the aggregate and bitumen emulsion application rates determined in the chip seal design section. According to the surface area of the samples, which is 0.017 m^2, the corresponding aggregate and bitumen emulsion contents were calculated, reported in Table 3.7.

Table 3.7 Specimen area and materials application rates

Chip seal type	Binder rate (L/m²)	Aggregate rate (kg/m²)	Sample surface area (m^2)	Required emulsion (g)	Required aggregates (g)
Concrete	1.50	7.88	0.017	26	134
Yellow brick	1.88	6.11	0.017	32	104
Red brick	1.90	6.02	0.017	32	102
Glass	1.44	4.85	0.017	25	82

After applying the required amounts of bitumen emulsion and aggregates, the chip seals were compacted using a 5 kg roller compactor. Curing followed the same procedure as the sand patch test, which was 48 hours at 35°C, followed by 48 hours at ambient temperature (23 °C ± 2 °C) to allow for water evaporation of the emulsion. Considering one of the highest asphalt pavement surface temperatures in Canada, which is approximately 60 °C, this temperature was also used for skid resistance (Mills et al., 2009). Since high pavement temperatures can increase binder viscosity and cause aggregate movement under traffic, potentially reduce friction. Thus, skid resistance was evaluated at both 23°C and 60°C, the latter representing the highest pavement temperatures recorded in Canada by Mills et al (2009).

In total, 24 specimens were produced (four aggregate types, each with three replicates for two temperature conditions). The British Pendulum Number (BPN) was measured five times for each specimen, and the average value was recorded for each aggregate type. For the 60°C condition, specimens were heated on a hot plate for 2 hours until reaching the target temperature, confirmed using a portable thermometer, before conducting the BPT measurements. Testing procedures at both temperatures are illustrated in Figure 3.9.

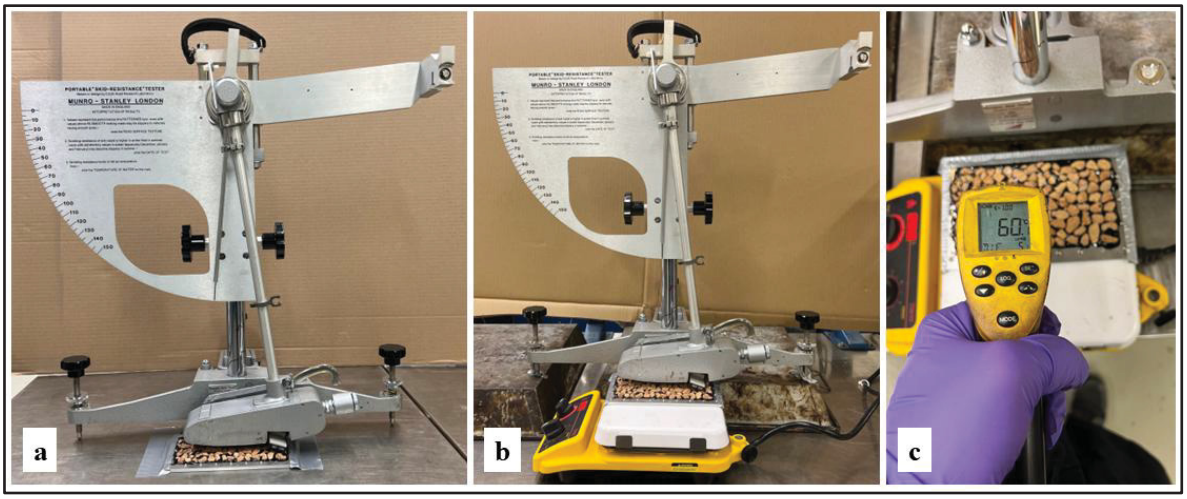

Figure 3.9 Skid resistance testing: (a) conducted at 23 °C, (b) conducted at 60 °C, and (c) measurement of chip seal surface temperature

3.2.4.4 The Interface Bond Test

The objective of the interface bond test in this study was to compare the bond strength between recycled aggregate chip seals and asphalt pavement surfaces under dry conditions using a consistent and reproducible methodology. A strong interface bond is essential for chip seal performance, as inadequate adhesion can lead to premature stripping and reduce the effectiveness of pavement preservation treatments.

A limitation of this method is that it evaluates bond strength only under dry conditions, as no internationally recognized standard currently exists for assessing chip seal interface bond performance under wet conditions. Although wet adhesion is an important factor, this study focused on dry condition testing to ensure direct comparability between aggregate types within the constraints of the available testing procedure. The method applied is based on the protocol developed by Michigan Technological University (You et al., 2019), which is specifically designed for dry-condition assessment. Additionally, while other parameters such as displacement and fracture energy can provide further insight into adhesion mechanics, these were not included because the test energy was constant across all specimens, and the primary goal is to compare peak pull-off stress for different recycled aggregate types, using a uniform testing framework, as an indicator of relative interface bond performance.

As mentioned, the interface bond test was first introduced at Michigan Technological University as a suitable method for investigating chip seal and asphalt pavement bonding. In this study, the same approach was used to assess the relative bond strength of recycled aggregate chip seals. 36 cylindrical asphalt concrete specimens were prepared (100 mm in diameter and 60 mm in height). Aggregate and bitumen emulsion application rates were calculated based on the surface area of the asphalt specimens, which was around 0.0079 m^2, as reported in Table 3.8.

Table 3.8 Asphalt surface area and materials application rates

Chip seal type	Binder rate (L/m^2)	Aggregate rate (kg/m^2)	Sample surface area (m^2)	Required emulsion (g)	Required aggregates (g)
Concrete	1.50	7.88	0.0079	12	62
Yellow brick	1.88	6.11	0.0079	15	48
Red brick	1.90	6.02	0.0079	15	47
Glass	1.44	4.85	0.0079	12	38

The required bitumen emulsion was applied to the asphalt specimens, followed by uniform aggregate distribution. A 5 kg roller compactor was then used to ensure proper embedment. Curing was carried out at 35°C for 48 hours, followed by 48 hours at ambient temperature (23 °C ± 2 °C) to allow water in the emulsion to evaporate. For the load application, each specimen was fitted with aluminum caps at the top and bottom using a slow-setting epoxy adhesive with a tensile strength of 13 MPa. After 4 hours of epoxy curing, the specimens were stored at -10°C, 0°C, and 23°C for 24 hours to simulate Canada's critical temperature conditions. Testing was performed using a Material Testing System (MTS) at a loading rate of 50 mm/min, recommended by the previous studies (You et al., 2019). As the loading rate is equal for all chip seal types, it is suitable for the comparison of different aggregates. The interface bond strength was calculated by dividing the peak load by the specimen's cross-sectional area. The procedure is illustrated in Figure 3.10.

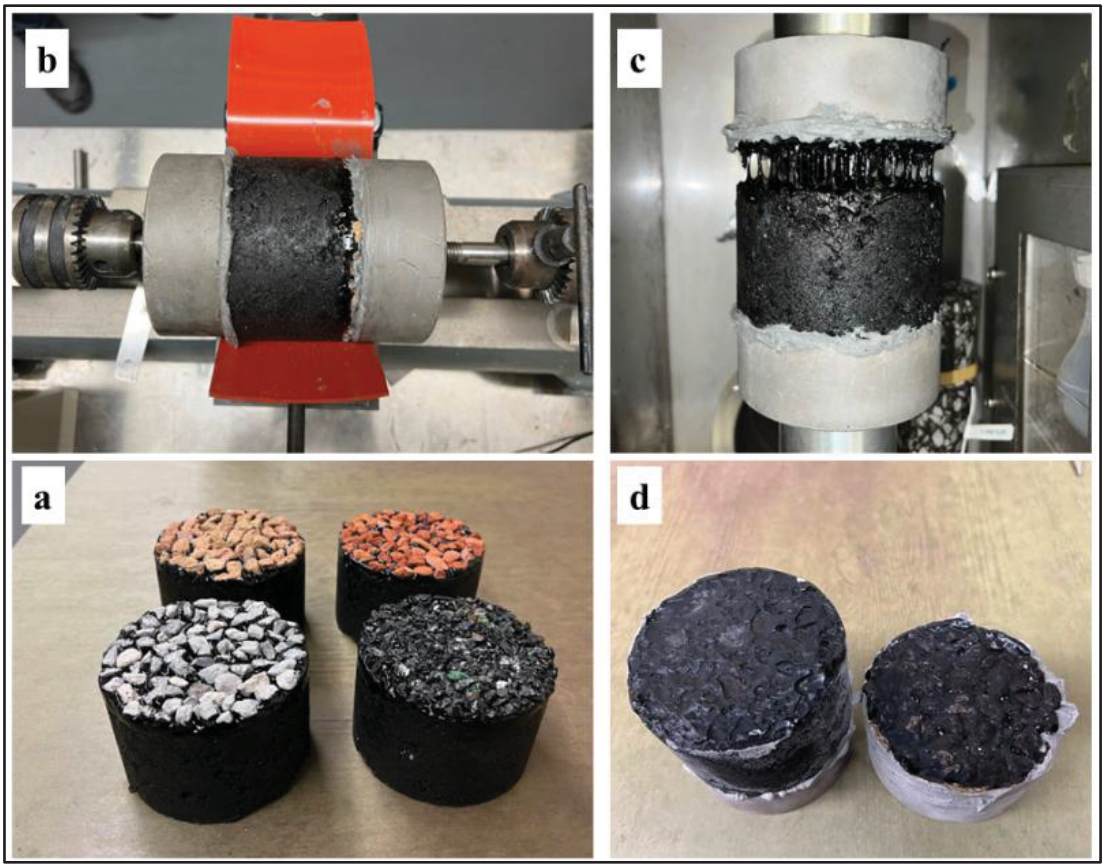

Figure 3.10 Interface bond strength test: (a) asphalt mixture specimens overlaid with chip seals, (b) attachment of aluminum caps to the specimen, (c) specimen under testing at 23 °C, and (d) specimen after testing at -10 °C

3.2.4.5 The Vialit Test

The Vialit test is a standardized method for assessing aggregate–bitumen adhesion in chip seals (BS EN 12272-3, 2003), particularly under conditions relevant to cold climates. While it is an impact-based test, its relevance lies in simulating the detachment forces aggregates may experience during service, such as traffic-induced impact, vibration, or dynamic loading, especially when binder stiffness increases at low temperatures. Therefore, the Vialit test provides a practical, repeatable measure of adhesion performance under realistic service stresses rather than a purely theoretical analysis of the microscopic adhesion mechanism. Considering the lack of other internationally recognized cold-climate adhesion tests for chip seals, the Vialit test remains a widely accepted tool for quality control and material comparison. In this study, it was used to compare the retention performance of recycled aggregates under

three low-temperature conditions representative of Canadian winter climates. Although adhesion is a complex, multi-scale process involving surface chemistry, binder rheology, and mechanical interlock, the Vialit test offers a standardized way to assess how well aggregates remain bonded under sudden impact loading at low temperatures.

In this research, the adhesion between bitumen emulsion and various aggregates under cold-climate conditions was evaluated using the Vialit test (BS EN 12272-3, 2003). Testing was conducted at three temperatures, -10°C, -20°C, and -30°C to reflect severe winter conditions in Canada. According to the standard, stainless steel molds measuring 200 mm × 200 mm were used. The specified quantities of bitumen emulsion were applied to each mold surface (62 g for concrete, 78 g for yellow brick, 78 g for red brick, and 59 g for glass aggregates). For each specimen, 100 pre-washed aggregates of the selected type were placed on the freshly applied emulsion and compacted with a 1 kg rubber roller. The samples were cured at 35°C for 48 hours, followed by 48 hours at ambient temperature (23 °C ± 2 °C) to allow for emulsion water evaporation. After curing, the specimens were conditioned at the target test temperatures (-10°C, -20°C, -30°C) for 4 hours based on the BS standard.

For testing, the molds were inverted, and a 500 g steel ball was dropped from a height of 500 mm onto each mold three times. This impact simulated aggregate dislodgement forces under service conditions. 36 specimens (four aggregate types × three repetitions × three temperatures) were tested. After completing the test, the number of aggregates remaining adhered to each mold was counted, and the average retention ratio for each aggregate type at each temperature was calculated. The Vialit test specimens before and after the test are demonstrated in Figure 3.11.

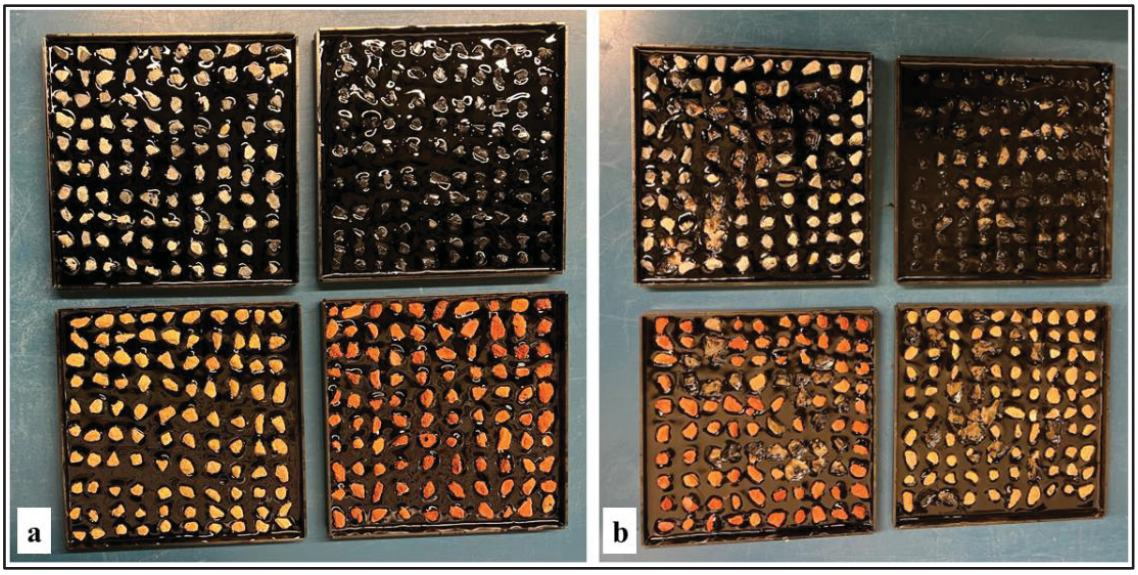

Figure 3.11 Vialit test specimens: (a) before testing and (b) after testing

3.2.4.6 The Bleeding Susceptibility Test

Bleeding is one of the most common and problematic chip seal distresses, characterized by the upward movement of binder to the surface, which fills surface voids, reduces macrotexture, and increases the risk of skidding, particularly in wet conditions. This phenomenon can significantly compromise road safety and shorten chip seal service life. As there is no standardized international bleeding test for chip seals, in this thesis, a new testing approach by modifying an existing microsurfacing test method was developed (ASTM D6372, 2015). The goal was to create a quantitative index for assessing the bleeding susceptibility of chip seals, enabling direct comparison between different aggregate types.

The bleeding potential of chip seals containing glass and limestone aggregates was assessed using a modified Loaded Wheel Test (LWT), originally standardized for microsurfacing in ASTM D6372 (2015). In the standard method, a specimen is subjected to a 76.2 mm diameter rubber tire wheel applying a 57.6 kg load for 1000 cycles at a rate of 44 cycles per minute. After weighing the specimen, 100 g of Ottawa sand heated to 85°C is evenly spread over the wheel–specimen contact area, followed by an additional 100 cycles. Any sand that does not adhere is removed, and the percentage increase in specimen weight is used as an indicator of bleeding potential. 12 chip seal specimens (four aggregate types × three replicates) were

prepared using the same material quantities (Table 3.6) and curing procedures as the sand patch test. Because the LWT machine is designed for microsurfacing specimens, some adjustments were made to accommodate chip seal specimens. The original steel plate was replaced with a larger steel plate equipped with custom specimen holders. To simulate more realistic pavement conditions with flexible behavior and prevent excessive aggregate loss (observed when the wheel had direct contact with specimens), a 10 mm thick neoprene rubber pad was placed between the wheel and the specimen surface to simulate load distribution in actual field conditions. After testing, the weight increase due to adhered sand was recorded for each specimen. This value served as the bleeding susceptibility index for comparison between aggregate types. The modified LWT setup and the chip seal specimens after testing are shown in Figure 3.12.

Figure 3.12 The modified LWT setup: (a) test apparatus, (b) chip seal specimens after testing, (c) detailed components: (1) steel plate, (2) neoprene rubber pad, (3) specimen holder

3.2.5 Description of Reflectivity, Thermal Properties, and Cooling Effect Tests

After completing the mechanical properties, durability, and safety tests of the developed chip seals, their effects on the UHI mitigation were examined. In detail, a combination of laboratory and field experiments was conducted to evaluate the reflective properties and cooling potential of these surfaces. Laboratory testing included spectral reflectance measurements across ultraviolet (UV), visible, and near-infrared (NIR) wavelengths (called UV–Visible–NIR in this study), thermal property measurements using a C-Therm Trident system, and infrared solar simulation. In the field, albedo measurements were taken with a pyranometer, while surface and subsurface temperatures were monitored using an infrared camera and type T thermocouples with a precision of about 0.5 ℃ calibrated with a cold bath.

3.2.5.1 Ultraviolet (UV)-Visible-Near Infrared (NIR) Spectrometer Test

A UV–Visible–NIR spectrometer (Model: Perkin Elmer, Lambda 750) was used to measure the reflectance and absorption properties of the chip seal specimens. This device is capable of recording absorbance and reflectance across wavelengths from 175 nm to 3000 nm, and it can operate at temperatures ranging from 0°C to 100°C during testing. Although the instrument can accommodate solid samples up to 100 × 100 mm, the chip seal specimens were prepared at 50 × 50 mm to improve measurement accuracy and reduce potential errors.

Based on the chip seal mix designs, the corresponding aggregate and bitumen emulsion application rates of the sample areas (0.0025 m^2) were calculated and reported in Table 3.9.

Table 3.9 UV–Visible–NIR sample materials rates

Chip seal type	Binder rate (L/m^2)	Aggregate rate (kg/m^2)	Sample surface area (m^2)	Required emulsion (g)	Required aggregates (g)
Concrete	1.50	7.88	0.0025	4	20
Yellow brick	1.88	6.11	0.0025	5	16
Red brick	1.90	6.02	0.0025	5	15
Glass	1.44	4.85	0.0025	4	12

Accordingly, the required amount of bitumen emulsion was poured into the designed mold on asphalt sheets, followed by the placement of aggregates, compacted using a 1 kg roller

compactor. The specimens were then cured at 35°C for 48 hours, followed by an additional 48 hours at ambient temperature (23 °C ± 2 °C) to allow water in the emulsion to evaporate. For comparison, additional specimens were extracted and cut from new hot mix asphalt (HMA) and aged HMA (after three years of service), preparing 18 specimens in total with 3 repetitions for each one. The absorbance and reflectance of each specimen were measured five times, with the specimen rotated and repositioned before each reading. The average values were then calculated. The Lambda 750 spectrometer and the prepared specimens for this test are shown in Figure 3.13.

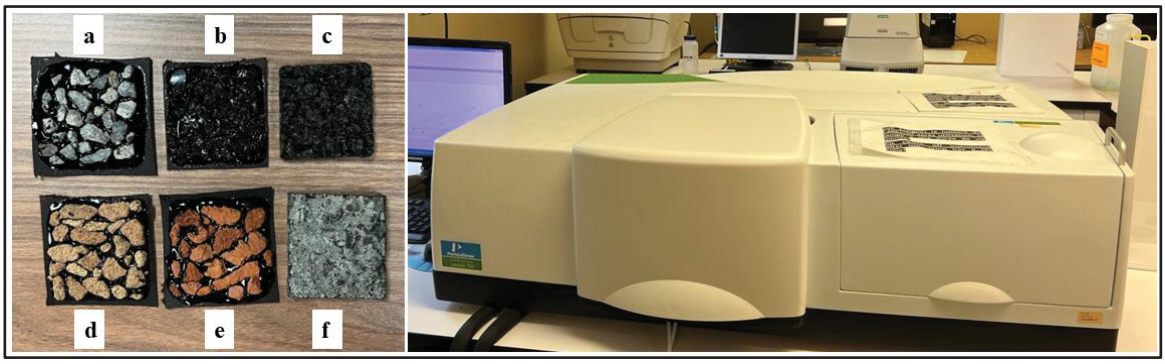

Figure 3.13 Specimens used for the reflectivity test (left): (a) concrete, (b) glass, (c) new HMA, (d) yellow brick, (e) red brick, (f) aged HMA; and the Lambda 750 spectrometer

3.2.5.2 Materials Thermal Properties Measurement

Since these recycled aggregates are directly exposed to solar radiation and form the top layer of asphalt pavement, their thermal properties play a critical role in surface temperature behavior. To assess their heat transfer characteristics, a C-Therm Trident thermal conductivity instrument was employed, working in accordance with ASTM D7984 (2021). This device is equipped with various sensors that operate based on the transient heat transfer method. For aggregates and asphalt pavement thermal properties evaluation, the Modified Transient Plane Source (MTPS) sensor was selected for measuring thermal conductivity and thermal effusivity, as it is recommended for testing solid materials by the manufacturer.

The MTPS sensor requires solid samples with a minimum diameter of 18 mm and a flat surface. Due to the rough texture and aggregate size (5–10 mm) of the prepared chip seals, it was not

possible to meet these requirements and test the chip seals. Therefore, testing was performed on the aggregates before crushing. The four waste materials, along with new and aged asphalt pavement samples, were cut into 50 × 50 mm pieces to create smooth, flat surfaces suitable for testing, preparing 18 samples, including 3 replicates for each one. To ensure proper contact between the samples and the MTPS sensor, a special thermal paste (supplied by the device supplier) was applied to fill any surface voids, and a 500 g weight was placed on each specimen during measurement. Provided reference samples tested with and without this paste showed no change in measured thermal properties, confirming that its use did not affect results. For each specimen, thermal conductivity was measured five times at different sample's areas, and the average was recorded. The C-Therm device and the prepared specimens are shown in Figure 3.14.

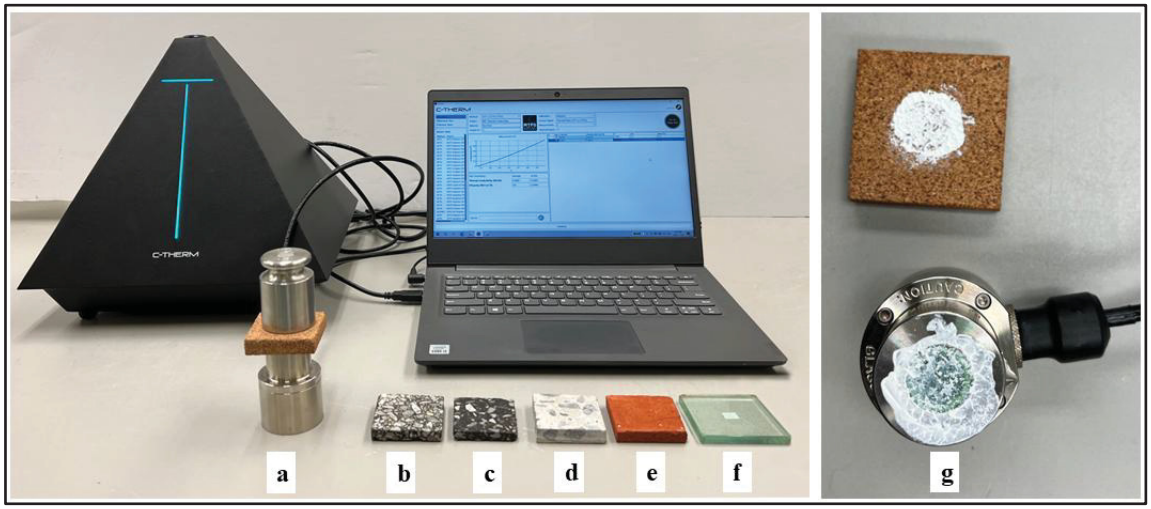

Figure 3.14 Thermal properties testing of materials: (a) yellow brick, (b) aged HMA, (c) new HMA, (d) concrete, (e) red brick, and (g) MTPS sensor with thermal contact paste

3.2.5.3 Indoor Solar Simulation Test

An experimental setup was designed to simulate one-directional heat transfer in asphalt mixtures coated with chip seals under controlled indoor conditions. A 175 W infrared lamp (wavelength range: 300–3000 nm) was used to simulate solar radiation on the test specimens. To minimize airflow and ventilation over the specimen surfaces, which can affect the accuracy of data due to possible different convention rate during the test, a transparent pipe matching

the asphalt mixture diameter (150 mm) was positioned above them. This pipe also helped concentrate heat and achieve a target surface temperature for the control HMA specimen. The asphalt mixture specimens' diameter was the same as the pipe diameter (150mm), and their height was 150mm. The test aimed to achieve the highest asphalt pavement surface temperatures recorded in Canada, as UHI effects are most significant in hot weather. Based on reported maximum pavement temperatures (Mills et al., 2009), the proper lamp height was determined through trial and error to be 85 cm.

In the first stage, control asphalt mixture specimens were placed in the setup and exposed to the infrared lamp for 15 hours, raising the surface temperature to 63°C. The lamp was then switched off, and temperatures were recorded for 9 hours to monitor reverse heat transfer from the specimens to the ambient air. The developed experimental setup is shown in Figure 3.15. As shown, 7 type T thermocouples with a precision of about 0.5 ℃, calibrated with a cold bath, were placed inside each specimen, exactly in the middle and at the center of the specimen, secured with bitumen, preparing a total of 15 specimens for control HMA and HMA coated with chip seals. An air temperature sensor (outside the tube with white color, which is shown in Figure 3.15/g) was also used to measure the laboratory temperature. This air temperature sensor was used to show the laboratory air temperature during the test. Thermocouples and sensors were connected to a data logger to continuously record temperature changes during both heating and cooling phases. Surface temperatures were additionally measured using an infrared camera. To limit heat loss from the sides and bottom of the specimens, they were surrounded with liquid foam insulation throughout the test. The conducted experimental tests and the number of samples for each test are summarized in Table 3.10.

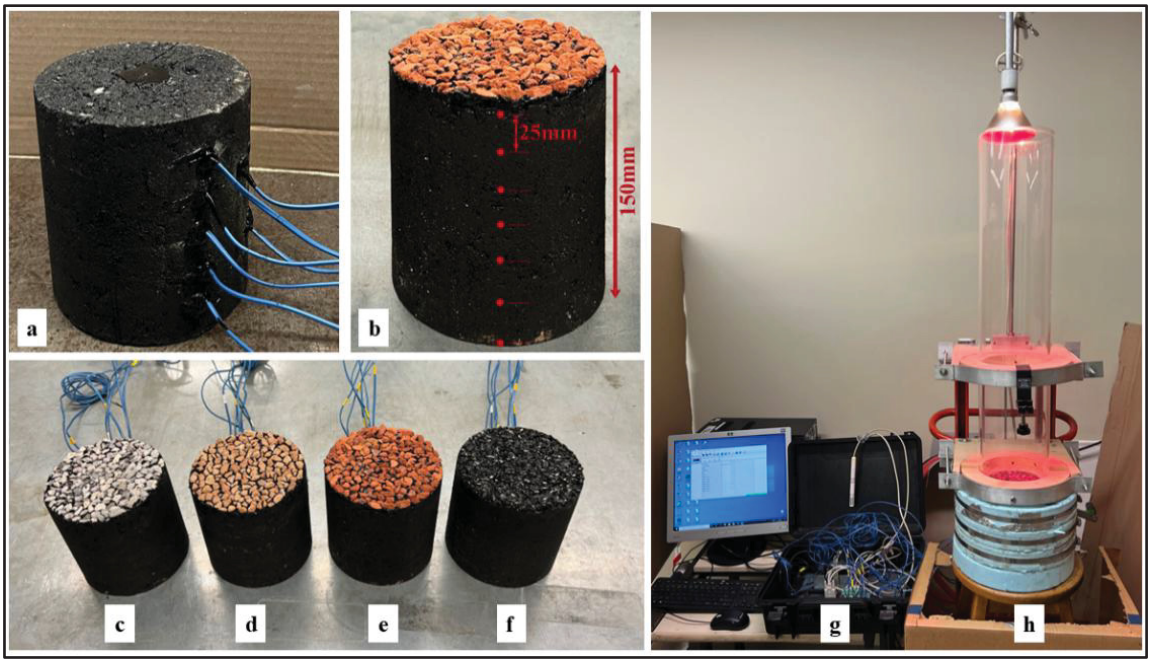

Figure 3.15 Solar simulation test: (a) thermocouple installation, (b) thermocouple layout, (c) concrete chip seal, (d) yellow brick chip seal, (e) red brick chip seal, (f) glass chip seal, (g) data logger and computer, (h) insulated specimen with lamp

Table 3.10 The summary of the conducted laboratory tests and the number of samples

Test	Goals for the laboratory tests	Number of samples
Sand patch test	Measuring the texture depth to verify the materials' application rates	12
Sweep test	Durability of chip seals by measuring aggregate retention	12
British Pendulum Tester	Evaluating the skid resistance of chip seals	24
Interface bond test	Assessing the adhesion and bond strength between chip seals and the asphalt surface	36
Vialit test	Measuring the adhesion between aggregate and bitumen emulsion at cold temperatures	36
Bleeding susceptibility test	Evaluating the bleeding susceptibility of chip seals	12
Spectrometer test	Measuring the reflectance of specimens	18
C-Therm thermal test	Evaluating the thermal properties of materials	18
Indoor Solar Simulation Test	Assessing the cooling effects and temperature reductions of pavements coated with chip seals	15

3.2.5.4 Albedo and Temperature Variation Measurement Experiment

The solar spectrum has wavelengths from 200 nm to 2500 nm, accounting for roughly 96.3% of total irradiance. While infrared lamps are one of the most practical tools for simulating solar radiation on pavements (Jiang and Wang, 2020), their color temperature is approximately 3200 K, whereas natural sunlight ranges between 5600 K and 6000 K. This difference, particularly in shortwave visible output and low ultraviolet content, means that solar radiation and simulated radiation are not identical (Pirouzfam and Sendur, 2021).

Considering these factors, the albedo and cooling effects of chip seals were assessed through an outdoor field test. Four circular asphalt pavement sections (4 m in diameter) were coated with bitumen emulsion and covered with recycled aggregates (yellow and red bricks, concrete, and glass). For comparison with new and aged HMA, two additional circular sections, one with new asphalt pavement and one with aged asphalt pavement, were also tested.

The albedo measurement was conducted based on ASTM E1918 (2021). This Standard specifies that readings should be taken under cloudless conditions when the sun's angle to the pavement surface normal is less than 45°. For horizontal or low-sloped surfaces, this means testing between 9:00 a.m. and 3:00 p.m. in summer local time, or between 10:00 a.m. and 2:00 p.m. in winter when the sun's incidence angle is lower. In this study, testing took place on September 30, 2022, in Orford, Quebec, Canada, under sunny and cloudless conditions. Three measurements were taken for each area between 11:00 a.m. and 2:00 p.m. local time to calculate the average.

According to previous studies (Li et al., 2013b), it was assumed that air temperature and wind speed do not influence albedo results. For each reading, reflection values were stabilized for at least 10 seconds, with three measurements (incoming and reflected radiation) in 2 minutes. The albedo meter was positioned 500 mm above the pavement surface. After recording incoming solar radiation, the device was flipped to measure reflected radiation.

Additionally, 6 type T thermocouples were installed at the center of each section at a 25 mm depth to monitor pavement temperature. These thermocouples, along with a pyranometer and air temperature sensor, were connected to a data logger that transmitted data to a computer. Surface temperatures were also recorded using an infrared camera. To reduce measurement error, the data logger and air temperature sensor were shaded from direct sunlight during testing. The field test setup and details are shown in Figure 3.16.

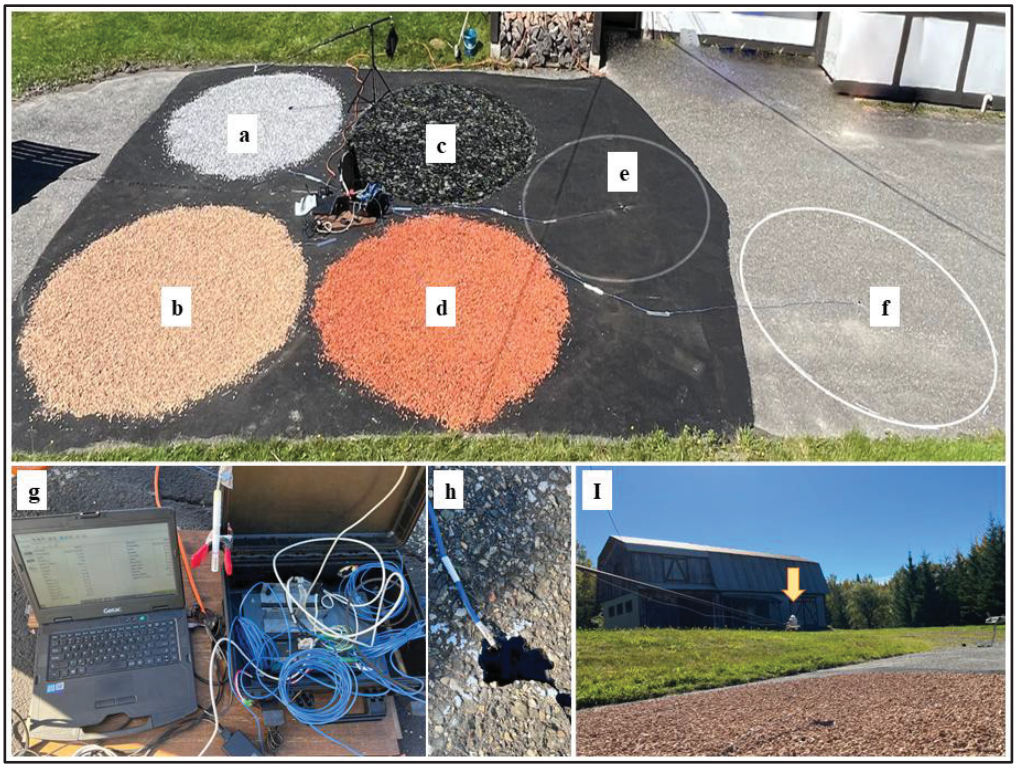

Figure 3.16 Details of the field reflection test: (a) concrete, (b) yellow brick, (c) glass, (d) red brick chip seals, (e) new HMA, (f) aged HMA, (g) data logger, (h) thermocouples, (i) pyranometer with clear sky

3.3 Results and Discussion

In this section, the results of mechanical, reflectance, and thermal performance tests for the developed chip seals are presented. Mechanical evaluation included texture depth, skid resistance, the sweep test, interface bond strength, the Vialit test, and a bleeding potential test. After confirming adequate performance of the developed chip seals, thermal behavior and reflectance were assessed through UV–Visible–NIR reflectance, thermal property measurements, indoor solar simulation, and field albedo and temperature monitoring. These results provide a comprehensive assessment of chip seals with recycled materials under Canadian climate conditions.

3.3.1 Mechanical and Safety Performance of Chip Seals

This section presents and discusses the results of the mechanical and safety performance evaluation of the developed chip seals. Emphasis is placed on surface functionality, durability, and adhesion characteristics, with detailed results from each test provided in the following subsections.

3.3.1.1 The Macrotexture of Chip Seal

The Mean Texture Depth (MTD) of the chip seal specimens was measured using the volumetric sand patch method, and the results are summarized in Table 3.11. All four recycled aggregate types exceeded the minimum macrotexture thresholds specified in chip seal standards, 0.90 mm for posted speeds above 70 km/h and 0.70 mm for speeds below 70 km/h, indicating that all mixes meet the basic safety and performance requirements (Pierce et al., 2015). Furthermore, the MTD values for all materials fall within the typical 1–3 mm range reported for conventional chip seals (Buss et al., 2016), suggesting that using these recycled aggregates does not compromise macrotexture quality.

The results reveal that concrete aggregates produced the highest MTD (2.79 mm), followed closely by yellow brick (2.70 mm) and red brick (2.68 mm). These materials share angular, irregular particle shapes, which promote greater surface roughness and, consequently, higher macrotexture depths. In contrast, the glass aggregates had a significantly lower MTD (1.91 mm), a difference attributable to several physical characteristics. Glass aggregates had partially flaky morphology (flakiness index = 31) with a smaller average particle size compared to the other aggregates, and relatively smooth surface texture. These factors reduce measured texture depth. The low coefficients of variation (3.26%–6.58%) across all materials indicate high consistency within each aggregate type, reinforcing the reliability of the macrotexture measurements. Overall, while glass chip seals present lower macrotexture values, they remain above the minimum performance thresholds, having acceptable skid resistance potential for roadway applications.

Table 3.11 The MTD values of developed chip seals

Material	Avg MTD (mm)	Variance	Standard Deviation (SD)	Coefficient of Variation (CV) (%)	Number of samples	Minimum required MTD (mm)
Yellow brick	2.70	0.0274	0.17	6.12%	3	0.90
Red brick	2.68	0.0076	0.09	3.26%	3	0.90
Glass	1.91	0.0107	0.10	5.42%	3	0.90
Concrete	2.79	0.0336	0.18	6.58%	3	0.90

3.3.1.2 The Sweep Test

The sweep test results, presented in Figure 3.17, quantify the percentage of aggregate loss for each chip seal mix and provide critical insight into the durability of the aggregate–binder interface under mechanical disturbance. According to the NCHRP Report 680 guidelines, chip seals exhibiting aggregate loss below 10% are considered to have satisfactory early-life performance (Shuler et al., 2011). In this study, all tested specimens met this performance threshold, indicating that each aggregate type achieved adequate binder adhesion under the applied construction and curing conditions.

Concrete chip seals exhibited an aggregate loss of 7.43%, which can be attributed to their inherently rough surface texture, high angularity, and irregular particle morphology. These characteristics enhance mechanical interlocking and promote effective adhesion through improved binder–aggregate contact. In particular, higher angularity not only contributes to macro-scale interlock but also increases the effective surface area available for binder bonding, improving resistance to dislodgement under mechanical disturbance.

Yellow and red brick chip seals exhibited aggregate losses of 5.56% and 7.05%, respectively. In addition to angularity and surface roughness, these materials possess relatively high porosity, which may promote partial penetration and absorption of the bitumen emulsion into the aggregate surface. Although this micro-scale absorption was not directly measured in this study, the observed aggregate retention performance is consistent with the formation of enhanced mechanical anchoring at the binder–aggregate interface, thereby increasing the

energy required for particle detachment under sweep loading. However, excessive binder absorption can also reduce binder availability for surface film formation, highlighting the importance of carefully calibrating binder application rates when using porous recycled aggregates.

Glass aggregates exhibited the lowest aggregate loss (2.36%), indicating superior retention performance. This behavior may be attributed to a combination of physicochemical and geometric factors. Based on findings reported in the literature, the silica-rich surface of glass aggregates can promote polar interactions with bitumen emulsions, potentially enhancing interfacial adhesion beyond what is achieved through mechanical interlock alone (You et al., 2019). Although surface chemical interactions were not directly characterized in this study, the observed retention performance is consistent with such mechanisms. In addition, the relatively smaller particle size and lower mean texture depth (MTD) of the glass chip seal resulted in deeper aggregate embedment within the binder film, thereby reducing the exposed surface area subjected to mechanical shear forces during the sweep test.

Overall, the sweep test results suggest that while all mixes meet conventional performance criteria, the retention mechanisms were different for aggregates. For angular and rough-textured aggregates (concrete and brick), mechanical interlock and binder penetration played a critical role. Whereas for glass aggregates, chemical competition and embedment depth play a more substantial role. These findings highlight that aggregate loss resistance is a function of integrated material characteristics, including particle size distribution, surface texture, shape, and binder coverage, rather than a single dominant chemical mechanism. These distinctions have important implications for aggregate selection in chip seals, particularly when optimizing binder formulation, application rate, and curing conditions to be compatible with aggregate mineralogy and morphology.

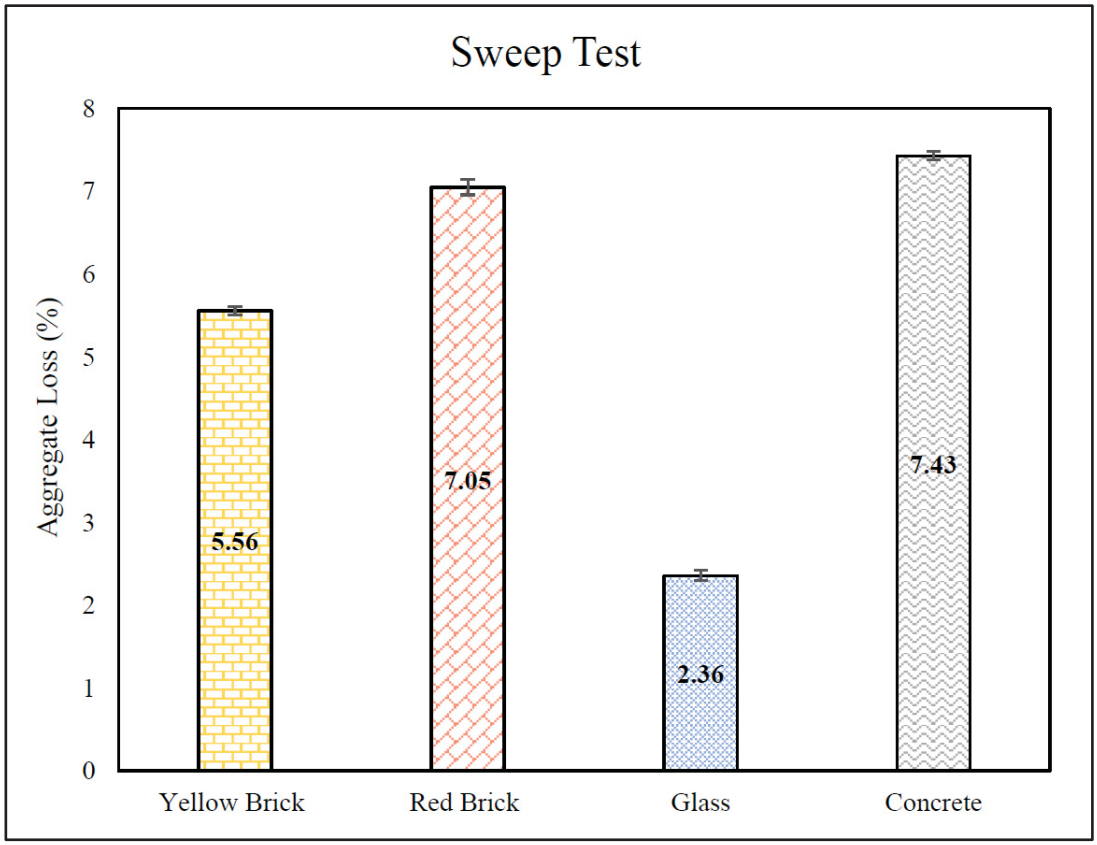

Figure 3.17 The percentages of aggregate loss for chip seals

3.3.1.3 The Skid Resistance

A known limitation of several reflective surface coatings proposed for UHI mitigation is their potential to reduce skid resistance, particularly under wet or high-speed traffic conditions. Reduced skid resistance poses a critical safety concern for pavements. In contrast, chip seals are widely recognized as an effective surface treatment for restoring and enhancing skid resistance by increasing both macrotexture and microtexture (Pierce et al., 2015). According to established performance thresholds, a British Pendulum Number (BPN) above 55 is considered to provide good skid resistance, while values above 70 indicate an excellent level of friction (Ahammed and Tighe, 2012; J. Lee et al., 2012). The BPN reflects contributions from the macrotexture (wavelength 0.5–50 mm and amplitude 0.1–20 mm) and microtexture (wavelength <0.5 mm and amplitude <0.2 mm) of the surface, both of which are strongly influenced by aggregate geometry, surface roughness, and binder embedment (Henry, 2000).

The measured BPN values for all chip seal mixes at 23 °C exceeded 70, confirming excellent skid resistance under ambient conditions, as presented in Table 3.12. Concrete aggregates had the highest value (BPN = 108), followed by yellow brick (102) and red brick (94), while glass aggregates recorded the lowest (74). This performance trend closely followed the measured MTD values, where concrete and brick showed higher macrotexture than glass. Additionally, glass aggregates' higher flakiness index and smoother surface morphology reduced microtexture, limiting frictional resistance despite adequate macrotexture.

The strong linear relationship between MTD and BPN at 23 °C ($R^2 = 0.92$), demonstrated in Figure 3.18, proved that skid resistance is a combined outcome of texture scales. In detail, macrotexture promotes water drainage and initial tire contact, while microtexture governs actual friction generation at the aggregate–tire interface. The high R^2 suggests that texture geometry alone explains the majority of the variation in BPN for these chip seals, indicating its predictive value in surface performance assessment.

Regarding tests at higher temperature (60 °C), all mixes had a reduction in BPN due to binder softening and reduced stiffness. The lower bitumen stiffness was observed by visual evidence of aggregate displacement during the British Pendulum Test. When the molds were heated before testing, the binder visibly softened, and slight shifts in aggregate positioning were observed under the applied pendulum load. These movements likely reduced surface microtexture and macrotexture engagement with the pendulum slider, contributing to the observed BPN reduction across all aggregate types. The softened binder allows minor displacement or rotation of aggregates under the pendulum's dynamic load, decreasing surface roughness and, consequently, skid resistance. The extent of reduction was different for chip seals. Glass chip seals showed the greatest drop (28.2%), followed by yellow brick (26%), red brick (23.4%), and concrete (22.3%). The relatively smaller loss for concrete chip seal suggested adequate mechanical stability at high temperature, potentially due to the higher angularity and rigidity of its aggregates.

Thermal conductivity characteristics of the aggregates can influence these results. While concrete exhibits thermal conductivity values similar to conventional aggregates, bricks and glass have significantly lower thermal conductivity (Dondi et al., 2004; Asadi et al., 2018; Peng et al., 2023), which can reduce heat transfer to the binder and prevent excessive binder

softening. This insulating effect may be advantageous for chip seals in hot climates, potentially limiting binder softening and preserving skid resistance. However, the results from this study do not conclusively demonstrate a significant thermal protection benefit under the laboratory conditions. Although the high-temperature BPN tests revealed that all materials experienced performance loss, the magnitude of reduction was not substantially smaller for the low-conductivity materials compared to concrete. This indicates that while thermal insulation properties may contribute marginally to slowing binder softening, the effect alone is insufficient to maintain better skid resistance at high temperatures. Therefore, the potential advantage of using such aggregates in hot-climate chip seals should be considered as a complementary factor rather than the most influential one, and its practical effect can be evaluated with field tests and chip seals under traffic loads. The reduction in skid resistance with temperature increase verifies that binder softening at higher temperatures reduces microtexture friction. The comparison of the BPN values of the studied chip seals at ambient and high temperatures is illustrated in Figure 3.9.

Table 3.12 The skid resistance and BPN values for chip seals

Temperature (°C)	Materials	BPN (Avg)	Variance	Standard Deviation (SD)	Coefficient of Variation (CV) (%)	Number of Samples
23	Yellow brick	102	6.64	2.58	2.52	3
	Red brick	94	6.56	2.56	2.72	3
	Glass	74	5.36	2.32	3.14	3
	Concrete	108	6.64	2.58	2.39	3
60	Yellow brick	76	4.96	2.23	2.94	3
	Red brick	72	7.76	2.79	3.86	3
	Glass	53	6.80	2.61	4.92	3
	Concrete	84	3.44	1.85	2.22	3

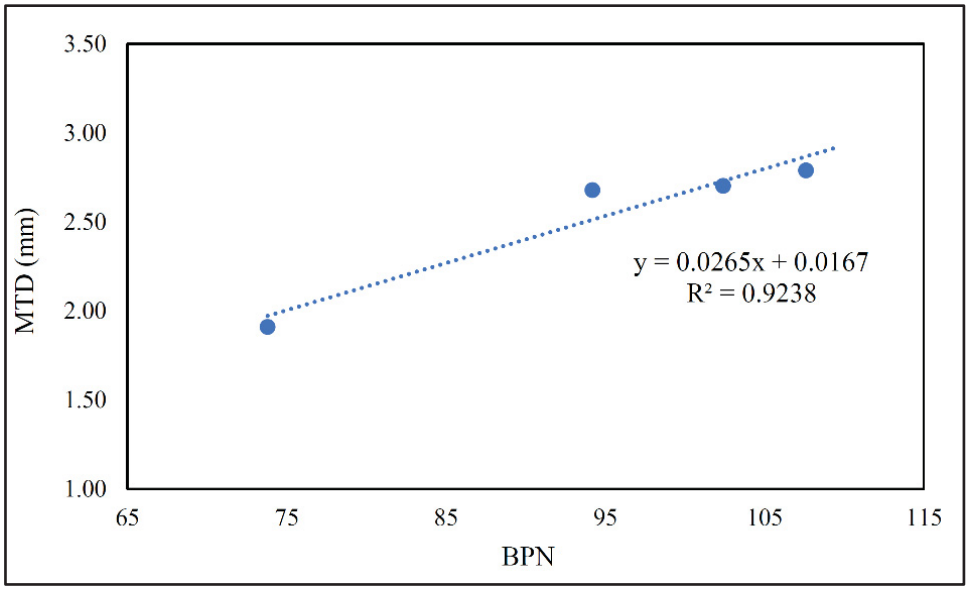

Figure 3.18 The correlation between MTD and BPN at the ambient temperature

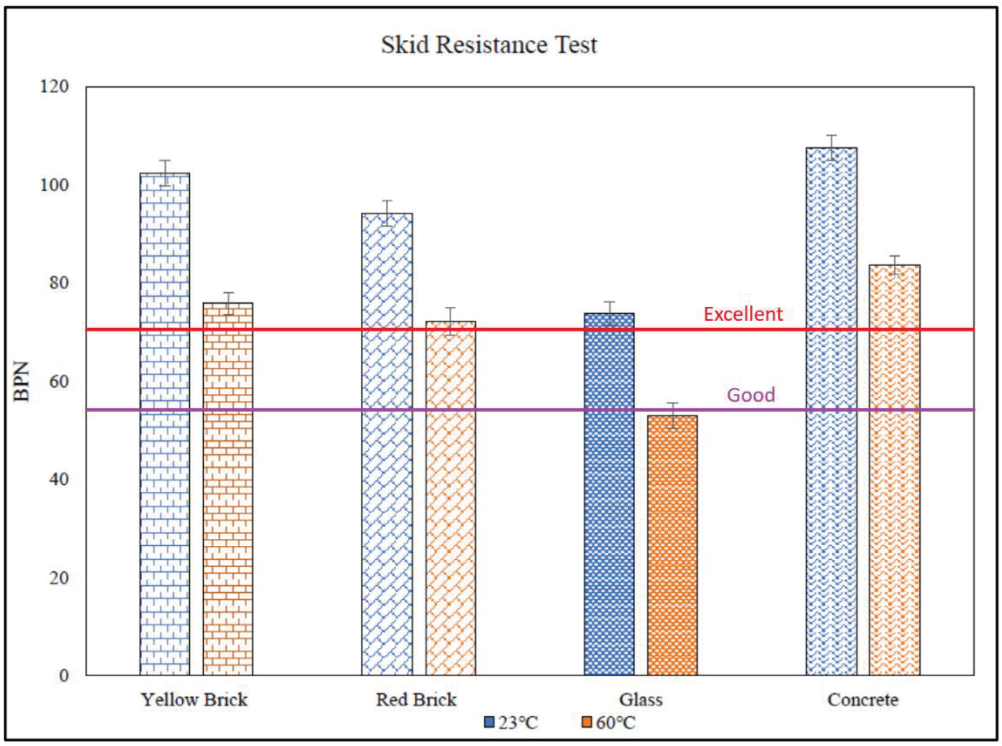

Figure 3.19 The comparison of BPN values at ambient and high temperatures

3.3.1.4 The Interface Bond Between the Asphalt Mixture and Chip Seals

The interface bond between chip seals and the asphalt pavement surface is a critical parameter influencing their structural performance and service life. A strong bond ensures effective stress transfer between the chip seal and the asphalt mixture, while weak adhesion can result in early-life distress such as stripping, debonding, and surface raveling. In bituminous surfacing systems, this bond is affected by a complex interplay of mechanical interlock, physico-chemical adhesion, binder rheology, and aggregate morphology.

In this research, the interface bond strength was measured under only dry conditions at three temperatures, including -10 °C, 0 °C, and 23 °C, whose results are shown in Figure 3.20. It is important to note that the test method employed did not include moisture conditioning. The presented results should be considered as relative performance measures of the materials tested in dry conditions. The reason why wet conditioning has not been done is the lack of standardized wet-conditioning protocols for this specific test method and chip sealing. Hence, wet conditioning is a recognized limitation and should be addressed in future research with a novel developed test method.

Across all test temperatures, concrete chip seals demonstrated the highest tensile bond strength, peaking at approximately 1185 kPa at 0 °C. At -10 °C, a 13 % reduction was recorded, attributable to increased binder brittleness at low temperatures, which limits its capacity to dissipate fracture energy despite higher stiffness. At 23 °C, bond strength fell to 750 kPa, reflecting binder softening and increased aggregate mobility under tensile load. The performance of concrete aggregates can be attributed to multiple interacting mechanisms. First, their rough and angular morphology promotes mechanical interlocking, which enhances resistance to aggregate movement under tensile and shear loading (Omar et al., 2020). Second, acid–base adhesion mechanisms may contribute to improved bonding at the aggregate–binder interface. In particular, cationic bitumen emulsions contain positively charged amine functional groups that can form electrostatic and chemical interactions with negatively charged or polar mineral surfaces commonly present in concrete aggregates (Omar et al., 2020; You et al., 2019). In addition, the relatively high alkaline content of concrete aggregates can promote acid–base reactions with polar functional groups in the bitumen, further enhancing interfacial

adhesion (Omar et al., 2020). Moreover, non-specific physical interactions such as van der Waals forces, although weaker than chemical bonding, act over the entire contact area and contribute cumulatively to the overall adhesion between the binder and aggregate surface (Xu and Wang, 2016).

Glass aggregates produced the second-highest bond strengths, close to concrete at -10 °C and 23 °C. Their smaller particle size reduces interfacial voids and increases real contact area, while their high silica content supports electrostatic attraction with the cationic emulsion through acid–base interactions between silanol groups (Si-OH) and the amine groups of the binder (Omar et al., 2020; You et al., 2019). However, their smoother surfaces slightly reduce mechanical interlock compared to concrete. Moreover, brick aggregates had lower interface bond strengths, 950 kPa at -10 °C and 0 °C, decreasing by 30% at 23 °C. Although their rough and porous surfaces promote good adhesion and mechanical interlock, the aggregate tensile strength of bricks can become a limiting factor. Some failures were observed within the aggregate itself during testing (Figure 3.21), indicating that aggregate-bitumen adhesion exceeded the internal strength of the aggregate.

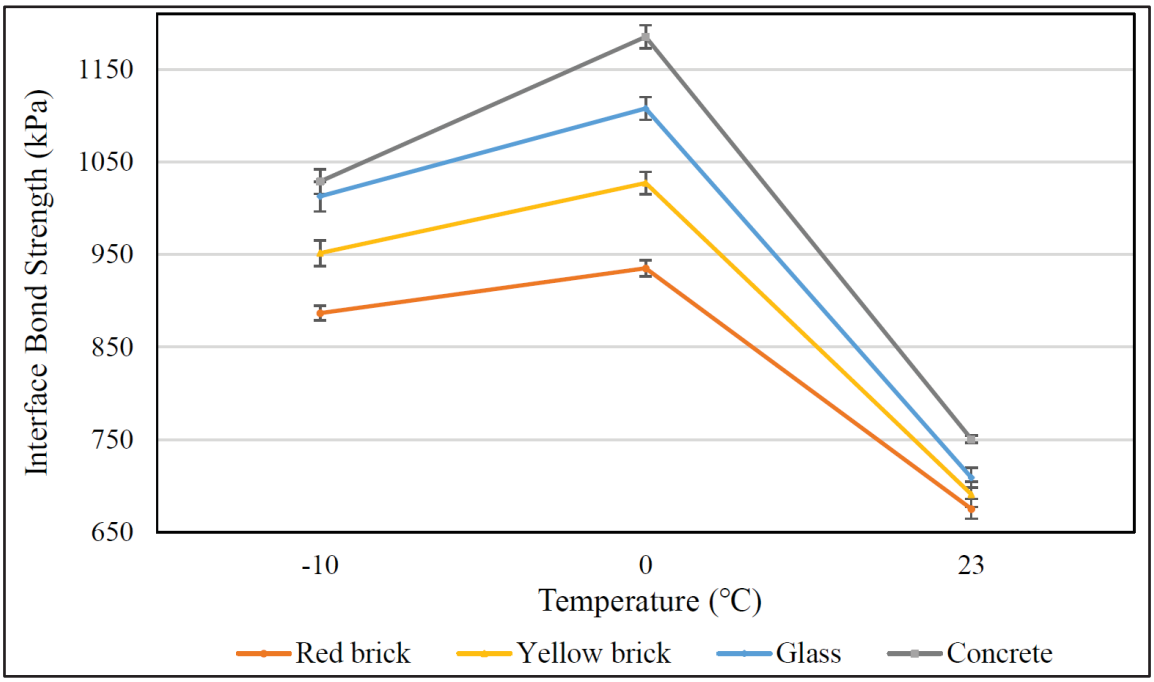

Figure 3.20 The interface bond strength of chip seals

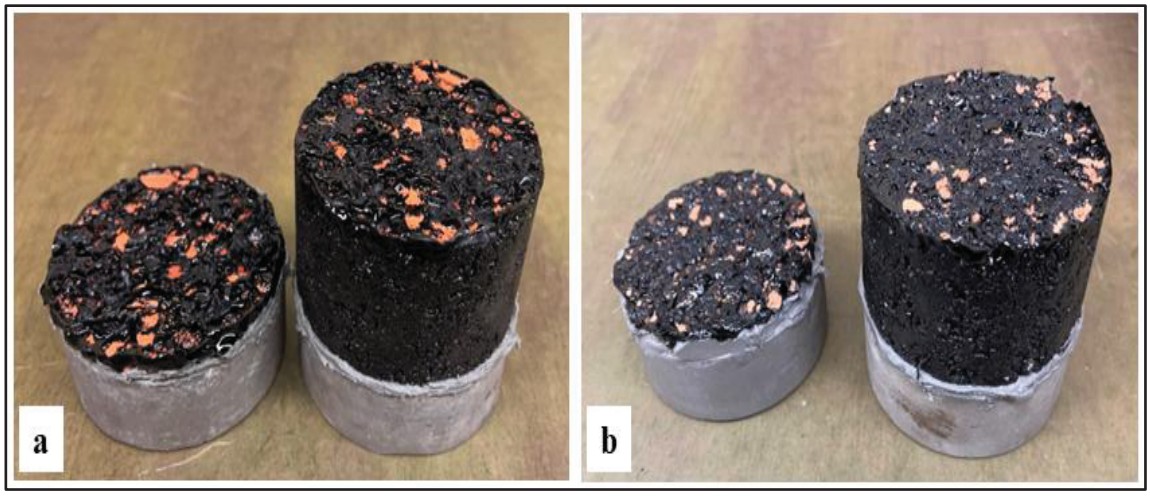

Figure 3.21 (a) Red, and (b) yellow brick chip seals after the interface bond strength test

Overall, the interface bond results revealed that aggregate surface chemistry, texture, and size distribution all contribute to adhesion under dry conditions. The cationic nature of the emulsion favors aggregates with negatively charged surface groups or alkaline mineral phases capable of strong acid–base interactions, supplemented by mechanical interlock and van der Waals forces.

The results of this test had a limitation in terms of wet conditioning. All adhesion and bond strength results were obtained under dry conditions without water conditioning. Moisture is a primary degradation agent for bitumen–aggregate bonds, capable of displacing binder from the aggregate surface through stripping mechanisms. Although the reported findings provide valuable insight into relative performance under dry service conditions for these aggregates, they cannot be directly used to predict moisture susceptibility or long-term durability in wet climates. As there is no standard test method for evaluating the interface bond under wet conditions, future work should develop a standardized moisture conditioning test to quantify the impact of water on interface bond strength and aggregate retention of chip seals.

3.3.1.5 Aggregate-Bitumen Emulsion Adhesion at Low Temperatures

The Vialit test results, illustrated in Figure 3.22, showed that decreasing temperature reduces the adhesion between aggregates and the cationic bitumen emulsion for all aggregate types. This decline is attributed to the temperature-related change in binder mechanical properties.

Below the freezing point, the binder becomes brittle, reducing its capacity to dissipate impact energy and making it more susceptible to fracture at the aggregate–binder interface. Under repeated impact loading in the Vialit test, this brittleness leads to higher aggregate detachment. At -10 °C, glass and concrete aggregates showed the highest retention ratios (almost 75%), performing better than brick aggregates (around 69%). This better performance is attributed to the combination of physicochemical and mechanical factors, including acid–base adhesion of cationic bitumen emulsion, silica-based adhesion, and surface texture of materials (Omar et al., 2020; You et al., 2019). In detail, the cationic bitumen emulsion contains positively charged amine functional groups, which can develop strong electrostatic and chemical bonds with negatively charged or polar mineral surfaces (Omar et al., 2020). Concrete aggregates have relatively high calcium ion content (Table 3.2), providing alkaline sites that interact strongly with the polar carbonyl groups in the bitumen emulsion, increasing bond durability even in low-temperature conditions (You et al., 2019). Besides, glass aggregates, which are rich in silica, present silanol (Si–OH) groups that can engage in acid–base interactions with the cationic binder (Park et al., 2000). Although hydrogen bonding between silanol groups and polar binder components can enhance the adhesion, under dry test conditions, the dominant mechanism is still the acid–base attraction between the negatively charged silanol surfaces and the cationic bitumen emulsion (Omar et al., 2020; You et al., 2019). Furthermore, as glass aggregates were smaller than other aggregate types, this reduced interfacial voids and increased real contact area. A smaller aggregate size also improves impact resistance in the Vialit test because the force is distributed over a greater binder–aggregate contact proportion, lowering detachment probability (You et al., 2019).

At -20 °C and -30 °C, the retention ratios for both glass and concrete aggregates decreased significantly. Glass aggregates exhibited reductions of 37% at -20 °C and 41% at -30 °C, while concrete aggregates showed reductions of 39% and 44% at -20 °C and -30 °C, respectively. Although the percentage losses were comparable, this similarity does not imply identical failure mechanisms. At very low temperatures, the adhesion performance of chip seals becomes increasingly governed by the mechanical response of the binder. As the bitumen emulsion stiffens and becomes brittle, its capacity to absorb impact energy diminishes, making the system more susceptible to fracture under impact loading (You et al., 2019).

Yellow and red bricks showed similar retention ratios (approximately 69%) at -10 °C, dropping to about 35% and 30% respectively, at -20 °C and -30 °C. Their lower calcium and silica content reduces opportunities for strong acid–base bonding with the cationic emulsion (Omar et al., 2020). Their rough and porous texture can enhance mechanical interlock at moderate cold temperatures, though. This advantage reduced sharply once the binder became too brittle (very cold temperatures) to sustain micro-scale interlocking stresses (Omar et al., 2020; You et al., 2019). Therefore, more temperature reduction from -20 °C to -30 °C caused a smaller proportional drop in retention ratio for all aggregates. It can be concluded that once the binder's brittle state is fully developed, further temperature reduction has a minor additional negative effect on fracture susceptibility.

Adhesion between aggregates and binder in chip seals at low temperatures is a critical performance parameter for cold regions such as Canada. Insufficient adhesion can result in early chip loss and accelerate stripping or raveling of the underlying asphalt pavement. The results indicated that aggregates with high alkaline mineral content or high silica content with smaller particle sizes are more resistant to adhesion loss in sub-zero conditions.

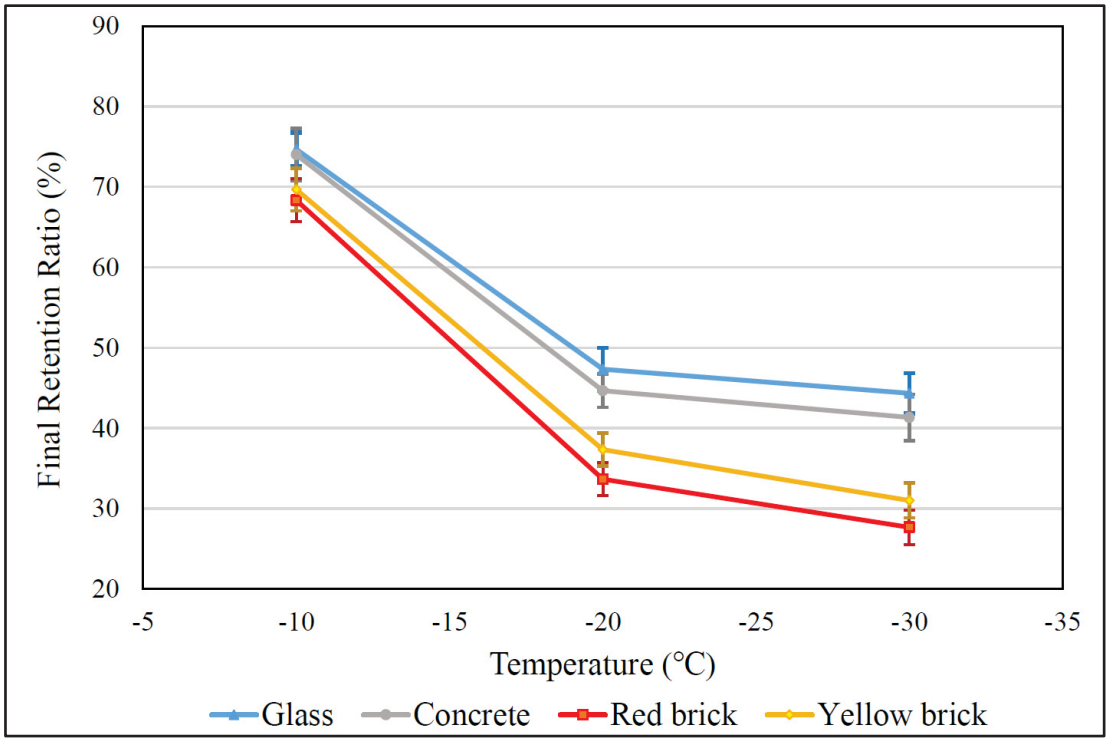

Figure 3.22 The aggregates' retention ratios

3.3.1.6 Chip Seal Bleeding Susceptibility

Because no international standard exists to quantify bleeding in chip seals, in this study, a modified Loaded Wheel Test (LWT), adapted from the microsurfacing standard, was developed to generate a bleeding susceptibility index. This index is defined as the percent weight gain from hot Ottawa sand adhering to the surface after controlled loading. Concrete chip seals exhibited the lowest weight increase (6.56%), determining the baseline for minimal bleeding susceptibility among all studied chip seal types. However, brick chip seals showed almost up to 33% higher (8.73%), and glass chip seals were approximately 62% higher weight increase than concrete (10.65%).

The higher bleeding resistance observed for concrete chip seals may be related to several aggregate characteristics reported in the literature (Zheng et al., 2022). Concrete aggregates typically exhibit higher compressive and abrasion strength (Table 3.1), which can limit particle breakdown during rolling and trafficking. Reduced aggregate crushing may result in fewer generated fines, thereby limiting binder film thickening and localized void filling that can

promote bleeding. In addition, concrete chip seals exhibited higher measured MTD values, which are associated with improved macrotexture and reduced binder rise. The combination of adequate macrotexture and angular aggregate geometry likely limited over-embedment, helping maintain a thinner residual binder film and reducing susceptibility to binder flow.

In contrast, the higher bleeding potential observed for brick and glass chip seals may be associated with their lower abrasion and compressive strength, as well as differences in particle size distribution. Brick and glass aggregates are more prone to fines generation under the Lightweight Wheel Tracking (LWT) test due to their lower mechanical strength (Table 3.1). These fines can blend with the binder to form a richer mastic at contact points, reducing macrotexture and facilitating upward binder migration. In addition, the smaller effective particle size of glass aggregates resulted in lower MTD values and higher embedment. Excessive embedment reduces surface texture and increases effective surface continuity, which can shift load accommodation from aggregate interlock to binder deformation, thereby increasing bleeding susceptibility.

Overall, the bleeding susceptibility index indicated that concrete chips are appropriate for all types of roads due to their low bleeding potential. However, brick and glass chips are suitable for low-volume facilities, including residential streets, driveways, parking areas, and bike routes. This new test method for chip seal durability produces a repeatable relative index that aligns with known mechanisms, including texture loss, binder enrichment, and chip integrity. It intentionally stresses the chip seal with controlled high surface temperature (hot sand) to reveal bleeding tendencies. Finally, the consistent ranking of bleeding index (concrete < brick < glass) and the mechanistic observed pathways provide chip seal designers with actionable guidance and a clear basis for future standardization.

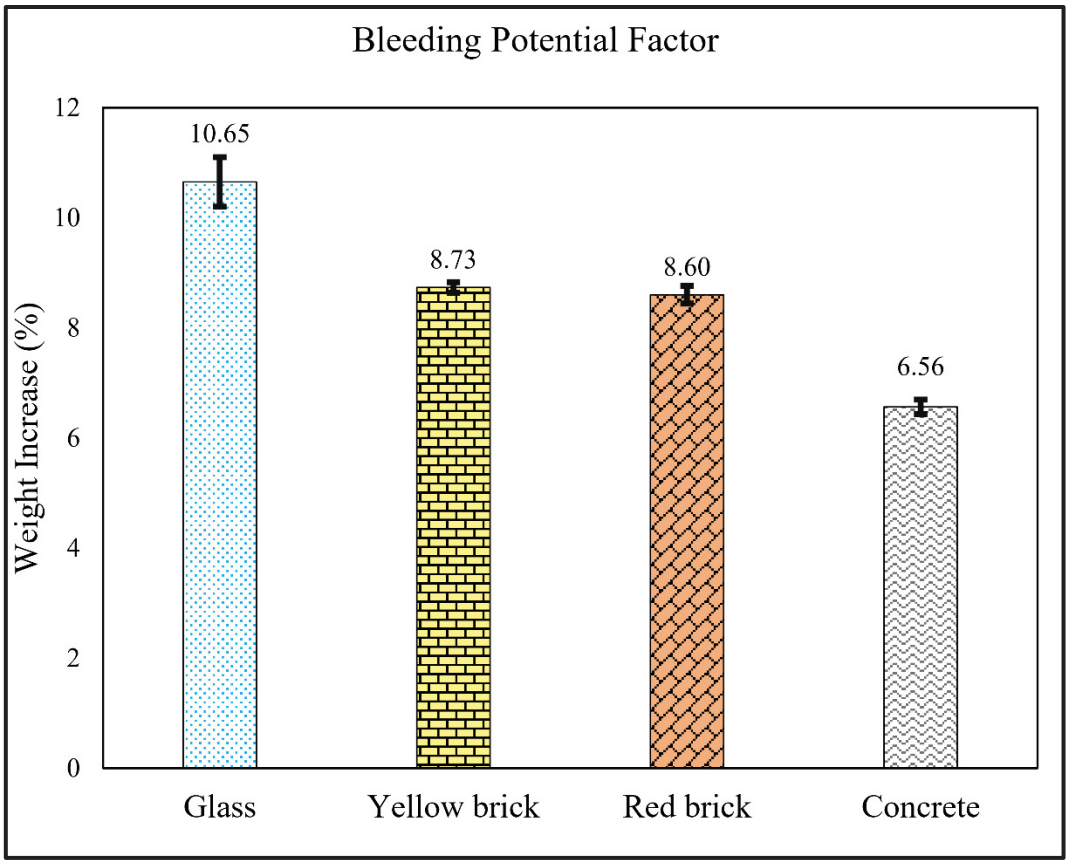

Figure 3.23 The comparison of chip seals' bleeding susceptibility

3.3.2 Thermal Behavior and Reflectance Evaluation

This section summarizes the detailed results of the thermal behavior and reflectance evaluation of the developed chip seals. The evaluation included UV–Visible–NIR reflectance analysis, thermal property measurements, indoor solar simulation tests, and field albedo and temperature monitoring. These experiments were conducted to investigate the materials' ability to reflect solar radiation, dissipate heat, and reduce surface temperature. The results of each test are described and discussed in the following subsections.

3.3.2.1 The Spectrometer Reflectance

When a surface is exposed to incoming solar radiation, it responds through three primary mechanisms, including absorption, reflection, and transmission. This relationship is expressed in Equation 3.3 (Bergman et al., 2017).

$$\rho + \varepsilon + \tau = 1 \tag{3.3}$$

Here, ρ represents reflectance, ε absorption, and τ transmittance. Since both asphalt pavements and chip seals are opaque, the transmittance component can be assumed negligible ($\tau = 0$). Consequently, surface energy balance becomes a direct interplay between reflectance and absorption, making high reflectivity and low absorptivity the desirable characteristics for reducing surface heating.

From a solar radiation perspective, only a fraction of the spectrum reaches the Earth's surface. Ultraviolet (UV) radiation with wavelengths shorter than 300 nm is largely absorbed by stratospheric ozone, and almost 5% reaches the Earth's surface. The remaining solar energy is distributed across the visible (VIS) and near-infrared (NIR) bands, which form the majority of ground-level solar irradiance. In detail, the VIS range (400–780 nm) accounts for about 43% and the NIR (800–2500 nm) forms roughly 52%, as shown in Figure 3.24 (ASTM G173, 2008; Cleveland and Morris, 2013). Direct Normal Irradiance (DNI) refers to this perpendicular solar input, excluding radiation reflected or scattered by atmospheric components.

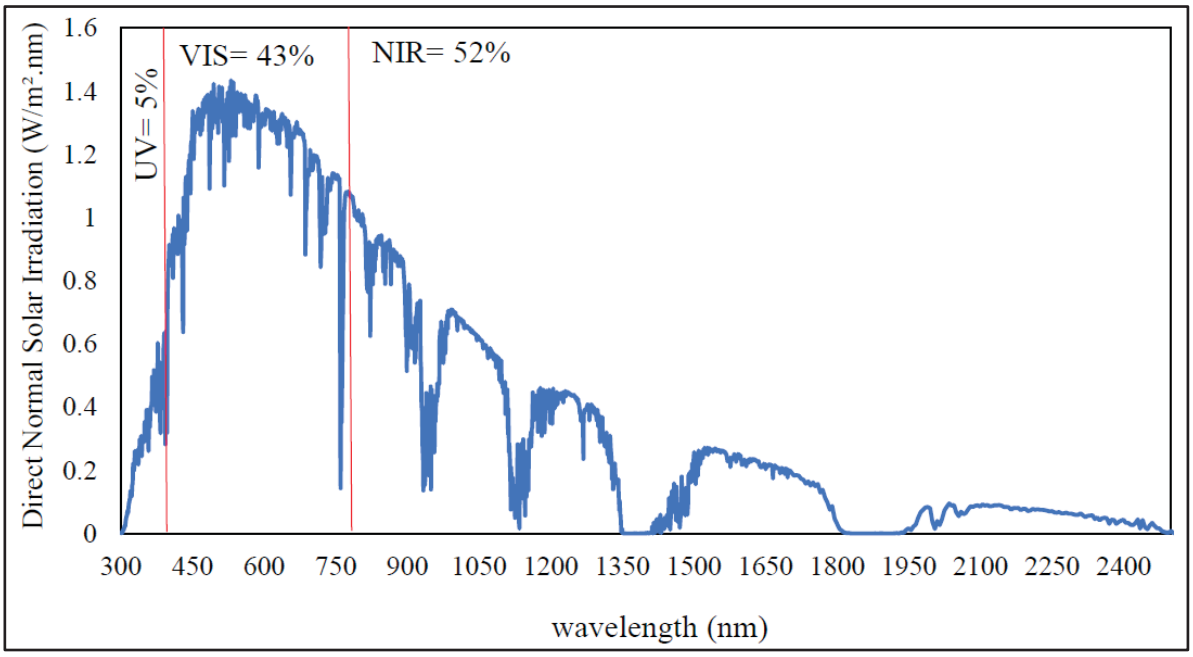

Figure 3.24 The solar spectrum energy (direct normal irradiance)
Adapted from ASTM G173 (2008)

Figure 3.25 demonstrates the spectrometer-measured reflectance curves of different chip seals, new HMA, and aged HMA across the 300–2000 nm wavelength range. Among all these tested specimens, the yellow brick chip seal consistently had the highest reflectance. It was followed by red brick and concrete, while aged HMA, glass chip seals, and new HMA showed significantly lower values.

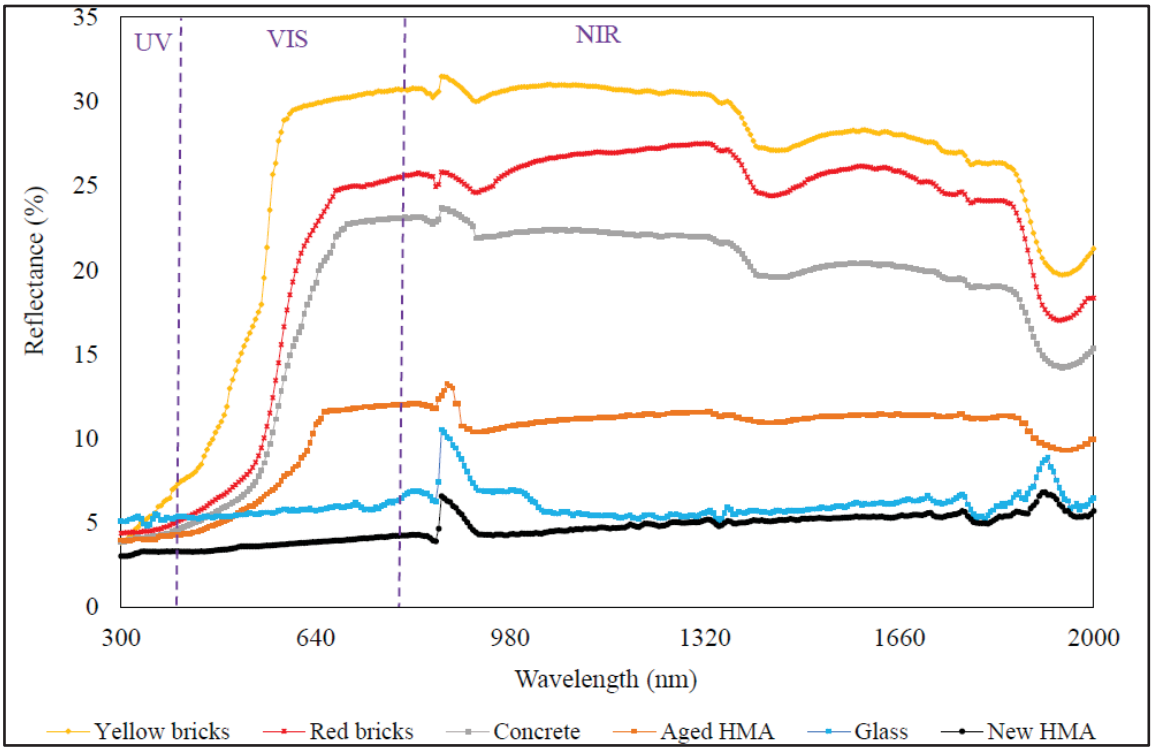

Figure 3.25 Different chip seals, aged and new HMA spectral reflectance

The combinations of the solar spectrum (Figure 3.24) and reflection data (Figure 3.25) were analyzed to account for the non-uniform distribution of solar energy across wavelengths. Thus, Equation 3.4 was employed to provide integrated solar reflectance (R_s) values of chip seals for each wavelength category.

$$R_s = \frac{\int_{\lambda_2}^{\lambda_1} R(\lambda)E(\lambda)d\lambda}{\int_{\lambda_2}^{\lambda_1} E(\lambda)d\lambda} \quad (3.4)$$

Where R_s is the solar reflectance (%), $R(\lambda)$ the spectral reflectance of the specimen, and $E(\lambda)$ the spectral irradiance. The resulting values are summarized in Table 3.13.

Table 3.13 Chip seals, aged and new HMA solar reflectance

Type of surface	Reflectance (%)			
	UV	VIS	NIR	Total (based on wavelengths)
Yellow brick chip seal	5.33	22.58	26.45	24.36
Red brick chip seal	4.57	16.15	23.36	20.61
Concrete chip seal	4.20	14.19	19.20	17.18
Glass chip seal	5.20	5.71	5.75	5.71
Aged HMA	4.07	8.38	10.36	9.54
New HMA	3.23	3.76	4.70	4.40

Regarding the UV band, all surfaces demonstrated very low reflectance, ranging from 3.23% for new HMA to 5.33% for yellow brick chip seals. These small variations are expected, as most construction materials strongly absorb UV due to their mineralogical composition and surface texture. These findings are consistent with previous studies (Turner and Parisi, 2018; Kim and Uh, 2021). As UV contributes only a minor fraction of total ground-level solar energy, these differences have little practical influence on reflectance and thermal performance. Therefore, chip seals behave similarly to other opaque construction materials in this range.

By stark contrast, in the visible (VIS) region, which has about 43% of total solar energy, more significant differentiation was revealed among chip seals and HMA specimens. Yellow brick chip seals reflected 22.58% of incoming visible light, performing better than red brick (16.15%) and concrete (14.19%). However, glass chip seals (5.71%) and new HMA (3.76%) reflected substantially less. These differences can be directly linked to aggregate color and mineral composition. Lighter-colored materials, such as clay brick and concrete, reflect more visible wavelengths, especially those close to their natural color tones, whereas darker materials absorb more energy. Although glass chip seals performed well in UV reflection, their VIS reflectance was poor, owing to the translucence of particles, which allowed light penetration and absorption by the binder. These results are consistent with results reported in studies in which reflective coatings and surface pigmentation were used (Synnefa et al., 2007; Kim and Uh, 2021; Miao et al., 2022).

Because NIR forms the largest share of solar energy (52%), performance in this band is of great importance. Similarly, the yellow brick chip seal had the highest reflectance (26.45%), followed by red brick (23.36%) and concrete (19.20%). Aged HMA reflected just over 10%, while glass and new HMA reflected less than 6% and 5%, respectively. This trend matches the VIS results, indicating the role of chemical composition and microstructural roughness. In particular, lighter aggregates with rougher textures reflected more NIR radiation, while smoother and darker surfaces, like glass and new asphalt, absorbed more NIR radiation. The obtained results were in agreement with previous studies in which the enhancing NIR reflection was emphasized for UHI mitigation (Revel et al., 2013; Coser et al., 2015; Jiang et al., 2019).

After the integration of chip seals' reflectance across the solar spectrum, the total reflectance values highlighted the advantages of clay brick and concrete chip seals. In detail, yellow brick (24.36%) and concrete (17.18%) surfaces significantly outperformed aged HMA (9.54%) and new HMA (4.40%). These higher reflection rates suggest that brick and concrete chip seals can substantially lower surface temperature, reducing UHI effects. Glass chip seals, despite their comparable UV reflectance, demonstrated poor VIS and NIR performance, limiting their cooling potential. As a result, glass chip seals are not recommended for UHI mitigation.

Overall, the spectrometer reflectance results provided the first proof for the cooling potential of recycled chip seals. After quantifying how much energy is reflected across the UV, VIS, and NIR regions, these results predicted the extent to which each surface will absorb solar radiation and, consequently, heat up under field conditions. Surfaces with higher reflectivity, such as clay brick and concrete chip seals, are expected to have lower surface temperatures, since less incoming energy is converted into heat. Conversely, the low VIS and NIR reflectance of glass chip seals and new HMA suggests higher absorptivity and higher surface heating. The effects of higher reflectivity on pavement temperature reduction are evaluated with other laboratory and field tests.

3.3.2.2 Thermal Properties of Chip Seal Aggregates

The experimentally obtained average thermal effusivity and thermal conductivity values of CDW aggregates, as well as aged and new HMA, are summarized in Table 3.14. Thermal effusivity describes a material’s capacity to exchange heat with its ambient air (Ahmad et al.,

2021). Since chip seal aggregates form the pavement's exposed surface, their thermal effusivity influences how quickly the absorbed heat from solar radiation can be released back to the atmosphere. From the UHI mitigation point of view, lower thermal effusivity is advantageous since it slows down heat transfer to the ambient air, moderating the surface temperature during heating and cooling cycles.

Table 3.14 CDW materials and HMA thermal properties

Aggregates & mixtures	Thermal conductivity (obtained from experiments)		Thermal effusivity (obtained from experiments)		Specific heat capacity (J. kg^{-1}. K^{-1}, calculated)	Thermal diffusivity ($mm^2.s^{-1}$, calculated)
	Avg values (W. m^{-1}. K^{-1})	Standard deviation (SD)	Avg values (W. $s^{1/2}$. m^{-2}. K^{-1})	Standard deviation (SD)		
Yellow brick	0.95	0.01	1270.38	9.40	876.84	0.56
Red brick	1.03	0.02	1381	12.87	967.61	0.56
Concrete	2.45	0.05	2162.05	24.33	806.46	1.29
Glass	1.19	0.00	1472.55	1.77	729.74	0.66
Aged HMA	1.91	0.02	1875.97	10.42	808.48	1.04
New HMA	1.65	0.02	1815.22	14.67	872.97	0.82

The results show that yellow and red bricks had the lowest thermal effusivity values (1270.38 and 1381 $W \cdot s^{½} \cdot m^{-2} \cdot K^{-1}$, respectively). This indicates that clay brick aggregates exchange heat with their surroundings more slowly compared to other materials, reducing the intensity of UHI effects. This is attributed to their porous texture and lower density, having air voids in their microstructure. Because air is a poor thermal conductor, its presence lowers the number of atoms available for lattice vibrations and slows heat transfer, which was also observed in previous studies (Chen et al., 2018). Although glass aggregates had slightly higher thermal effusivity (1472.55 $W \cdot s^{½} \cdot m^{-2} \cdot K^{-1}$), they still emit less heat to the surroundings compared to HMA and concrete aggregates.

Concrete, aged HMA, and new HMA all had higher thermal effusivity than yellow brick, with values 70%, 48%, and 43% greater, respectively. Their dense structures and higher bulk density facilitate more efficient vibrational heat transfer. A further distinction is the fundamental structural differences between glass and concrete. Glass, as a non-crystalline amorphous solid with a random molecular arrangement, has lower thermal effusivity (Gupta, 1996; Ramachandran and Feldman, 1996).

Likewise, the thermal conductivity results showed that yellow and red bricks exhibited the lowest conductivity values (0.95 and 1.03 W. $m^{-1}.K^{-1}$), followed by glass (1.19 W. $m^{-1}.K^{-1}$). In contrast, aged and new HMA, and especially concrete, showed substantially higher conductivity values (1.91, 1.65, and 2.45 W. $m^{-1}.K^{-1}$, respectively). These consistent trends indicate that aggregate density and internal structure play an important role in governing heat transfer behavior. Aggregates with higher thermal conductivity, such as concrete, may facilitate greater downward heat transfer from the pavement surface into the asphalt mixture and underlying layers. This enhanced heat transfer is consistent with the observed reduction in surface temperature gradients during peak heating periods. Regarding the conducted tests, the proposed heat-transfer mechanism is discussed as a plausible explanation of the obtained results. While increased heat conduction may contribute to lower surface temperatures, it can also increase heat exposure within the binder layer, potentially accelerating binder softening under hot weather and heavy traffic conditions, as reported in previous studies (Holmgreen et al., 1985; Gransberg, 2005).

Nevertheless, aggregates with lower conductivity (such as clay bricks) limit downward heat transfer, as observed for the HMA surface temperature coated with these aggregates, which maintains binder stiffness by reducing the temperature rise of bitumen. In such cases, the pavement surface may warm more than chip seals with conductive aggregates, but the reduced heating of the binder delays deterioration mechanisms like aggregate movement or bleeding. Thus, the suitability of a material depends on balancing UHI mitigation at the surface with structural durability of the binder–aggregate adhesion.

Specific heat capacity (C_p) values, calculated with Equation 3.5, are the required heat to raise a unit mass of material by 1 °C.

$$e = \left(k.\rho.C_p\right)^{\frac{1}{2}} \tag{3.5}$$

Where e is thermal effusivity (W. $s^{1/2}$. m^{-2}. K^{-1}), k denotes thermal conductivity (W. m^{-1}. K^{-1}), ρ represents the material's density (kg.m^{-3}), and C_p is the specific heat capacity (J. kg^{-1}. K^{-1}). Calculated results ranged between 729.74 J·kg^{-1}·K^{-1} for glass and 967.61 J·kg^{-1}·K^{-1} for red brick, with little variation among other materials at the test temperature (24 °C). Although C_p changes with temperature, and crystalline solids like concrete have a higher C_p at higher temperatures (Pan et al., 2017), the differences are minor. Nonetheless, higher C_p means that more heat energy is needed for the surface to warm, contributing to reduced surface heating under solar exposure. Moreover, thermal diffusivity was calculated via Equation 3.6 (Bergman et al., 2017).

$$\alpha = \frac{k}{C_p \rho} \tag{3.6}$$

Where α is the thermal diffusivity (m^2.s^{-1}), k is the thermal conductivity (W. m^{-1}. K^{-1}), C_p is the specific heat capacity (J. kg^{-1}. K^{-1}), and ρ is the density of the material (kg.m^{-3}). Thermal diffusivity has a direct relationship with thermal conductivity. The thermal diffusivity reveals the rate at which heat spreads through a material. The calculated results showed that bricks and glass had the lowest values, 0.56 and 0.66 $mm^2 \cdot s^{-1}$, respectively. While concrete showed more than double in comparison to these materials (1.29 $mm^2 \cdot s^{-1}$). This outcome again emphasizes the link between density, composition, and heat transport efficiency. Materials with high diffusivity, such as concrete and HMA, quickly distribute absorbed energy throughout their volume. While this rapid distribution can dissipate surface heat and reduce UHI intensity, it also increases the temperature of the binder layer, exacerbating bleeding and raveling in hot climates. Therefore, diffusivity must be evaluated as well as reflectivity and conductivity to assess the UHI and durability performance.

All measured and calculated thermal parameters were consistent with values reported in previous studies for similar materials, confirming the validity of the adopted test methodology (Howlader et al., 2012; Kanellopoulos et al., 2017; Bodian et al., 2018; Hoivik et al., 2019; Byzyka et al., 2021). The findings show the complex trade-offs between thermal behavior,

UHI mitigation, and chip seal durability. Therefore, aggregate selection must be done considering environmental conditions, expected traffic, and thermal loads.

3.3.2.3 The Indoor Cooling Effect Evaluation

The indoor solar simulation tests provided beneficial results regarding the cooling potential of the chip seals compared to uncoated HMA. Figure 3.26 illustrates the surface temperatures increase under 15 hours of continuous exposure to an infrared lamp, which simulates daytime solar radiation. Among all tested specimens, the yellow brick chip seal had the most effective cooling performance, with a surface temperature stabilizing around 48 ℃. This represents a 23% reduction compared to uncoated HMA, whose temperature peaked at nearly 63 ℃. Such a cooling effect is directly related to the high visible and near-infrared reflectance of the yellow brick aggregates, as demonstrated in Section 3.3.7. By reflecting a larger proportion of incoming solar radiation, less energy was absorbed at the surface, reducing the surface temperature. Red brick and concrete chip seals ranked second and third, reducing surface temperatures by approximately 18% and 15%, respectively. These findings confirm that lighter-colored aggregates with higher VIS/NIR reflectivity are effective in reducing daytime surface temperature. These results are consistent with prior research on reflective coatings for pavements (Synnefa et al., 2007; Miao et al., 2022).

In contrast, the performance of the glass chip seal was markedly different. Although its surface temperature was slightly less than HMA during the first 7 hours, by the end of the 15-hour heating period, it peaked at 63.79 ℃, approximately identical to the uncoated HMA. This behavior is attributed to two interconnected mechanisms. Firstly, the transparency of glass allows radiation to penetrate through the aggregate layer and be absorbed by the black bitumen binder underneath. Secondly, the low thermal conductivity and diffusivity of glass cause the absorbed heat to remain near the surface instead of dissipating. Consequently, while glass aggregates had acceptable UV reflectivity, their overall thermal performance is insufficient for surface cooling of pavements.

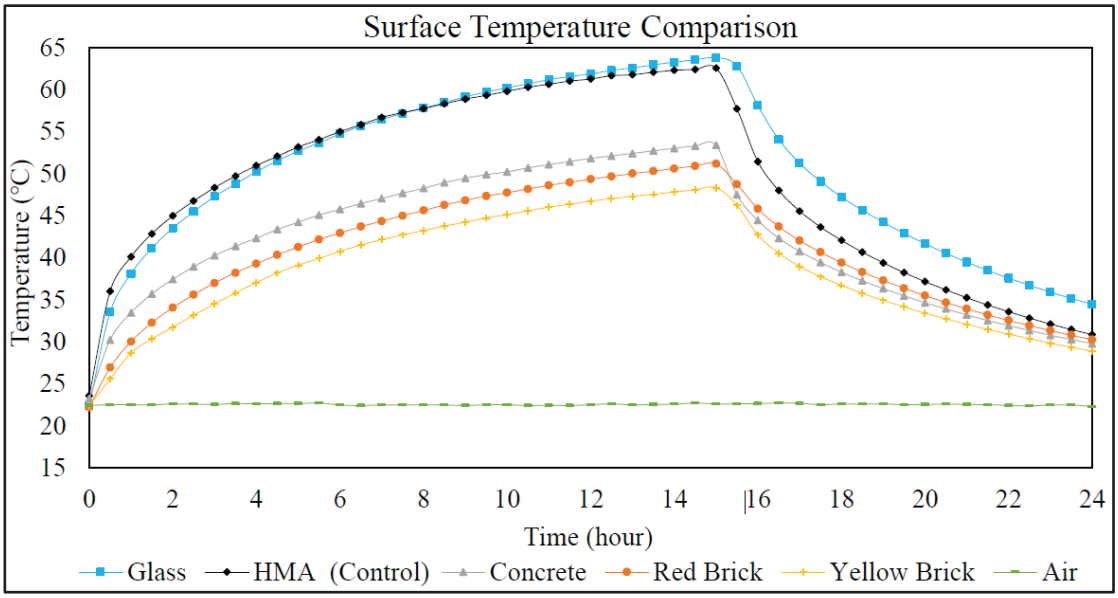

Figure 3.26 Chip seals surface temperature variations in 24 hours

When the lamp was switched off (simulating nighttime conditions), the specimens released accumulated heat to the ambient air. Concrete chip seals showed the fastest cooling rate, surpassing even red brick during the early hours of cooling. This is a direct outcome of concrete's higher thermal conductivity and effusivity (Table 3.14), promoting rapid heat exchange with the surrounding air. However, bricks and glass chip seals cooled more gradually because of their lower thermal conductivity and effusivity. This retention of heat is attributed to their porous textures, which tend to store energy rather than release it. Despite this, the total heat released by conductive surfaces (HMA and concrete) was higher at night. Nevertheless, the considerable benefit of concrete over HMA was its higher reflectivity. Although both materials conduct heat, concrete absorbed less in the first place and released less during the night, contributing less to UHI effects.

The temperature reduction rates after 9 hours of cooling highlighted important results. Yellow and red brick chip seals cooled by 40% and 41%, respectively. While concrete and glass cooled by 44% and 46%, HMA had the greatest reduction at 51%. HMA's higher reduction percentage was a result of its higher initial peak temperature and greater thermal gradient with the surrounding air. The glass chip seal also showed a relatively high percentage reduction, but this is because of its peak temperature (63.79 °C). The specific heat capacity of chip seal

aggregates at the same temperature was in a similar range (Table 3.14), and there is a direct relationship between the temperature change and the heat exchange with the ambient air (Bergman et al., 2017). Therefore, the more the surface temperature reduction during the night is observed, the more heat is released to the ambient air.

The analysis of subsurface temperatures provided insightful results, depicted in Figure 3.27. As the temperature variations in different depths followed a similar trend, only temperatures at a depth of 25 mm are reported in this section. Similarly, after 15 hours of heating, the 25 mm-depth temperatures of the yellow and red brick chip seals were lower than that of the concrete chip seal. This is owing to the lower heat absorption of clay bricks and their insulating properties due to their low thermal conductivity and diffusivity, reducing heat penetration into the underlying asphalt mixture. Similarly, the glass chip seal had a higher subsurface temperature due to lower thermal conductivity, preventing vertical heat transfer and trapping thermal energy near the surface. These results were consistent with previous research in which insulation and conductive materials were used as HMA materials (Yinfei et al., 2014).

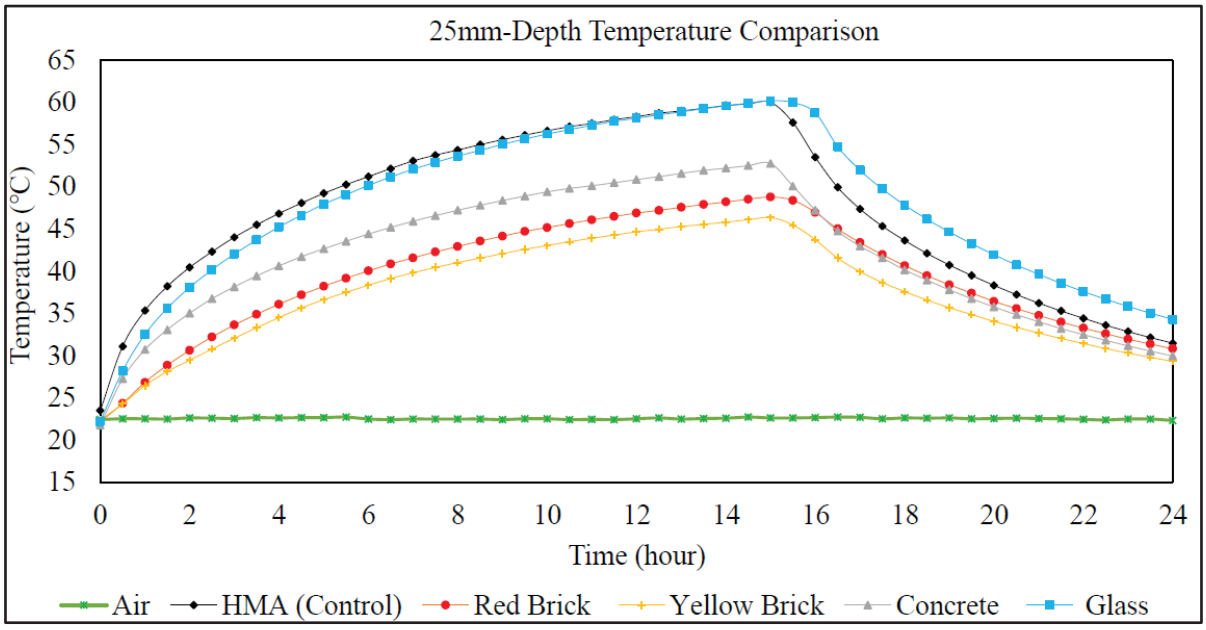

Figure 3.27 25mm-depth HMA temperatures coated with chip seals

The results of this test confirmed the importance of spectral reflectivity and thermal conductivity in determining the cooling efficiency of chip seals. Materials such as yellow and

red bricks combine favorable reflectance characteristics with low conductivity, making them effective at both limiting heat absorption and insulating the underlying pavement. Concrete had a balance by reflecting sufficient radiation while allowing rapid heat release due to higher conductivity, mitigating daytime heating and accelerating nighttime cooling. In contrast, glass aggregates are disadvantaged by their transparency and low thermal conductivity, resulting in high surface heating. Thus, the indoor solar simulation test not only revealed the suitable thermal performance of brick and concrete chip seals but also showed the roles of color, chemical composition, molecular structure, and thermal transport properties.

3.3.2.4 Albedo Assessment and Outdoor Cooling Effects

The outdoor albedo assessment provided valuable results of the cooling potential of chip seals under real solar radiation, complementing the findings from the indoor spectrometer and solar simulation tests. The average albedo, incident, and reflected radiation of six surfaces, including yellow brick, red brick, concrete, glass, aged HMA, and new HMA, were measured over three consecutive hours. The recorded error bars indicated negligible variations between repeated measurements, confirming the consistency of the test procedure, as demonstrated in Figure 3.27.

As shown in this figure, the albedo followed the reflectance behavior observed in the UV–VIS–NIR spectrometer results (Section 3.3.7). In detail, yellow brick chip seals achieved the highest albedo of 0.24, which was nearly double that of aged HMA (0.12) and more than six times that of new HMA (0.04). Red brick and concrete followed with values of 0.22 and 0.21, respectively. In stark contrast, glass chip seals and new HMA consistently showed the lowest albedo values (around 0.05), reflecting their darker appearance and higher absorption of incident solar radiation. The lighter surfaces and mineralogical composition of brick and concrete allowed them to reflect more radiation, while darker surfaces like HMA and transparent aggregates like glass absorbed and transmitted more energy into the pavement.

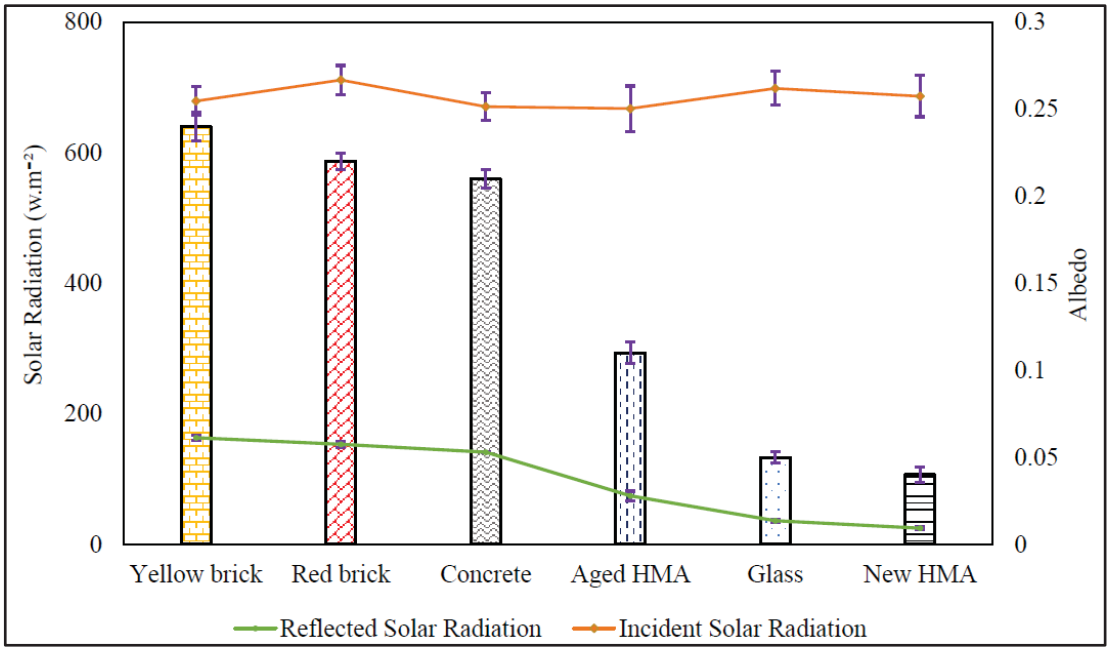

Figure 3.28 The average of albedo, incident, and reflected solar radiation

The difference between aged and new HMA was also considerable. Aged HMA showed a much higher albedo (over double) than new HMA. This shift is attributed to weathering processes that lighten asphalt surfaces through oxidation of asphaltenes and surface degradation (Xie et al., 2020). This finding suggests the advantage of using light-colored aggregates such as bricks or concrete to provide long-term reflective stability. These results were in agreement with the previous findings related to the construction materials and coatings albedo (Li et al., 2013b; Li and Xie, 2020). Pavement's albedo plays a significant part in outgoing heat. Although pavements with higher albedo release more heat during the day (because of higher reflectivity), they release less heat at night, alleviating the UHI effects. Therefore, both bricks and concrete chip seals can mitigate the UHI.

The results indicated that the albedo differences directly affected surface and subsurface thermal responses. Figure 3.29 illustrates the maximum surface and 25 mm-depth temperatures at the end of the albedo test. Yellow brick chip seals again showed the lowest temperatures, with a surface temperature of 25.1 °C and subsurface temperature of 21.2 °C, corresponding to 17% and 27% surface temperature reductions compared to aged and new HMA, respectively. Red brick and concrete also demonstrated considerable cooling, lowering surface

temperatures by 23% and 19% compared with new HMA. Clay bricks also decreased the in-depth temperatures effectively due to the lower thermal conductivity and thermal diffusivity. These results are consistent with the spectrometer outcomes, confirming that high VIS and NIR reflectivity play significant roles in surface cooling.

The behavior of the glass chip seal was similar to the indoor reflectance test. In detail, its overall albedo was extremely low (0.05), and its surface temperature was close to new HMA, and even around 3 °C higher than aged HMA. This performance is attributed to the transparency of glass aggregates, allowing solar radiation to penetrate deeper into the pavement surface and be absorbed, exacerbating rather than mitigating UHI effects. The in-depth temperature of the glass chip seal was much less than the new HMA due to its insulation effects, though.

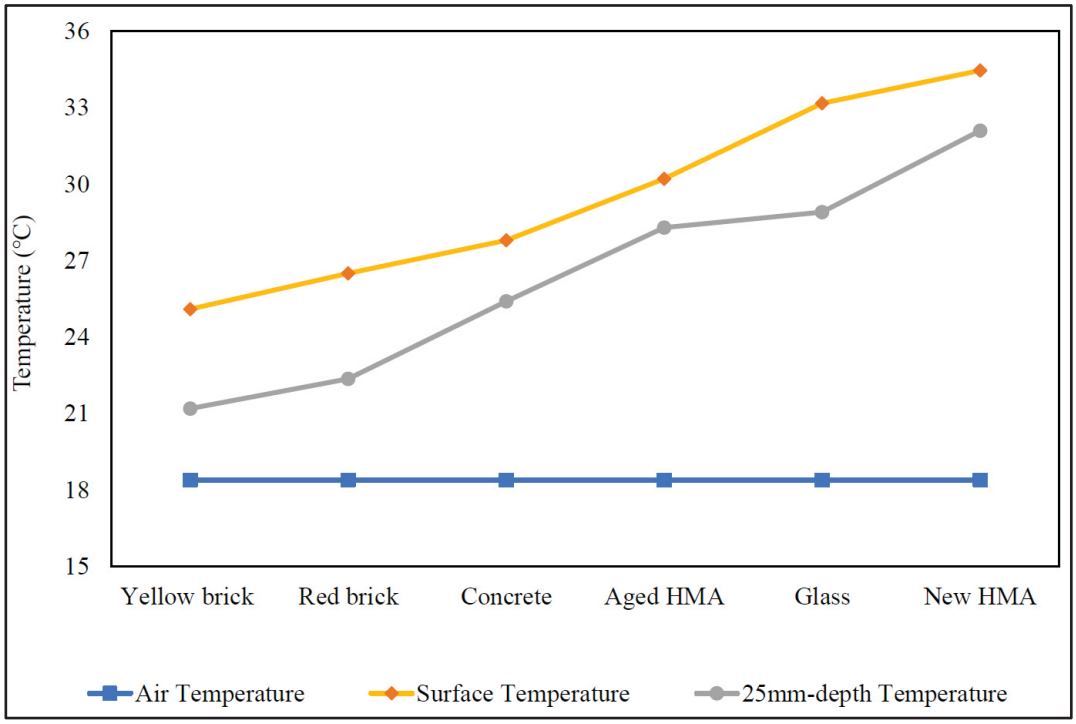

Figure 3.29 The surface and 25 mm-depth temperatures of chip seals, aged and new HMA

Overall, these results indicated the role of albedo and thermal properties in determining pavement cooling potential. Yellow and red brick chip seals, with their higher albedo and

insulation nature, emerged as the most effective solutions for reducing both surface and subsurface temperatures under outdoor conditions. Concrete offered a balanced performance, combining moderate albedo with adequate nighttime cooling effect. Nevertheless, glass chip seals performed poorly due to their transparency, making them unsuitable for UHI mitigation.

3.4 Conclusion

The conducted tests and analyses revealed beneficial results, mitigating urban heat island effects as well as proposing novel chip seal materials. The mechanical evaluation of chip seals produced with recycled construction and demolition waste aggregates confirmed these materials can be used for chip seals using the modified McLeod method without compromising design embedment criteria. This supports the hypothesis that CDW materials can be employed as chip seal aggregates, satisfying the structural requirements for surface treatments while offering potential environmental benefits. The findings also indicate that CDW materials with irregular shapes or higher absorption require slight adjustments in binder application rates, and all of them cannot be used for all roads, defining the practical limits for their use under various traffic loads. In detail, these materials can provide adequate and, in some cases, great performance compared to conventional aggregates. MTD measurements showed that all developed chip seals had minimum thresholds specified in chip seal standards, ensuring compliance with safety requirements for both high-speed and low-speed traffic. Concrete, yellow brick, and red brick chip seals showed higher MTD values than glass, due to their angular and irregular particle morphologies, which promoted greater surface roughness.

Sweep test resistance, as a durability factor, revealed the role of aggregate morphology and binder–aggregate interaction. While all mixes demonstrated aggregate losses below 10%, which is satisfactory performance, the adhesion mechanisms were different for chip seals. The higher retention observed for concrete and brick chip seals is consistent with their rough and angular surface characteristics, which are known to promote mechanical interlocking and improve resistance to aggregate dislodgement. In contrast, glass chip seals exhibited high retention, which may be associated with their smaller particle size and deeper embedment within the binder film, as indicated by lower measured MTD values. Previous studies have also reported that mineralogical composition can influence aggregate–binder affinity when cationic

emulsions are used. However, chemical interactions were not directly characterized in this study. These results emphasize that aggregate mineralogy, morphology, and binder compatibility collectively influence chip seal performance. It should be noted that the sweep test reflects short-term aggregate retention under dry conditions and does not account for moisture effects or long-term aging. Therefore, the observed trends are interpreted as indicators of early-life durability rather than long-term performance.

Interface bond strength results, another durability factor, emphasized the significance of aggregate–binder interactions. Concrete had the strongest adhesion at all tested temperatures, because of negatively charged aggregate surfaces with the cationic binder and strong mechanical interlock. Glass also performed well due to high silica content and reduced interfacial voids, while bricks showed bond strength limited due to their low compressive and abrasion strengths, rather than poor adhesion. At sub-zero temperatures, Vialit test results confirmed that glass and concrete had high retention ratios, while brick aggregates showed greater losses, revealing the critical role of aggregate mineralogy in cold-climate adhesion. However, at very low temperatures (-20 to -30 °C), binder brittleness became the main failure mechanism, reducing retention of all materials.

Moreover, skid resistance tests confirmed excellent safety potential, with all surfaces achieving BPN values above 70 at ambient temperature (23 °C ± 2 °C), which is over thresholds for excellent friction. Performance trends closely followed MTD values, highlighting the combined role of macro- and microtexture in providing adequate tire–pavement friction. At elevated temperatures, BPN values decreased due to binder softening and aggregate displacement, but concrete chip seals retained the highest resistance, reflecting both the stability of their angular aggregates and their suitable bond strength. Although insulating materials such as bricks and glass theoretically slow binder heating, the effect was marginal under laboratory conditions, indicating that aggregate geometry and mechanical stability dominate high-temperature skid resistance, and full-scale field tests can reveal more results for this subject.

Bleeding susceptibility, assessed through a novel test, revealed chip seal performance. Concrete chip seals had the lowest bleeding potential due to high aggregate strength, well-

preserved macrotexture, and resistance to over-embedment. By contrast, brick and glass chip seals showed greater bleeding tendencies, attributed to lower aggregate compressive and abrasion strengths, and smaller glass aggregates. These results indicated that while all recycled materials can be used in low-volume roadways, concrete chip seals are most suitable for high-traffic applications, where both safety and durability are critical.

Overall, the mechanical, early-life durability, and safety evaluations demonstrated that several recycled aggregates can produce chip seals that meet standard performance thresholds under the test conditions considered in this study. Performance outcomes, however, varied depending on aggregate type. Concrete aggregates consistently exhibited adequate adhesion, skid resistance, and bleeding resistance across all evaluated tests, showing their potential to be used for all roads after assessing their long-term durability under freeze-thaw conditions. Yellow brick chip seals achieved high skid resistance but showed lower aggregate retention and higher sensitivity in durability-related tests conducted under dry and short-term conditions. As a result, their performance should be interpreted as indicative of early-life behavior rather than long-term durability. Based on the measured results, these materials may be considered for applications with limited mechanical and environmental demand, such as low-traffic roads, residential streets, driveways, parking areas, and bicycle paths, where loading levels and service conditions are less severe.

The reflectivity and thermal measurement tests also revealed the role of using these chip seals in urban heat island mitigation. Temperature measurements revealed that chip seals made with light-colored recycled aggregates (brick and concrete) showed lower surface temperatures. This directly confirms the first research hypothesis that reflective CDW materials can reduce pavement temperature, mitigating UHI intensity.

Spectral reflectance analysis confirmed that reflectivity is dependent on aggregate type, color, and microstructural characteristics. Yellow brick chip seals consistently performed better than other materials, with integrated solar reflectance of 24.36% across UV, VIS, and NIR regions, almost six times higher than new HMA. Red brick and concrete chip seals also showed good reflectance performance, ranked after yellow bricks. While glass had minimal reflectivity due to its light-transmitting nature. As visible and near-infrared bands dominate incoming energy,

the high reflectance of brick and concrete directly shows significant surface cooling potential of these chip seals.

Thermal property measurements deepened this understanding by linking cooling performance to thermal parameters, including conductivity, effusivity, thermal capacity, and diffusivity. Bricks, with their porous microstructure and low density, had the lowest thermal effusivity and conductivity, insulating the underlying binder and slowing heat penetration. Glass also had relatively low conductivity, but its transparency caused no cooling benefit by transmitting radiation directly into the pavement surface. In contrast, concrete showed high conductivity and effusivity, which may increase heat release during nighttime. However, its higher reflectivity reduced the heat absorption, resulting in less heat in comparison to uncoated HMA. These findings emphasize the importance of balancing surface reflectivity and thermal transport properties for chip seal aggregate selection.

Indoor solar simulation confirmed these theoretical results under controlled heating and cooling cycles. Yellow brick chip seals had the coolest surface temperatures (48 °C) after 15 hours of lamp exposure, 23% lower than uncoated HMA. After yellow brick chip seals, red brick, and concrete provided considerable cooling results. However, glass reached peak temperatures similar to HMA, confirming its limited thermal benefit. Furthermore, nighttime cooling indicated material differences. Concrete released heat faster than bricks and glass due to its higher thermal effusivity and conductivity. Subsurface measurements revealed similar trends for chip seals.

Outdoor albedo and temperature measurements validated these laboratory findings under real solar conditions. Yellow brick chip seals achieved the highest albedo (0.24), over six times greater than new HMA, with red brick and concrete following closely. This higher albedo caused substantial surface cooling. In detail, yellow brick surfaces were 17% and 27% cooler than aged and new HMA, respectively. Red brick and concrete similarly decreased surface and in-depth temperatures, confirming their effectiveness for UHI mitigation. Glass, however, demonstrated the poorest performance, with an albedo near 0.05 and surface temperatures comparable to new HMA.

All in all, these thermal and reflectivity evaluations demonstrated that clay brick and concrete chip seals provide the most effective UHI mitigation. Yellow brick, with its high reflectivity and insulating properties, was the optimal material for surface cooling. Concrete also balanced daytime reflectivity and nighttime heat exchange, offering stable performance. Glass, despite adequate aggregate retention in mechanical tests, consistently failed in thermal performance, showing its unsuitability for UHI reduction.

In conclusion, the comprehensive evaluation of recycled chip seals confirmed that some aggregates from construction and demolition waste can produce functional, durable, and safe chip seals while also contributing to urban heat island alleviation. Mechanical performance results proved that aggregate morphology and mineralogy dictate adhesion, skid resistance, and bleeding susceptibility. More importantly, thermal and reflectivity analyses showed that color, conductivity, and effusivity play critical parts in cooling potential and long-term environmental benefits. Although yellow brick represented the highest thermal benefit for UHI mitigation among all chip seals, its lower mechanical performance limits its application for high-volume roads. However, concrete provided the strongest mechanical durability and adhesion, making it suitable for high-volume roads, with suitable cooling effects to mitigate the UHI. Glass showed some poor mechanical properties and thermal performance, making it unsuitable for thermal mitigation and restricting its application to low-traffic roads.

Finally, this chapter explains that CDW materials can be strategically selected to optimize both mechanical durability and thermal performance of chip seals, confirming some of the research hypotheses. Depending on the traffic volumes, municipalities can design recycled chip seals for existing pavements in urban areas that not only meet safety and durability standards but also contribute to sustainable urban infrastructure through decreased construction waste, reduced pavement heating, and UHI mitigation. After examining the effects of surface reflectivity using recycled chip seals in this chapter, the next chapter focuses on the thermal behavior of subsurface pavement layers. In detail, Chapter 4 investigates the influence of the interface and base course, particularly when modified with conductive materials, on downward heat transfer, overall pavement temperature, and heat release, evaluating how different pavement structures contribute to mitigating UHI effects.

CHAPTER 4

THE EFFECTS OF CONVENTIONAL, CONDUCTIVE PRIME COATS, AND CONDUCTIVE BASE COURSES ON THE ASPHALT PAVEMENT TEMPERATURE AND URBAN HEAT ISLAND EFFECTS

4.1 Introduction

In Chapter 3, novel chip seals using CDW materials were developed to enhance surface reflectivity and reduce heat absorption from solar radiation, mitigating the UHI effects. These reflective surface treatments declined pavement temperatures, reducing the thermal gradient between the pavement and ambient air and resulting in lower heat exchange with the ambient air. However, the results also proved that even with improved reflectance, a considerable fraction of heat is inevitably absorbed by the asphalt mixture. If this absorbed heat is accumulated in the asphalt mixture layer, it brings about a higher surface temperature, and some of this energy is released during the night. Another goal of this thesis is to use the multi-layered structure of asphalt pavement to dissipate the absorbed heat into layers below and use the higher thermal capacity of these layers, reducing the asphalt mixture temperature and lowering the heat exchange with the ambient air. Therefore, the challenge extends beyond surface reflectivity. In fact, it is vital to develop strategies that facilitate efficient dissipation of absorbed heat into deeper pavement layers, preventing its accumulation and release into the urban atmosphere.

Although most heat absorption occurs at the asphalt mixture surface, and this layer has the heat exchange with the ambient air, the rate of heat transfer to the base course plays a critical role in how much heat remains near the pavement surface. The presence of air-filled pores at the asphalt mixture and base course interface reduces the heat conduction to the base course, limiting the downward transfer of absorbed energy. Traditionally, this interface is treated with a prime coat, a thin bituminous binder layer applied on top of the compacted base course to seal surface pores and improve adhesion between layers (Freeman et al., 2010). As using this layer is not mandatory based on most road construction guides, it is often omitted for cost-

saving reasons. One of the overlooked aspects of using prime coats is its role in downward heat transfer. This thin layer of bitumen has the potential to influence the thermal behavior of the pavement by reducing trapped air at the interface and enhancing conductivity. If modified with conductive additives, the prime coat may act as a thermal bridge, enabling more effective dissipation of absorbed heat into the base course and subgrade.

In addition to the asphalt mixture–base course interface, the properties of base course materials may influence heat transfer and dissipation within the pavement structure. Conductive base courses incorporating materials such as steel slag have been reported in the literature to enhance thermal conductivity and potentially facilitate heat transfer away from the asphalt mixture layer. Replacing conventional limestone with varying percentages of steel slag may increase the effective thermal conductivity of the base course, which could promote greater heat redistribution within the pavement system. Under daytime heating conditions, such enhanced conductivity may contribute to lower surface temperatures by reducing near-surface heat accumulation, while during cooling periods, it may influence the release of stored heat. However, the direction and magnitude of heat transfer depend on temperature gradients, boundary conditions, and pavement configuration.

Considering the potential benefits of using prime coats, modified prime coats, and base courses on the pavement surface temperature reduction and UHI mitigation, the effect of using steel slag aggregates and powders was evaluated using different experimental techniques in this chapter. Firstly, the effect of using a conventional prime coat on the asphalt pavement temperature and the released heat was evaluated with a laboratory setup. Different percentages of steel slag powders (up to 40%) were added to this prime coat to assess the impact of using a conductive prime coat on surface temperature reduction and UHI mitigation. Moreover, different proportions of limestone aggregates in the base course, specifically 33%, 66%, and 100%, were substituted with steel slag aggregates to develop a conductive base course for the same aim of pavement surface temperature reduction and mitigating the UHI effects. These modified base courses were first assessed for optimum moisture content and mechanical strength using the Modified Proctor and California Bearing Ratio (CBR) tests. Subsequently, the thermal behavior of both the conductive prime coat and base courses was evaluated with a C-Therm trident thermal conductivity device, employing the modified transient plane source

(MTPS) and transient line source (TLS) needle sensors. To simulate solar radiation, an infrared lamp was used to examine the cooling potential of the developed pavement structures. Furthermore, a heat flux sensor (FluxTeq) was employed to quantify incoming and outgoing heat fluxes. The outline of Chapter 4 is demonstrated in Figure 4.1.

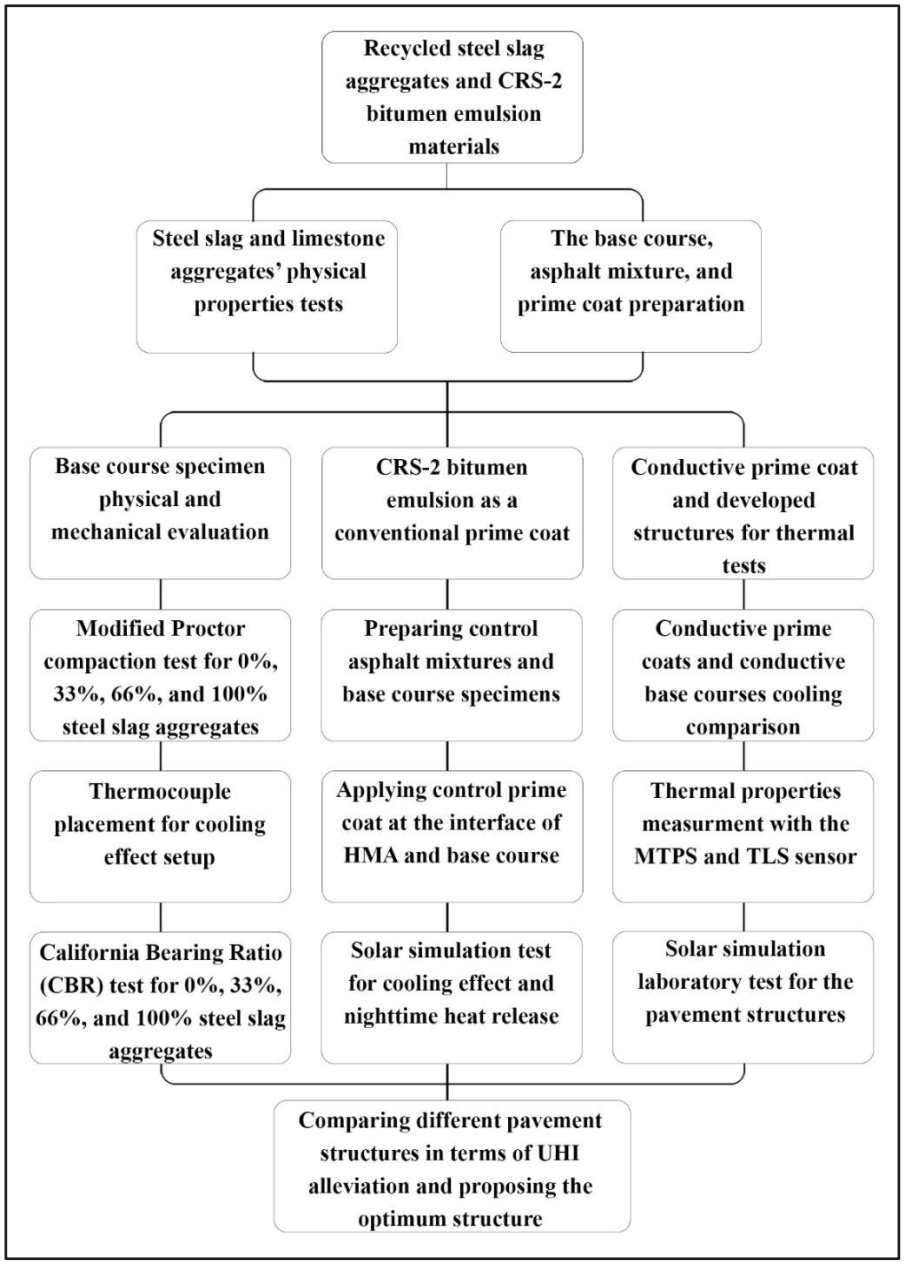

Figure 4.1 The outline of Chapter 4

4.2 Materials and Methods

The section describes the materials used in the construction of the pavement structures. The properties of limestone and steel slag aggregates, and the prime coat are explained. Besides, the asphalt mixture design, consistent with regional practices, for the laboratory specimens, is presented. After the material characterization, the mechanical performance of the developed base course structures was assessed. The Modified Proctor test was performed to establish the optimum moisture content and maximum dry density (MDD), while CBR tests were conducted to determine the load-bearing capacity of the developed base course using steel slag aggregates.

In addition to physical and mechanical properties tests, the thermal properties of both the base course and the prime coat were measured using advanced techniques, including the MTPS and TLS sensors, to quantify thermal conductivity. To evaluate the cooling potential of the developed pavement structures under solar radiation, an indoor solar simulation setup was employed using an infrared lamp, as explained in this section. These tests allowed for a comprehensive evaluation of how conductive base courses and prime coats influence pavement thermal behavior and their potential contribution to mitigating UHI effects.

4.2.1 Materials

Limestone aggregates, which are widely used as conventional base course materials in Montreal (Canada), were selected in accordance with Grading C of the AASHTO specification (AASHTO M 147-65, 2012). The allowable gradation limits specified by AASHTO, along with the gradation curves and representative images of both limestone and Electric Arc Furnace (EAF) steel slag aggregates, are presented in Figures 4.2 and 4.3.

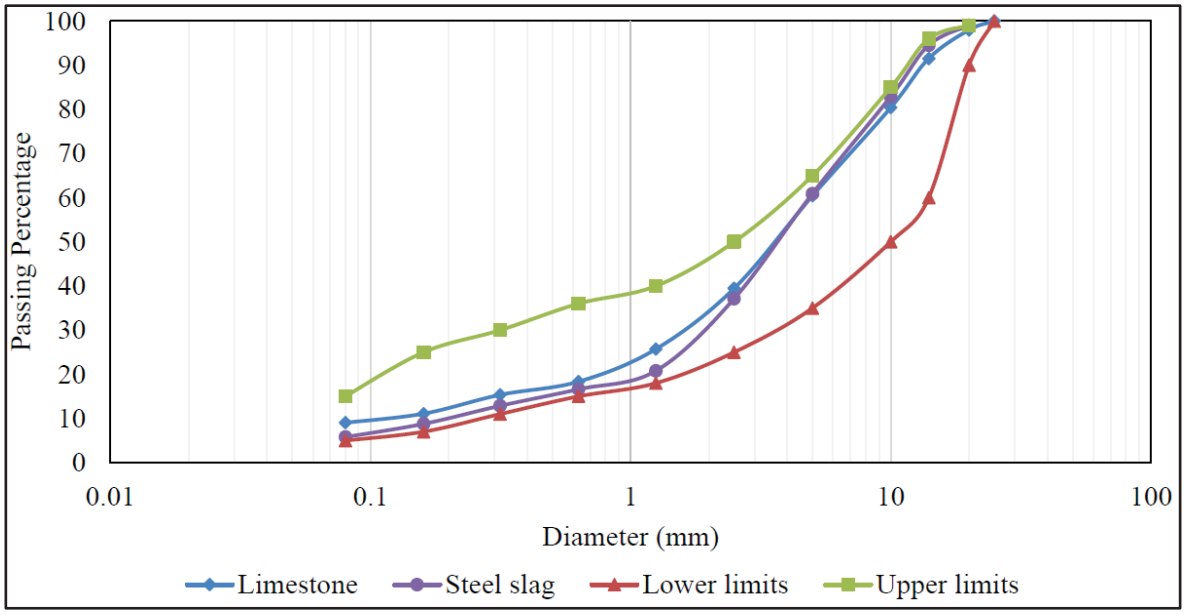

Figure 4.2 The steel slag and limestone gradation for base course specimens

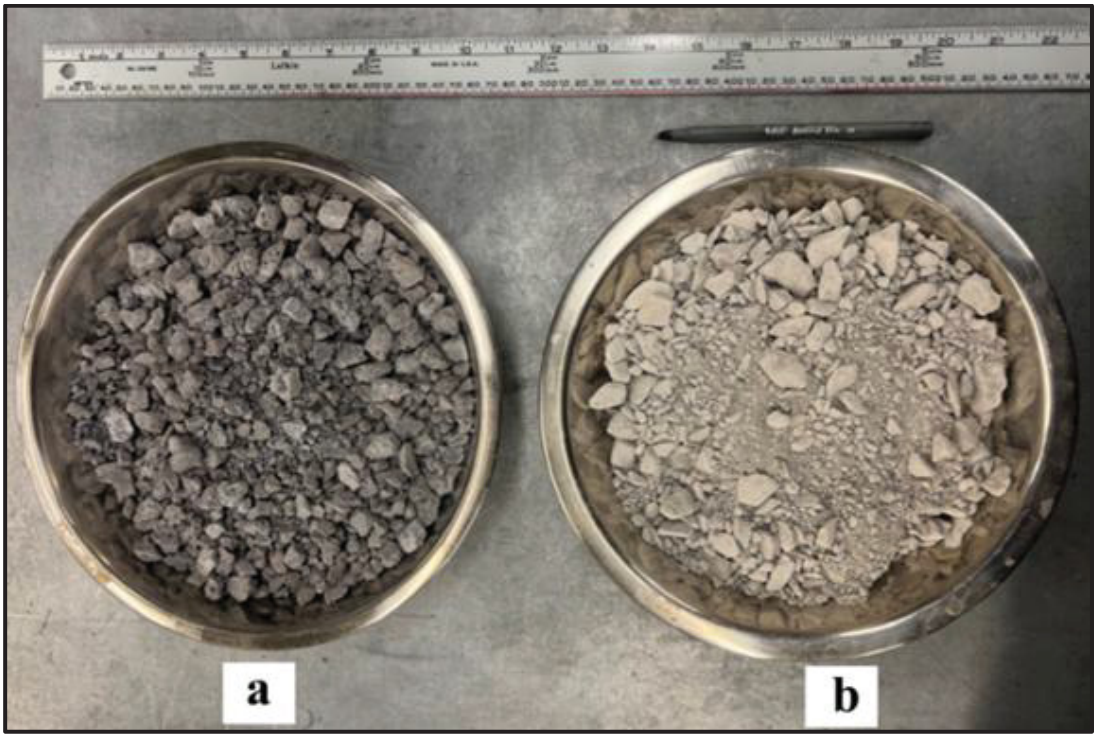

Figure 4.3 The used aggregates: (a) Steel slag and (b) limestone

The steel slag aggregates were supplied by Harsco Environmental. In Quebec, the Bauval Group has already used a partial amount of this by-product in asphalt mixture production. Therefore, a full curing treatment was applied by them to ensure the material achieved acceptable volumetric stability before use. As specified by ASTM D2940 standard, the expansion of steel slag aggregates intended for highway base and subbase applications must remain below 0.50%, which was satisfied by the aggregates utilized in this study (ASTM D2940, 2020). Furthermore, the physical properties of both limestone and steel slag aggregates were experimentally determined and are summarized in Table 4.1.

Table 4.1 The physical properties of the utilized aggregates

Properties	Standard	Limestone	Steel Slag
Coarse aggregates density ($kg.m^{-3}$)	(ASTM C127, 2015)	2690	3570
Fine aggregates density ($kg.m^{-3}$)	(ASTM C128, 2022)	2536	3450
Coarse aggregates water absorption (%)	(ASTM C127, 2015)	0.92	0.88
Fine aggregates water absorption (%)	(ASTM C128, 2022)	1.44	1.36
Blend maximum dry density ($kg.m^{-3}$)	(ASTM D1557, 2021)	2355	2785
Blend optimum water content (%)	(ASTM D1557, 2021)	5	4.4
Los Angeles abrasion (%)	(ASTM C131/C131M, 2020)	26	15

4.2.2 Asphalt Mixture Design

For the solar simulation experiments, laboratory asphalt mixture specimens were placed over the compacted base layers to form two pavement layers. The asphalt mixtures were produced in accordance with the Quebec provincial standards (Québec, 2016). Specifically, a dense-graded hot mix asphalt known as ESG-10 was selected, and a PG 58-28 performance grade asphalt binder modified with anti-stripping agents was used, improving durability and moisture resistance. The nominal maximum aggregate size used in this mixture was 10 mm, ensuring appropriate gradation for surface course applications. The specimens' diameter and height were 150 mm and 100 mm, respectively. The detailed aggregate gradation curve, including MTMD limits, and mixture specifications are presented in Figure 4.4 and Table 4.2, respectively.

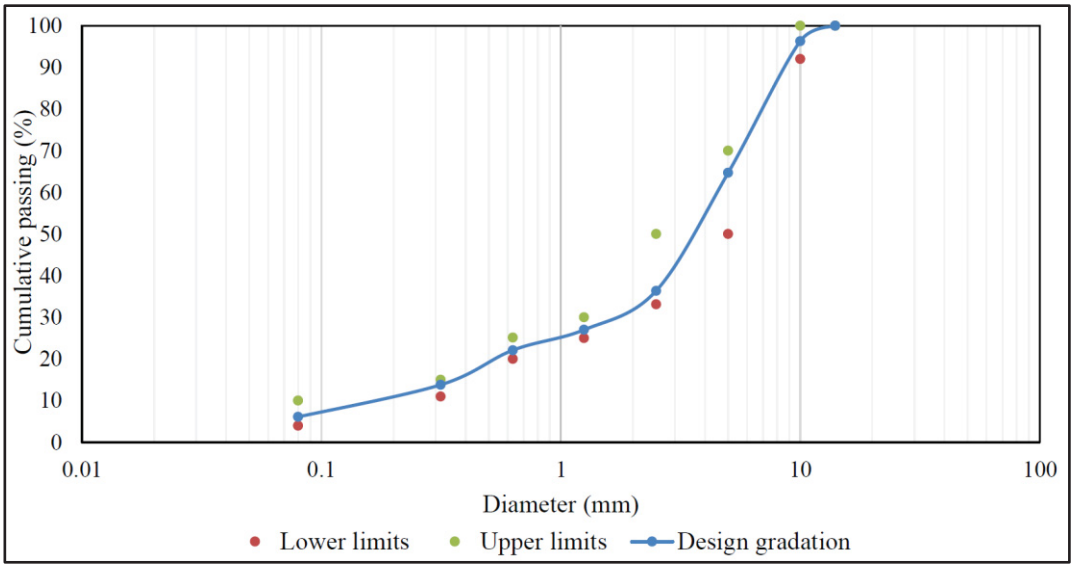

Figure 4.4 Aggregate gradation of asphalt mixture specimens

Table 4.2 Asphalt binder and asphalt mixture characteristics

PG 58-28 asphalt binder specifications	Values
Density at 25 °C ($g.cm^{-3}$)	1.025
Viscosity at 135 °C (Pa·s)	0.247
Viscosity at 165 °C (Pa·s)	0.075
G*/sin δ at 58°C for virgin binder (kPa)	1.254
ESG-10 asphalt mixture specifications	**Values**
G_{mm} ($g.cm^{-3}$)	2.538
Binder (%)	5.45
Absorbed binder (%)	1.02
Effective binder (%)	12.2

4.2.3 Conventional and Conductive Prime Coats

Cationic rapid-setting bitumen emulsion (CRS-2) was used as the conventional prime coat in this study. The detailed specifications of the CRS-2 emulsion are provided in Table 4.3. To explore the potential influence of interfacial thermal properties, the emulsified binder was modified by incorporating steel slag powder, producing a prime coat formulation with increased solid mineral content. For asphalt mastic preparation, the slag was sieved, and particles smaller than 0.075 mm were collected. This gradation was selected to promote uniform dispersion of slag particles within the CRS-2 emulsion and to enhance particle–binder contact at the interface. The resulting formulation was intended to increase the effective thermal conductivity of the prime coat layer.

Table 4.3 The bitumen emulsion specifications

Tests	Unit	Test method	Result For CRS-2	Specifications	
				Min	Max
Residue by distillation (weight)	%	(ASTM D6997, 2020)	69.1	65	-
Oil Distillate, (volume)	%	(ASTM D6997, 2020)	0.32	-	3
Demulsibility	%	(ASTM D6936, 2017)	85.1	40	-
Saybolt Furol viscosity at 50 °C	Sec	(ASTM D7496, 2018)	223.4	100	400
Settlement and storage stability, 1 day	%	(ASTM D6930, 2019)	0.312		Max 1
Penetration, 25°C, 100 g., 5 s.	0/1mm	(ASTM D5, 2013)	153.3	100	250
Particle Charge	-	(ASTM D7402, 2017)	Positive	-	-
Ductility, 4°C, 5 cm/min	cms	(ASTM D113, 2017)	75.1	40	-
Solubility in TCE	%	(ASTM D2042, 2015)	99.51	98.5	-

To determine the maximum possible filler dosage, six different percentages of steel slag powder, including 10%, 20%, 30%, 40%, 45%, and 50% by weight of CRS-2, were prepared with 3 replicates, providing 18 samples. The bitumen emulsion was preheated and maintained at 60 °C on a heating plate before adding steel slag filler, ensuring proper workability and preventing premature breaking of the emulsion. Mixing was performed using a mechanical IKA RW16 Basic Overhead Stirrer operating at 1000 rpm. This mixing protocol was selected

to promote adequate dispersion of filler particles and homogeneous blending of the asphalt mastic.

The blending trials revealed that the maximum feasible loading of steel slag powder was 40% by weight of the bitumen emulsion. After increasing the filler percentage, the mixture showed signs of instability, including non-uniform dispersion and premature emulsion breaking, due to the strong physico-chemical interaction between the highly alkaline steel slag powder and the cationic binder (Jiao et al., 2020b). As a result, all conductive asphalt mastics of this research contained 40% steel slag filler, which represented the optimal balance between conductivity enhancement and mixture stability. The steel slag filler particles, the mechanical stirrer setup, and the final asphalt mastic blends are illustrated in Figure 4.5, demonstrating the preparation process and the resulting homogeneity of the asphalt mastics.

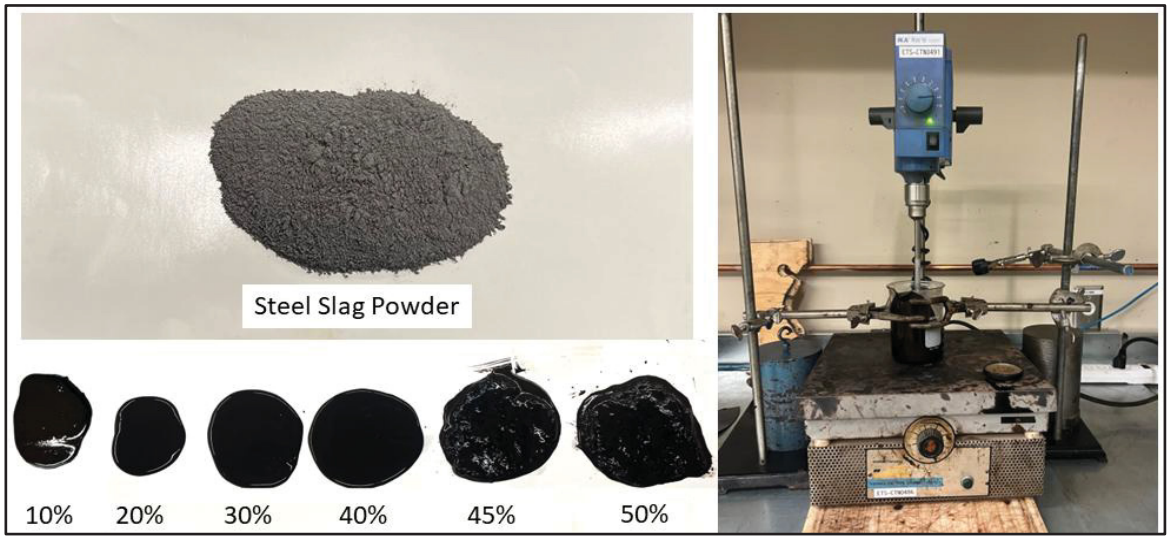

Figure 4.5 Steel slag powder, asphalt mastics, the stirrer, and the heating plate

4.2.4 The Mechanical and Physical Properties of Base Course Specimens

To assess the influence of conductive steel slag aggregates on the structural behavior of base courses, four distinct mixtures were prepared. The control specimen was composed of 100% conventional limestone aggregates, reflecting typical practice in Montreal. In addition, three modified blends were produced, in which limestone was partially or fully replaced with steel

slag aggregates at proportions of 33%, 66%, and 100% by weight. This gradation allowed for a systematic evaluation of the mechanical and physical effects of increasing steel slag aggregates.

The developed base course specimens were subjected to two key compaction and strength characterization tests. First, the Modified Proctor Test was conducted to determine the Optimum Moisture Content (OMC) and the Maximum Dry Density (MDD) of each mixture. These parameters are critical indicators of compaction behavior and aggregate packing efficiency, directly influencing pavement stability and long-term performance. Second, the California Bearing Ratio (CBR) test was performed to assess the load-bearing capacity of the mixtures, simulating field conditions where base layers must resist repetitive traffic loading.

4.2.4.1 Modified Proctor Compaction Test

The Modified Proctor compaction test was conducted to determine the OMC and MDD of the base course mixtures, following the standard procedure outlined in ASTM D1557 (2021). This test is crucial because achieving proper compaction ensures adequate strength, durability, and stiffness of the base course, which directly affects pavement performance under traffic and environmental loads.

Cylindrical Modified Proctor molds and standard rammers were used to prepare the specimens. Each specimen was compacted in five layers, and each layer was subjected to 56 blows from a rammer dropped from a height of 457.2 mm. This procedure applied an equivalent compaction effort of approximately 2700 kN-m.m^{-3}, simulating heavy field compaction conditions. Such energy levels simulate realistic densification of pavement layers, ensuring that the laboratory-derived MDD values represent field performance more accurately than lighter compaction protocols (ASTM D1557, 2021).

For the control mixture (100% limestone) and each replacement level of steel slag aggregates (33%, 66%, and 100% by weight), water was added incrementally at five moisture contents (2%, 4%, 6%, 8%, and 10% by weight) with 3 repetitions, preparing 60 specimens. After compaction, the dry density of each specimen was calculated and plotted against its corresponding water content to produce the characteristic compaction curve. The peak of this

curve was used to determine the MDD, while the associated moisture level represented the OMC.

This test not only quantifies fundamental compaction parameters but also provides indirect insights into the aggregate packing behavior and moisture sensitivity of limestone–steel slag blends. Identifying these factors is essential for mix design optimization because insufficient moisture leads to incomplete compaction, while excess water reduces dry density by occupying voids and creating instability during compaction. The Modified Proctor compaction test procedure is shown in Figure 4.6.

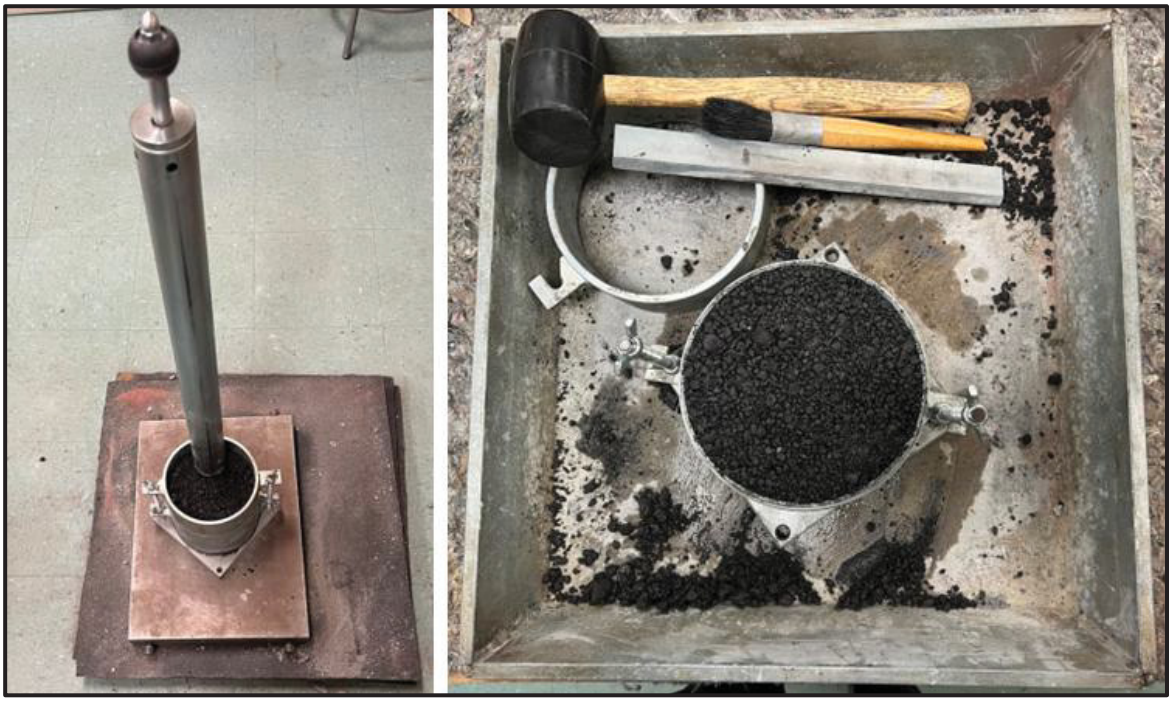

Figure 4.6 Modified Proctor compaction test method

4.2.4.2 California Bearing Ratio (CBR) Test

The California Bearing Ratio (CBR) test was performed to evaluate the load-bearing capacity of base course materials prepared with limestone and different percentages of steel slag aggregates. The CBR is a critical parameter for assessing the structural adequacy of pavement

foundations, as it directly influences pavement thickness design and long-term performance under traffic loads.

In accordance with ASTM D1883 (2021), the maximum aggregate size for this test was limited to 19 mm to ensure consistency and comparability with standard penetration load–deformation curves. All specimens were prepared at their OMC, which had been previously determined using section 4.2.4.1. Compaction was carried out using the same method to ensure uniformity between density, moisture characteristics, and strength assessment.

The cylindrical CBR specimens were compacted into molds with a height of 178 mm and a diameter of 152.4 mm, based on the standard procedure. A spacer disk (61.4 mm in height) was placed at the bottom of the mold to adjust specimen height and maintain uniform penetration geometry. After preparation, the specimens were subjected to loading in the CBR machine at a uniform penetration rate of 1.27 mm/min, simulating realistic traffic-induced penetration stresses. To simulate the pressure from the above pavement layers, two surcharge weights with a combined mass of 4.5 kg were placed on the compacted specimens before testing. The load–penetration response was then recorded continuously from 0.64 mm to 13 mm penetration depth. The CBR value was calculated as the ratio of the measured load at 2.5 mm or 5 mm penetration to the standard load values defined by ASTM D1883 (2021), multiplied by 100. This testing procedure not only can show the mechanical stability of limestone–steel slag mixtures but also allows comparison of strength improvements across different slag replacement levels (33%, 66%, and 100%). 12 specimens were tested to calculate the average CBR values for the control and studied samples.

4.2.5 Thermal Properties and Heat Transfer Assessment

The thermal properties of the developed base course and prime coat specimens play a critical role in heat flow inside the pavement structure. Since the surface asphalt mixture layer inevitably absorbs solar radiation, the efficiency of heat transfer into the deeper layer can directly influence both the surface temperature and the overall UHI effects. By modifying the thermal characteristics of the base course and the interface, it is possible to change the pavement’s heat dissipation, decreasing nighttime heat release and mitigating UHI intensity.

To investigate this aspect, conductive prime coat and compacted base course specimens with different steel slag replacement ratios were tested using experimental methods designed to quantify their key thermal parameters. In detail, thermal conductivity and thermal effusivity of prime coat specimens were measured using an MTPS sensor, and thermal conductivity of base course samples was assessed using a TLS needle probe. In addition to the directly measured parameters, other important thermal parameters, including thermal diffusivity and specific heat capacity, were calculated using equations 3.5 and 3.6. The cooling effect of the developed pavement structures was also investigated using a solar simulation setup. Overall, these tests and parameters offer a comprehensive understanding of how different pavement structures influence the storage, transfer, and release of thermal energy.

4.2.5.1 Thermal Properties Measurement

The thermal properties of both the conductive base course and prime coat specimens were measured. Regarding the base course samples, four different base course mixtures, including the control mixture containing 100% limestone, and three blends incorporating 33%, 66%, and 100% steel slag by weight, were evaluated. To achieve this, a C-Therm Trident thermal conductivity instrument was employed. For granular materials such as base course aggregates, the TLS needle sensor, operated based on the transient heat transfer principle, in accordance with the IEEE 442 (2017) standard, making it a reliable choice for measuring thermal characteristics of construction materials, which is recommended for granular unbounded materials.

The TLS sensor had a length of 150 mm, requiring a specimen volume of at least 80 mL to ensure measurement reliability. Therefore, the base course materials were first compacted according to the Modified Proctor Standard to simulate field-like density and structural integrity. Following compaction, the specimens were subjected to 48 hours of curing at 110 °C to achieve complete drying and minimize the influence of moisture on heat transfer measurements. To facilitate sensor insertion, five uniform holes, matching the diameter of the TLS probe, were drilled into each specimen. For each mixture type, thermal conductivity was measured at five different locations of each sample with 3 replicates (a total of 12 samples),

using the TLS sensor coated with a special thermal paste to maximize contact quality and minimize thermal contact resistance. The average thermal conductivity for each steel slag replacement ratio was then calculated to represent the blend's heat conduction potential. Figure 4.7 illustrates the compacted base course specimens, the TLS sensor, and the C-Therm device used for the experiments.

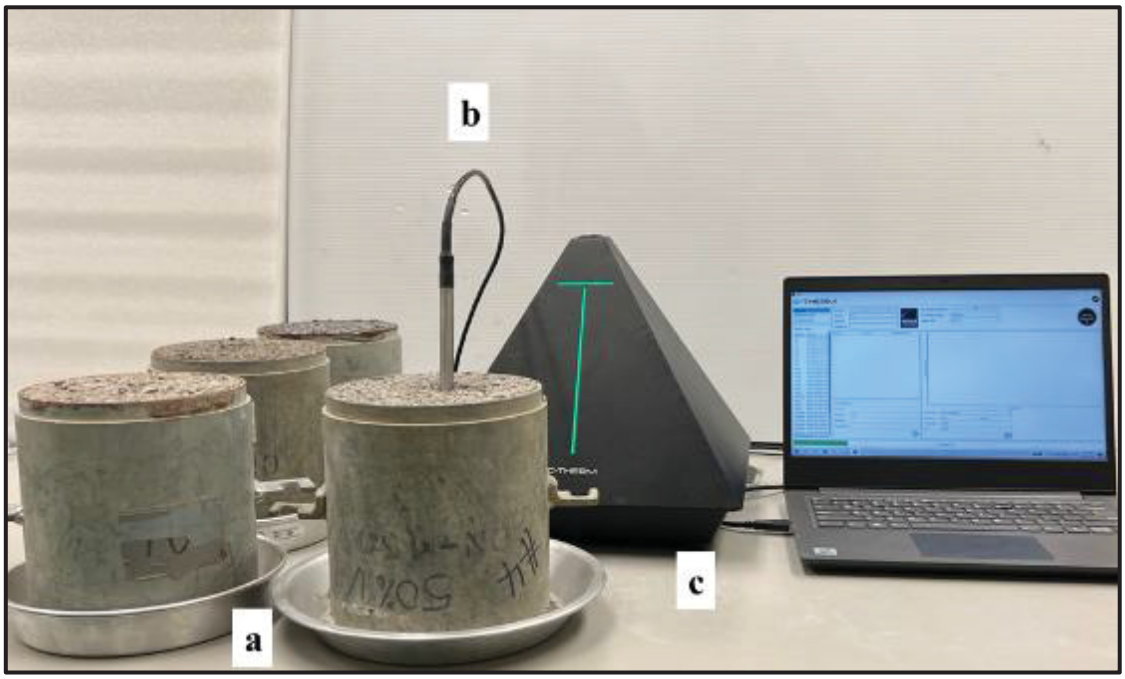

Figure 4.7 Thermal parameter test; (a) base course specimens, (b) TLS sensor, (c) C-Therm

In addition to the base course mixtures, the thermal properties of CRS-2 as a control prime coat and the bitumen emulsion, including 40% steel slag powder, were also assessed. In this case, both thermal conductivity and thermal effusivity were measured with the MTPS sensor of the same C-Therm instrument, in accordance with the ASTM D7984 (2021) standard. The MTPS method is particularly effective for solid and semi-solid specimens with smooth flat surfaces, making it appropriate for asphalt mastics. Each mastic specimen was prepared and loaded with a 500g weight to ensure consistent surface contact during testing. The test was conducted on six specimens, with each specimen tested five times to reduce variability. The reported values represent the average of all measurements. Figure 4.8 presents this testing process. Using both TLS and MTPS sensors allowed a comprehensive characterization of the

thermal performance of both granular base course aggregates and prime coats, ensuring methodological compatibility with material type. Finally, these measurements provide the baseline for quantifying how conductive base courses and prime coats contribute to vertical heat transfer within pavement structures, which directly affects surface temperature moderation and UHI mitigation potential.

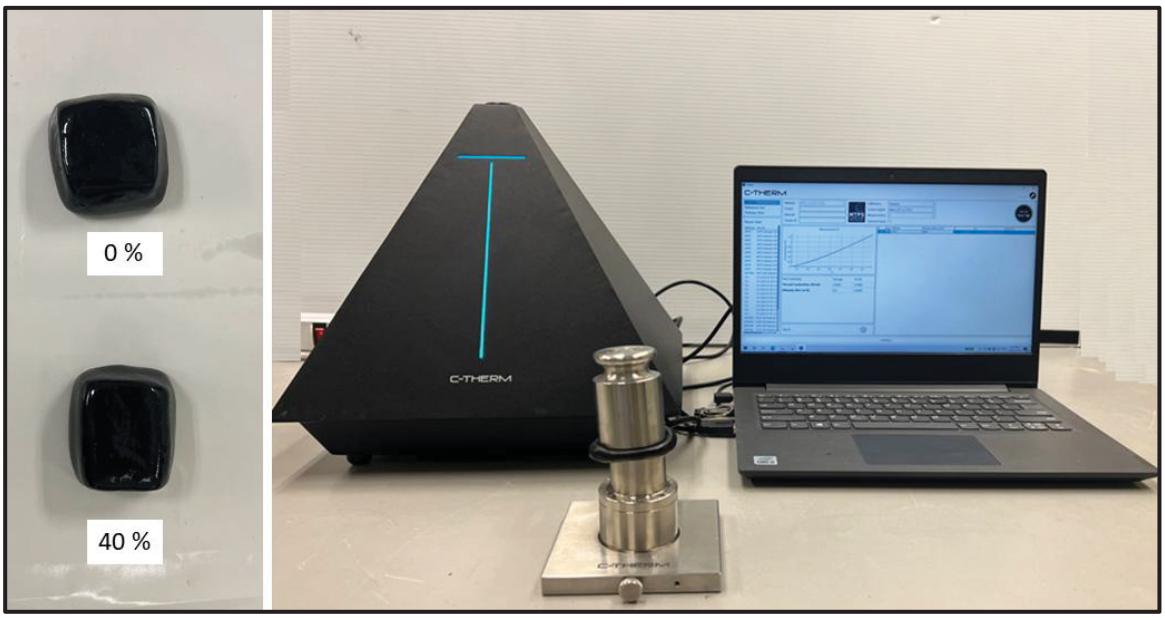

Figure 4.8 Prime coat samples and the C-Therm device with an MTPS sensor

4.2.5.2 Base Course Specimen Preparation for Cooling Effect Tests

Preparing compacted base course specimens for pavement cooling effect testing presents challenges due to the unbound and granular nature of the materials. Achieving compact levels equivalent to field conditions required adherence to the Modified Proctor standard, but the conventional molds and configurations can transfer the heat from the side of the specimens. On the one hand, metal molds, which are typically used for mechanical compaction, were unsuitable in this case because of their high thermal conductivity. Using metal containers could have introduced boundary heat transfer effects, distorting the thermal measurements by allowing rapid lateral heat dissipation through the mold walls. On the other hand, standard

plastic molds do not have the strength to withstand repeated impacts from the Proctor rammer, particularly when compacting steel slag aggregates.

To address these issues, a durable PVC cylinder with identical dimensions to a standard Proctor mold (152.4 mm in diameter and 178 mm in height) was used in this study. PVC provided the dual advantages of sufficient structural durability under compaction process and low thermal conductivity, reducing lateral heat transfer during thermal testing and ensuring more representative results. A Proctor collar was fitted at the top of the PVC cylinder to facilitate uniform layers' compaction.

The specimens were compacted in five layers, each subjected to 56 blows of the Proctor rammer, similar to the Modified Proctor compaction method, to prepare base course specimens with a 150 mm diameter and 100 mm height. Regarding the installation of type T thermocouples inside the specimens, three thermocouples were positioned at predefined depths, including surface level (0 mm), mid-depth (50 mm), and bottom depth (100 mm). This configuration allowed for monitoring of the vertical heat gradient, critical in analyzing how conductive base courses affect heat dissipation toward the subgrade.

To minimize errors associated with voids around the sensors, thermocouples were carefully positioned during compaction, not after the compaction. Adhesive material was used to seal them in place against the PVC mold walls. During installation, the upper sensors were temporarily folded to allow the lower sensors to be embedded at certain depths. The compaction mold and thermocouple placement are illustrated in Figure 4.9. This method ensured that the prepared specimens had similar field-compacted base courses, while also enabling accurate measurement of temperature variations at different depths under controlled laboratory thermal loading with minimum air void around the thermocouples. By combining Proctor compaction protocols with a carefully designed thermal measurement method, this specimen preparation method provided reliable test samples for assessing the impact of conventional and conductive base courses on heat transfer within asphalt pavement structures. A total of 12 specimens were prepared to have the average values for the indoor solar simulation test.

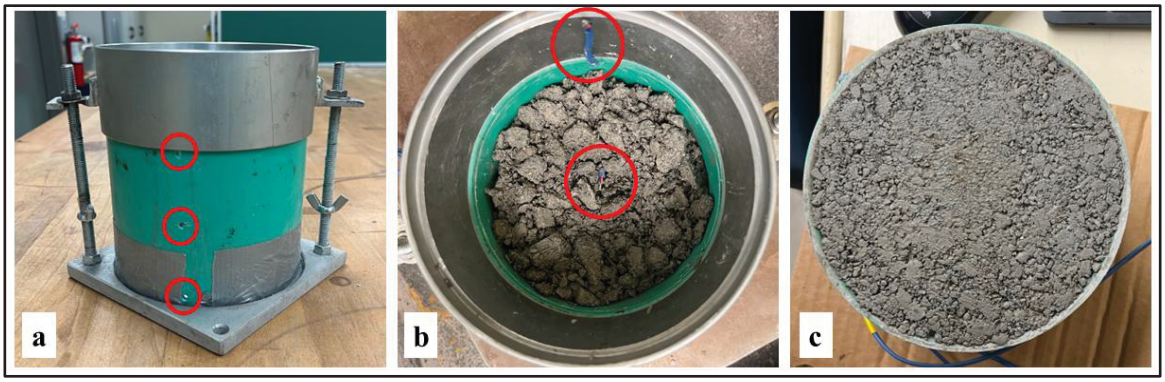

Figure 4.9 Compaction mold (a), thermocouples' placement (b), and final specimen (c)

4.2.5.3 Control and Conductive Prime Coat Application

The control prime coat and conductive asphalt mastics, including 40% steel slag powder by weight of CRS-2 emulsion, were applied to the compacted base course surfaces at an application rate of 0.45 L/m², which is the recommended application rate of prime coat (Mantilla and Button, 1994). This rate was selected to ensure adequate pore sealing at the base course surface while avoiding excessive binder accumulation.

The prime coat was then uniformly spread across the base course surface using a glass rod, which provided a smooth and even distribution while maintaining consistent film thickness. The intent was to achieve uniform coverage and ensure a well-distribution across the interface, maximizing the continuity of thermal conduction between the asphalt mixture and the base course. After placement, the specimens were subjected to a curing process at 35 °C for 24 hours, which allowed sufficient evaporation of the water phase from the cationic emulsion.

After curing, laboratory-prepared asphalt mixture specimens were placed on top of the treated base course samples, preparing 6 samples in total (3 repetitions) and simulating the pavement structure. Using control and conductive prime coats, the experimental setup can reveal how control and conductive prime coats can enhance vertical heat dissipation, reduce surface temperatures under solar radiation, and contribute to the mitigation of UHI effects. The application process is illustrated in Figure 4.10.

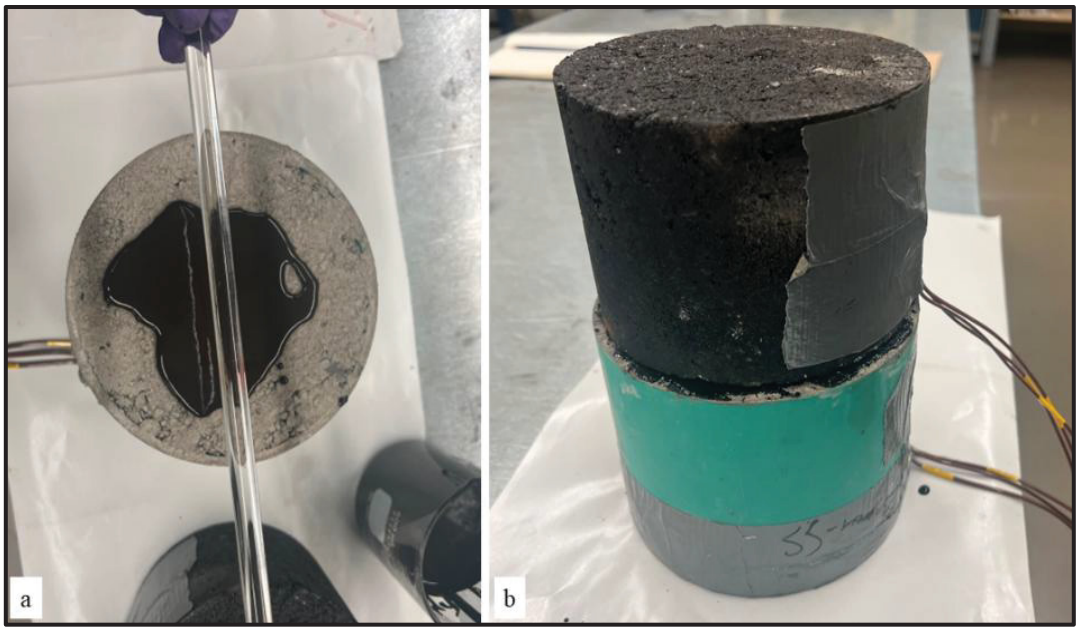

Figure 4.10 (a) applying the prime coat, (b) placing the HMA specimen

4.2.5.4 Indoor Solar Simulation and Cooling Effect Evaluation

Evaluating the cooling effects of the developed asphalt pavement under solar radiation might be complex, as it depends on multiple variables, such as wind. To assess the impact of developed structures under controlled conditions, an indoor solar simulation setup was used, including a 175 W infrared lamp. The lamp produced a broad wavelength range (300–3000 nm), covering most parts of the visible and near-infrared regions that dominate natural solar irradiance at the Earth's surface.

The test configuration simulates a one-directional heat transfer system, simulating how solar energy penetrates and dissipates through asphalt pavement' layers. Each specimen consisted of an asphalt mixture layer positioned over a compacted base course, with type T thermocouples embedded at three depths (surface, 50 mm, and 100 mm). This allowed continuous monitoring of the vertical temperature gradient within the pavement structure. To recreate realistic pavement heating conditions comparable to the maximum asphalt surface temperatures recorded in Canadian climates (Mills et al., 2009), a transparent acrylic cylinder (150 mm diameter) was positioned around the lamp and on top of the specimens. This was used for minimizing airflow and convection losses, and concentrating radiant energy directly

onto the specimen's surface. The lamp height was optimized at 85 cm, producing a maximum asphalt surface temperature of 57.5 °C after 15 hours of continuous irradiation. After the heating phase, the lamp was switched off to simulate nighttime cooling, during which the pavement released stored heat to the ambient air. Temperatures at each thermocouple depth were continuously recorded using a data acquisition system. To prevent lateral heat losses that could distort results, specimens were insulated with liquid foams along their sides and base. This ensured that heat transfer was restricted to the vertical direction. In addition to the conventional base course and conductive base course samples, specimens with control and conductive prime coats applied at the interface were also tested, evaluating 6 specimens for prime coats and 12 specimens for base courses (3 replicates for each percentage). Hence, the cooling effect of developed asphalt pavement structures could be compared with the control pavement structure. Furthermore, a heat flux sensor (FluxTeq) was placed at the surface of asphalt mixtures to measure both incoming flux during heating and outgoing thermal flux during cooling. This provided direct evidence of the effect of conductive prime coats and base course modifications on reducing heat release to the urban atmosphere, which is a critical aspect of UHI mitigation. The experimental setup and key components are illustrated in Figure 4.11. The summary of laboratory tests and the number of specimens is shown in Table 4.4.

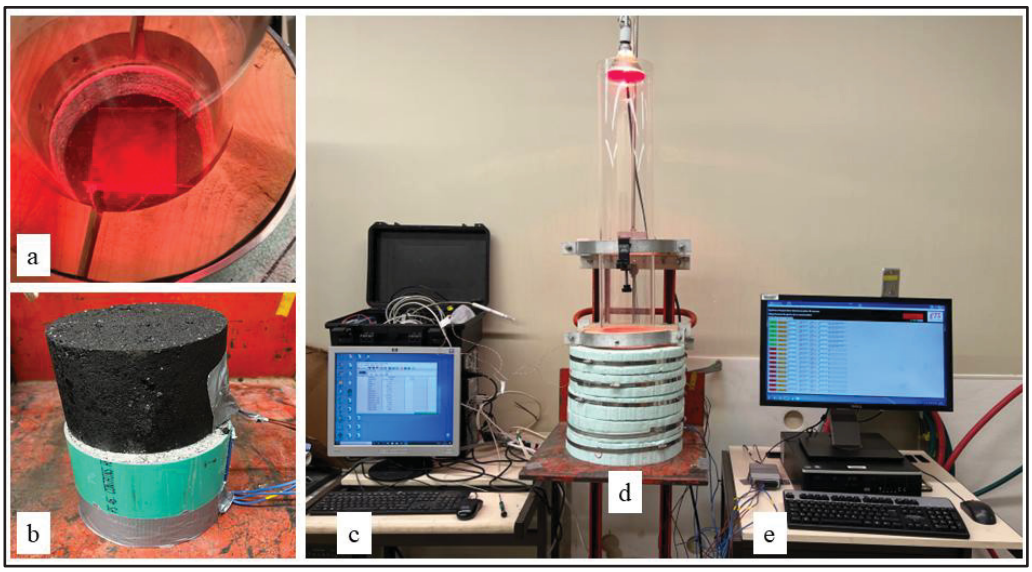

Figure 4.11 The cooling effect setup: (a) heat flux sensor, (b) pavement specimens, (c & e) data loggers, (d) heat lamp, and insulated specimens

Table 4.4 The summary of laboratory tests and the number of specimens

Test	Goals for the laboratory tests	Number of samples
Conductive prime coat preparation	Finding the maximum percentage of conductive powder with suitable stability	18
Modified Proctor compaction test	Measuring the OMC and MDD of base course mixes	60
CBR Test	Evaluating the load-bearing capacity of base course mixes	12
C-Therm device using MTPS sensor	Measuring the thermal properties of control and conductive prime coat samples	6
C-Therm device using TLS sensor	Assessing the thermal properties of control and conductive base course specimens	12
Indoor solar simulation test for prime coat samples	Measuring the cooling effects, heat release, and temperature reduction of control and conductive prime coats	6
Indoor solar simulation test for base course specimens	Evaluating the cooling effects, heat release, and temperature reduction of control and conductive base course	12

4.3 Results and Discussion

In this section, the outcomes of the experimental program are presented and critically analyzed. The discussion is divided into two main parts. Firstly, the physical and mechanical properties of the developed base course mixtures are evaluated. These results can indicate how the replacement of limestone with different proportions of steel slag aggregates influences the

compaction characteristics, water content, density, strength, and suitability of the base course for pavement applications. Secondly, the thermal behavior of the developed structures is examined. The thermal properties of the base course specimens and conductive prime coat are analyzed to assess their capacity to transfer or retain heat. These results are then integrated with the outcomes of the indoor solar simulation tests, which quantify the cooling potential, surface and subsurface temperature variations, and outgoing heat flux of different pavement structures. Thus, the mechanical and thermal analyses reveal the dual role of conductive prime coats and base courses, ensuring adequate structural performance while simultaneously reducing heat storage and release and mitigating UHI effects.

4.3.1 Physical Properties and Strength Evaluation of Base Course Specimens

The compaction characteristics of the base course specimens, as determined from the Modified Proctor test, are illustrated in Figure 4.12. The results demonstrate a clear influence of steel slag replacement on both the OMC and MDD. In detail, increasing the proportion of steel slag reduced the OMC of the mixtures. The control specimens prepared with 100% limestone aggregates exhibited an OMC of 5%, which declined to 4.4% after full replacement with steel slag, a 12% reduction. This decline can be attributed to the lower water absorption of steel slag compared to limestone, meaning less water was required for compaction of particles. Another reason is the reduced content of fine particles (smaller than 1.25 mm) in the steel slag blends, reducing the required water for compaction.

While OMC decreased, the MDD showed the opposite trend, rising from 2355 $kg.m^{-3}$ for limestone control to 2785 $kg.m^{-3}$ for the 100% steel slag mixture, representing an 18% increase. This improvement is attributed to the higher specific gravity and density of steel slag particles compared to limestone, which allows for a denser packing under identical compaction energy. The rough, angular morphology of slag particles may also have contributed to improved interlock, further limiting air voids within the compacted structure. Comparable increases in dry density with steel slag replacement have been reported in previous studies as well (Behiry, 2013; Shiha et al., 2020). Therefore, a higher MDD in the base course can contribute not only

to enhanced load-bearing capacity but also to reduced deformation under traffic loads, reinforcing the mechanical and structural benefits of using slag aggregates.

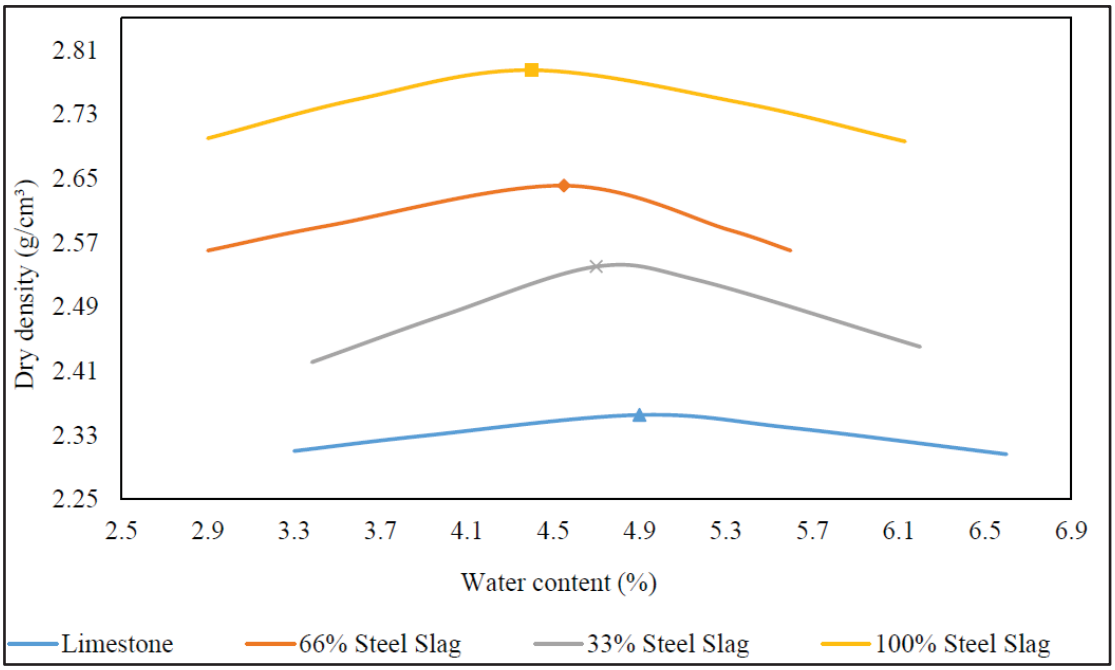

Figure 4.12 The water content-dry density correlation of steel slag and limestone specimens

The results of the CBR test, presented in Figure 4.13, indicate the significant improvement in strength characteristics after steel slag replacement. The CBR index of the control limestone mixture was measured at 92.4%, while the mixture with 100% steel slag reached 218.8%, a 137% increase. This enhancement in bearing capacity is attributed to two factors. First, steel slag aggregates had higher compressive strength and abrasion resistance compared to limestone, enabling them to resist crushing and degradation under load, maintaining structural integrity. Second, the increased density and angular particle shapes of steel slag promote higher interparticle friction and interlock, directly contributing to greater resistance against penetration under the standard CBR load. These mechanisms explain the large increase in measured strength, which again aligns with trends reported in earlier research (Shiha et al., 2020).

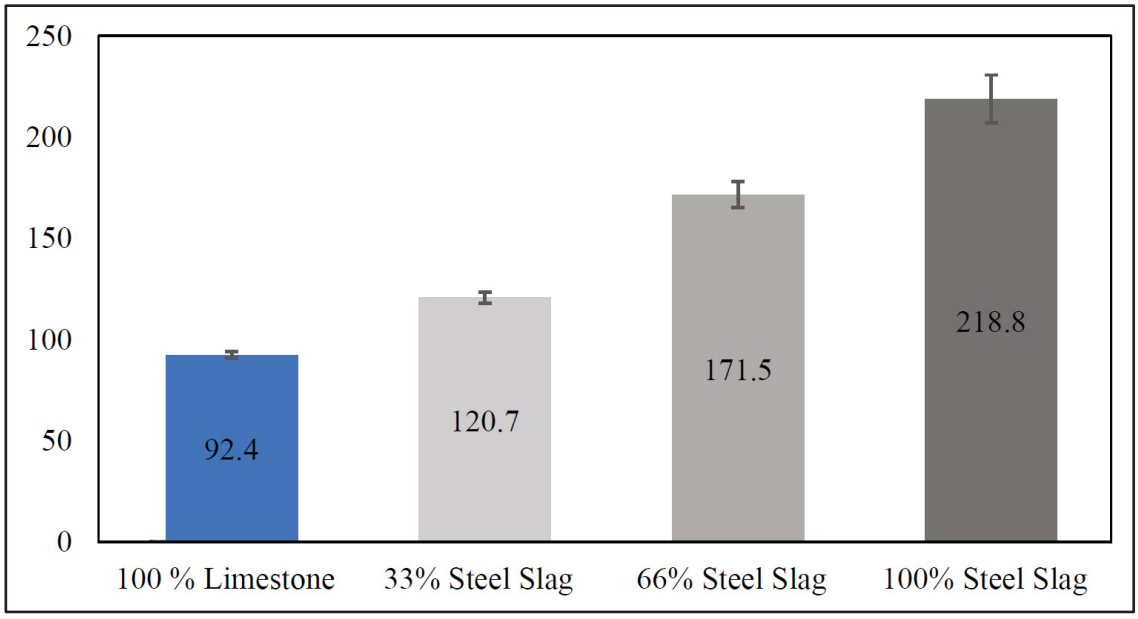

Figure 4.13 Limestone and steel slag base course CBR values

Overall, the results of the Proctor and CBR tests reveal that steel slag replacement not only improves compaction efficiency (higher MDD at lower OMC) but also makes an improvement in strength and load-bearing capacity. This finding is beneficial for pavement engineering because it suggests that the use of steel slag as a base course material can simultaneously reduce water sensitivity (lower OMC) and increase structural performance (higher CBR). Furthermore, by ensuring a stronger and denser base course, these results establish a mechanical foundation for integrating thermal performance improvements in subsequent sections, linking material selection with both structural and environmental objectives. The optimum percentage of steel slag substitution will be determined based on heat transfer enhancement in the following sections of this chapter. These results revealed that steel slag aggregates can be used as base course materials, which was one of the research hypotheses.

4.3.2 Thermal Properties of Base Course and Prime Coat Specimens

The thermal properties of the base course specimens, comprised of different proportions of steel slag aggregates, as well as the modified prime coat prepared with steel slag powder, are summarized in Table 4.5. Both thermal conductivity and thermal effusivity were measured

using the MTPS sensor, and thermal conductivity was evaluated using the TLS sensor, while specific heat capacity and thermal diffusivity of prime coat samples were derived from Equations 4.1 and 4.2 (Bergman et al., 2017). These results provided important information about how material composition and microstructural features influence heat transfer in pavement layers.

$$e = \left(k.\rho.C_p\right)^{\frac{1}{2}} \tag{4.1}$$

In this equation, e represents the thermal effusivity (W. $s^{1/2}$. m^{-2}. K^{-1}), k is the thermal conductivity (W. m^{-1}. K^{-1}), ρ indicates the material's density ($kg.m^{-3}$), and C_p denotes the specific heat capacity (J. kg^{-1}. K^{-1}). In this study, thermal parameters were measured at room temperature (around 24 ℃).

$$\alpha = \frac{k}{C_p\rho} \tag{4.2}$$

Where α is thermal diffusivity ($m^2.s^{-1}$), k denotes the thermal conductivity (W. m^{-1}. K^{-1}), ρ is the material's density ($kg.m^{-3}$), and C_p is specific heat capacity (J. kg^{-1}. K^{-1}).

The results show that replacing limestone with steel slag aggregates significantly enhanced the thermal conductivity of the base course. The conductivity of the limestone control mixture was measured at 0.73 $W{\cdot}m^{-1}{\cdot}K^{-1}$, while the mixture with 66% steel slag reached 1.44 $W{\cdot}m^{-1}{\cdot}K^{-1}$, reflecting an almost 96% increase. This increase demonstrates the higher conductivity of steel slag due to its dense crystalline structure and high metal oxide content, particularly Fe_2O_3, which facilitates phonon and electron-based heat transport (Jiao et al., 2020b). However, another trend was observed when limestone was fully replaced. The 100% steel slag mixture showed a slight reduction in conductivity (1.23 $W{\cdot}m^{-1}{\cdot}K^{-1}$), approximately 15% lower than the 66% blend. This decline is attributed to the lower content of fine particles (smaller than 1.25 mm) and the porous surfaces of coarser slag particles in the fully substituted mixture. These characteristics can increase internal air voids, which act as insulators and reduce heat transfer efficiency. This trend emphasizes the importance of gradation in maximizing conductivity, which was in agreement with previous relevant studies (Jiao et al., 2020b).

Table 4.5 Base course and prime coat specimens' thermal properties

Types of Specimens	Thermal conductivity (Experimented)		Specific heat capacity (J. kg^{-1}. K^{-1}, calculated)	Thermal diffusivity ($mm^2.s^{-1}$, calculated)
	Avg values (W. m^{-1}. K^{-1})	Standard deviation (SD)		
100% Limestone (Base)	0.73	0.02	909.40	0.34
33% Steel Slag (Base)	1.04	0.03	827.54	0.49
66% Steel Slag (Base)	1.44	0.01	753.34	0.72
100% Steel Slag (Base)	1.23	0.03	746.49	0.59
Prime coat (Control)	0.16	0.01	1377.42	0.12
Conductive prime coat (40% Steel Slag)	0.37	0.02	845.68	0.27

Moreover, thermal diffusivity (α) results also showed similar trends. Diffusivity increased substantially after using steel slag, peaking at 0.72 $mm^2.s^{-1}$ for the 66% blend, more than double the limestone control (0.34 $mm^2.s^{-1}$). However, the 100% slag mixture showed a lower value (0.59 $mm^2.s^{-1}$), due to the adverse influence of increased voids and reduced fine particles. Higher diffusivity indicates that heat spreads more rapidly within the material volume, accelerating the downward redistribution of absorbed solar energy in the pavement structure. The calculated specific heat capacities (C_p) ranged from 746 to 909 $J.kg^{-1}.K^{-1}$ for base courses. These values indicate that the mixtures require moderate amounts of energy to raise their temperature by 1 °C. In general, the limestone mixtures displayed slightly higher C_p, consistent with their structure and greater moisture-holding capacity. The specific heat did not vary as widely as conductivity, though.

For the prime coats, modification with steel slag powder produced a considerable enhancement. The thermal conductivity of the control CRS-2 emulsion was 0.16 $W.m^{-1}.K^{-1}$, and after using 40% slag filler, this value was increased by more than doubled to 0.37 $W.m^{-1}.K^{-1}$. This improvement is directly related to the fine slag powders providing dense conductive channels within the asphalt mastic. Their high Fe_2O_3 and CaO contents enhance both ionic and

lattice vibrational heat transfer, giving the conductive prime coat significantly greater capacity to dissipate heat compared to the control sample. Besides, diffusivity also increased from 0.12 $mm^2.s^{-1}$ (control prime coat) to 0.27 $mm^2.s^{-1}$ (conductive prime coat). Higher diffusivity indicates that heat spreads more rapidly within the material volume, accelerating the redistribution of absorbed solar energy from the asphalt mixture to the base course. The increase in thermal performance of the prime coat suggests that conductive modifiers at the interface between the asphalt mixture and base course can play an important role in redistributing heat flux within the pavement structure.

In summary, the thermal characterization of base course and prime coat specimens demonstrates that partial replacement of limestone with steel slag (particularly at 66%) provides the most favorable balance of enhanced conductivity and diffusivity. Fully replacing limestone with slag, although still beneficial compared to the control, risks diminishing performance due to gradation-related increases in void content. Meanwhile, modifying the prime coat with steel slag powder substantially improved its conductive capacity, suggesting a promising strategy for improving interfacial heat transfer between asphalt mixtures and base courses. These findings emphasize the dual role of material chemistry and microstructural design in determining the thermal behavior of pavements, with direct implications for UHI mitigation.

4.3.3 Cooling Effects and Heat Release of Different Pavement Structures

The impacts of different studies on pavement structures on the pavement temperature are evaluated in this section. Firstly, the conventional pavement structure with and without a prime coat is assessed. Other structures, including conventional and conductive base courses without a prime coat, and finally the conventional pavement structure with a conductive prime coat, are investigated. These comparisons can reveal the optimal structures based on the project requirements and field conditions.

4.3.3.1 The Impact of Using a Prime Coat on the Asphalt Mixture Temperature

The solar simulation experiments revealed that although the overall trend of temperature variation across the asphalt mixture depths was similar for all pavement structures, the absolute temperature values differed depending on the presence of a prime coat. Figure 4.14 illustrates

the 24-hour variation in asphalt mixture surface temperatures for structures with and without a prime coat. For the control specimen without a prime coat, the HMA surface temperature increased steadily under infrared lamp exposure, reaching a maximum of 57.5 °C after 15 hours. In comparison, the specimen with a prime coat showed a cooler surface, peaking at about 54.5 °C, representing a 6% reduction. This reduction is attributed to the improved thermal conduction at the asphalt mixture–base course interface, which enhanced the transfer of absorbed heat away from the surface. By dissipating heat more effectively into the underlying base course, the prime coat helped to avoid excessive heat accumulation within the asphalt mixture, reducing surface overheating during daytime simulation.

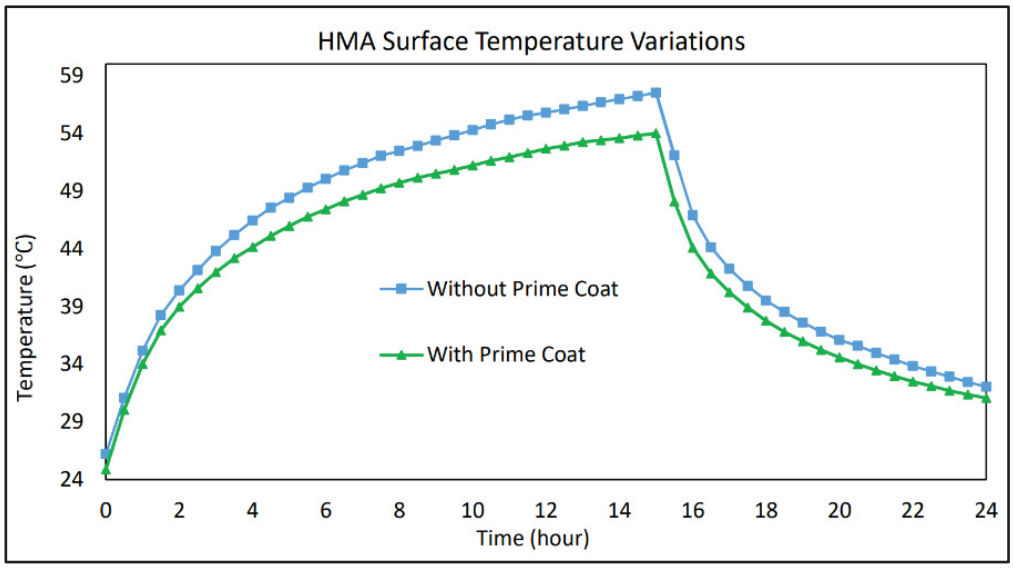

Figure 4.14 The asphalt pavement surface temperature variation over 24 hours

During the cooling phase (nighttime simulation), both structures demonstrated a similar overall trend of temperature decline. However, the prime-coated pavement consistently maintained lower residual surface temperatures than the control. This was due to its greater capacity to transfer absorbed heat into the base course, which resulted in a smaller thermal gradient between the pavement surface and air. The reduced gradient slowed the upward release of heat, meaning that less energy was emitted into the atmosphere during the night. This outcome is

highly significant for UHI mitigation, as conventional pavements exacerbate UHI effects by releasing large amounts of stored heat after sunset.

The achieved results are consistent with prior studies, such as Jiang and Wang (2020), where the use of artificial conductive channels inside pavement layers reduced surface temperatures and nighttime heat release. In this study, the prime coat essentially acted as a passive conductive interface, demonstrating that even relatively thin interfacial modifications can considerably change the thermal behavior of multi-layer pavement systems. This shows the importance of not only surface reflectivity (as examined in chip seal studies in Chapter 3) but also subsurface heat dissipation mechanisms in reducing surface temperature, developing comprehensive UHI mitigation strategies. The interface temperature gradients revealed that the prime coat layer affects heat transfer between the asphalt mixture and base course. Modifying the interface with a prime coat improved downward heat flow, reducing surface temperature. These findings validate the hypothesis that the interface plays a critical role in transferring absorbed heat, mitigating the UHI.

4.3.3.2 Cooling Effects of Conductive Base Course and Conductive Prime Coat

The thermal response of the developed pavement structures demonstrated significant differences in both surface and in-depth temperatures, despite following similar variation trends across the asphalt mixture and base layers during daytime simulation. To avoid redundancy, this section focuses on the surface temperatures of the asphalt mixture and base course, which are the most critical indicators of pavement contribution to the UHI phenomenon. First, the surface temperature of the base course and then the asphalt mixture are discussed. Figure 4.15 shows the 24-hour base course surface temperature variations for three pavement structures. The control base course with limestone aggregates, conductive base courses having different proportions of steel slag aggregates, and a control base course with a conductive prime coat at the asphalt mixture–base interface.

Regarding base courses' surface temperature results, the control structure consistently had the highest surface temperatures, with its base course reaching approximately 47 °C during the daytime heating simulation. In comparison, the surface of base courses containing 33% and 100% steel slag reached temperatures nearly 3 °C lower, demonstrating their cooling potential.

More importantly, the 66% steel slag mixture and the base course with conductive prime coat showed the lowest maximum surface temperatures, around 40 °C, a reduction of nearly 7 °C relative to the control. This performance denotes the different involved mechanisms. Steel slag aggregates, owing to their higher thermal conductivity, facilitated faster vertical heat transfer to deeper layers, preventing excessive accumulation at the surface. The conductive prime coat acted at the interface by sealing pores and creating a continuous conductive channel, reducing interfacial resistance to heat flow. This dual role (mechanical adhesion and enhanced conduction) allowed even the conventional limestone base to perform more effectively when coupled with the conductive prime coat due to the prevention of heat accumulation in the asphalt mixture layer and transferring the heat to the base layer depth. These outcomes are consistent with prior findings on engineered conduction channels inside pavement structures (Jiang and Wang, 2020).

During the nighttime cooling phase, the control base course again had the highest retained surface temperature, stabilizing around 35 °C after 9 hours of upward heat release. This corresponds to a 26% reduction from its peak, indicating substantial emission of stored energy into the atmosphere. By contrast, the conductive prime coat and the 66% steel slag specimens reached only 32 °C after 9 hours, releasing less heat. Although the conductive prime coat specimen was marginally warmer than the 66% steel slag mixture during daytime heating, it became slightly cooler at night. This is linked to the reduced air voids and greater continuity at the interface in specimens with conductive prime coat, which allowed more efficient transfer of heat downward during the day, reducing the residual heat available for nighttime emission. However, the heat penetration depth was less for these specimens, as shown in Figure 4.17. The effect of these structures was not only lower peak daytime temperatures but also smaller nighttime thermal gradients, reducing nocturnal heat release into the ambient air.

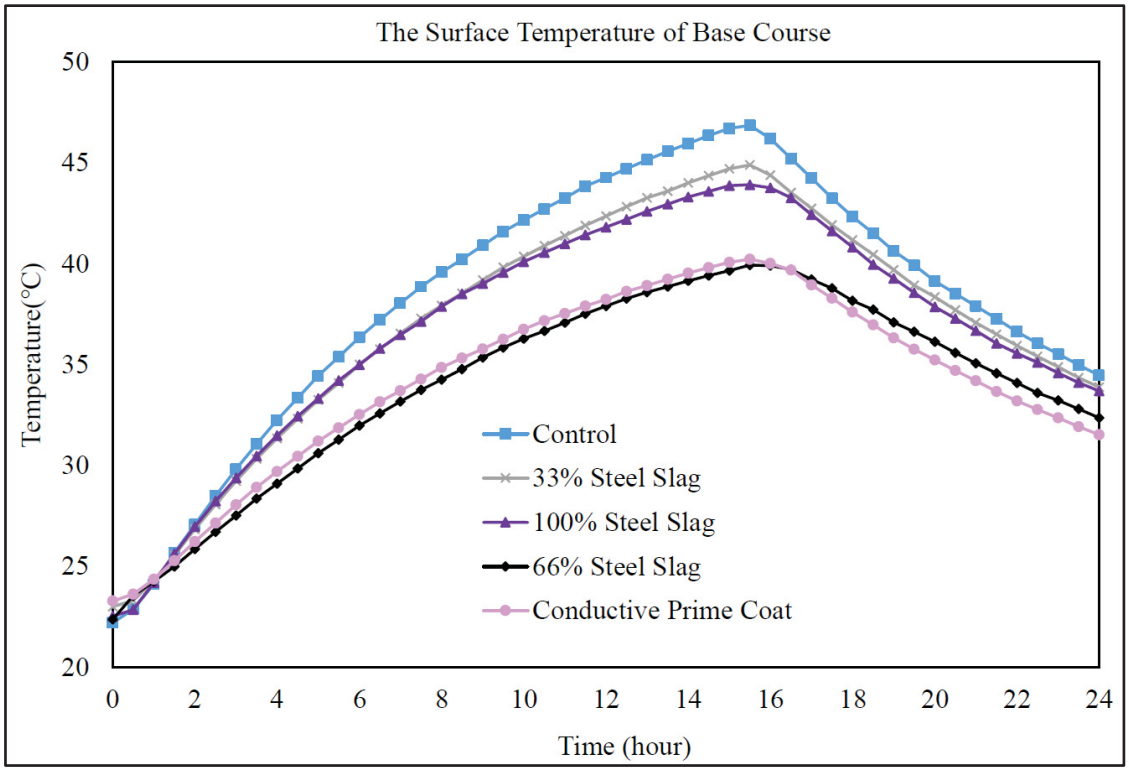

Figure 4.15 The base course surface temperature variations of pavement structures

Regarding the asphalt mixture surface temperature, Figure 4.16 demonstrates the surface temperature variations of the asphalt mixture layers above these base courses. All mixtures were fabricated from the same batch to eliminate variability in surface composition, ensuring that observed differences stemmed solely from base course and interface modifications.

Similarly, the control pavement had the highest surface temperature, peaking at 57.5 °C after 15 hours. Pavements with 33% and 100% steel slag base courses showed slight improvements, with surface temperatures about 4% lower than the control. The 66% steel slag base course and the conductive prime coat specimens showed the highest surface temperature reduction, which both achieved reductions of approximately 13% relative to the control, showing the effectiveness of conductive modifications in channeling absorbed heat away from the asphalt mixture surface. These reductions directly confirm that UHI mitigation can be achieved not only by reflective surfaces (Chapter 3) but also by enhancing the interface and base course heat transfer.

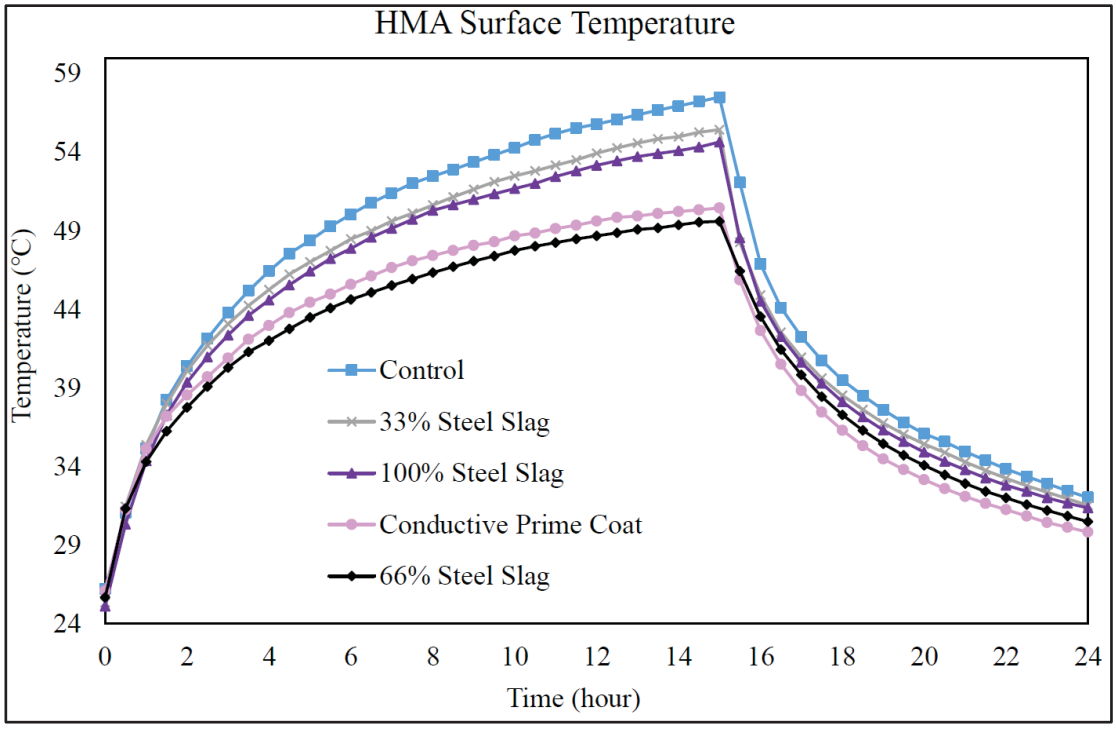

Figure 4.16 The studied pavement structures' asphalt mixture surface temperature

Nighttime results also reinforced these findings. The control pavement had the largest surface temperature reduction (45%), reflecting its high daytime heat accumulation and high thermal gradient with the cooler ambient air. This led to the highest nocturnal heat release, exacerbating UHI effects. However, both the 66% steel slag and conductive prime coat pavements recorded smaller temperature reductions (40%), releasing less heat upward into the air. Although both of these structures performed similarly, the 66% slag mixture showed slightly lower absolute temperatures and slightly smaller nighttime reductions, indicating deeper penetration of heat into the conductive base course.

The difference between the two approaches, conductive base course versus conductive prime coat, was clarified by monitoring the temperatures at the bottom of base course specimens, as shown in Figure 4.17. The 66% steel slag base course reached temperatures about 5% and 10% higher than the prime coat and control specimens, respectively. This confirms the conductive base course transferred heat deeper into this layer rather than keeping it near the surface. The prime coat, however, improved interfacial conduction but did not transfer heat as deeply as the

conductive base course, resulting in heat accumulation in the upper parts of the base course. This distinction illustrates the different functional advantages of these structures. The conductive base course acts as a long-term heat dissipation channel, while the prime coat ensures efficient interfacial conduction and moderate surface gradients. Both strategies reduce surface heating and nighttime release, but the steel slag base course is particularly effective in distributing thermal loads more evenly throughout the base layer. The analysis of conductive base course and prime coat temperature profiles confirmed that base course and prime coat containing steel slag had higher thermal conductivity than natural aggregates. Pavements including these layers showed enhanced heat dissipation and lower surface temperatures, confirming the hypothesis that conductive materials in the interface and base course promote vertical heat transfer, assisting in UHI mitigation. These findings support the proposed hypotheses regarding using conductive base course and prime coats, including finding the optimum percentages of steel slag.

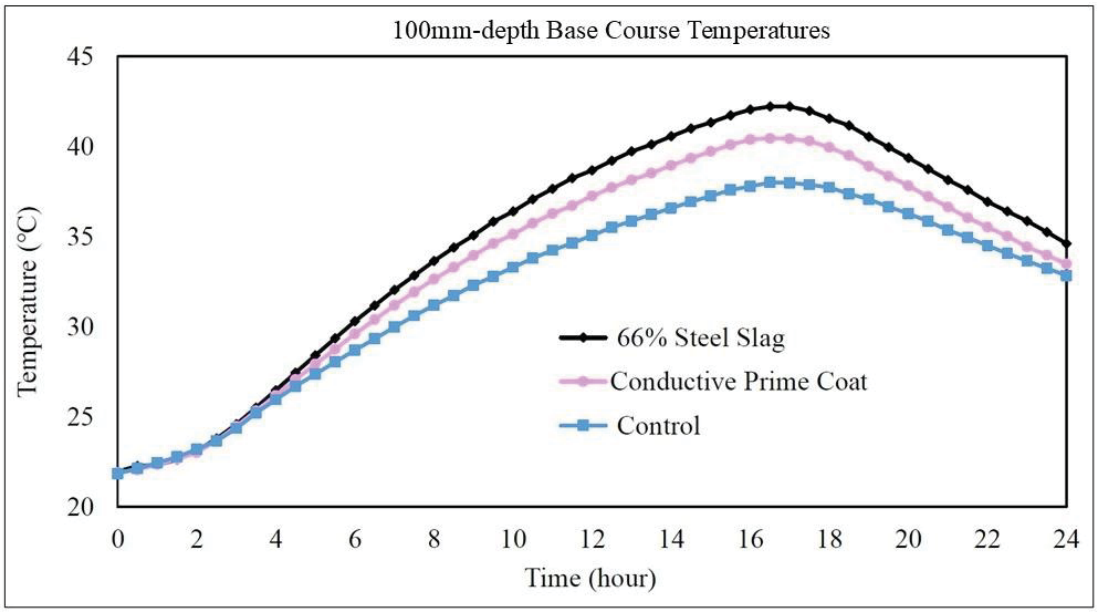

Figure 4.17 The studied pavement structures' base course bottom temperatures

4.3.3.3 Outgoing Heat Flux of Pavement with Control Prime Coat

One of the most critical contributors to the UHI phenomenon is the outgoing surface heat flux of pavements at night. The magnitude and rate of this heat release determine not only the

thermal comfort of urban areas but also the duration of higher nighttime urban temperatures. Thus, understanding how different pavement structures modify outgoing heat flux is critical to evaluating their UHI mitigation potential. A heat flux sensor was used to continuously record both incoming heat flux during the simulated daytime heating period and outgoing flux during the nighttime cooling period. Since the nighttime release directly impacts the intensity of UHI, the focus was on the initial 9 hours after the lamp was turned off. The results for conventional pavement structure with and without a control prime coat are presented in Figure 4.18.

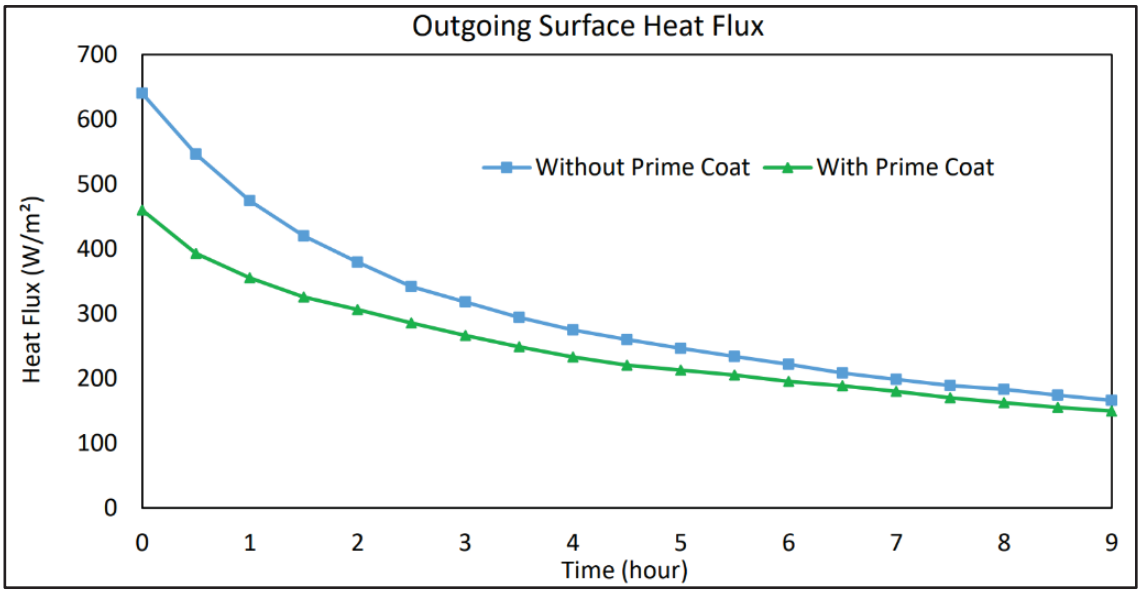

Figure 4.18 Outgoing heat flux of pavement with and without control prime coat

Starting the nighttime cooling, the control pavement (without prime coat) had a peak outgoing heat flux of about 640 $W.m^{-2}$. This rapid release of stored energy reflects the higher daytime heat accumulation in the asphalt mixture layer. Nevertheless, the pavement structure with the control prime coat showed a significantly lower initial outgoing flux of 460 $W \cdot m^{-2}$, representing an almost 28% reduction. This difference indicates that the prime coat effectively enhanced downward heat conduction into the base course, reducing the thermal gradient between the pavement surface and the surrounding air.

The heat flux patterns over time also indicate different thermal behaviors when a prime coat was used. In the first four hours of cooling, the pavement without the prime coat consistently released more energy, owing to its higher stored heat and thermal gradient. The structure with prime coat, on the other hand, demonstrated a more gradual and sustained release profile, reflecting reduced surface heat storage and improved subsurface dissipation. This trend was also observed in previous research on porous asphalt mixtures that reported slower and lower magnitude nighttime heat fluxes due to altered heat transport pathways (Liu et al., 2023).

The slower nighttime release in specimens with the control prime coat is advantageous for UHI mitigation. By moderating surface gradients and distributing heat flux over longer periods, the prime coat contributes to lower overall nocturnal air heating. The prime coat serves as a conduction bridge, sealing voids and increasing the effective thermal contact area between the asphalt mixture and base course. This prevents excessive energy accumulation in the upper pavement layers and lowers the rate of heat emission into the urban air. These promising results led to evaluating the outgoing heat flux of a conductive prime coat, as explained in the next section.

4.3.3.4 Outgoing Heat of Pavement with Conductive Base Course and Prime Coat

In this section, using the same method, the outgoing nighttime heat flux of pavement structures with a conductive base course and conductive prime coat is evaluated. The magnitude and rate of nocturnal heat release dictate how much thermal energy is emitted back into the urban atmosphere, contributing to UHI effects. Therefore, analyzing outgoing heat flux patterns from different pavement structures is crucial for evaluating their potential to mitigate UHI effects.

The laboratory simulation provided continuous records of incoming daytime flux and outgoing nighttime flux. Due to the importance of outgoing nighttime heat flux, Figure 4.19 presents the outgoing flux profiles over a 9-hour cooling cycle for different conductive pavement structures. Similar to Section 4.3.3.3, the control pavement without a prime coat had the highest outgoing heat flux, beginning at approximately 640.25 $W.m^{-2}$ immediately after the heat source was turned off, and declining to 166.26 $W.m^{-2}$ after 9 hours. This rapid and high-magnitude release reflects the significant daytime heat accumulation in the asphalt mixture layer, which resulted in a high thermal gradient with the surrounding air during early cooling.

By comparison, the steel slag-modified base courses and conductive prime coat structures released considerably less energy. Pavements with 33% and 100% steel slag replacement showed approximately 21% lower initial flux than the control, confirming that using slag enhances downward heat conduction, redistributing part of the stored energy into deeper layers instead of keeping it in the surface layer. The most important heat release reduction, however, was observed in the 66% steel slag and conductive prime coat specimens, which released 38% and 33% less outgoing heat, respectively, compared with the control specimens at the start of the cooling process. This demonstrates the efficiency of these two structures in decreasing nocturnal heat discharge.

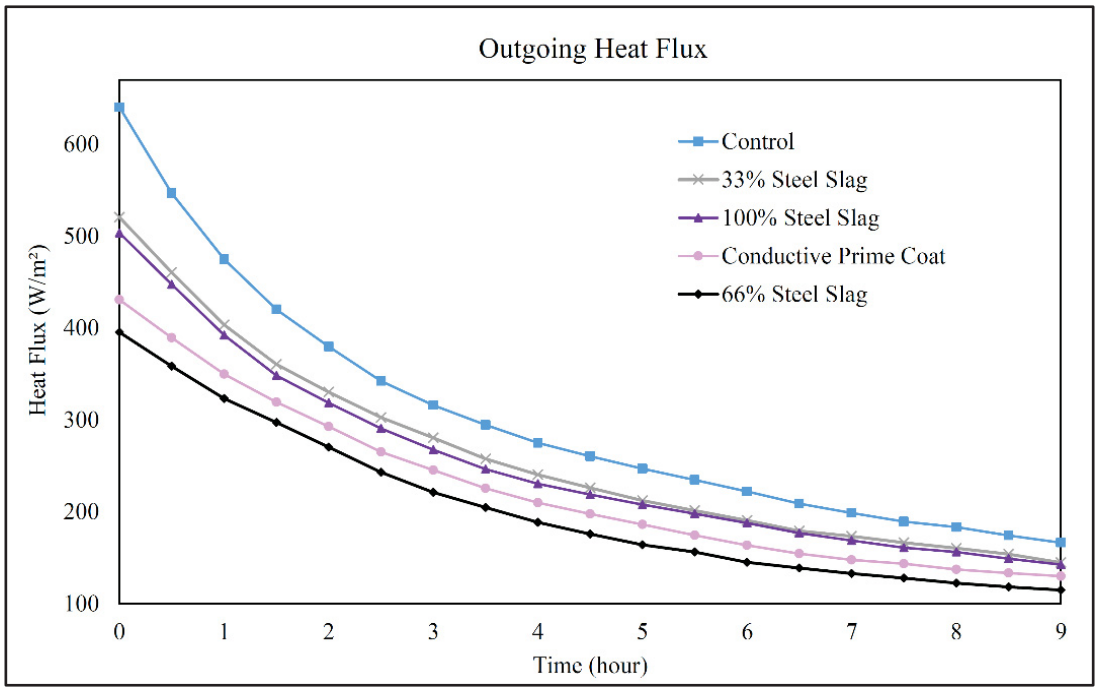

Figure 4.19 The surface outgoing heat flux of the studied pavement structures

As the nighttime simulation progressed, outgoing flux declined across all specimens due to diminishing thermal gradients between the pavement surface and ambient air. After 9 hours, the control pavement still released the most energy, while the 66% steel slag and conductive prime coat specimens maintained their advantage, showing 31% and 22% lower flux, respectively, compared to the control pavement structure. This reduction indicates that

conductive modifications not only had lower peak flux but also reduced the cumulative heat discharge into the urban atmosphere throughout the night.

Moreover, the 66% slag mixture consistently performed better than the fully substituted (100%) slag mixture, reflecting the importance of aggregate gradation and packing density in maintaining optimal thermal performance. Higher coarse slag and slag surface air in the 100% blend increased internal voids, limiting effective conductivity despite the material's high thermal capacity. The conductive prime coat, however, filled the interface voids and enhanced thermal contact between the asphalt mixture and base course. This mechanism facilitated smoother energy transfer downward, reducing asphalt layer heat accumulation and moderating nocturnal heat release.

The combined results reveal that outgoing heat flux can be strategically controlled by modifying subsurface conduction pathways. The 66% steel slag base course and conductive prime coat both proved capable of substantially lowering nocturnal outgoing heat flux. By redistributing stored heat deeper into the base layer rather than allowing it to escape rapidly at night, these solutions can be directly used for mitigating UHI effects. Besides, as both prime coats and conductive bases can improve the mechanical stability of pavements, they may extend their service life as well.

4.4 Conclusion

This chapter investigated the role of conductive base courses and prime coats in improving the thermal behavior and mechanical performance of asphalt pavement systems, with a focus on their contribution to UHI mitigation. The experimental program includes Proctor compaction and CBR strength evaluation, thermal property characterization, solar simulation tests, and nighttime heat flux analysis. The results provide evidence that material modifications at the base and interface levels can simultaneously enhance structural capacity and thermal performance of pavements.

Regarding the mechanical and physical properties, the utilization of steel slag aggregates in the base course mixtures had a clear and measurable impact on compaction and strength performance. Increasing slag content reduced the OMC up to 12%. This was attributed to the

lower water absorption capacity and reduced fines of steel slag, which required less moisture to achieve optimum compaction. In contrast, the MDD increased by 18%, reflecting the higher specific gravity and angular morphology of steel slag, which improved packing efficiency and reduced voids. Strength results showed similar trends. The CBR increased more than double after full steel slag replacement, 137% improvement. This dramatic growth stems from the slag's higher compressive strength, abrasion resistance, and interparticle friction. These improvements not only confirm steel slag's suitability as a base course material but also suggest its capacity to extend pavement service life, reduce deformation under traffic, and improve resilience under heavy loads.

More importantly, thermal characterization and pavement cooling effects revealed the advantages of using steel slag base course and conductive prime coats for UHI mitigation. The thermal conductivity of the base course almost doubled when 66% of limestone was replaced with slag, rising from 0.73 to 1.44 $W.m^{-1}.K^{-1}$. Thermal diffusivity also showed a similar enhancement. These results confirm that steel slag aggregates facilitate faster and more efficient heat transfer, redistributing absorbed solar energy away from the asphalt mixture surface and into deeper pavement layers. However, the percentage of using this by-product is important, and the fully substituted 100% slag base course performed slightly less efficiently than the 66% blend due to gradation imbalances and excessive voids, demonstrating that optimal steel slag content is critical. The conductive prime coat showed similar compelling improvements. Modifying the CRS-2 emulsion with 40% slag filler increased thermal conductivity from 0.16 to 0.37 $W.m^{-1}.K^{-1}$. Thermal diffusivity also showed a similar increase. These enhancements indicate the prime coat's role as an interfacial conduction bridge, sealing voids and creating conductive channels between the asphalt mixture and base course layers. This modification ensures smoother downward heat transfer and prevents surface overheating, while still maintaining structural adhesion.

These conductive subsurface pavements showed promising surface cooling effects. The solar simulation experiments provided direct evidence of how these thermal improvements have cooling benefits. Pavement structures with either a conductive base course (66% slag) or a conductive prime coat recorded maximum surface temperatures approximately 13% lower than

the control pavement, reducing peak asphalt mixture temperatures from 57.5 °C (control) to around 50 °C. This confirms that slag aggregates and conductive prime coats prevented heat accumulation near the surface by transferring it to deeper layers.

Nighttime performance was more significant. While the control pavement showed the largest surface temperature drop (45%), reflecting its higher heat storage and release, the conductive base and prime coat structures recorded smaller reductions (40%), releasing less energy into the atmosphere. Measurements at the bottom of the base course revealed that the 66% slag structure transferred heat more deeply, showing temperatures 5–10% higher than both the prime coat and control structures. This indicates that while both strategies are effective, the 66% slag base course performed better in long-term heat dissipation, while the conductive prime coat optimizes interfacial transfer.

Finally, the most direct measure of UHI mitigation can be the nighttime outgoing heat flux. The control pavement released the most energy, beginning at 640 $W.m^{-2}$ and declining to 166 $W.m^{-2}$ after 9 hours. By contrast, pavements with conductive modifications released substantially less. Starting the nighttime simulation, the 66% slag and conductive prime coat pavements achieved reductions of 38% and 33%, respectively. After 9 hours, reductions of 31% (steel slag base) and 22% (conductive prime coat) were still observed, showing that these designs not only lower peak flux but also reduce the cumulative nocturnal energy discharge, directly addressing the UHI effect.

In conclusion, the experimental program demonstrated that both steel slag base courses and conductive prime coats have substantial and complementary benefits. Mechanically, they enhance density, reduce water sensitivity, and increase load-bearing strength, ensuring structural viability. Thermally, more importantly, they increase conductivity and diffusivity, enabling effective redistribution of absorbed heat. The cooling simulations and flux analyses confirmed that these modifications reduce daytime peak temperatures, lower residual nighttime heat, and decrease outgoing flux, combating UHI effects.

Among the tested pavement structures, the 66% steel slag base course provided the most balanced performance, combining superior mechanical properties with optimized thermal behavior. Meanwhile, the conductive prime coat offered an efficient interfacial solution,

improving downward conduction without requiring full base course replacement. All in all, these strategies show the importance of focusing on pavement subsurface heat transfer, which is neglected in most studies. Hence, thermal improvement of pavement as a multilayer system, and looking at it from different perspectives, such as reflective surface treatments (Chapter 3) and conductive subsurface modifications, can propose practical ways to mitigate the UHI. Finally, the outcomes presented in this chapter verify the study's central hypotheses. In detail, conductive interface and base layers improved subsurface heat dissipation, which were previously neglected questionable subjects. The integration of reflective surface and conductive subsurface strategies validated the conceptual framework introduced in Chapter 1, demonstrating that UHI mitigation can be achieved through a combination of high-reflectivity surfaces and thermally conductive subsurface pavements. These findings not only confirm the hypotheses but also extend existing literature by showing the importance of considering pavements as a multilayer system to combat the UHI effects.

CONCLUSION AND RECOMMENDATIONS

In this thesis, several novel cool asphalt pavement structures were developed to mitigate urban heat island (UHI) effects associated with conventional asphalt pavements. The research was motivated by the need to reduce excessive heat absorption and storage caused by dark asphalt surfaces, which elevate pavement and ambient air temperatures. Traditional mitigation techniques, such as surface chemical coatings or water-based cooling methods, were found to have limited durability, safety concerns, and high construction and maintenance costs. Therefore, this study aimed to develop sustainable, durable, and thermally efficient pavement structures using recycled and industrial by-product materials. The selection of recycled concrete, clay bricks, glass, and steel slag as pavement materials was driven by their distinct thermal, mechanical, and physicochemical characteristics, as well as their availability as construction and industrial by-products. Some of these materials offer contrasting thermal conductivities, surface chemistries, porosities, and mechanical strengths, allowing a systematic evaluation of how aggregate properties influence surface reflectivity, heat transfer, adhesion, and durability.

Based on previous studies, three common approaches are used to mitigate the UHI effects of pavements, including using the cooling effect of water inside asphalt mixtures, enhancing the surface reflectivity of pavements, and changing the asphalt pavement materials to modify the thermal properties. According to different test methods in this research, the albedo of asphalt pavement plays an important part in reducing its temperature. This means the higher albedo is available, the lower surface and in-depth temperatures are observed. However, the current solutions found by these methods have drawbacks. For example, chemical paints and coatings were used to increase surface reflectivity; these coatings mostly compromised road safety, and they were costly in terms of regular maintenance. Thus, in this thesis, the problematic parts or the neglected aspects (such as subsurface heat dissipation) that can be influential in providing cooler pavements and air temperatures are evaluated. This chapter consolidates the experimental findings and critically analyzes their significance. It also explains the limitations

of the present work, suggests subjects for future research, and highlights the original contributions of the thesis.

In this research, the defined objectives were achieved successfully. The first objective was to increase the surface reflectivity without compromising the road safety, evaluated with a friction test, using reflective chip seals made of recycled CDW materials to improve albedo and maintain high skid resistance. The developed reflective layers could decrease the surface and air temperature, assisting in UHI mitigation. The second objective was to design pavement structures to dissipate the absorbed heat to subsurface layers using conductive base courses and prime coats, employing steel slag to provide cooler pavements and releasing less heat to the ambient air as a UHI mitigation policy. Each objective was achieved through experimental validation and analysis of thermal, mechanical, and reflective properties, demonstrating measurable improvements in surface cooling, heat dissipation, less outgoing heat, and overall pavement performance in terms of UHI alleviation effects.

This thesis has investigated the performance of multiple cool pavement strategies at different structural levels. On the one hand, in Chapter 3, the modification at the surface level with recycled chips was done to increase reflectivity, improve skid resistance, and reduce surface heating and heat absorption to mitigate the UHI effects. On the other hand, in Chapter 4, the subsurface modification with conductive base courses and prime coats was conducted to enhance thermal conductivity, redistributing absorbed heat and reducing surface temperature and nocturnal heat release. The results obtained from both chapters confirm that UHI mitigation requires a wider perspective and considers asphalt pavement as a system. Each layer of pavement, surface, base, and their interface, plays a significant role in cooling. This integrated understanding forms one of the key novel contributions of this thesis.

While the individual chapters provided the performance of these solutions, considering all of them revealed that effective UHI mitigation requires looking at pavements as a multi-layered system, each of which plays an important role in cooling. Pavements are not passive absorbers of solar energy but dynamic heat storage and release systems, where surface reflectivity, interfacial conduction, and base-layer heat transfer interact to shape thermal outcomes.

Regarding the mechanical and durability performance, both strategies demonstrated that UHI mitigation need not be achieved at the expense of structural performance. At the surface level, recycled chip seals using concrete aggregates delivered the strongest bond, lowest bleeding potential, and highest skid resistance, making them suitable for high-volume roads. Importantly, most developed chip seals satisfied minimum skid resistance and durability requirements, demonstrating that recycled aggregates can provide safe, durable surface treatments for different roadway contexts, and the type of aggregate must be chosen based on the traffic volume of the road. These results highlight the practical applicability of the proposed materials for real pavement construction, supporting their inclusion in performance-based specifications for chip seal design.

At the structural (subsurface) level, the use of steel slag in base courses significantly enhanced density and strength. Modified Proctor and CBR tests demonstrated that steel slag reduced water demand, increased dry density by 18%, and more than doubled load-bearing capacity compared to limestone. These results confirm that steel slag-modified base courses benefit from adequate structural strength and may extend pavement service life under heavy loads. Therefore, the thermal benefits achieved through conductive base courses are complemented by mechanical advantages, making this approach technically viable for adoption by transportation agencies.

The integration of mechanical and structural findings suggests that recycled chip seals and conductive base courses are not mutually exclusive. In fact, chip seals enhance safety and skid resistance at the surface, while steel slag enhances stability at depth. Therefore, they can form a framework for sustainable pavements that are both mechanically strong and thermally optimized. This dual functionality, simultaneously improving safety and cooling, forms one of the most significant and novel contributions of this thesis.

The central focus of this thesis was the thermal behavior of pavement systems, measured through reflectivity, thermal parameters, surface and in-depth temperatures, and outgoing heat flux. Regarding chip seals as a reflectivity strategy, clay brick aggregates provided the highest VIS/NIR reflectivity, reducing daytime surface temperatures by 15–23% compared to

uncoated HMA. Concrete chip seals performed slightly less effectively in reflectance but considerably higher than uncoated HMA. These reflective pavements showed the least surface temperature difference during the night, releasing less heat into the ambient air. In stark contrast, glass chip seals absorbed and transmitted solar energy, failing to reduce surface heating and outgoing heat. This confirmed the hypothesis that the selection of aggregate type is critical to the thermal behavior of the pavement and that reflectivity-based solutions must be carefully compatible with local traffic and climatic conditions.

The subsurface strategy for dissipation of the absorbed heat, through conductive base courses, reduced the surface temperature of asphalt pavement effectively. The 66% steel slag base course was the most effective combination, reducing asphalt surface temperature by 13% and lowering outgoing nocturnal heat flux by 31%. Fully substituted steel slag (100%) was less effective due to gradation-related voids, indicating the importance of optimal steel slag content. These results establish a quantitative benchmark for designing conductive base layers and provide a practical reference for engineers when specifying slag proportions for base course construction.

In addition to surface and subsurface methods, the interfacial strategy also showed a promising thermal performance. The steel slag–modified prime coat doubled conductivity and diffusivity compared with the control prime coat. As a result, it reduced peak asphalt surface temperatures by 13% and lowered outgoing nighttime heat flux by 22%, confirming its role as a conduction bridge between the asphalt mixture and base course. This intermediate layer design is another novel element of the thesis, demonstrating that relatively small modifications at the interface can produce meaningful thermal improvements.

The integrated analysis of these results reveals that reflective chip seals minimize heat gain, while conductive base course and prime coats regulate heat storage and release. These mechanisms can mitigate the UHI associated with asphalt pavements, since the surface reflectivity strategy reduces absorbed solar energy, and conductive subsurface redistributes and dissipates what is absorbed into layers below, lowering both daytime overheating and nighttime UHI emissions.

This thesis introduces several novel aspects to pavement engineering. Firstly, some new CDW materials are introduced to develop chip seals. These chip seals can be used in urban areas as a reflective layer to minimize the pavement heat absorption and heat release, mitigating the UHI effects. The privilege of this novel method over previous chemical coatings is its role in extending pavement life by sealing the surface cracks and increasing the skid resistance. Another important aspect of this approach is that it can be used for all existing pavements in urban areas, and there is no need to reconstruct pavements at high cost. Secondly, the overlooked role of the interface between the asphalt mixture and base course and base course thermal behavior for heat dissipation, reducing the surface temperature, and heat release was comprehensively investigated. In fact, previous research has focused on the asphalt mixture thermal behavior rather than considering the layers below and their role in cooling the surface and mitigating the UHI. Hence, the novel aspect was to show the role of using a conductive prime coat and base course to transfer the accumulated heat in the asphalt mixture surface temperature and reduce the nighttime outgoing heat to the ambient air. Last but not least, all proposed solutions were prepared using recycled materials and by-products, showing the dual environmental and mechanical benefits of them, contributing to circular economy practices.

Another critical contribution of this work is the detailed quantification of the outgoing heat flux of subsurface and interfacial modifications. Results demonstrated that the control pavement without modifications released 640 $W.m^{-2}$ at the start of cooling, declining to 166 $W.m^{-2}$ after 9 hours. However, the 66% steel slag base course reduced initial flux by 38% and cumulative release by 31%. Likewise, the conductive prime coat reduced initial flux by 33% and cumulative release by 22%. These results proved that to mitigate the UHI, researchers should not rely on only surface reflectivity, which is mostly studied in UHI research projects. Subsurface conduction strategies can significantly alter the timing and magnitude of heat release, influencing urban temperatures. These results provide a new scientific approach and practical guidance for pavement engineers, helping them design thermally responsive pavement systems with predictable cooling behavior.

The results of this thesis have practical implications for pavement design and environmental policy. Transportation agencies could add reflectivity and thermal efficiency requirements to

pavement design specifications, similar to mechanical performance criteria, due to their important roles in UHI effects. Municipalities and ministries of transportation could consider updating their pavement design manuals to include sustainable material alternatives such as recycled CDW and steel slag to have cool pavements and cities in hot seasons. Hence, implementing these strategies in urban infrastructure could contribute to achieving climate resilience goals and reducing cooling energy demand in cities.

This thesis advances knowledge on urban heat island (UHI) mitigation in pavement engineering in three main ways. First, it demonstrates that effective UHI mitigation requires an integrated pavement system by highlighting the combined influence of surface and subsurface layers on pavement surface temperature, rather than focusing solely on the top layer as in most previous studies. Second, it shows that recycled CDW aggregates and steel slag by-products can satisfy mechanical, durability, and thermal performance requirements simultaneously, offering a safer and more sustainable alternative to slippery reflective coatings while supporting circular economy practices. Third, this research quantifies nighttime outgoing heat flux for different pavement structures, providing a direct and realistic indicator of pavement contributions to urban thermal environments. Although combining surface and subsurface mitigation strategies shows promising results, practical implementation may be limited by material availability and agency standards, and such combined approaches may not always be feasible in practice.

Despite the contributions of this thesis, there were some limitations. Although the laboratory cooling effect setup is the most common method for comparing laboratory samples with each other, it cannot fully simulate the variability of real-world solar radiation, wind, humidity, and traffic loading. Another limitation was associated with the reflectance and albedo of chip seals. Although the albedo data assisted in comparing chip seals with aged and new HMA, their long-term stability under traffic and weathering remains untested. Finally, the conductive prime coat and steel slag-modified base courses were tested at the laboratory scale. If their effects in full pavement layers are investigated, more realistic thermal and mechanical behavior can be achieved.

Although many aspects of the proposed solutions have been investigated, there are beneficial relevant subjects that can be examined in future studies. These subjects are as follows:

- Conducting full-scale outdoor trials of chip seals, conductive base courses, and conductive prime coats to validate laboratory results under real traffic and environmental conditions is recommended.
- Developing numerical models coupling the proposed pavement structures with mesoscale urban climate models to directly quantify air temperature reductions after using these novel systems at neighborhood scales can also be interesting.
- As the recycled materials have not been used before for the studied purposes, the long-term monitoring of chip seal reflectivity and base course conductivity under seasonal cycles, aging, and traffic loads is also recommended.
- Carrying out life-cycle and economic assessments to evaluate environmental benefits, energy savings, and cost-effectiveness of the proposed strategies relative to conventional pavements is suggested.

In conclusion, this thesis has successfully developed and validated novel cool asphalt pavement structures that address both the UHI problem and the need for sustainable recycling of waste materials. It also confirms that cool pavements must be perceived as engineered multi-layer systems rather than reflective surface treatments or modified asphalt mixture layers alone. Reflective chip seals reduce solar heat absorption, while conductive base courses and prime coats control heat transfer and nighttime heat release. Therefore, they create pavements that are mechanically durable, environmentally sustainable, and thermally optimized. Overall, the results provide a pathway toward climate-responsive infrastructure design, integrating sustainability, safety, and performance. The findings also point out that pavements should no longer be designed solely for mechanical performance but also as active thermal systems contributing to climate resilience. By integrating recycled materials, industrial by-products, and thermal engineering principles, this work establishes a strategy toward sustainable urban infrastructure that reduces construction waste, mitigates UHI, and enhances human thermal comfort. A list of the papers derived from this research, published in international journals and presented at international conferences, is also provided at the end of this thesis.

The published journal and conference papers obtained from this thesis are as follows:

International Journal Papers:

1. **Shamsaei, M**., Carter, A., & Vaillancourt, M. (2025). Utilization of steel slag aggregates to propose novel asphalt pavement structures alleviating urban heat islands. Road Materials and Pavement Design, 1–26. https://doi.org/10.1080/14680629.2024.2438340.
2. **Shamsaei, M**., Carter, A., & Vaillancourt, M. (2024). Using construction and demolition waste materials to alleviate the negative effect of pavements on the urban heat island: A laboratory, field, and numerical study, Case Studies in Construction Materials, Volume 20, 2024, e03346. https://doi.org/10.1016/j.cscm.2024.e03346.
3. **Shamsaei, M**., Carter, A., & Vaillancourt, M. (2023). Using Construction and Demolition Waste Materials to Develop Chip Seals for Pavements. Infrastructures, 8(5), 95.https://doi.org/10.3390/infrastructures8050095
4. **Shamsaei, M**., Carter, A., & Vaillancourt, M. (2022). A review on the heat transfer in asphalt pavements and urban heat island mitigation methods, Construction and Building Materials, Volume 359, 2022, 129350. https://doi.org/10.1016/j.conbuildmat.2022.129350.

International Conference Papers:

1. **Shamsaei, M**., Carter, A., Vaillancourt, M. (2024). The effects of using prime coat on the surface temperature of asphalt pavement and urban heat island mitigation. RILEM Conference on Sustainable Materials & Structures (SMS 2024): Meeting the major challenges of the 21st century, Toulouse, France.
2. **Shamsaei, M**., Carter, A., Vaillancourt, M. (2023). The Comparison of the Bleeding Potential of Chip Seals Developed with Recycled Materials and Limestone Aggregates. Smart & Sustainable Infrastructure: Building a Greener Tomorrow. ISSSI 2023. RILEM Bookseries, vol 48. Springer, Cham. Vancouver, Canada.

APPENDIX I

CHIP SEAL MIX DESIGN – CHAPTER 3

The chip seal mix design calculation is based on the Modified McLeod method, which is the most common method in Canada (Shuler et al., 2011; Wood et al., 2006). The details of the step-by-step calculation are explained in this section. Based on the McLeod method, the aggregate rate depends on the aggregate shape, gradation, and specific gravity. Moreover, the binder rate depends on other factors, including absorption and shape of aggregates, traffic volume, the current pavement condition, and the asphalt content of the binder. Hence, the aggregate gradation, bulk specific gravity, and aggregate binder absorption are determined in the first step. The median particle size is then determined by the gradation curve. Indeed, this is the size through which 50 percent of aggregates passed the sieve. Following that, the flakiness index (FI) will be calculated. For this purpose, a certain amount of aggregate is sieved from the sieve 1/2" inch to the sieve No.4. The FI is calculated by Equation AI. 1.

$$FI\ (percent) = \frac{(weight\ of\ flat\ chips, retained\ on\ the\ sieves)}{(Total\ weight\ of\ the\ sample)} \times 100 \qquad \text{(AI.1)}$$

The average least dimension (H) is determined in the next step. This parameter is the estimation for the thickness (mm) of the seal after passing the traffic, and the flat chips are oriented. This can be calculated from the provided graph in the guide or the equation based on M, which is the median particle size (mm), and FI is the flakiness index of aggregates. The loose weight of aggregates, W (kg/m^3), is then measured. For this goal, a cylinder is filled with aggregates, and this parameter is calculated by Equation A I. 2. It is recommended to measure this parameter 3 times and use the average value.

$$W = \frac{Weight\ of\ aggregate\ (kg)}{Volume\ of\ the\ cylinder\ (m^3)} \qquad \text{(AI. 2)}$$

In the next step, the void in loose aggregates (V_d) is assessed. This parameter is achieved by Equation AI. 3.

$$V_d = 1 - \frac{W}{1000G} \qquad \text{(AI. 3)}$$

Where W is the loose weight of aggregate (kg/m^3), and G is the bulk specific gravity of aggregates. Finally, the application rate of aggregate for the chip seal layer is calculated by Equation AI. 4.

$$C = (1 - (0.4)(V_d))(H)(G)(E) \quad \text{(AI. 4)}$$

Where C is the aggregate application rate (kg/m^2), V_d is the void in loose aggregates (percent and decimal), H is the average least dimension (mm), G is the bulk specific gravity, and E is the wastages factor for traffic whip-off, which a factor considering the number of aggregates that will get thrown to the side of the roadway while the chip seal is curing and traffic loads are applied. If the roadway has a low volume of traffic (residential type traffic), this parameter is assumed to be 5 percent, and for high-speed roads like main roads is considered to be 10 percent. Hence, the E parameter can be obtained from Table AI. 1. Once the aggregate amount is determined, it can be tested by a 1 m^2 plywood box. The aggregate must be a one-stone thick layer.

Table AI. 1 Aggregate wastage factor

Allowed Percentage Waste	Wastage Factor (E)
1	1.01
2	1.02
3	1.03
4	1.04
5	1.05
6	1.06
7	1.07
8	1.08
9	1.09
10	1.10
11	1.11
12	1.12
13	1.13
14	1.14
15	1.15

After calculating the aggregate application rate, the binder application rate will be calculated with the following steps. In addition to the parameters that were mentioned, some other parameters are essential to calculate the application binder rate. One of these parameters is the aggregate absorption rate. Aggregates absorb a part of the binder. So, the amount of binder should be corrected in the design process. According to the McLeod method, this factor must be adjusted based on the aggregate's water absorption. Traffic is also another important factor that should be taken into consideration. Hence, the traffic correction factor (T) is used based on the traffic volume per day, which is depicted in Table AI. 2.

Table AI. 2 Traffic correction factor (T)

Traffic factor (percentage, expressed as a decimal)				
Traffic (vehicles per day)				
Under 100	100 to 500	500 to 1000	1000 to 2000	Over 2000
0.85	0.75	0.7	0.65	0.6

Finally, the existing pavement surface is important for the required binder of the chip seal. Thus, the McLeod method proposes a surface correction factor (S), shown for different types of surfaces in Table AI. 3.

Table AI. 3 Surface correction factors

The current pavement surface texture	Correction factor S (L/m^2)
Black and flushed surface	-0.04 to -0.27
Smooth and non-porous	0.00
Slightly porous and oxidized	+0.14
Slightly pocked, porous, and oxidized	+0.27
Badly pocked, porous, and oxidized	+0.40

The other influential parameter is the residual asphalt content of binder (R), which is mentioned as a percent (decimal) in the calculation. A good and desirable residual asphalt content should be around 0.7. Therefore, the application binder rate can be calculated from Equation AI. 5.

$$B = \frac{(0.4)(H)(T)(V_d)+S+A}{R} \quad \text{(AI. 5)}$$

Where B is the binder application rate (L/m^2), H is the average least dimension (mm), T is the traffic factor, V_d is the voids in loose aggregate, S is the surface condition factor (L/m^2), A is the aggregate absorption factor (L/m^2), and R is the residual asphalt content of binder. Considering the physical properties of recycled aggregates and emulsified binder, the aggregate and binder application rates are calculated as follows:

Recycled Concrete Aggregates Chip Seal Design:

Aggregates Application Rate:

$FI\ (\%) = \frac{150}{1000} \times 100 = 15$ & M = 6.5 & H= 3.70 mm

$W_1 = \frac{2.386}{0.00157} = 1520$ kg/m^3

$W_2 = \frac{2.367}{0.00157} = 1508$ kg/m^3

$W_3 = \frac{2.372}{0.00157} = 1511$ kg/m^3

$W_{avg} = \frac{1520+1508+1511}{3} = 1513$ kg/m^3

$V_d = 1 - \frac{1513}{1000 \times 2.37} = 0.36$ & G = 2.37 E = 1.05

$C = (1 - (0.4)(0.36))(3.70)(2.37)(1.05) = 7.88$ kg/m^2

Binder Application Rate:

T = 0.7 & S = 0.27 & A = 0.39 & R = 0.69

$$B = \frac{(0.4)(3.70)(0.7)(0.36) + 0.27 + 0.39}{0.69} = 1.5 \text{ L/m}^2$$

Recycled Yellow Brick Chip Seal Mix Design:

Aggregates Application Rate:

$FI\ (\%) = \frac{200}{1000} \times 100 = 20$ & M = 6.7 & H= 3.62 mm

$W_1 = \frac{1.760}{0.00157} = 1121$ kg/m^3

$W_2 = \frac{1.741}{0.00157} = 1109$ kg/m^3

$W_3 = \frac{1.755}{0.00157} = 1118$ kg/m^3

$W_{avg} = \frac{1121+1109+1118}{3} = 1116$ kg/m^3

$V_d = 1 - \frac{1116}{1000 \times 1.93} = 0.42$ & G = 1.93 E = 1.05

$C = (1 - (0.4)(0.42))(3.62)(1.93)(1.05) = 6.11$ kg/m^2

Binder Application Rate:

T = 0.7 & S = 0.27 & A = 0.60 & R = 0.69

$$B = \frac{(0.4)(3.62)(0.7)(0.42) + 0.27 + 0.60}{0.69} = 1.88\ \text{L/m}^2$$

Recycled Red Brick Chip Seal Mix Design:

Aggregates Application Rate:

$FI\ (\%) = \frac{220}{1000} \times 100 = 22$ & M = 6.8 & H= 3.59 mm

$W_1 = \frac{1.768}{0.00157} = 1126$ kg/m^3

$W_2 = \frac{1.750}{0.00157} = 1115$ kg/m^3

$W_3 = \frac{1.762}{0.00157} = 1122$ kg/m^3

$W_{avg} = \frac{1126+1115+1122}{3} = 1121$ kg/m^3

$V_d = 1 - \frac{1121}{1000 \times 1.91} = 0.41$ & G = 1.91 E = 1.05

$C = (1 - (0.4)(0.41))(3.59)(1.91)(1.05) = 6.02$ kg/m^2

Binder Application Rate:

T = 0.7 & S = 0.27 & A = 0.63 & R = 0.69

$$B = \frac{(0.4)(3.59)(0.7)(0.41) + 0.27 + 0.63}{0.69} = 1.90\ \text{L/m}^2$$

Recycled Glass Chip Seal Mix Design:

Aggregates Application Rate:

$FI\ (\%) = \frac{310}{1000} \times 100 = 31$ & M = 4.7 & H= 2.21 mm

$W_1 = \frac{2.313}{0.00157} = 1473$ kg/m^3

$W_2 = \frac{2.333}{0.00157} = 1486$ kg/m^3

$W_3 = \frac{2.349}{0.00157} = 1496$ kg/m^3

$W_{avg} = \frac{1473+1486+1496}{3} = 1485$ kg/m^3

$V_d = 1 - \frac{1485}{1000 \times 2.49} = 0.40$ & G = 2.49 E = 1.05

$C = (1 - (0.4)(0.40))(2.21)(2.49)(1.05) = 4.85$ kg/m^2

Binder Application Rate:

T = 0.7 & S = 0.27 & A = 0.48 & R = 0.69

$$B = \frac{(0.4)(2.21)(0.7)(0.40) + 0.27 + 0.48}{0.69} = 1.44\ \mathrm{L/m^2}$$

The chip seal mix designs for four recycled aggregate types, recycled concrete, yellow brick, red brick, and glass, were calculated using the Modified McLeod Method, as commonly used in Canada. All designs are based on the materials' measured physical properties, summarized in Table AI 4.

Table AI. 4 Summary of chip seal mix designs for recycled aggregates

Material	Aggregate Rate (kg/m²)	Binder Rate (L/m²)
Recycled Concrete	7.88	1.50
Recycled Yellow Brick	6.11	1.88
Recycled Red Brick	6.02	1.90
Recycled Glass	4.85	1.44

In summary, recycled concrete chip seal has the highest aggregate application rate, which was expected due to its relatively high specific gravity and lower flakiness. This chip seal has a moderate binder requirement, which is suitable for most traffic conditions. Brick aggregates are more porous and less dense, have lower aggregate rates but higher binder rates due to greater absorption. Recycled glass chip seals have the lowest thickness and smaller gradation, resulting in the least amount of aggregate. However, the flakiness and brittleness of glass could affect skid resistance and durability, requiring careful field validation.

LIST OF BIBLIOGRAPHICAL REFERENCES

A basic asphalt emulsion manual, 1997. A basic asphalt emulsion manual. Manual Series No. 19. Third edition.

AASHTO M 147-65, 2012. Standard specification for materials for aggregate and soil-aggregate subbase, base, and surface courses. American Association of State Highway and Transportation Officials ….

Abedin Khan, Z., Balunaini, U., Costa, S., 2024. Environmental feasibility and implications in using recycled construction and demolition waste aggregates in road construction based on leaching and life cycle assessment – A state-of-the-art review. Clean. Mater. 12, 100239. https://doi.org/10.1016/j.clema.2024.100239

Adams, J., Castorena, C., Im, J.H., Ilias, M., Kim, Y.R., 2017. Addressing Raveling Resistance in Chip Seal Specifications. Transp. Res. Rec. 2612, 39–46. https://doi.org/10.3141/2612-05

Adesanya, O., 2015. Determining the Emissivity of Roofing Samples: Asphalt, Ceramic and Coated Cedar. University of North Texas.

Afshinnia, K., Rangaraju, P.R., 2015. Influence of fineness of ground recycled glass on mitigation of alkali–silica reaction in mortars. Constr. Build. Mater. 81, 257–267.

Aghayan, I., Khafajeh, R., Shamsaei, M., 2021. Life cycle assessment, mechanical properties, and durability of roller compacted concrete pavement containing recycled waste materials. Int. J. Pavement Res. Technol. 14, 595–606. https://doi.org/10.1007/s42947-020-0217-7

Ahammed, M.A., Tighe, S.L., 2012. Asphalt pavements surface texture and skid resistance — exploring the reality. Can. J. Civ. Eng. 39, 1–9. https://doi.org/10.1139/l11-109

Ahmad, M., Al-Dala'ien, R.N.S., Beddu, S., Itam, Z.B., 2021. Thermo-Physical Properties of Graphite Powder and Polyethylene Modified Asphalt Concrete. Eng. Sci. Volume 17 (March 2022), 121–132.

Ahmad Nazki, M., Chopra, T., Chandrappa, A.K., 2020. Rheological properties and thermal conductivity of bitumen binders modified with graphene. Constr. Build. Mater. 238, 117693. https://doi.org/10.1016/j.conbuildmat.2019.117693

Akbari, H., Matthews, H.D., 2012. Global cooling updates: Reflective roofs and pavements. Energy Build., Cool Roofs, Cool Pavements, Cool Cities, and Cool World 55, 2–6. https://doi.org/10.1016/j.enbuild.2012.02.055

Akbari, H., Rose, L.S., 2008. Urban Surfaces and Heat Island Mitigation Potentials. J. Hum.-Environ. Syst. 11, 85–101. https://doi.org/10.1618/jhes.11.85

Aletba, S.R.O., Abdul Hassan, N., Putra Jaya, R., Aminudin, E., Mahmud, M.Z.H., Mohamed, A., Hussein, A.A., 2021. Thermal performance of cooling strategies for asphalt pavement: A state-of-the-art review. J. Traffic Transp. Eng. Engl. Ed. 8, 356–373. https://doi.org/10.1016/j.jtte.2021.02.001

Allahdin, O., Wartel, M., Mabingui, J., Boughriet, A., 2015. Implication of Electrostatic Forces on the Adsorption Capacity of a Modified Brick for the Removal of Divalent Cations from Water. Am. J. Anal. Chem. 6, 11–25. https://doi.org/10.4236/ajac.2015.61002

Anand, J., Sailor, D.J., 2022. Role of pavement radiative and thermal properties in reducing excess heat in cities. Sol. Energy 242, 413–423. https://doi.org/10.1016/j.solener.2021.10.056

Anderson, G.B., Bell, M.L., 2011. Heat Waves in the United States: Mortality Risk during Heat Waves and Effect Modification by Heat Wave Characteristics in 43 U.S. Communities. Environ. Health Perspect. 119, 210–218. https://doi.org/10.1289/ehp.1002313

Anting, N., Din, M.F.M., Iwao, K., Ponraj, M., Siang, A.J.L.M., Yong, L.Y., Prasetijo, J., 2018. Optimizing of near infrared region reflectance of mix-waste tile aggregate as coating material for cool pavement with surface temperature measurement. Energy Build. 158, 172–180. https://doi.org/10.1016/j.enbuild.2017.10.001

Asadi, I., Shafigh, P., Abu Hassan, Z.F.B., Mahyuddin, N.B., 2018. Thermal conductivity of concrete – A review. J. Build. Eng. 20, 81–93. https://doi.org/10.1016/j.jobe.2018.07.002

Asaeda, T., Ca, V.T., Wake, A., 1996. Heat storage of pavement and its effect on the lower atmosphere. Atmos. Environ., Conference on the Urban Thermal Environment Studies in Tohwa 30, 413–427. https://doi.org/10.1016/1352-2310(94)00140-5

Asphalt Institute, 2007. The Asphalt handbook. Asphalt Institute, Lexington, Ky.

ASTM, C1371, 2015.Standard Test Method for Determination of Emittance of Materials near Room Temperature Using Portable Emissometers. Am. Soc. Test. Mater. West Conshohocken PA.

ASTM C29/C29M, 2017. Standard Test Method for Bulk Density (“Unit Weight”) and Voids in Aggregate. American Society for Testing and Materials, West Conshohocken, PA, USA.

ASTM C127, 2015. Standard test method for relative density (specific gravity) and absorption of coarse aggregate. Am. Soc. Test. Mater. West Conshohocken PA USA.

ASTM C128, 2022. Standard Test Method for Relative Density (Specific Gravity) and Absorption of Fine Aggregate.

ASTM C131/C131M, 2020. Standard test method for resistance to degradation of small-size coarse aggregate by abrasion and impact in the Los Angeles machine. Am. Soc. Test. Mater. West Conshohocken PA USA.

ASTM C136/C136M, 2019. Standard Test Method for Sieve Analysis of Fine and Coarse Aggregates. American Society for Testing and Materials, West Conshohocken, PA, USA.

ASTM C177-19, A., 2019. Standard Test Method for Steady-State Heat Flux Measurements and Thermal Transmission Properties by Means of the Guarded-Hot-Plate Apparatus. ASTM International West Conshohocken, PA.

ASTM D5, 2013. Standard test method for penetration of bituminous materials. Am. Soc. Test. Mater. West Conshohocken PA USA.

ASTM D113, 2017. Standard test method for ductility of asphalt materials. Am. Soc. Test. Mater. West Conshohocken PA USA.

ASTM D1557, 2021. Standard Test Methods for Laboratory Compaction Characteristics of Soil Using Modified Effort (56,000 Ft-Lbf/Ft3 (2,700 KN-M/M3)) 1. American Society for Testing and Materials, West Conshohocken, PA, USA.

ASTM D1883, 2021. Standard Test Method for California Bearing Ratio (CBR) of Laboratory-Compacted Soils.

ASTM D2042, 2015. Standard test method for solubility of asphalt materials in trichloroethylene. American Society for Testing and Materials, West Conshohocken, PA, USA.

ASTM D2940, 2020. Standard specification for graded aggregate material for bases or subbases for highways or airports.

ASTM D4791, 2019. Standard test method for flat particles, elongated particles, or flat and elongated particles in coarse aggregate, D4791-10. American Society for Testing and Materials, West Conshohocken, PA, USA.

ASTM D5334, 2022. Standard Test Method for Determination of Thermal Conductivity of Soil and Rock by Thermal Needle Probe Procedure.

ASTM D5930, 2017. Standard Test Method for Thermal Conductivity of Plastics by Means of a Transient Line-Source Technique. Am. Soc. Test. Mater. West Conshohocken PA USA.

ASTM D6372, 2015. Standard Practice for Design, Testing, and Construction of Microsurfacing. Am. Soc. Test. Mater. West Conshohocken PA USA.

ASTM D6930, 2019. Standard Test Method for Settlement and Storage Stability of Emulsified Asphalts. Am. Soc. Test. Mater. West Conshohocken PA USA.

ASTM D6936, 2017. Standard Test Method for Determining Demulsibility of Emulsified Asphalt. Am. Soc. Test. Mater. West Conshohocken PA USA.

ASTM D6997, 2020. Standard Test Method for Distillation of Emulsified Asphalt. American Society for Testing and Materials, West Conshohocken, PA, USA.

ASTM D7000, 2019. Standard Test Method for Sweep Test of Emulsified Asphalt Surface Treatment Samples. Am. Soc. Test. Mater. West Conshohocken PA USA.

ASTM D7402, 2017. Standard Practice for Identifying Cationic Emulsified Asphalts. Am. Soc. Test. Mater. West Conshohocken PA USA.

ASTM D7496, 2018. Standard test method for viscosity of emulsified asphalt by saybolt furol viscometer. Annual book of ASTM standards. American Society for Testing and Materials, West Conshohocken, PA, USA.

ASTM D7984, 2021. Standard Test Method for Measurement of Thermal Effusivity of Fabrics Using a Modified Transient Plane Source (MTPS) Instrument. Am. Soc. Test. Mater. West Conshohocken PA USA.

ASTM E408. Standard test methods for total normal emittance of surfaces using inspection-meter techniques. Annu. Book ASTM Stand. 15.

ASTM E303, 2013. Standard test method for measuring surface frictional properties using the British pendulum tester. Am. Soc. Test. Mater. West Conshohocken PA USA.

ASTM E965, 2019. Standard test method for measuring pavement macrotexture depth using a volumetric technique. Am. Soc. Test. Mater. West Conshohocken PA USA.

ASTM E1918, 2021. Standard Test Method for Measuring Solar Reflectance of Horizontal and Low-Sloped Surfaces in the Field, in: American Society for Testing and Materials, West Conshohocken, PA, USA.

ASTM G173, 2008. Standard Tables for Reference Solar Spectral Irradiances: Direct Normal and Hemispherical on 37° Tilted Surface. Am. Soc. Test. Mater. West Conshohocken PA USA.

Baran, S., Sukhija, M., Coleri, E., 2025. Assessment of aggregate-binder adhesion through field-applicable modified sweep, Vialit, and pull-off tests. Constr. Build. Mater. 490, 142495. https://doi.org/10.1016/j.conbuildmat.2025.142495

Behiry, A.E.A.E.-M., 2013. Evaluation of steel slag and crushed limestone mixtures as subbase material in flexible pavement. Ain Shams Eng. J. 4, 43–53. https://doi.org/10.1016/j.asej.2012.07.006

Behrens, S.H., Grier, D.G., 2001. The charge of glass and silica surfaces. J. Chem. Phys. 115, 6716–6721. https://doi.org/10.1063/1.1404988

Bergman, T.L., Lavine, A.S., Incropera, F.P., DeWitt, D.P., 2017. Fundamentals of Heat and Mass Transfer. Wiley.

BNQ 2560-600, 2024. Aggregates — Recycled materials made from concrete, asphalt mix and bricks —Classification and characteristics.

Bobes-Jesus, V., Pascual-Muñoz, P., Castro-Fresno, D., Rodriguez-Hernandez, J., 2013. Asphalt solar collectors: A literature review. Appl. Energy, Special Issue on Advances in sustainable biofuel production and use - XIX International Symposium on Alcohol Fuels - ISAF 102, 962–970. https://doi.org/10.1016/j.apenergy.2012.08.050

Bodian, S., Faye, M., Sene, N.A., Sambou, V., Limam, O., Thiam, A., 2018. Thermo-mechanical behavior of unfired bricks and fired bricks made from a mixture of clay soil and laterite. J. Build. Eng. 18, 172–179. https://doi.org/10.1016/j.jobe.2018.03.014

Brennan, M.P., Abramase, A.L., Andrews, R.W., Pearce, J.M., 2014. Effects of spectral albedo on solar photovoltaic devices. Sol. Energy Mater. Sol. Cells 124, 111–116. https://doi.org/10.1016/j.solmat.2014.01.046

BS EN 12272-3, 2003. Determination of binder aggregate adhesivity by the Vialit plate shock test method. Br. Stand. Inst. 389 Chiswick High Road Lond. UK.

Buss, A.F., Guriguis, M., Claypool, B., Gransberg, D.D., Williams, R.C., Oregon. Dept. of Transportation. Research Section, 2016. Chip seal design and specifications : final report. (No. FHWA-OR-RD-17-03).

Byzyka, J., Rahman, M., Chamberlain, D.A., 2021. A laboratory investigation on thermal properties of virgin and aged asphalt mixture. Constr. Build. Mater. 305, 124757. https://doi.org/10.1016/j.conbuildmat.2021.124757

Cao, X., Tang, B., Zou, X., He, L., 2015. Analysis on the cooling effect of a heat-reflective coating for asphalt pavement. Road Mater. Pavement Des. 16, 716–726. https://doi.org/10.1080/14680629.2015.1026383

Cao, Y., Sha, A., Liu, Z., Zhang, F., Li, J., Liu, H., 2022. Thermal Conductivity Evaluation and Road Performance Test of Steel Slag Asphalt Mixture. Sustainability 14, 7288. https://doi.org/10.3390/su14127288

Chen, J., Wang, H., Li, L., 2015. Determination of Effective Thermal Conductivity of Asphalt Concrete with Random Aggregate Microstructure. J. Mater. Civ. Eng. 27, 04015045. https://doi.org/10.1061/(ASCE)MT.1943-5533.0001313

Chen, J., Wang, H., Xie, P., 2019. Pavement temperature prediction: Theoretical models and critical affecting factors. Appl. Therm. Eng. 158, 113755. https://doi.org/10.1016/j.applthermaleng.2019.113755

Chen, J., Wang, H., Zhu, H., 2017. Analytical approach for evaluating temperature field of thermal modified asphalt pavement and urban heat island effect. Appl. Therm. Eng. 113, 739–748. https://doi.org/10.1016/j.applthermaleng.2016.11.080

Chen, J., Yin, X., Wang, H., Ding, Y., 2018. Evaluation of durability and functional performance of porous polyurethane mixture in porous pavement. J. Clean. Prod. 188, 12–19. https://doi.org/10.1016/j.jclepro.2018.03.297

Chen, Y., Li, Z., Ding, S., Yang, X., Guo, T., 2022. Research on heat reflective coating technology of asphalt pavement. Int. J. Pavement Eng. 23, 4455–4464. https://doi.org/10.1080/10298436.2021.1952410

Chen, Y., Lyu, L., Pei, J., Zhang, G., Wen, Y., Zhang, J., 2020. Novel Asphalt-Mix Design with High Thermal Diffusivity for Alleviating the Urban Heat Island. J. Mater. Civ. Eng. 32, 04020321. https://doi.org/10.1061/(ASCE)MT.1943-5533.0003325

Chip Seal Best Practices, 2005. Transportation Research Board, Washington, D.C. https://doi.org/10.17226/13814

Chiu, C.-T., Hsu, T.-H., Yang, W.-F., 2008. Life cycle assessment on using recycled materials for rehabilitating asphalt pavements. Resour. Conserv. Recycl. 52, 545–556. https://doi.org/10.1016/j.resconrec.2007.07.001

Chu, L., He, L., Fwa, T.F., 2020. 3-Dimensional finite element modelling of asphalt mixtures for thermal conductivity determination. Int. J. Pavement Eng. 0, 1–10. https://doi.org/10.1080/10298436.2020.1834109

Cleveland, C.J., Morris, C. (Eds.), 2013. Section 10 - Solar, in: Handbook of Energy. Elsevier, Amsterdam, pp. 405–450. https://doi.org/https://doi.org/10.1016/B978-0-08-046405-3.00010-3

Coleri, E., Tsai, B.-W., Monismith, C.L., 2008. Pavement Rutting Performance Prediction by Integrated Weibull Approach. Transp. Res. Rec. 2087, 120–130. https://doi.org/10.3141/2087-13

Cong, P., Xu, P., Chen, S., 2014. Effects of carbon black on the anti aging, rheological and conductive properties of SBS/asphalt/carbon black composites. Constr. Build. Mater. 52, 306–313. https://doi.org/10.1016/j.conbuildmat.2013.11.061

Coser, E., Moritz, V.F., Krenzinger, A., Ferreira, C.A., 2015. Development of paints with infrared radiation reflective properties. Polímeros 25, 305–310. https://doi.org/10.1590/0104-1428.1869

Davidson, J.K., Houston, G., Linton, P., Croteau, J.M., 2005. Overview of the Design of Emulsion Based Seal Coating Systems Available in Canada and Abroad. Presented at the Fiftieth Annual Conference of the Canadian Technical Asphalt Association (CTAA)Canadian Technical Asphalt Association.

Dawson, A.R., Dehdezi, P.K., Hall, M.R., Wang, J., Isola, R., 2012. Enhancing thermal properties of asphalt materials for heat storage and transfer applications. Road Mater. Pavement Des. 13, 784–803. https://doi.org/10.1080/14680629.2012.735791

Deb, P., Singh, Kh.L., 2022. Experimental Investigation on the Mechanical Performance of Cold Mix Asphalt Using Construction Demolition Waste as Filler. Int. J. Pavement Res. Technol. https://doi.org/10.1007/s42947-022-00216-4

Deng, H., Deng, D., Du, Y., Lu, X., 2019. Using Lightweight Materials to Enhance Thermal Resistance of Asphalt Mixture for Cooling Asphalt Pavement. Adv. Civ. Eng. 2019, e5216827. https://doi.org/10.1155/2019/5216827

Díaz-Piloneta, M., Terrados-Cristos, M., Álvarez-Cabal, J.V., Vergara-González, E., 2021. Comprehensive Analysis of Steel Slag as Aggregate for Road Construction: Experimental Testing and Environmental Impact Assessment. Materials 14, 3587. https://doi.org/10.3390/ma14133587

Ding, T., Xiao, J., Tam, V.W., 2016. A closed-loop life cycle assessment of recycled aggregate concrete utilization in China. Waste Manag. 56, 367–375.

Dondi, M., Mazzanti, F., Principi, P., Raimondo, M., Zanarini, G., 2004. Thermal Conductivity of Clay Bricks. J. Mater. Civ. Eng. 16, 8–14. https://doi.org/10.1061/(ASCE)0899-1561(2004)16:1(8)

Doulos, L., Santamouris, M., Livada, I., 2004. Passive cooling of outdoor urban spaces. The role of materials. Sol. Energy 77, 231–249. https://doi.org/10.1016/j.solener.2004.04.005

Du, Y., Xu, L., Deng, H., Deng, D., Ma, C., Liu, W., 2020. Characterization of thermal, high-temperature rheological and fatigue properties of asphalt mastic containing fly ash cenosphere. Constr. Build. Mater. 233, 117345. https://doi.org/10.1016/j.conbuildmat.2019.117345

Duan, H., Li, J., Liu, G., 2017. Growing threat of urban waste dumps. Nature 546, 599–599. https://doi.org/10.1038/546599b

Duan, H., Miller, T.R., Liu, G., Tam, V.W.Y., 2019. Construction debris becomes growing concern of growing cities. Waste Manag. 83, 1–5. https://doi.org/10.1016/j.wasman.2018.10.044

Durrani, A., 2021. Analysis of Reclaimed Asphalt Pavement (RAP) Proposed for Use as Aggregate in Microsurfacing and Chip Seal Mixes for Local Roadways Applications in Ohio. Ohio University.

Epa, U., 2015. Advancing sustainable materials management: 2014 fact sheet. U. S. Environ. Prot. Agency Off. Land Emerg. Wash. DC USA.

Epps, A., 2000. Design and Analysis System for Thermal Cracking in Asphalt Concrete. J. Transp. Eng. 126, 300–307. https://doi.org/10.1061/(ASCE)0733-947X(2000)126:4(300)

Fang, M., Park, D., Singuranayo, J.L., Chen, H., Li, Y., 2019. Aggregate gradation theory, design and its impact on asphalt pavement performance: a review. Int. J. Pavement Eng. 20, 1408–1424. https://doi.org/10.1080/10298436.2018.1430365

Fatemi, S., Imaninasab, R., 2016. Performance evaluation of recycled asphalt mixtures by construction and demolition waste materials. Constr. Build. Mater. 120, 450–456. https://doi.org/10.1016/j.conbuildmat.2016.05.117

Feng, D., Yi, J., Wang, D., 2013. Performance and Thermal Evaluation of Incorporating Waste Ceramic Aggregates in Wearing Layer of Asphalt Pavement. J. Mater. Civ. Eng. 25, 857–863. https://doi.org/10.1061/(ASCE)MT.1943-5533.0000788

Founda, D., 2011. Evolution of the air temperature in Athens and evidence of climatic change: A review. Adv. Build. Energy Res. 5, 7–41. https://doi.org/10.1080/17512549.2011.582338

Freeman, T.J., Button, J.W., Estakhri, C.K., 2010. Effective Prime Coats for Compacted Pavement Bases.

Gao, Q., Huang, Y., Li, M., Liu, Y., Yan, Y.Y., 2010. Experimental study of slab solar collection on the hydronic system of road. Sol. Energy 84, 2096–2102. https://doi.org/10.1016/j.solener.2010.09.008

Garcia, A., Hassn, A., Chiarelli, A., Dawson, A., 2015. Multivariable analysis of potential evaporation from moist asphalt mixture. Constr. Build. Mater. 98, 80–88. https://doi.org/10.1016/j.conbuildmat.2015.08.061

Geng, W., Heitzman, M., 2019. Measuring Specific Heat Capacity of Pavement Materials, in: Steyn, Wj., Holleran, I., Nam, B. (Eds.), Pavement Materials and Associated Geotechnical Aspects of Civil Infrastructures, Sustainable Civil Infrastructures. Springer International Publishing, Cham, pp. 126–135. https://doi.org/10.1007/978-3-319-95759-3_11

Georgiou, P., Loizos, A., 2021. Environmental assessment of warm mix asphalt incorporating steel slag and high reclaimed asphalt for wearing courses: a case study. Road Mater. Pavement Des. 22, S662–S671. https://doi.org/10.1080/14680629.2021.1906305

Gheni, A.A., Abdelkarim, O.I., Abdulazeez, M.M., ElGawady, M.A., 2017. Texture and design of green chip seal using recycled crumb rubber aggregate. J. Clean. Prod. 166, 1084–1101. https://doi.org/10.1016/j.jclepro.2017.08.127

Gilbert, H.E., Rosado, P.J., Ban-Weiss, G., Harvey, J.T., Li, H., Mandel, B.H., Millstein, D., Mohegh, A., Saboori, A., Levinson, R.M., 2017. Energy and environmental consequences of a cool pavement campaign. Energy Build. 157, 53–77. https://doi.org/10.1016/j.enbuild.2017.03.051

Givoni, B., 1998. Climate considerations in building and urban design. John Wiley & Sons.

Golden, J.S., Kaloush, K.E., 2006. Mesoscale and microscale evaluation of surface pavement impacts on the urban heat island effects. Int. J. Pavement Eng. 7, 37–52. https://doi.org/10.1080/10298430500505325

González-Corrochano, B., Alonso-Azcárate, J., Rodas, M., Barrenechea, J.F., Luque, F.J., 2011. Microstructure and mineralogy of lightweight aggregates manufactured from mining and industrial wastes. Constr. Build. Mater. 25, 3591–3602. https://doi.org/10.1016/j.conbuildmat.2011.03.053

Gransberg, D.D., 2005. Chip Seal Program Excellence in the United States. Transp. Res. Rec. 1933, 72–82. https://doi.org/10.1177/0361198105193300109

Gransberg, D.D., Zaman, M., 2005. Analysis of Emulsion and Hot Asphalt Cement Chip Seal Performance. J. Transp. Eng. 131, 229–238. https://doi.org/10.1061/(ASCE)0733-947X(2005)131:3(229)

Grimmond, S., 2007. Urbanization and global environmental change: local effects of urban warming. Geogr. J. 173, 83–88. https://doi.org/https://doi.org/10.1111/j.1475-4959.2007.232_3.x

Gudipudi, P.P., Underwood, B.S., Zalghout, A., 2017. Impact of climate change on pavement structural performance in the United States. Transp. Res. Part Transp. Environ. 57, 172–184. https://doi.org/10.1016/j.trd.2017.09.022

Gui, J. (Gavin), Phelan, P.E., Kaloush, K.E., Golden, J.S., 2007. Impact of Pavement Thermophysical Properties on Surface Temperatures. J. Mater. Civ. Eng. 19, 683–690. https://doi.org/10.1061/(ASCE)0899-1561(2007)19:8(683)

Gupta, P.K., 1996. Non-crystalline solids: glasses and amorphous solids. J. Non-Cryst. Solids 195, 158–164.

Hassan, H.F., Al-Shamsi, K., Al-Jabri, K., 2024. Effect of Steel Slag on the Permanent Deformation and Life Cycle Cost of Asphalt Concrete Pavements. Int. J. Pavement Res. Technol. 17, 1513–1530. https://doi.org/10.1007/s42947-023-00314-x

Hassn, Abdushafi, Aboufoul, M., Wu, Y., Dawson, A., Garcia, A., 2016. Effect of air voids content on thermal properties of asphalt mixtures. Constr. Build. Mater. 115, 327–335. https://doi.org/10.1016/j.conbuildmat.2016.03.106

Hassn, Abdushaffi, Chiarelli, A., Dawson, A., Garcia, A., 2016. Thermal properties of asphalt pavements under dry and wet conditions. Mater. Des. 91, 432–439. https://doi.org/10.1016/j.matdes.2015.11.116

Hatvani-Kovacs, G., Belusko, M., Skinner, N., Pockett, J., Boland, J., 2016. Heat stress risk and resilience in the urban environment. Sustain. Cities Soc. 26, 278–288. https://doi.org/10.1016/j.scs.2016.06.019

Hendel, M., Colombert, M., Diab, Y., Royon, L., 2015. An analysis of pavement heat flux to optimize the water efficiency of a pavement-watering method. Appl. Therm. Eng. 78, 658–669. https://doi.org/10.1016/j.applthermaleng.2014.11.060

Henry, J.J., 2000. Evaluation of Pavement Friction Characteristics. Transportation Research Board.

Hestin, M., de Veron, S., Burgos, S., 2016. Economic study on recycling of building glass in Europe. Deloitte Sustain.

Higashiyama, H., Sano, M., Nakanishi, F., Takahashi, O., Tsukuma, S., 2016. Field measurements of road surface temperature of several asphalt pavements with temperature rise reducing function. Case Stud. Constr. Mater. 4, 73–80. https://doi.org/10.1016/j.cscm.2016.01.001

Hoivik, N., Greiner, C., Barragan, J., Iniesta, A.C., Skeie, G., Bergan, P., Blanco-Rodriguez, P., Calvet, N., 2019. Long-term performance results of concrete-based modular thermal energy storage system. J. Energy Storage 24, 100735. https://doi.org/10.1016/j.est.2019.04.009

Holmgreen, R.J., Epps, J.A., Hughes, C.H., Gallaway, B.M., 1985. Field evaluation of the Texas seal coat design method.

Holtz, R.D., Kovacs, W.D., Sheahan, T.C., 2011. An Introduction to Geotechnical Engineering. Pearson.

Hou, S., Chen, C., Zhang, J., Shen, H., Gu, F., 2018. Thermal and mechanical evaluations of asphalt emulsions and mixtures for microsurfacing. Constr. Build. Mater. 191, 1221–1229. https://doi.org/10.1016/j.conbuildmat.2018.10.091

Howlader, M.K., Rashid, M.H., Mallick, D., Haque, T., 2012. Effects of aggregate types on thermal properties of concrete. ARPN J. Eng. Appl. Sci. 7, 900–906.

Hu, J., Yu, X. (Bill), 2016. Innovative thermochromic asphalt coating: characterisation and thermal performance. Road Mater. Pavement Des. 17, 187–202. https://doi.org/10.1080/14680629.2015.1068215

Hu, J., Yu, X. (Bill), 2013. Experimental Study of Sustainable Asphalt Binder: Influence of Thermochromic Materials. Transp. Res. Rec. 2372, 108–115. https://doi.org/10.3141/2372-12

Huang, B., Dong, Q., Burdette, E.G., 2009. Laboratory evaluation of incorporating waste ceramic materials into Portland cement and asphaltic concrete. Constr. Build. Mater. 23, 3451–3456. https://doi.org/10.1016/j.conbuildmat.2009.08.024

Huang, B., Wang, X., Kua, H., Geng, Y., Bleischwitz, R., Ren, J., 2018. Construction and demolition waste management in China through the 3R principle. Resour. Conserv. Recycl. 129, 36–44. https://doi.org/10.1016/j.resconrec.2017.09.029

Huang, Y.H., 2004. Pavement Analysis and Design, Pavement Analysis and Design. Pearson Prentice Hall.

Ichinose, T., Matsumoto, F., Kataoka, K., 2008. Chapter 15 - Counteracting Urban Heat Islands in Japan, in: Droege, P. (Ed.), Urban Energy Transition. Elsevier, Amsterdam, pp. 365–380. https://doi.org/10.1016/B978-0-08-045341-5.00015-3

IEA, E., 2007. International Energy Agency Tracking Industrial Energy Efficiency and CO2 Emissions. URL Httpsru Scribd Comdocument214804328IEAEE-2007-Track.-Ind.-Energy-Effic.-AndCO2-Emiss. Дата Обращения 1909 2018.

IEEE 442, 2017. Guide for Thermal Resistivity Measurements of Soils and Backfill Materials.

Irfeey, A.M.M., Chau, H.-W., Sumaiya, M.M.F., Wai, C.Y., Muttil, N., Jamei, E., 2023. Sustainable Mitigation Strategies for Urban Heat Island Effects in Urban Areas. Sustainability 15, 10767. https://doi.org/10.3390/su151410767

ISO 14044 Standard, I., 2006. Environmental management-Life cycle assessment-Requirements and guidelines. Lond. ISO.

ISO 22007-2, 2022. specifies a method for the determination of the thermal conductivity and thermal diffusivity, and hence the specific heat capacity per unit volume of plastics.

Jiang, L., Wang, L., Wang, S., 2019. A novel solar reflective coating with functional gradient multilayer structure for cooling asphalt pavements. Constr. Build. Mater. 210, 13–21. https://doi.org/10.1016/j.conbuildmat.2019.03.180

Jiang, L., Wang, S., 2020. Enhancing heat release of asphalt pavement by a gradient heat conduction channel. Constr. Build. Mater. 230, 117018. https://doi.org/10.1016/j.conbuildmat.2019.117018

Jiao, W., Sha, A., Liu, Z., Jiang, W., Hu, L., Li, X., 2020a. Utilization of steel slags to produce thermal conductive asphalt concretes for snow melting pavements. J. Clean. Prod. 261, 121197. https://doi.org/10.1016/j.jclepro.2020.121197

Jiao, W., Sha, A., Liu, Z., Li, W., Jiang, W., Qin, W., Hu, Y., 2020b. Study on thermal properties of steel slag asphalt concrete for snow-melting pavement. J. Clean. Prod. 277, 123574. https://doi.org/10.1016/j.jclepro.2020.123574

Kabirifar, K., Mojtahedi, M., Wang, C., Tam, V.W.Y., 2020. Construction and demolition waste management contributing factors coupled with reduce, reuse, and recycle strategies for effective waste management: A review. J. Clean. Prod. 263, 121265. https://doi.org/10.1016/j.jclepro.2020.121265

Kadirgamar, K., 2014. The applications of recycled crushed glass in civil construction in the Northern Territory.

Kanellopoulos, G., Koutsomarkos, V.G., Kontoleon, K.J., Georgiadis-Filikas, K., 2017. Numerical Analysis and Modelling of Heat Transfer Processes through Perforated Clay Brick Masonry Walls. Procedia Environ. Sci., Sustainable synergies from Buildings to the Urban Scale 38, 492–499. https://doi.org/10.1016/j.proenv.2017.03.112

Kataoka, K., Matsumoto, F., Ichinose, T., Taniguchi, M., 2009. Urban warming trends in several large Asian cities over the last 100 years. Sci. Total Environ., Human Impacts on Urban Subsurface Environments 407, 3112–3119. https://doi.org/10.1016/j.scitotenv.2008.09.015

Kearby, J.P., 1953. Tests and theories on penetration surfaces, in: Highway Research Board Proceedings.

Khan, A., Mrawira, D., 2008. Influence of Selected Mix Design Factors on the Thermal Behavior of Lightweight Aggregate Asphalt Mixes. J. Test. Eval. 36, 492–499. https://doi.org/10.1520/JTE101687

Kim, T., Uh, J., 2021. A Study on the Effect on UV Exposure in Coastal Buildings. J. Soc. Disaster Inf. 17, 195–205. https://doi.org/10.15683/kosdi.2021.6.30.195

Kolokotroni, M., Ren, X., Davies, M., Mavrogianni, A., 2012. London's urban heat island: Impact on current and future energy consumption in office buildings. Energy Build. 47, 302–311. https://doi.org/10.1016/j.enbuild.2011.12.019

Kuvandykova, D., Bateman, R., 2013. A new transient method to measure thermal conductivity of asphalt. Therm. Conduct. 31.

Lachance-Tremblay, É., Vaillancourt, M., Perraton, D., 2016. Evaluation of the impact of recycled glass on asphalt mixture performances. Road Mater. Pavement Des. 17, 600–618. https://doi.org/10.1080/14680629.2015.1103778

Le, M.-T., Nguyen, Q.-H., Nguyen, M.L., 2020. Numerical and Experimental Investigations of Asphalt Pavement Behaviour, Taking into Account Interface Bonding Conditions. Infrastructures 5, 21. https://doi.org/10.3390/infrastructures5020021

Lee, J., Ahn, H., 2016. Effect of Electrical Surface Charge on Seal Coat Curing and Aggregate Loss Performance. J. Test. Eval. 44, 1661–1670. https://doi.org/10.1520/JTE20140318

Lee, J., Lee, Jaejun, Kim, Y., Mun, S., 2012. A Comparison Study of Friction Measurements for Chip Seal. J. Test. Eval. 40, 603–611. https://doi.org/10.1520/JTE103863

Lee, K.W., Craver, V.O., Kohm, S., Chango, H., 2012. Cool Pavements As a Sustainable Approach to Green Streets and Highways 235–247. https://doi.org/10.1061/41148(389)20

Li, H., 2015. 4 - A comparison of thermal performance of different pavement materials, in: Pacheco-Torgal, F., Labrincha, J.A., Cabeza, L.F., Granqvist, C.-G. (Eds.), Eco-Efficient Materials for Mitigating Building Cooling Needs. Woodhead Publishing, Oxford, pp. 63–124. https://doi.org/10.1016/B978-1-78242-380-5.00004-2

Li, H., 2012. Evaluation of Cool Pavement Strategies for Heat Island Mitigation.

Li, H., Harvey, J., Kendall, A., 2013a. Field measurement of albedo for different land cover materials and effects on thermal performance. Build. Environ. 59, 536–546. https://doi.org/10.1016/j.buildenv.2012.10.014

Li, H., Harvey, J., Kendall, A., 2013b. Field measurement of albedo for different land cover materials and effects on thermal performance. Build. Environ. 59, 536–546. https://doi.org/10.1016/j.buildenv.2012.10.014

Li, H., Xie, N., 2020. 7 - Reflective coatings for high albedo pavement, in: Pacheco-Torgal, F., Amirkhanian, S., Wang, H., Schlangen, E. (Eds.), Eco-Efficient Pavement Construction Materials, Woodhead Publishing Series in Civil and Structural Engineering. Woodhead Publishing, pp. 127–146. https://doi.org/10.1016/B978-0-12-818981-8.00007-2

Li, N., Zhan, H., Yu, X., Tang, W., Yu, H., Dong, F., 2021. Research on the high temperature performance of asphalt pavement based on field cores with different rutting development levels. Mater. Struct. 54, 70. https://doi.org/10.1617/s11527-021-01672-3

Liu, Dengao, Zhang, H., Liu, Z., Liu, Dongjie, He, D., Yu, T., 2023. The heat flux evolution of porous asphalt mixture based on meso-structure and its influence on heat transfer property. Therm. Sci. Eng. Prog. 43, 102020. https://doi.org/10.1016/j.tsep.2023.102020

Liu, J., Xu, J., Liu, Q., Wang, S., Yu, B., 2022. Steel Slag for Roadway Construction: A Review of Material Characteristics and Application Mechanisms. J. Mater. Civ. Eng. 34, 03122001. https://doi.org/10.1061/(ASCE)MT.1943-5533.0004230

Liu, Q., Yu, W., Wu, S., Schlangen, E., Pan, P., 2017. A comparative study of the induction healing behaviors of hot and warm mix asphalt. Constr. Build. Mater. 144, 663–670. https://doi.org/10.1016/j.conbuildmat.2017.03.195

Liu, X., Wu, S., 2011. Study on the graphite and carbon fiber modified asphalt concrete. Constr. Build. Mater. 25, 1807–1811. https://doi.org/10.1016/j.conbuildmat.2010.11.082

Liu, Y., Li, T., Peng, H., 2018. A new structure of permeable pavement for mitigating urban heat island. Sci. Total Environ. 634, 1119–1125. https://doi.org/10.1016/j.scitotenv.2018.04.041

Luca, J., Mrawira, D., 2005. New Measurement of Thermal Properties of Superpave Asphalt Concrete. J. Mater. Civ. Eng. 17, 72–79. https://doi.org/10.1061/(ASCE)0899-1561(2005)17:1(72)

Ma, B., Zhou, X., Liu, J., You, Z., Wei, K., Huang, X., 2016. Determination of Specific Heat Capacity on Composite Shape-Stabilized Phase Change Materials and Asphalt Mixtures by Heat Exchange System. Materials 9, 389. https://doi.org/10.3390/ma9050389

Ma, Y., Zhu, B., 2009. Research on the preparation of reversibly thermochromic cement based materials at normal temperature. Cem. Concr. Res. 39, 90–94. https://doi.org/10.1016/j.cemconres.2008.10.006

Mallick, R.B., Hooper, F.P., O'Brien, S., Kashi, M., 2004. Evaluation of Use of Synthetic Lightweight Aggregate in Hot-Mix Asphalt. Transp. Res. Rec. 1891, 1–7. https://doi.org/10.3141/1891-01

Mammeri, A., Lallam, M., Guellati, S.E., Shamsaei, M., 2023a. Using Tuff and Limestone Sand to Minimize Water Consumption of Pavement Construction in Arid Regions. Civ. Environ. Eng. 19, 630–639. https://doi.org/10.2478/cee-2023-0057

Mammeri, A., Vaillancourt, M., Shamsaei, M., 2023b. Experimental and numerical investigation of using waste glass aggregates in asphalt pavement to mitigate urban heat islands. Clean Technol. Environ. Policy. https://doi.org/10.1007/s10098-023-02481-8

Mantilla, C.A., Button, J.W., 1994. Prime coat methods and materials to replace cutback asphalt.

Marceau, M., VanGeem, M., 2007. Solar Reflectance of Concretes for LEED Sustainable Sites Credit: Heat Island Effect.

Maria V.D., Rahman M., Collins P., Dondi G., Sangiorgi C., 2013. Urban Heat Island Effect: Thermal Response from Different Types of Exposed Paved Surfaces. Int. J. Pavement Res. Technol. 6, 414–422. https://doi.org/10.6135/ijprt.org.tw/2013.6(4).414

McHattie, R.L., 2001. Asphalt Surface Treatment Guide (No. FHWA/AK/RD-85/08).

McLEOD, N.W., Chaffin, C.W., Holberg, A.E., Parker, C.F., Obrcian, V., Edwards, J.M., Campen, W.H., Kari, W.J., 1969. A general method of design for seal coats and surface treatments, in: Proceedings of the Association of Asphalt Paving Technologists. pp. 537–630.

Medina, T., Calmon, J.L., Vieira, D., Bravo, A., Vieira, T., 2023. Life Cycle Assessment of Road Pavements That Incorporate Waste Reuse: A Systematic Review and Guidelines Proposal. Sustainability 15, 14892. https://doi.org/10.3390/su152014892

Memon, R.A., Leung, D.Y.C., Liu, C.-H., 2009. An investigation of urban heat island intensity (UHII) as an indicator of urban heating. Atmospheric Res. 94, 491–500. https://doi.org/10.1016/j.atmosres.2009.07.006

Menegaki, M., Damigos, D., 2018. A review on current situation and challenges of construction and demolition waste management. Curr. Opin. Green Sustain. Chem., Reuse and Recycling / UN SGDs: How can Sustainable Chemistry Contribute? / Green Chemistry in Education 13, 8–15. https://doi.org/10.1016/j.cogsc.2018.02.010

Miao, C., Li, Z., Li, K., Lv, Y., Wu, X., Cao, X., Wu, Y., 2022. A super-cooling solar reflective coating with waterborne polyurethane for asphalt pavement. Prog. Org. Coat. 165, 106741. https://doi.org/10.1016/j.porgcoat.2022.106741

Mills, B.N., Tighe, S.L., Andrey, J., Smith, J.T., Huen, K., 2009. Climate Change Implications for Flexible Pavement Design and Performance in Southern Canada. J. Transp. Eng. 135, 773–782. https://doi.org/10.1061/(ASCE)0733-947X(2009)135:10(773)

Mills, G., 2008. Luke Howard and the climate of London. Weather 63, 153–157.

Mirzanamadi, R., Johansson, P., Grammatikos, S.A., 2018. Thermal properties of asphalt concrete: A numerical and experimental study. Constr. Build. Mater. 158, 774–785. https://doi.org/10.1016/j.conbuildmat.2017.10.068

Mohajerani, A., Bakaric, J., Jeffrey-Bailey, T., 2017a. The urban heat island effect, its causes, and mitigation, with reference to the thermal properties of asphalt concrete. J. Environ. Manage. 197, 522–538. https://doi.org/10.1016/j.jenvman.2017.03.095

Mohajerani, A., Vajna, J., Cheung, T.H.H., Kurmus, H., Arulrajah, A., Horpibulsuk, S., 2017b. Practical recycling applications of crushed waste glass in construction materials: A review. Constr. Build. Mater. 156, 443–467. https://doi.org/10.1016/j.conbuildmat.2017.09.005

Molla, A.S., Tang, P., Sher, W., Bekele, D.N., 2021. Chemicals of concern in construction and demolition waste fine residues: A systematic literature review. J. Environ. Manage. 299, 113654. https://doi.org/10.1016/j.jenvman.2021.113654

Montoya, M.A., Jason Weiss, W., Haddock, J.E., 2017. Using electrical resistance to evaluate the chip seal curing process. Road Mater. Pavement Des. 18, 98–111. https://doi.org/10.1080/14680629.2017.1389090

Morea, F., Agnusdei, J.O., Zerbino, R., 2011. The use of asphalt low shear viscosity to predict permanent deformation performance of asphalt concrete. Mater. Struct. 44, 1241–1248. https://doi.org/10.1617/s11527-010-9696-3

Mullaney, J., Lucke, T., 2014. Practical Review of Pervious Pavement Designs. CLEAN – Soil Air Water 42, 111–124. https://doi.org/10.1002/clen.201300118

Nakayama, T., Fujita, T., 2010. Cooling effect of water-holding pavements made of new materials on water and heat budgets in urban areas. Landsc. Urban Plan. 96, 57–67. https://doi.org/10.1016/j.landurbplan.2010.02.003

Narasimhan, B., Bhallamudi, S.M., Mondal, A., Ghosh, S., Mujumdar, P., 2016. Chennai floods 2015: A rapid assessment. Interdiscip. Cent. Water Res. Rep.

Nellis, G., Klein, S., 2009. Heat Transfer. Cambridge University Press.

Nippon Slag Association, 2016. Production and uses of steel slag in Japan.

Nishioka, M., Nabeshima, M., Wakama, S., Ueda, J., 2006. Effects of surface temperature reduction and thermal environment on high albedo coating asphalt pavement. J Heat Isl. Inst Int 1, 46–52.

Novo, A.V., Bayon, J.R., Castro-Fresno, D., Rodriguez-Hernandez, J., 2013. Monitoring and Evaluation of the Thermal Behavior of Permeable Pavements for Energy Recovery Purposes in an Experimental Parking Lot: Preliminary Results. J. Energy Eng. 139, 230–237. https://doi.org/10.1061/(ASCE)EY.1943-7897.0000106

Omar, H.A., Yusoff, N.I.Md., Mubaraki, M., Ceylan, H., 2020. Effects of moisture damage on asphalt mixtures. J. Traffic Transp. Eng. Engl. Ed. 7, 600–628. https://doi.org/10.1016/j.jtte.2020.07.001

Pai, R.R., Bakare, M.D., Patel, S., Shahu, J.T., 2021. Structural Evaluation of Flexible Pavement Constructed with Steel Slag–Fly Ash–Lime Mix in the Base Layer. J. Mater. Civ. Eng. 33, 04021097. https://doi.org/10.1061/(ASCE)MT.1943-5533.0003711

Pan, J., Zou, R., Jin, F., 2017. Experimental Study on Specific Heat of Concrete at High Temperatures and Its Influence on Thermal Energy Storage. Energies 10, 33. https://doi.org/10.3390/en10010033

Pancar, E.B., 2016. Using Recycled Glass and Zeolite in Concrete Pavement to Mitigate Heat Island and Reduce Thermal Cracks. Adv. Mater. Sci. Eng. 2016, e8526354. https://doi.org/10.1155/2016/8526354

Park, D.-W., Dessouky, S., Hwang, S.-D., 2014. Thermo-physical properties of graphite-modified asphalt mixture and numerical analyses for snow melting pavement. Sustain. Eco-Effic. Conserv. Transp. Infrastruct. Asset Manag. 87–94.

Park, S., Jo, M.-C., Park, J.-B., 2000. Adsorption and Thermal Desorption Behaviour of Asphalt-like Functionalities on Silica. Adsorpt. Sci. Technol. 18, 675–684. https://doi.org/10.1260/0263617001493729

Parker, D.E., 2010. Urban heat island effects on estimates of observed climate change. WIREs Clim. Change 1, 123–133. https://doi.org/10.1002/wcc.21

Pascual-Muñoz, P., Castro-Fresno, D., Serrano-Bravo, P., Alonso-Estébanez, A., 2013. Thermal and hydraulic analysis of multilayered asphalt pavements as active solar collectors. Appl. Energy 111, 324–332. https://doi.org/10.1016/j.apenergy.2013.05.013

Pasetto, M., Baliello, A., Giacomello, G., Pasquini, E., 2023. The Use of Steel Slags in Asphalt Pavements: A State-of-the-Art Review. Sustainability 15, 8817. https://doi.org/10.3390/su15118817

Pasetto, M., Pasquini ,E., Giacomello ,G., and Baliello, A., 2019. Innovative pavement surfaces as urban heat islands mitigation strategy: chromatic, thermal and mechanical characterisation of clear/coloured mixtures. Road Mater. Pavement Des. 20, S533–S555. https://doi.org/10.1080/14680629.2019.1593230

Peng, B., Li, J., Ling, T., Li, X., Diao, H., Huang, X., 2023. Semi-flexible pavement with glass for alleviating the heat island effect. Constr. Build. Mater. 367, 130275. https://doi.org/10.1016/j.conbuildmat.2022.130275

Petkova-Slipets, R., Zlateva, P., 2018. Thermal Properties of a New Pavement Material for Using in Road Construction. Civ. Environ. Eng. 14, 99–104. https://doi.org/10.2478/cee-2018-0013

Pierce, L.M., Kebede, N., Applied Pavement Technology, Inc., 2015. Chip seal performance measures : best practices. (No. WA-RD 841.1).

Pirouzfam, N., Sendur, K., 2021. Tungsten Based Spectrally Selective Absorbers with Anisotropic Rough Surface Texture. Nanomaterials 11, 2018. https://doi.org/10.3390/nano11082018

Pomerantz, M., Akbari, H., Chang, S.-C., Levinson, R., Pon, B., 2003. Examples of cooler reflective streets for urban heat-island mitigation: Portland cement concrete and chip seals.

Pouranian, M.R., Haddock, J.E., 2020. Effect of Aggregate Gradation on Asphalt Mixture Compaction Parameters. J. Mater. Civ. Eng. 32, 04020244. https://doi.org/10.1061/(ASCE)MT.1943-5533.0003315

Qin, Y., 2015. A review on the development of cool pavements to mitigate urban heat island effect. Renew. Sustain. Energy Rev. 52, 445–459. https://doi.org/10.1016/j.rser.2015.07.177

Québec, G.D., 2016. Hot mix asphalt formulated according to the Pavement Laboratory formulation method. 4 Liants Enrobés 17.

Rakrueangdet, K., Nunak, N., Suesut, T., Sritham, E., 2016. Emissivity measurements of reflective materials using infrared thermography, in: International MultiConference of Engineers and Computer Scientists (IMECS).

Ramachandran, V.S., Feldman, R.F., 1996. 1 - Concrete Science, in: Ramachandran, V.S. (Ed.), Concrete Admixtures Handbook (Second Edition). William Andrew Publishing, Park Ridge, NJ, pp. 1–66. https://doi.org/10.1016/B978-081551373-5.50005-2

Ren, J., Ma, B., Si, W., Zhou, X., Li, C., 2014. Preparation and analysis of composite phase change material used in asphalt mixture by sol–gel method. Constr. Build. Mater. 71, 53–62. https://doi.org/10.1016/j.conbuildmat.2014.07.100

Revel, G.M., Martarelli, M., Bengochea, M.Á., Gozalbo, A., Orts, M.J., Gaki, A., Gregou, M., Taxiarchou, M., Bianchin, A., Emiliani, M., 2013. Nanobased coatings with improved NIR reflecting properties for building envelope materials: Development and natural aging effect measurement. Cem. Concr. Compos., Special issue: Nanotechnology in Construction 36, 128–135. https://doi.org/10.1016/j.cemconcomp.2012.10.002

Richard, C., Doré, G., Lemieux, C., Bilodeau, J.-P., Haure-Touzé, J., 2015. Albedo of Pavement Surfacing Materials: In Situ Measurements 181–192. https://doi.org/10.1061/9780784479315.017

Roesler, J., Sen, S., 2016. Impact of Pavements on the Urban Heat Island.

Rossi, F., Castellani, B., Presciutti, A., Morini, E., Anderini, E., Filipponi, M., Nicolini, A., 2016. Experimental evaluation of urban heat island mitigation potential of retro-reflective pavement in urban canyons. Energy Build. 126, 340–352. https://doi.org/10.1016/j.enbuild.2016.05.036

Rossi, F., Pisello, A.L., Nicolini, A., Filipponi, M., Palombo, M., 2014. Analysis of retro-reflective surfaces for urban heat island mitigation: A new analytical model. Appl. Energy 114, 621–631. https://doi.org/10.1016/j.apenergy.2013.10.038

Santamouris, M. (Ed.), 2013a. Energy and Climate in the Urban Built Environment. Routledge, London. https://doi.org/10.4324/9781315073774

Santamouris, M., 2013b. Using cool pavements as a mitigation strategy to fight urban heat island—A review of the actual developments. Renew. Sustain. Energy Rev. 26, 224–240. https://doi.org/10.1016/j.rser.2013.05.047

Serigos, P.A., Smit, A. de F., Prozzi, J.A., University of Texas at Austin. Center for Transportation Research, 2017. Performance of preventive maintenance treatments for flexible pavements in Texas. (No. FHWA/TX-16/0-6878-2).

Sha, A., Liu, Z., Tang, K., Li, P., 2017. Solar heating reflective coating layer (SHRCL) to cool the asphalt pavement surface. Constr. Build. Mater. 139, 355–364. https://doi.org/10.1016/j.conbuildmat.2017.02.087

Shamberger, P.J., Bruno, N.M., 2020. Review of metallic phase change materials for high heat flux transient thermal management applications. Appl. Energy 258, 113955. https://doi.org/10.1016/j.apenergy.2019.113955

Shamsaei, M., Carter, A., Vaillancourt, M., 2025. Utilisation of steel slag aggregates to propose novel asphalt pavement structures alleviating urban heat islands. Road Mater. Pavement Des. 0, 1–26. https://doi.org/10.1080/14680629.2024.2438340

Shamsaei, M., Carter, A., Vaillancourt, M., 2024a. Using construction and demolition waste materials to alleviate the negative effect of pavements on the urban heat island: A laboratory, field, and numerical study. Case Stud. Constr. Mater. 20, e03346. https://doi.org/10.1016/j.cscm.2024.e03346

Shamsaei, M., Carter, A., Vaillancourt, M., 2024b. The Comparison of the Bleeding Potential of Chip Seals Developed with Recycled Materials and Limestone Aggregates, in: Banthia, N., Soleimani-Dashtaki, S., Mindess, S. (Trans.), Smart & Sustainable Infrastructure: Building a Greener Tomorrow. Springer Nature Switzerland, Cham, pp. 521–531.

Shamsaei, M., Carter, A., Vaillancourt, M., 2022. A review on the heat transfer in asphalt pavements and urban heat island mitigation methods. Constr. Build. Mater. 359, 129350. https://doi.org/10.1016/j.conbuildmat.2022.129350

ShengYue, W., QiYang, Z., YingNa, D., PeiDong, S., 2014. Unidirectional Heat-Transfer Asphalt Pavement for Mitigating the Urban Heat Island Effect. J. Mater. Civ. Eng. 26, 812–821. https://doi.org/10.1061/(ASCE)MT.1943-5533.0000872

Shi, X., 2014. Controlling Thermal Properties of Asphalt Concrete and its Multifunctional Applications (Thesis).

Shi, X., Rew, Y., Ivers, E., Shon, C.-S., Stenger, E.M., Park, P., 2019. Effects of thermally modified asphalt concrete on pavement temperature. Int. J. Pavement Eng. 20, 669–681. https://doi.org/10.1080/10298436.2017.1326234

Shiha, M., El-Badawy, S., Gabr, A., 2020. Modeling and performance evaluation of asphalt mixtures and aggregate bases containing steel slag. Constr. Build. Mater. 248, 118710. https://doi.org/10.1016/j.conbuildmat.2020.118710

Shuler, S., Epps-Martin, A., Lord, A., Hoyt, D., 2011. Manual for Emulsion-Based Chip Seals for Pavement Preservation. National Academies Press, Washington, D.C. https://doi.org/10.17226/14421

Si, W., Ma, B., Ren, J., Hu, Y., Zhou, X., Tian, Y., Li, Y., 2020. Temperature responses of asphalt pavement structure constructed with phase change material by applying finite element method. Constr. Build. Mater. 244, 118088. https://doi.org/10.1016/j.conbuildmat.2020.118088

Silva, H.R., Phelan, P.E., Golden, J.S., 2010. Modeling effects of urban heat island mitigation strategies on heat-related morbidity: a case study for Phoenix, Arizona, USA. Int. J. Biometeorol. 54, 13–22. https://doi.org/10.1007/s00484-009-0247-y

Singh, P.P., Garg, R.D., 2013. Study of spectral reflectance characteristics of asphalt road surface using geomatics techniques, in: 2013 International Conference on Advances in Computing, Communications and Informatics (ICACCI). Presented at the 2013 International Conference on Advances in Computing, Communications and Informatics (ICACCI), pp. 516–520. https://doi.org/10.1109/ICACCI.2013.6637225

Stempihar, J.J., Pourshams-Manzouri, T., Kaloush, K.E., Rodezno, M.C., 2012. Porous Asphalt Pavement Temperature Effects for Urban Heat Island Analysis. Transp. Res. Rec. 2293, 123–130. https://doi.org/10.3141/2293-15

Stockton, W.R., Epps, J.A., 1975. ENGINEERING ECONOMY AND ENERGY CONSIDERATIONS. SEAL COAT ECONOMICS AND DESIGN.

Stone Brian, Hess Jeremy J., Frumkin Howard, 2010. Urban Form and Extreme Heat Events: Are Sprawling Cities More Vulnerable to Climate Change Than Compact Cities? Environ. Health Perspect. 118, 1425–1428. https://doi.org/10.1289/ehp.0901879

Stripple, H., 2001. Life cycle assessment of road. Pilot Study Inventory Anal. 96.

Synnefa, A., Karlessi, T., Gaitani, N., Santamouris, M., Assimakopoulos, D.N., Papakatsikas, C., 2011. Experimental testing of cool colored thin layer asphalt and estimation of its potential to improve the urban microclimate. Build. Environ. 46, 38–44. https://doi.org/10.1016/j.buildenv.2010.06.014

Synnefa, A., Santamouris, M., Apostolakis, K., 2007. On the development, optical properties and thermal performance of cool colored coatings for the urban environment. Sol. Energy 81, 488–497. https://doi.org/10.1016/j.solener.2006.08.005

Teh, S.H., Wiedmann, T., Castel, A., de Burgh, J., 2017. Hybrid life cycle assessment of greenhouse gas emissions from cement, concrete and geopolymer concrete in Australia. J. Clean. Prod. 152, 312–320. https://doi.org/10.1016/j.jclepro.2017.03.122

Thuillier, G., Hersé, M., Labs, D., Foujols, T., Peetermans, W., Gillotay, D., Simon, P.C., Mandel, H., 2003. The Solar Spectral Irradiance from 200 to 2400 nm as Measured by the SOLSPEC Spectrometer from the Atlas and Eureca Missions. Sol. Phys. 214, 1–22. https://doi.org/10.1023/A:1024048429145

Tian, Y., Yu, M., 2017. A novel crater recognition based visual navigation approach for asteroid precise pin-point landing. Aerosp. Sci. Technol. 70, 1–9. https://doi.org/10.1016/j.ast.2017.07.014

Ting, D.S.-K., 2012. Heat Islands – Understanding and Mitigating Heat in Urban Areas. Int. J. Environ. Stud. 69, 1008–1011. https://doi.org/10.1080/00207233.2012.670477

Tong, J., Ma, T., Shen, K., Zhang, H., Wu, S., 2020. A criterion of asphalt pavement rutting based on the thermal-visco-elastic-plastic model. Int. J. Pavement Eng. 0, 1–11. https://doi.org/10.1080/10298436.2020.1792470

Tran, N., Powell, B., Marks, H., West, R., Kvasnak, A., 2009. Strategies for Design and Construction of High-Reflectance Asphalt Pavements. Transp. Res. Rec. 2098, 124–130. https://doi.org/10.3141/2098-13

Transportation Association of Canada, 2013. Best Practices Guide for the Use of Recycled Materials in Transportation Infrastructure. URL https://www.tac-atc.ca/en/knowledge-centre/technical-resources-search/publications/ptm-urmti-e/ (accessed 8.4.25).

Turner, J., Parisi, A.V., 2018. Ultraviolet Radiation Albedo and Reflectance in Review: The Influence to Ultraviolet Exposure in Occupational Settings. Int. J. Environ. Res. Public. Health 15, 1507. https://doi.org/10.3390/ijerph15071507

Ulubeyli, S., Kazaz, A., Arslan, V., 2017. Construction and Demolition Waste Recycling Plants Revisited: Management Issues. Procedia Eng., Modern Building Materials, Structures and Techniques 172, 1190–1197. https://doi.org/10.1016/j.proeng.2017.02.139

Umar, U.A., Shafiq, N., Malakahmad, A., Nuruddin, M.F., Khamidi, M.F., 2017. A review on adoption of novel techniques in construction waste management and policy. J. Mater. Cycles Waste Manag. 19, 1361–1373. https://doi.org/10.1007/s10163-016-0534-8

Vo, H.V., Park, D.-W., 2017. Application of Conductive Materials to Asphalt Pavement. Adv. Mater. Sci. Eng. 2017, e4101503. https://doi.org/10.1155/2017/4101503

Vo, H.V., Park, D.-W., Dessouky, S., 2015. Simulation of snow melting pavement performance using measured thermal properties of graphite-modified asphalt mixture. Road Mater. Pavement Des. 16, 696–706. https://doi.org/10.1080/14680629.2015.1020847

Vo, H.V., Park, D.-W., Seo, W.-J., Yoo, B.-S., 2017. Evaluation of Asphalt Mixture Modified with Graphite and Carbon Fibers for Winter Adaptation: Thermal Conductivity Improvement. J. Mater. Civ. Eng. 29, 04016176. https://doi.org/10.1061/(ASCE)MT.1943-5533.0001675

Vorhauer, N., Metzger, T., Tsotsas, E., 2010. Empirical Macroscopic Model for Drying of Porous Media Based on Pore Networks and Scaling Theory. Dry. Technol. 28, 991–1000. https://doi.org/10.1080/07373937.2010.497088

Wang, C., Fu, H., Fan, Z., Li, T., 2019. Utilization and properties of road thermal resistance aggregates into asphalt mixture. Constr. Build. Mater. 208, 87–101. https://doi.org/10.1016/j.conbuildmat.2019.02.154

Wang, H., Wu, S., Chen, M., Zhang, Y., 2010. Numerical simulation on the thermal response of heat-conducting asphalt pavements. Phys. Scr. 2010, 014041. https://doi.org/10.1088/0031-8949/2010/T139/014041

Wang, J., Zhang, Z., Guo, D., Xu, C., Zhang, K., 2018. Study on Cooling Effect and Pavement Performance of Thermal-Resistant Asphalt Mixture. Adv. Mater. Sci. Eng. 2018, e6107656. https://doi.org/10.1155/2018/6107656

Wang, W.-C., Wang, H.-Y., Chang, K.-H., Wang, S.-Y., 2020. Effect of high temperature on the strength and thermal conductivity of glass fiber concrete. Constr. Build. Mater. 245, 118387. https://doi.org/10.1016/j.conbuildmat.2020.118387

Watkins, R., Palmer, J., Kolokotroni, M., Littlefair, P., 2002. The London Heat Island: results from summertime monitoring. Build. Serv. Eng. Res. Technol. 23, 97–106.

Weil, M., Jeske, U., Schebek, L., 2006. Closed-loop recycling of construction and demolition waste in Germany in view of stricter environmental threshold values. Waste Manag. Res. 24, 197–206.

Wong, N.H., Chen, Y., 2008. Tropical Urban Heat Islands: Climate, Buildings and Greenery, Spon Research. Taylor & Francis.

Wood, T.J., Janisch, D.W., Gaillard, F.S., 2006. Minnesota seal coat handbook 2006.

Wu, Q., Niu, F., 2013. Permafrost changes and engineering stability in Qinghai-Xizang Plateau. Chin. Sci. Bull. 58, 1079–1094. https://doi.org/10.1007/s11434-012-5587-z

Xie, N., Li, H., Abdelhady, A., Harvey, J., 2019. Laboratorial investigation on optical and thermal properties of cool pavement nano-coatings for urban heat island mitigation. Build. Environ. 147, 231–240. https://doi.org/10.1016/j.buildenv.2018.10.017

Xie, N., Li, H., Zhang, H., Zhang, X., Jia, M., 2020. Effects of accelerated weathering on the optical characteristics of reflective coatings for cool pavement. Sol. Energy Mater. Sol. Cells 215, 110698. https://doi.org/10.1016/j.solmat.2020.110698

Xu, G., Chen, X., Huang, X., Ma, T., Zhou, W., 2019. Characterization of Air Voids Distribution in the Open-Graded Asphalt Mixture Based on 2D Image Analysis. Appl. Sci. 9, 4126. https://doi.org/10.3390/app9194126

Xu, G., Wang, H., 2016. Study of cohesion and adhesion properties of asphalt concrete with molecular dynamics simulation. Comput. Mater. Sci. 112, 161–169. https://doi.org/10.1016/j.commatsci.2015.10.024

Xue, Q., Liu, L., Zhao, Y., Chen, Y.-J., Li, J.-S., 2013. Dynamic behavior of asphalt pavement structure under temperature-stress coupled loading. Appl. Therm. Eng. 53, 1–7. https://doi.org/10.1016/j.applthermaleng.2012.10.055

Yaghoubi, E., Yaghoubi, M., Guerrieri, M., Sudarsanan, N., 2021. Improving expansive clay subgrades using recycled glass: Resilient modulus characteristics and pavement performance. Constr. Build. Mater. 302, 124384. https://doi.org/10.1016/j.conbuildmat.2021.124384

Yamamoto, Y., 2006. Measures to mitigate urban heat islands. Q. Rev. DC. Nurses. Assoc. 18, 65–83.

Yang, B., Li, H., Sun, Y., Zhang, H., Liu, J., Yang, J., Zhang, X., 2023. Chemo-rheological, mechanical, morphology evolution and environmental impact of aged asphalt binder

coupling thermal oxidation, ultraviolet radiation and water. J. Clean. Prod. 388, 135866. https://doi.org/10.1016/j.jclepro.2023.135866

Yang, H., Huang, X., Thompson, J.R., Flower, R.J., 2016. Chinese landfill collapse: urban waste and human health. Lancet Glob. Health 4, e452. https://doi.org/10.1016/S2214-109X(16)30051-1

Yang, J., Hu, L., Wang, C., 2019. Population dynamics modify urban residents' exposure to extreme temperatures across the United States. Sci. Adv. 5, eaay3452. https://doi.org/10.1126/sciadv.aay3452

Yavuzturk, C., Ksaibati, K., Chiasson, A.D., 2005. Assessment of Temperature Fluctuations in Asphalt Pavements Due to Thermal Environmental Conditions Using a Two-Dimensional, Transient Finite-Difference Approach. J. Mater. Civ. Eng. 17, 465–475. https://doi.org/10.1061/(ASCE)0899-1561(2005)17:4(465)

Yazgan, B., 2003. A new testing protocol for seal coat (chip seal) aggregate-binder compatibility. Texas Tech University.

Yeheyis, M., Hewage, K., Alam, M.S., Eskicioglu, C., Sadiq, R., 2013. An overview of construction and demolition waste management in Canada: a lifecycle analysis approach to sustainability. Clean Technol. Environ. Policy 15, 81–91. https://doi.org/10.1007/s10098-012-0481-6

Yildirim, I.Z., Prezzi, M., 2017. Experimental evaluation of EAF ladle steel slag as a geo-fill material: Mineralogical, physical & mechanical properties. Constr. Build. Mater. 154, 23–33. https://doi.org/10.1016/j.conbuildmat.2017.07.149

Yinfei, D., Chen, J., Han, Z., Liu, W., 2018. A review on solutions for improving rutting resistance of asphalt pavement and test methods. Constr. Build. Mater. 168, 893–905. https://doi.org/10.1016/j.conbuildmat.2018.02.151

Yinfei, D., Mingxin, D., Haibin, D., Deyi, D., Peifeng, C., Cong, M., 2020. Incorporating hollow glass microsphere to cool asphalt pavement: Preliminary evaluation of asphalt mastic. Constr. Build. Mater. 244, 118380. https://doi.org/10.1016/j.conbuildmat.2020.118380

Yinfei, D., Qin, S., Shengyue, W., 2014. Highly oriented heat-induced structure of asphalt pavement for reducing pavement temperature. Energy Build. 85, 23–31. https://doi.org/10.1016/j.enbuild.2014.09.035

Yinfei, D., Shengyue, W., Jian, Z., 2015. Cooling asphalt pavement by a highly oriented heat conduction structure. Energy Build. 102, 187–196. https://doi.org/10.1016/j.enbuild.2015.05.020

Yinfei, D., Shengyue, W., Shuangjie, W., Jianbing, C., Dongpeng, Z., 2016. Integrative heat-dissipating structure for cooling permafrost embankment. Cold Reg. Sci. Technol. 129, 85–95. https://doi.org/10.1016/j.coldregions.2016.07.002

You, L., You, Z., Dai, Q., Xie, X., Washko, S., Gao, J., 2019. Investigation of adhesion and interface bond strength for pavements underlying chip-seal: Effect of asphalt-aggregate combinations and freeze-thaw cycles on chip-seal. Constr. Build. Mater. 203, 322–330. https://doi.org/10.1016/j.conbuildmat.2019.01.058

Yu, Q., Fan, K., You, Y., Guo, L., Yuan, C., 2015. Comparative analysis of temperature variation characteristics of permafrost roadbeds with different widths. Cold Reg. Sci. Technol. 117, 12–18. https://doi.org/10.1016/j.coldregions.2015.05.002

Yuan, L., Han, Z., Liu, L., Li, M., Mao, S., 2024. Six-synchronous construction technology-based fiber stone seal of road pavements: Design, optimization, and performance evaluation. Constr. Build. Mater. 450, 138594. https://doi.org/10.1016/j.conbuildmat.2024.138594

Zaika, Y., Djakfar, L., 2016. Gradation band of some types material for reservoir base of porous pavement. GEOMATE J. 11, 2486–2492.

Zaniewski, J.P., Yan, Y., 2014. Relationship Between Air Voids, Aggregate Gradation, Nominal Maximum Aggregate Size, and Permeability of Hot Mix Asphalt Mixtures. Presented at the Transportation Research Board 93rd Annual MeetingTransportation Research Board.

Zeng, Y., Qiu, X.F., Gu, L.H., He, Y.J., Wang, K.F., 2009. The urban heat island in Nanjing. Quat. Int., Larger Asian Rivers: Climate Change, River Flow and Sediment Flux 208, 38–43. https://doi.org/10.1016/j.quaint.2009.02.018

Zhang, C., Hu, M., Di Maio, F., Sprecher, B., Yang, X., Tukker, A., 2022. An overview of the waste hierarchy framework for analyzing the circularity in construction and demolition waste management in Europe. Sci. Total Environ. 803, 149892. https://doi.org/10.1016/j.scitotenv.2021.149892

Zhang, D., Chen, M., Wu, S., Riara, M., Wan, J., Li, Y., 2019. Thermal and rheological performance of asphalt binders modified with expanded graphite/polyethylene glycol composite phase change material (EP-CPCM). Constr. Build. Mater. 194, 83–91. https://doi.org/10.1016/j.conbuildmat.2018.11.011

Zhang, J., Ding, L., Li, F., Peng, J., 2020. Recycled aggregates from construction and demolition wastes as alternative filling materials for highway subgrades in China. J. Clean. Prod. 255, 120223. https://doi.org/10.1016/j.jclepro.2020.120223

Zhang, J., Tan, H., Pei, J., Qu, T., Liu, W., 2019. Evaluating Crack Resistance of Asphalt Mixture Based on Essential Fracture Energy and Fracture Toughness. Int. J. Geomech. 19, 06019005. https://doi.org/10.1061/(ASCE)GM.1943-5622.0001390

Zhao, Y., Goulias, D., Tefa, L., Bassani, M., 2021. Life Cycle Economic and Environmental Impacts of CDW Recycled Aggregates in Roadway Construction and Rehabilitation. Sustainability 13, 8611. https://doi.org/10.3390/su13158611

Zheng, M., Han, L., Wang, F., Mi, H., Li, Y., He, L., 2015. Comparison and analysis on heat reflective coating for asphalt pavement based on cooling effect and anti-skid performance. Constr. Build. Mater. 93, 1197–1205. https://doi.org/10.1016/j.conbuildmat.2015.04.043

Zheng, M., Tian, Y., He, L., 2019. Analysis on Environmental Thermal Effect of Functionally Graded Nanocomposite Heat Reflective Coatings for Asphalt Pavement. Coatings 9, 178. https://doi.org/10.3390/coatings9030178

Zheng, N., Bi, J., Dong, S., Lei, J., He, Y., Cui, Z., Chen, L., 2022. Testing and evaluation for long-term skid resistance of asphalt pavement composite seal using texture characteristics. Constr. Build. Mater. 356, 129241. https://doi.org/10.1016/j.conbuildmat.2022.129241

Zhou, Z., Hu, S., Zhang, X., Zuo, J., 2013. Characteristics and application of road absorbing solar energy. Front. Energy 7, 525–534. https://doi.org/10.1007/s11708-013-0278-2